université PARIS-SACLAY

NNT : 2018SACLN051

école normale supérieure paris-saclay

Design, synthesis and characterization of electron-acceptor aromatic and heterocyclic derivatives

Thèse de doctorat de l'Université Paris-Saclay
préparée à l'École Normale Supérieure Paris-Saclay

École doctorale n°571 Sciences Chimiques : Molécules, Matériaux, Instrumentation et Biosystèmes (2MIB)
Spécialité de doctorat: Chimie

Thèse présentée et soutenue à Cachan, le 19 Dec 2018, par

Mr. Yangyang QU

Composition du Jury :

Mr Jean-Cyrille HIERSO
Professeur, Université de Bourgogne (Laboratoire ICMUB) — Rapporteur

Mr Gilles ULRICH
Directeur de Recherche CNRS, Université de Strasbourg (Laboratoire ICPEES) — Rapporteur

Mme Françoise SPIRAU
Professeure, École Nationale Supérieure de Chimie de Montpellier (Laboratoire ICGM) — Examinatrice

Mr Przemyslaw DATA
Professeur, Silesian University of Technology (Department of Physical Chemistry and Technology of Polymers) — Examinateur

Mr Damien PRIM
Professeur, Université de Versailles Saint-Quentin-en-Yvelines (Laboratoire ILV) — Président

Mr Pierre AUDEBERT
Professeur, École Normale Supérieure Paris-Saclay (Laboratoire PPSM) — Directeur de thèse

Mr Gilles CLAVIER
Directeur de Recherche CNRS, École Normale Supérieure Paris-Saclay (Laboratoire PPSM) — Co-Directeur de thèse

Thèse de doctorat

Acknowledgement

First and foremost, I would like to express my deepest gratitude to my supervisor Prof. Pierre Audebert, a respectable, responsible and resourceful scholar. Without his continuous trust, enlightening instruction and impressive kindness, this thesis could not have been finalized. His wealthy knowledge and vigorous academic observation inspires me not only in this thesis but also in my future research.

I would also like to show my greatest appreciation to my second supervisor Dr. Gilles Clavier for continuous guidance and encouragement throughout this thesis. His assistance in routine laboratory operation, advices and discussion about research results, corrections for thesis, reports and posters are really precious to me. This thesis would not have materialized without him.

My warm and sincere thanks go to Prof. Fabien Miomandre, director of lab PPSM. His continuous support and help for both research and administrative affairs in the lab are deeply appreciated.

Furthermore, I wish to express my deep and sincere gratitude to Prof. Przemyslaw Data from Silesian University of Technology, for his great achievement to bring all the EXCILIGHT member together. I deeply thank him for his patient instruction and encouragement in University of Durham for photophysical studies. His wisdom enlightens me and surely has a lifelong impact on me.

I also wish to express my warm and sincere thanks to Prof. Peter Skabara from University of Glasgow, for his helpful discussions and suggestions regarding my research work during my secondment in his lab.

Special thanks go to Dr. Gilles Ulrich from Université de Strasbourg, who has kindly been my external supervisor for the last 3 years, and will be one of the rapporteurs of this thesis. I am really grateful for his helpful discussions and suggestions over the last 3 years.

In addition, I would also like to express my special gratitude to Prof. Jean-Cyrille Hierso for being another rapporteur of this thesis, Prof. Damien Prim for being the Président of the jury, Prof. Françoise Spirau and Prof. Przemyslaw Data for kindly taking part in the jury of this thesis.

I would like to extend my sincere thanks to all the members from PPSM, especially Dr. Laurent Galmiche, Dr. Clémence Allain and Dr. Stéphanne Maisonnneuve for their great help and support in the lab, Antonio Maggiore as a keen friend and co-worker in my research, Yayang Tian and Chaoqi Lin who helped me a lot in the lab as well as in my life, Andrée Husson and Christian Jean-Baptiste for administrate affairs, Jacky Fromont for IT management, and all the other current and previous members who worked with me

together in the lab or helped me in my work as well as in my life. I really appreciate the beautiful time I spent in PPSM, because of you, I feel so relaxing and grateful in the lab, I will always remember this experience with gratitude throughout my life.

Moreover, I would like to express my sincere gratitude to all the supervisors, researchers and students from EXCILIGHT project. I really learnt a lot from you after every EXCILIGHT meeting, not only about research, but also transferable skills. In particular, I'd like to thank Prof. Przemyslaw Data, Prof. Peter Skabara, Prof. Andrew Monkman, Dr. Fernando Dias, Anastasia Klimash, Oleh Vybornyi, Daniel Pereira and Piotr Pander for their hospitality during my research stay in University of Durham and University of Strathclyde. I must also thank Marharyta Vasylieva, Oleh Vybornyi, Antonio Maggiore and Piotr Pander for their great help in my research, especially Piotr Pander who taught me step by step about photophysical studies on TADF molecules when I had no experience with photophysical characterization techniques. I am also very grateful for the friendship with other ESRs Xiaofeng Tan, Ramin Pashazadeh, Amruth C, Marian Chapran, Gintautas Šimkus, Marco Colella, Pavel Chulkin and Manish Kumar.

Additionally, I am especially grateful to my wife, my daughter, my parents, and other family members for their constant supportive love and encouragement.

Finally, I would like to sincerely acknowledge the financial support from the European Union's Horizon 2020 research and innovation programme under the Marie Skłodowska-Curie grant agreement number 674990 (EXCILIGHT).

Table of Contents

Abbreviations ***1***

General introduction ***5***

Chapter 1: Introduction ***7***

1.1 Chemistry of 1,2,4,5-tetrazine 9

1.1.1 Introduction of 1,2,4,5-tetrazine 9

1.1.2 Synthesis of 1,2,4,5-tetrazines 10

1.1.2.1 Pinner synthesis and its modified versions 10

1.1.2.2 Other methods to form tetrazine ring 15

1.1.2.3 Nucleophilic aromatic substitution 17

1.1.2.4 Metal-catalyzed cross-coupling reactions 19

1.1.2.5 Other post-functionalization methods 22

1.1.3 Photophysical properties of 1,2,4,5-tetrazines 23

1.1.4 Electrochemistry of 1,2,4,5-tetrazines 24

1.1.5 Applications of 1,2,4,5-tetrazines 25

1.1.5.1 Inverse Electron Demand Diels–Alder (iEDDA) reaction 25

1.1.5.2 Functional molecules and molecular materials 31

1.2 Thermally-Activated Delayed Fluorescence (TADF) 34

1.2.1 Introduction of TADF phenomenon 34

1.2.2 TADF mechanism 35

1.2.3 Molecular designs to TADF molecules 37

1.2.4 Photophysics of TADF molecules 37

1.2.5 Application of TADF materials 40

1.3 PhD project 41

1.4 Reference 42

Chapter 2: Metal-free synthetic approach to 3-monosubstituted unsymmetrical 1,2,4,5-tetrazines ***51***

2.1 Introduction 53

2.2 Synthesis 54

2.3 Mechanism 58

2.4 Photophysical properties 60

2.5 Electrochemistry 60

2.6 Conclusion 62

2.7 Experimental details 63

2.8 Reference 70

Chapter 3: Novel donor-acceptor benzonitrile derivatives exhibiting TADF, AIE and mechanochromism ***73***

3.1 Introduction 75
3.2 Donor-acceptor benzonitriles for tetrazine synthesis 75
3.3 Molecular design of novel donor-acceptor benzonitriles 77
3.4 Novel benzonitrile compounds with mixed carbazole and phenoxazine substituents 82
3.5 Electrochemistry 88
3.6 Photophysical properties 90
3.7 Conclusion 99
3.8 Experimental details 100
3.9 Reference 117

Chapter 4: Novel donor-acceptor tetrazine derivatives prepared by Buchwald-Hartwig cross-coupling reaction 119

4.1 Introduction 121
4.2 Synthesis 122
4.3 Photophysical characterizations 126
4.4 Electrochemistry 128
4.5 Conclusion 129
4.6 Experimental details 131
4.7 Reference 136

Chapter 5: IEDDA reaction of 1,2,4,5-tetrazines: Synthesis of pyridazine derivatives 137

5.1 Introduction 139
5.2 Synthesis 139
5.3 Electrochemistry 142
5.4 Photophysical properties 143
5.5 Conclusion 153
5.6 Experimental details 154
5.7 Reference 159

Chapter 6: Modified Pinner synthesis: New convenient one-pot synthesis of thiatriazole derivatives 161

6.1 Introduction 163
6.2 Synthesis 164
6.3 Electrochemistry 168
6.4 Photophysical properties 169
6.5 Conclusion 173
6.6 Experimental details 175
6.7 Reference 182

***General conclusion and perspectives*.....185**

Abbreviations

ACQ	aggregation-caused quenching
AIE	aggregation induced emission
APPI	Atmospheric Pressure Photoionization
a.u.	arbitrary unit
CBZ	carbazole
CuAAC	copper(I)-catalyzed azide alkyne cycloaddition
CT	charge-transfer
CV	cyclic voltammetry
d	doublet (NMR)
DCM	dichloromethane
DDQ	dichlorodicyanobenzoquinone
DF	delayed fluorescence
DMAP	4-dimethylaminopyridine
DMF	dimethylformamide
DMSO	dimethyl sulfoxide
DPPF	bis(diphenylphosphino)ferrocene
D−A	donor−acceptor
EDG	electron donating group
E_g	optical gap
EL	electroluminescent
E_{ox}	oxidation potential
EQE	external quantum efficiency
equiv.	equivalents
E_{red}	reduction potential
ESIPT	excited-state intramolecular proton transfer
ESI	electrospray ionization
EWG	electron withdrawing group
Fc	ferrocene
HOMO	highest occupied molecular orbital
HPLC	high performance liquid chromatography
HRMS	high-resolution mass spectrometry
iEDDA	Inverse Electron Demand Diels–Alder
J	coupling constant (NMR)
k_r	rate constant

LHMDS	lithium bis(trimethylsilyl)amide
LUMO	lowest unoccupied molecular orbital
m	multiplet (NMR)
m/z	mass-to-charge ratio
MCH	methylcyclohexane
MW	microwave
m.p.	melting points
NAC	N-acetylcysteine
NLO	nonlinear optics
NMR	nuclear magnetic resonance spectroscopy
OFET	organic field-effect transistor
OLED	organic light-emitting diode
PF	prompt fluorescence
PFBN	2,3,4,5,6-pentafluorobenzonitrile
PL	photoluminescence
PLQY	photoluminescence quantum yield
PXZ	phenoxazine
RISC	reverse intersystem crossing
RTP	room temperature phosphorescence
s	singlet (NMR)
S_1	lowest singlet excited state
S_NAr	nucleophilic aromatic substitution
SOC	spin-orbit coupling
t	triplet (NMR)
T_1	lowest triplet excited state
TADF	thermally-activated delayed fluorescence
TBET	through-bond energy transfer
THF	tetrahydrofuran
TLC	Thin layer chromatography
TTA	triplet-triplet annihilation
UPLC	ultra performance liquid chromatography
v/v	volume/volume
w/w	weight/weight
XPhos	2-Dicyclohexylphosphino-2’,4’,6’-triisopropylbiphenyl
XRD	single crystal X-ray diffraction
δ	chemical shift (NMR)

τ_{DF}	delayed fluorescence lifetime
τ_{PF}	prompt fluorescence lifetime
λ_{Abs}	absorption wavelength
λ_{FL}	fluorescence wavelength
λ_{Phos}	phosphorescence wavelength
Φ_{PL}	photoluminescence quantum yield
ΔE_{ST}	energy difference between lowest singlet excited state and lowest triplet excited state

General introduction

This PhD thesis deals with the design, synthesis and characterization of several series of novel electron-acceptor derivatives. It is mostly focused on the study of 1,2,4,5-tetrazine derivatives, but also involves the study of benzonitrile derivatives which are the typical precursors for preparing 1,2,4,5-tetrazines, the study of pyridazine derivatives which are the products obtained from the Inverse Electron Demand Diels–Alder (iEDDA) reaction of 1,2,4,5-tetrazine molecules, and the study of 1,2,3,4-thiatriazole derivatives which are unpredicted products from the modified Pinner synthesis. The photophysical and electrochemical properties of the prepared electron-acceptor derivatives have also been studied and will be presented. Due to the charge-transfer (CT) states introduced in those donor-acceptor type molecules, they exhibit interesting electronic properties, and therefore are of particular interest in organic electronics. This thesis is conducted under the framework of European ITN project “EXCILIGHT”, therefore part of the work was carried out collaboratively in EXCILIGHT partner universities, e.g., University of Strathclyde for part of the synthetic work, and University of Durham for some photophysical characterizations.

Chapter 1: This chapter gives a brief introduction of the two main research fields involved in this thesis. It is first focused on the synthesis and application of 1,2,4,5-tetrazines. In particular, the background of the tetrazine Pinner synthesis as well as reactions involving tetrazines such as metal-catalyzed cross-coupling reactions, and inverse electron-demand Diels–Alder (iEDDA) reactions are introduced in detail. In the second part of the chapter the Thermally Activated Delayed Fluorescence (TADF) phenomenon is presented in terms of molecular design, characterization and applications because it is the major application aimed for the molecules in this work.

In **chapter 2** we demonstrate the design of a facile and efficient synthetic approach to 3-monosubstituted unsymmetrical 1,2,4,5-tetrazines. Dichloromethane (DCM) is for the first time recognized as a novel reactant in the chemistry of tetrazine synthesis. This synthetic approach offers an improved access to both 3-aryl and 3-alkyl unsymmetrical 1,2,4,5-tetrazines, which are expected to be widely utilized in various applications, particularly in tetrazine click chemistry.

In **chapter 3** we are firstly interested in the synthesis of donor-acceptor benzonitrile derivatives, and their subsequent reactions to prepare novel symmetrical and unsymmetrical 1,2,4,5-tetrazine derivatives, using both the classical Pinner synthesis and our novel approach described in chapter 2. More importantly, a stepwise and controlled synthetic approach is developed afterwards to prepare novel donor-acceptor benzonitrile

derivatives. Several series of these derivatives were conveniently prepared using a versatile starting material 2,3,4,5,6-pentafluorobenzonitrile (PFBN). These novel benzonitrile derivatives were found to exhibit interesting photophysical properties, such as thermally activated delayed fluorescence (TADF), aggregation induced emission (AIE) and mechanochromism.

Chapter 4 present the application of an important synthetic tool: Buchwald-Hartwig cross-coupling reaction, which was optimized for the functionalization of tetrazine compounds. Several factors influencing the Buchwald-Hartwig cross-coupling reaction on tetrazine are discussed, which are crucial when performing this reaction. A series of novel donor-acceptor 1,2,4,5-tetrazine molecules have been successfully prepared in high yields. This synthetic methodology is expected to facilitate future applications of 1,2,4,5-tetrazines as electron-deficient components in organic electronics and as valuable intermediates for the synthesis of natural products.

We firstly demonstrate in **Chapter 5** the successful use of our previously prepared donor-acceptor tetrazine derivatives in the inverse electron-demand Diels–Alder (iEDDA) reaction. The donor-acceptor tetrazine derivatives turned out to be fluorescence turn-on probes upon conversion into pyridazines. Then the electrochemical and photophysical properties of the novel donor-acceptor pyridazine derivatves prepared by the iEDDA reaction will be presented in details.

Finally, in **Chapter 6**, the important role of the solvent in the Pinner synthesis is studied and allowed us to uncover a novel convenient one-pot synthesis of 1,2,3,4-thiatriazoles in high yields, directly from commercially available aromatic nitrile compounds. The access to the 1,2,3,4-thiatriazole derivatives is significantly improved because the synthetic procedure is very easy and there is a large number of commercially available nitrile. Using this new synthetic route a novel donor-acceptor thiatriazole derivative has been prepared with a high yield. This molecule exhibits prominent TADF characteristics in both solution and film. This work provides an efficient and practical synthetic approach to functionalized 1,2,3,4-thiatriazole derivatives, and is expected to facilitate the application of 1,2,3,4-thiatriazole as an electron acceptor in organic electronics.

Chapter 1

Introduction

1.1 Chemistry of 1,2,4,5-tetrazine

1.1.1 Introduction of 1,2,4,5-tetrazine

Tetrazine is a six-membered aromatic ring which contains four nitrogen atoms with the chemical formula $C_2H_2N_4$. Three types of tetrazine isomers have been reported to date: 1,2,3,4-tetrazine, 1,2,3,5-tetrazine and 1,2,4,5-tetrazine. While 1,2,3,4-tetrazine and 1,2,3,5-tetrazine are relatively less explored, 1,2,4,5-tetrazine (also known as *s*-tetrazine) has attracted intensive interests from researchers worldwide for many decades.[1–4]

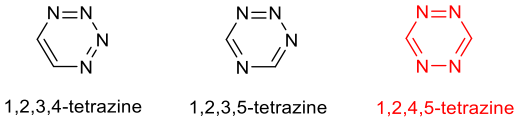

Figure 1: Three types of tetrazine isomers.

The first synthesis of 1,2,4,5-tetrazine can be traced back to the end of 19th century. In 1893, Adolf Pinner reacted imidoesters with excess hydrazine to form dihydrotetrazines, and after easy oxidation isolated 1,2,4,5-tetrazines as a beautiful red solid.[5] However, no further investigations on the properties of these tetrazines were performed during that period.

In 1959, Carboni and Lindsey demonstrated the ability of 1,2,4,5-tetrazine to react with unsaturated compounds (also known as Inverse Electron Demand Diels–Alder (iEDDA) reaction).[6] This reaction was found to boost the development of application of 1,2,4,5-tetrazine in many fields, such as total synthesis of natural products,[7,8] preparation of new tailored pyridazine molecules,[9–13] and more importantly, the recently developed tetrazine bioorthogonal click chemistry.[2,14–16]

In the 1970s, the photophysical properties of some 1,2,4,5-tetrazines have been reported, although in rather specific conditions, such as gas-phase spectroscopy, crystals, and spectrophysics (hole burning) of highly diluted compounds.[17–22] However, the interest for this field decreased in the early 1980s, due to the difficulties in the synthesis of new tetrazine derivatives, which also blocked the development of 1,2,4,5-tetrazine as functional materials.

In the 1990s, Hiskey and co-workers introduced the synthesis of bis(dimethylpyrazolyl)-1,2,4,5-tetrazine, and subsequently an easy synthesis of dichloro-1,2,4,5-tetrazine,[23–25] which paved the way to prepare various functional 1,2,4,5-tetrazine derivatives by nucleophilic aromatic substitution (S_NAr) leading to their application as molecular materials.[1]

The first metal-catalyzed cross-coupling reactions were discovered not until 2003 by Novák and Kotschy.[26] This allowed to prepare tetrazine derivatives by C–C bond formation directly onto the tetrazine core or onto the substituents attached to it (e.g. phenyl group), which proved to be particularly useful for the preparation of π-conjugated 1,2,4,5-tetrazines for bioorthogonal and materials chemistry.

As a strong electron-deficient aromatic system, 1,2,4,5-tetrazine possesses interesting optical and electrochemical properties, which have displayed significant application potentials in organic electronics (e.g., electrofluorochromism,[27–30] nonlinear optics,[31] photovoltaic devices,[32,33] etc.). Over the last two decades, our group and others have been involved in many developments of this exciting research field.

1.1.2 Synthesis of 1,2,4,5-tetrazines

The classical tetrazine synthetic methodology, also known as Pinner synthesis, is a two-step procedure starting from the addition of hydrazine to nitrile precursors, followed by oxidation of the resulting dihydrotetrazine.[1,34] Several modifications on the reaction conditions (vide infra) have significantly improved the applicability of this synthetic methodology.[35,36] Several other synthetic approaches to form the tetrazine ring have also been reported, although less popular.[37–39]

Apart from using Pinner synthesis to form the tetrazine ring, post-modification on a simple tetrazine building block is widely used to prepare tetrazines with reactive or complex functional groups. Among which, nucleophilic aromatic substitution (S_NAr) of a conventional 1,2,4,5-tetrazine precursor, commonly dichlorotetrazine, dipyrazolyltetrazine or dithiomethyltetrazine, has long been regarded as one of the most powerful methods to prepare functionalized 1,2,4,5-tetrazines for various applications.[1] More recently, new methodologies based on metal-catalyzed cross coupling reactions have started to attract researchers' interests for the preparation of various 1,2,4,5-tetrazines, especially those functionalized with fluorescent dyes.

In the following sections, these synthetic approaches will be reviewed in detail.

1.1.2.1 Pinner synthesis and its modified versions

In 1893, Adolf Pinner became the first person to isolate and identify 1,2,4,5-tetrazine. He reacted imidoester with hydrazine to form dihydrotetrazine, which was then easily oxidized to give 1,2,4,5-tetrazine (**Scheme 1a**).[5,40] The method was improved later by using nitrile as a precursor instead of imidoester to prepare dihydrotetrazine. This approach is now

commonly known as the tetrazine Pinner synthesis and became the most popular method for preparing 1,2,4,5-tetrazines until nowadays (**Scheme 1b**).[34]

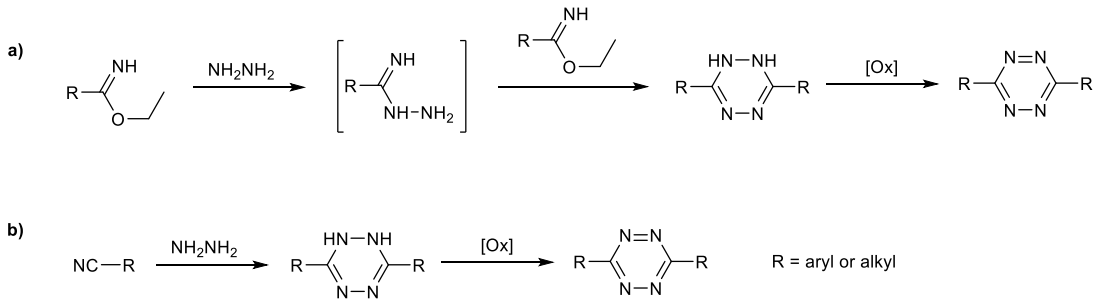

Scheme 1: Synthetic approach for 1,2,4,5-tetrazines using **a)** imidoester, **b)** nitrile as the precursor.

In the Pinner synthesis, the formation of dihydrotetrazine prior to oxidation is the crucial step to the final reaction yield, where the important factors include subtle energy factors, solubility variables and steric effects.[1,2,14] Depending on the reactivity of the starting nitrile precursors, hydrazine hydrate or anhydrous hydrazine is applied in the reaction. The common solvent is ethanol, while DMF may be used as co-solvent depending on the solubility of the nitriles.

In the oxidation step, nitrous gas (HNO_2), which can be easily produced from sodium nitrite ($NaNO_2$) in the presence of an acid, such as acetic acid or hydrochloric acid solution, is the most widely used oxidant for converting dihydrotetrazines to tetrazines.[1,2] However, this oxidant is not compatible with some widely used functional groups such as amines. DDQ (dichlorodicyanobenzoquinone) was reported to oxidize dihydrotetrazine with amino group successfully in good yield (81%), although it was difficult to separate the product from the hydroquinone byproducts.[41] Recently, $PhI(OAc)_2$ was reported as a mild and effective oxidant for the oxidation of dihydrotetrazine bearing amino group with high yield (86%).[42] And the byproduct iodobenzene could be easily removed. In this report, *m*-CPBA, benzoyl peroxide and benzoquinone were also shown to oxidize dihydrotetrazines to tetrazines successfully, however with poorer yields.[42] It was also found that metal oxides (e.g., MnO_2 and CrO_3) could be used for oxidation of dihydrotetrazines, however the moderate yields and toxic chromium waste limited their applications.[43,44] Moreover, $FeCl_3$ was also reported to oxidize dihydrotetrazine.[45] Interestingly, one recent report showed that both photocatalyst (methylene blue) and horseradish peroxidase could oxidize dihydrotetrazines with fast reaction rates.[46] In addition, it is also possible to slowly oxidize dihydrotetrazine by the oxygen from air.[39,47]

One of the most important modification of Pinner synthesis is the discovery that the addition of sulfur serves as an inducer in the reaction and largely improves the product yields.[35] It was found that the presence of sulfur in the reaction could promote the formation of

dihydrotetrazines, which is the determining step for the final product yields. Our group has proposed a reasonable mechanism for this improved synthesis (**Scheme 2**).[48] Based on the facts that the color of the solution changed from colorless to light orange, and the generation of H_2S was detected during the reaction. It is suggested that sulfur should react first with hydrazine to give the active nucleophile NH_2NHSH, which could then react with the nitrile, producing a reactive intermediate that eliminates H_2S, and finally form the dihydrotetrazine.

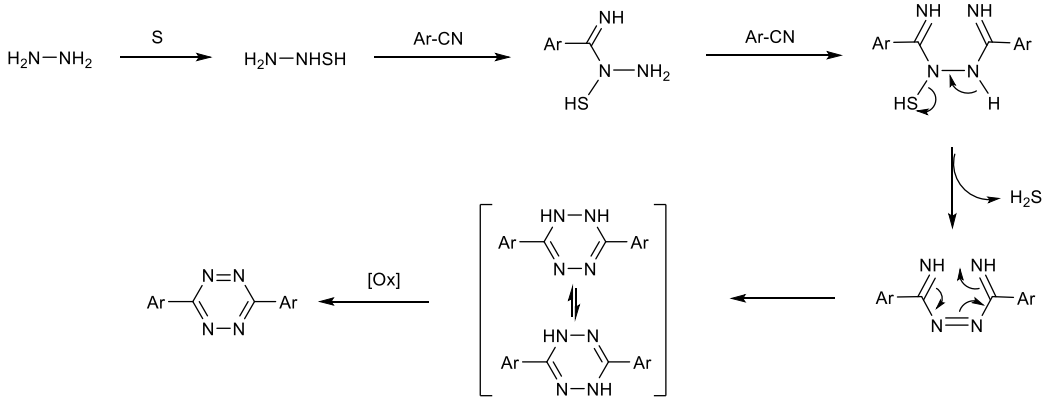

Scheme 2: Proposed mechanism for the sulfur-induced Pinner synthesis.

Recently, there has been a significant demand for the preparation of new unsymmetrical 1,2,4,5-tetrazines since the recent development of their application in bioorthogonal chemistry. However, they are tricky to prepare using the Pinner synthesis because a statistical mixture of products is obtained when an equimolar quantity of two different nitrile precursors is used resulting in poor yields.[2][38] It is usually suggested to use a large excess of one of the nitrile precursor (usually the more reactive one) when preparing unsymmetrical tetrazines to increase the yields (**Scheme 3a**).

It is important to note that when one of the nitrile precursor is replaced by formamidine salts, monosubstituted 1,2,4,5-tetrazines could be prepared, albeit in poor yields, typically between 10% to 20% (**Scheme 3b**).[49,50]

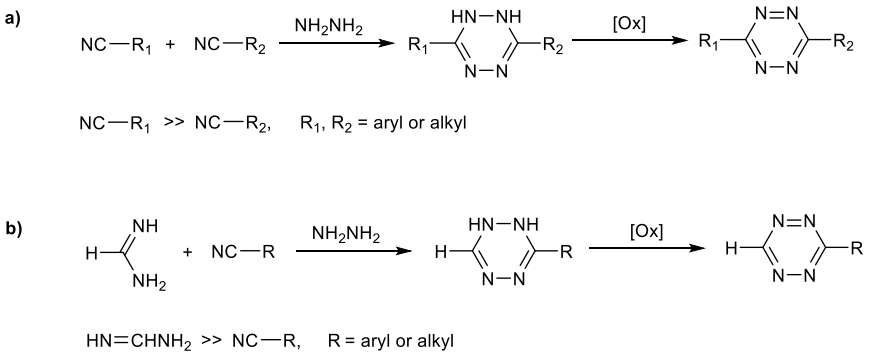

Scheme 3: Synthetic approach for **a)** unsymmetrical, and **b)** monosubstituted 1,2,4,5-tetrazines.

It is also important to mention that although the above-described conditions have been successfully used to convert aromatic nitriles to the corresponding tetrazines, they are not effective for aliphatic ones. This is probably due to the isomeric 4-amino-1,2,4-triazole intermediates formed during the first step.[51–53]

This frustrating situation has only been changed in 2012. Devaraj and co-workers reported a metal-catalyzed one-pot tetrazine synthesis based on the Pinner synthesis, directly from aliphatic nitriles and hydrazine, using nickel triflate ($Ni(OTf)_2$) or zinc triflate ($Zn(OTf)_2$).[36] The access to alkyl tetrazines significantly improved due to this promising modification. It was shown that this synthetic approach allowed to prepare both symmetrical and unsymmetrical dialkyl tetrazines in good to excellent yields (**Table 1**).

Table 1: Synthesis of symmetrical and unsymmetrical dialkyl tetrazines by metal-catalyzed one-pot tetrazine synthesis(a).

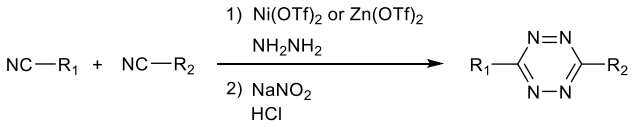

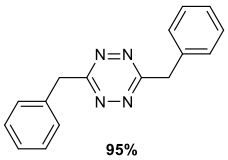 95%	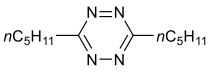 59%	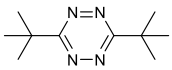 24%	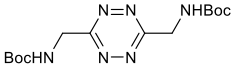 32%
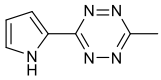 58%(b)	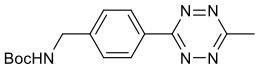 68%	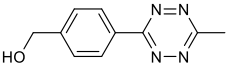 66%	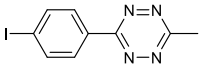 41%
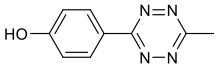 43%	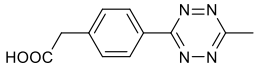 70%	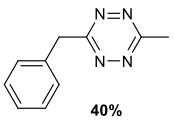 40%	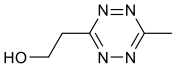 36%
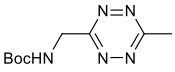 36%	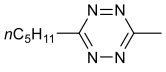 59%	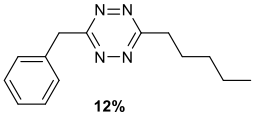 12%	

(a) Yields reported after isolation by silica flash chromatography. (b) The protective group (Boc) on the pyrrole nitrogen was lost during oxidative workup.

More importantly, it is also possible to prepare 3-monosubstitued 1,2,4,5-tetrazines using this metal-catalyzed one-pot synthesis (**Table 2**). Although these tetrazines have been previously prepared from aromatic nitriles and excess formamidine salts without catalysts,

poor yields were typically observed (10%-20%).[49] The yield of the reaction significantly increased to 64%-74% when employing $Ni(OTf)_2$ or $Zn(OTf)_2$ as a catalyst. These derivatives proved to be extremely useful to researchers interested in rapid bioorthogonal coupling applications.

Table 2: Synthesis of 3-monosubstitued 1,2,4,5-tetrazines by metal-catalyzed one-pot tetrazine synthesis(a).

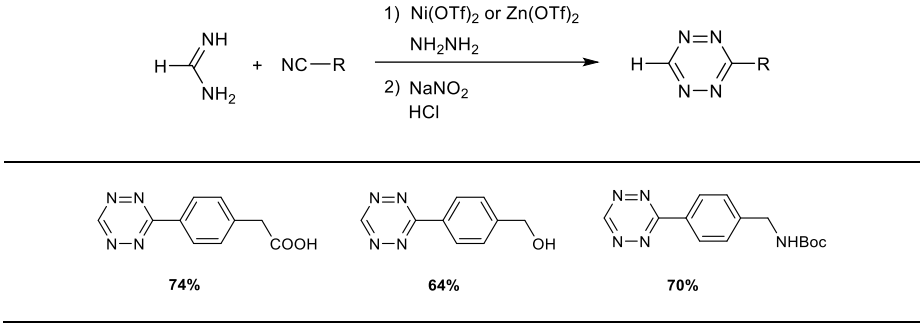

(a) Yields reported after isolation by silica flash chromatography.

It was shown in another report that this metal-catalyzed tetrazine synthesis could be used to prepare a similar 3-monosubstituted tetrazine in high yield (75%) on a gram-scale, while the sulfur-assisted reaction only gave a 14% yield.[54]

It was proposed by the authors that the metal acts as a Lewis acid and coordinates to the nitrile promoting the nucleophilic addition by hydrazine. It was also suggested that the metal binds both the nitrile and hydrazine, promoting synthesis of the amidrazone intermediate (**Scheme 4**).[36]

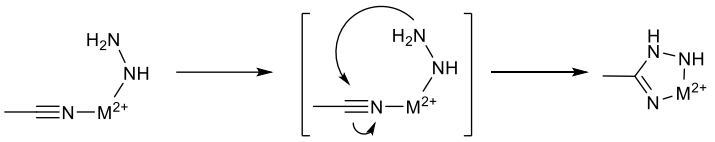

Scheme 4: Proposed role of the metal catalyst during synthesis process.

However, there are also limitations to this metal-catalyzed one-pot synthetic approach. The use of excess anhydrous hydrazine (usually 50 equivalents to the nitrile precursors) is indeed unfavorable. The harsh conditions are not compatible with several functional groups such as carbonyls and alkyl halides, which are susceptible to give either nucleophilic addition or reduction.[55] Moreover, the reaction requires use of large amounts of metal catalyst to proceed which is a major drawback with products containing good transition-

metal binding moieties such as the morpholinyl groups because intensive purification is then necessary to remove metal traces.[47]

Interestingly, Bianchi, Melguizo and co-workers recently demonstrated a non-metal-catalyzed Pinner synthesis of dialkyl tetrazine derivatives using hydrazine hydrate.[47] In their approach, N-acetylcysteine (NAC) was employed as the catalyst instead of $Ni(OTf)_2$ or $Zn(OTf)_2$. Dialkyl tetrazines were successfully prepared in moderate yields (35%-40%), although on a limited number of examples. It was suggested that NAC could act as a catalyst assisting the formation of an amidrazone intermediate from the nitrile precursor and hydrazine, which after dimerization leads to the isolable dihydrotetrazine.

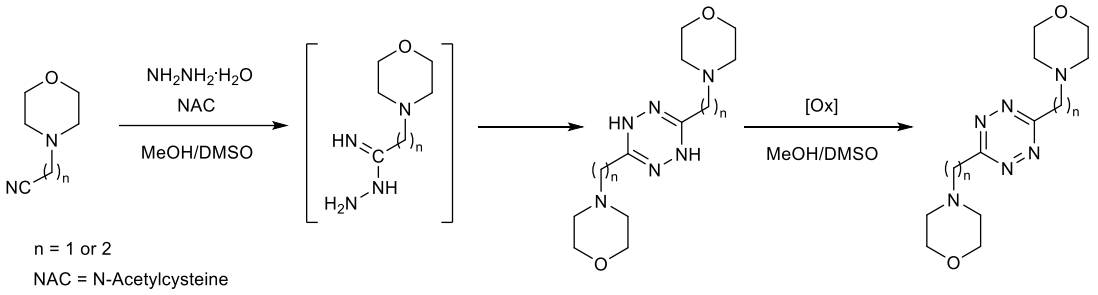

Scheme 5: Synthesis of dialkyl tetrazines using N-acetylcysteine (NAC) as the catalyst.

The different variants of the Pinner synthesis and their improvements are useful to prepare 1,2,4,5-tetrazines for various applications, although limitations still exist. We recently contributed to this area by introducing a novel metal-free synthetic approach to 3-monosubstitued 1,2,4,5-tetrazines (see **Chapter 2**).

1.1.2.2 Other methods to form tetrazine ring

There are also some other methods reported to prepare 1,2,4,5-tetrazines, which are usually difficult to obtain using the Pinner synthesis (e.g., alkyl tetrazines). One method is a stepwise procedure via a 1,2-dichloromethylene hydrazine intermediate, which was first reported by Stolle and co-workers in 1906.[37] This involves the synthesis of acylhydrazides, and subsequent treatment with PCl_5 to give 1,2-dichloromethylene hydrazines, then condensation with hydrazine to afford dihydrotetrazines which are finally oxidize to tetrazines (**Scheme 6**). With this stepwise method, both symmetrical and unsymmetrical alkyl tetrazines, and tetrazines with strong electron withdrawing groups (EWGs) could be synthesized in moderate yields.[38,56]

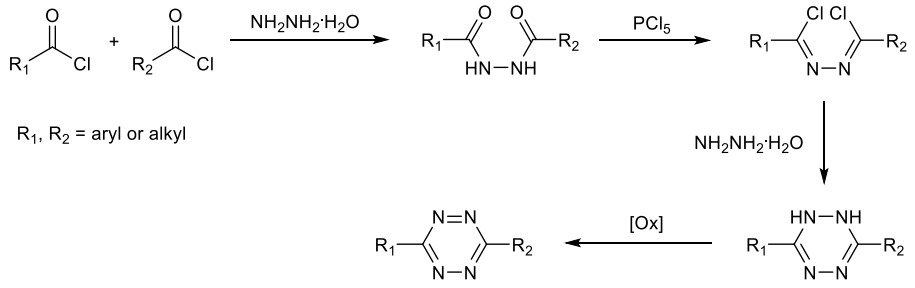

Scheme 6: Synthesis of 1,2,4,5-tetrazine via a stepwise method.

A further optimization of the reaction conditions showed that microwave irradiation could successfully reduce the reaction time and increase the yield of the condensation step between dichloromethylene hydrazine and hydrazine when compared to traditional refluxing conditions.[57]

Another interesting method to prepare 1,2,4,5-tetrazines is using *gem*-difluoroalkenes as the starting material (**Scheme 7**). This method was first reported by by Carboni and Linsey in 1958, but with low yields and limited substrate scope.[58] One recent report extended the scope of this synthetic approach and largely improved the product yields.[39] Both symmetrical and unsymmetrical dialkyl tetrazines could be prepared in high yields (61%-91%).

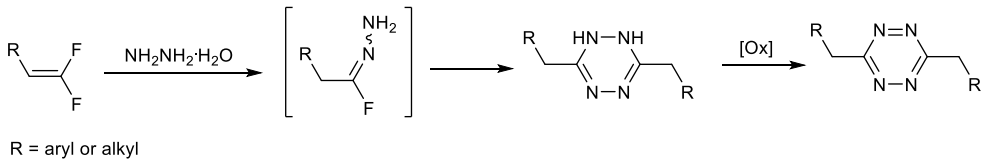

Scheme 7: Synthesis of 1,2,4,5-tetrazine from *gem*-difluoroalkenes.

Another alternative method was reported via a dialkyl-hexahydro-tetrazine intermediate, which can be prepared from the reaction of alkyl aldehydes with hydrazine. Then the dialkyl-hexahydro-tetrazines could be oxidized stepwise to give the dialkyl tetrazines (**Scheme 8**).[59,60]

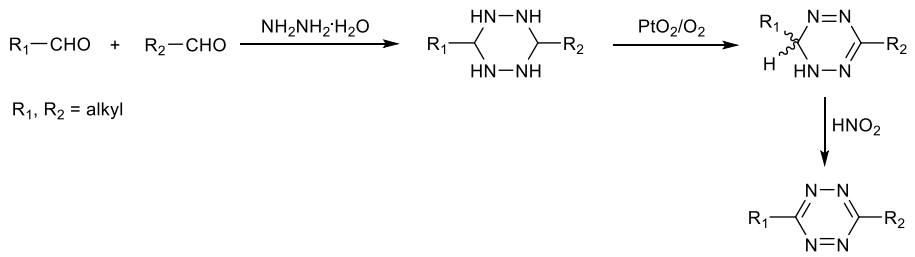

Scheme 8: Synthesis of 1,2,4,5-tetrazines via a dialkyl-hexahydro-tetrazine intermediate.

1.1.2.3 Nucleophilic aromatic substitution

In addition to the synthetic methods that directly give the tetrazine ring, post-modification on a simple tetrazine building block is widely used to prepare tetrazines with reactive or complex functional groups. Nucleophilic aromatic substitution (S_NAr) of a conventional 1,2,4,5-tetrazine precursor has long been regarded as one of the most powerful methods to prepare functionalized 1,2,4,5-tetrazines for various applications.[1]

For this purpose, bis(thiomethyl)-1,2,4,5-tetrazine was initially used as the starting precursor because of its relatively easy synthesis.[61] In the 1990s, Hiskey and and co-workers introduced an easy and quasi-quantitative synthetic procedure for bis(dimethylpyrazolyl)-1,2,4,5-tetrazine, and subsquently the easy synthesis of dichloro-1,2,4,5-tetrazine with an overall yield of ca. 80% (**Scheme 9**),[23–25] which paved the way to prepare various functional 1,2,4,5-tetrazine derivatives by nucleophilic aromatic substitution (S_NAr). An important modification to mention in this synthetic procedure is the replacement of the dangerous chlorine gas by trichloroisocyanuric acid introduced by Harrity and co-workers.[62]

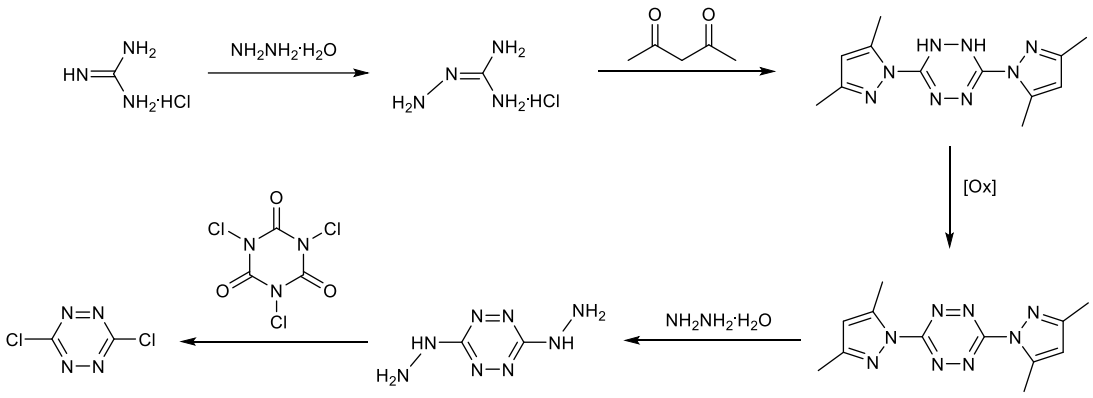

Scheme 9: Synthesis of bis(dimethylpyrazolyl)-1,2,4,5-tetrazine and subsquent synthesis of dichloro-1,2,4,5-tetrazine.

Dichlorotetrazine and dipyrazolyltetrazine are versatile starting synthons for the preparation of a number of functionalized 1,2,4,5-tetrazine derivatives using nucleophilic substitution reaction (**Scheme 10**). Various nucleophiles have been successfully employed, including alcohols, thiols, and amines, which highly improved the structural diversity of the target tetrazines. Monosubstitution usually occurs readily at room temperature, while disubstitution normally requires more forcing conditions (except for thiols), such as the use of ionic nucleophiles.[63] The use of 2,4,6-collidine or 2,6-lutidine allows to improve the efficiency of the substitution reaction to quite high yields.[64] Recently, it was shown that using 4-dimethylaminopyridine (DMAP) allows effecting the disubstitution of dichlorotetrazine with alcohols in good yields at room temperature.[65]

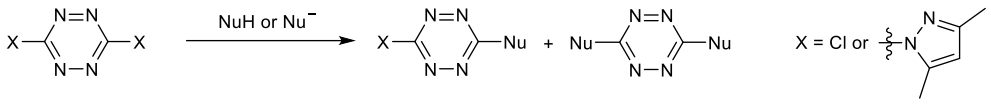

Scheme 10: Synthesis of 1,2,4,5-tetrazines by nucleophilic aromatic substitution (S_NAr).

Through this approach, numerous differently functionalized tetrazines have been prepared in our group and others, which find applications in various areas.[65] Some examples are shown below in **Table 3**.

Table 3: 1,2,4,5-tetrazine derivatives prepared by nucleophilic aromatic substitution (S_NAr).

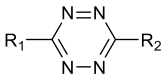

Entry	R1	R2
1	Cl	$O(CH_2)_4OH$
2	Cl	OMe
3	Cl	naphthalen-1-yloxy
4	Cl	pyrrolidin-1-yl
5	Cl	2,3-diphenylaziridin-1-yl
6	Cl	borneol
7	Cl	9*H*-fluoren-9-ylmethoxy
8	Cl	paracyclophan-4-ylmethoxy
9	Cl	adamantan-2-yloxy
10	Cl	adamantan-1-ylmethoxy
11	Cl	pentachlorophenoxy
12	Cl	*N*-phtalimidyl
13	OMe	OMe
14	OMe	$O(CH_2)_4OH$
15	$O(CH_2)_4OH$	$O(CH_2)_4OH$
16	adamantan-1-ylmethoxy	adamantan-1-ylmethoxy
17	OMe	SMe
18	SMe	SMe
19	S-*n*-butyl	S-*n*-butyl

20	pyrrolidin-1-yl	pyrrolidin-1-yl
21	3,5-dimethyl-1*H*-pyrazol-1-yl	OMe
22	3,5-dimethyl-1*H*-pyrazol-1-yl	pyrrol-1-yl
23	pyrrol-1-yl	pyrrol-1-yl

Although most heteroatomic nucleophiles have been successfully used in nucleophilic aromatic substitution (S_NAr), most carbanions (alkyl, aryl) are usually not suitable for nucleophilic substitution. Azaphilic addition on the tetrazine precursors to afford 1,4-dihydro-tetrazine is usually observed when the reaction is conducted at low temperature (-78 °C) (**Scheme 11**).[66] However, it was recently found in our group that when butyl lithium is reacted with chlorotetrazines at 0 °C, the products resulting from nucleophilic substitution are isolated (**Scheme 12**).[67]

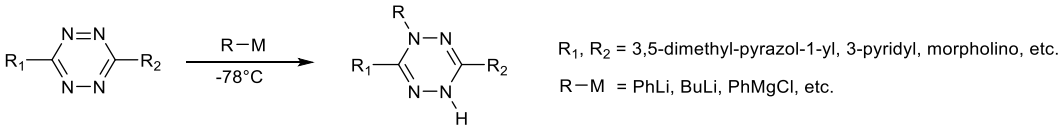

Scheme 11: Azaphilic addition on 1,2,4,5-tetrazine.

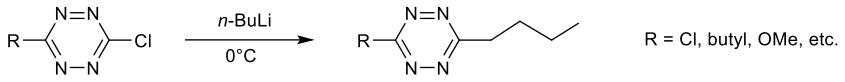

Scheme 12: Nucleophilic aromatic substitution of 1,2,4,5-tetrazines with *n*-BuLi.

1.1.2.4 Metal-catalyzed cross-coupling reactions

Metal-catalyzed cross coupling reaction is another useful method for preparing new functionalized 1,2,4,5-tetrazines by post-modification of a simple tetrazine precursor. This allows to prepare tetrazines by C–C bond formation directly onto the tetrazine core or onto the substituents attached to tetrazines (e.g. phenyl group). This is particularly useful to prepare π-conjugated 1,2,4,5-tetrazines, which are desirable for bioorthogonal chemistry and material chemistry.

In 2003, Novák and Kotschy reported the first cross-coupling reactions (Sonogashira and Negishi) on 1,2,4,5-tetrazines (**Scheme 13**).[26] It was demonstrated that the tetrazine core should be substituted with one donating group to allow the cross-coupling reactions to take place. Tetrazine precursors with electron-deficient substituents tended to decompose. The coupling reactions gave the respective products in low to good yields (23%-65%).

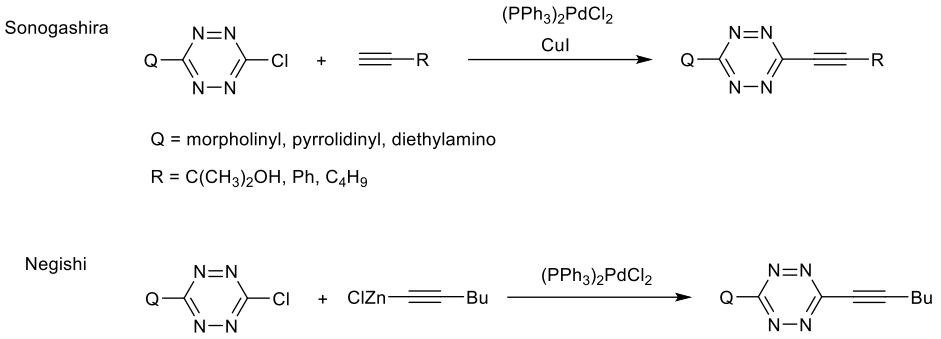

Scheme 13: Sonogashira and Negishi cross-coupling reactions on 1,2,4,5-tetrazines.

Later in 2007, Leconte and co-workers discovered that 3-methylthio-6-(morpholin-4-yl)-1,2,4,5-tetrazine could readily react with boronic acids and organostannane precursors, to undergo Suzuki and Stille couplings respectively with displacement of a methylthio group (**Scheme 14**).[68] The coupling reactions afforded products in moderate to good yields (30%-70%) under microwave conditions. Recently, Lindsley and co-workers expanded the scope of the Suzuki cross-coupling reaction with diverse unsymmetrical 1,2,4,5-tetrazines, and successfully obtained a tetrazine-containing biologically active molecules with improved drug metabolism and pharmacokinetic (DMPK) properties.[69]

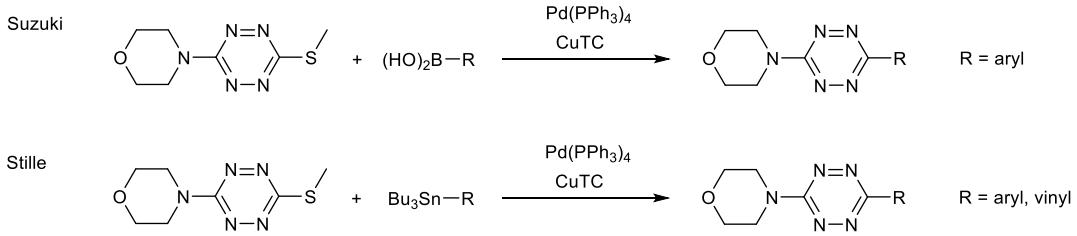

Scheme 14: Suzuki and Stille cross-coupling reactions on 1,2,4,5-tetrazines.

It is interesting to mention that using Stille coupling reaction, Wombacher and co-workers have recently successfully synthesized several fluorogenic tetrazine probes by coupling 3-bromo-6-methyl-1,2,4,5-tetrazine with protected fluorophore-organotin derivatives, although low yields (ca. 20%) were reported.[70] The synthesis of a tetrazine-fluorescein example is shown below in **Scheme 15**.

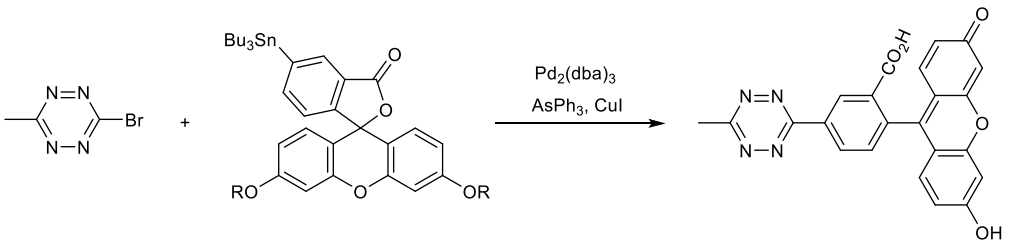

Scheme 15: Synthesis of a tetrazine-fluorescein derivative by Stille cross-coupling reaction.

The abovementioned examples refer to cross-coupling reactions that form a C–C bond directly onto the tetrazine core. Recently, with the increasing need for the preparation of π-conjugated tetrazine materials, various cross-coupling reactions have also been applied for the bond formation onto the substituents attached to tetrazines.

In 2014, Devaraj and co-workers developed a new cross-coupling reaction (Heck reaction) on tetrazine.[55] This in situ elimination–Heck cascade reaction allows to prepare (*E*)-3-substituted 6-alkenyl-1,2,4,5-tetrazine derivatives in good to high yields (47%-99%) (**Scheme 16**). A series of π-conjugated alkenyl tetrazine derivatives were also synthetized which can be used as fluorogenic probes for live-cell imaging (**Figure 2**). This method was later employed by Kele and co-workers to prepare new red-emitting tetrazine-phenoxazine fluorogenic labels with reasonable yields.[71]

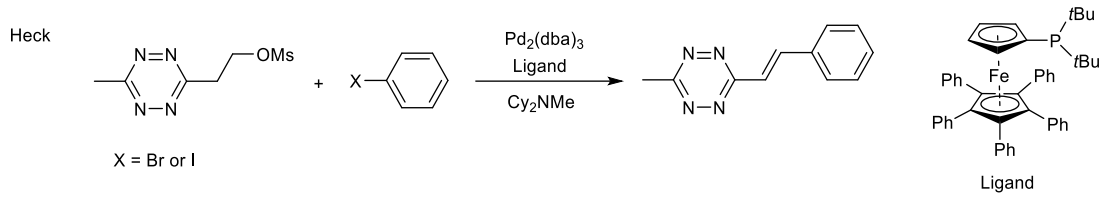

Scheme 16: In situ elimination–Heck cascade reaction to prepare 1,2,4,5-tetrazines.

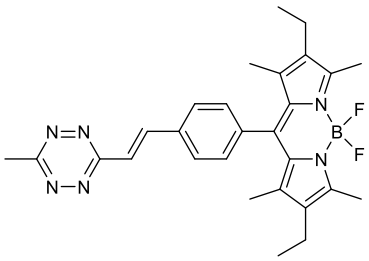

Figure 2: An example of alkenyl tetrazine-BODYPY fluorogenic probe.

In addition, Sonogashira,[72] Suzuki,[71] and Stille[72] cross-coupling reactions have also been used to successfully prepare π-conjugated tetrazine fluorogenic probes in recent years.

Other than preparing 1,2,4,5-tetrazines for bioorthogonal click chemistry, several reports also demonstrated the preparation of π-conjugated tetrazine derivatives by metal-catalyzed cross-coupling reactions, for applications in organic electronics.

In 2010, Ding and co-workers developed a tetrazine-based low-bandgap semiconducting polymer for efficient solar cells.[32] The copolymer was prepared by Stille coupling reaction with a good yield (36%), and was used to prepare simple polymer solar cells with a calibrated power conversion efficiency of 5.4% (**Scheme 17**). More recently, conjugated

donor-acceptor molecular systems based on triphenylamine and tetrazine have been developed in our group, by using Stille and Suzuki cross-coupling reactions, for application in organic solar cells.[73]

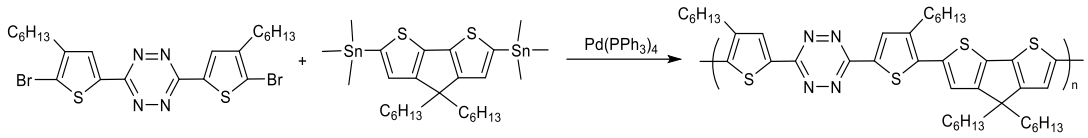

Scheme 17: Synthesis of a tetrazine-based copolymer by Stille coupling reaction.

In 2012, Kippelen and co-workers designed and synthesized a solution-processable small molecule containing electron-poor naphthalene diimide and tetrazine moieties by Stille coupling reactions (**Scheme 18**).[74] OFETs were fabricated using this molecule by spin-coating and inkjet-printing and exhibited good electron mobility performances.

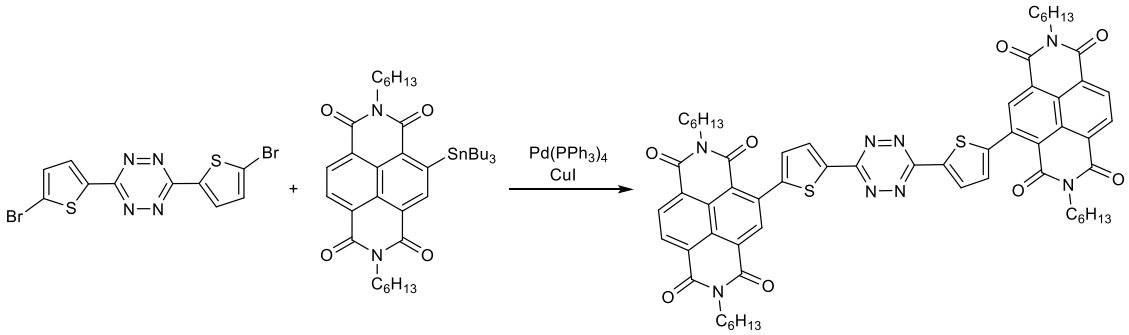

Scheme 18: Synthesis of a tetrazine-naphthalene diimide molecule by Stille coupling reaction.

1.1.2.5 Other post-functionalization methods

Recently, Hierso and co-workers demonstrated a direct palladium-catalyzed C−H functionalization of 1,2,4,5-tetrazines.[75] It was reported that the *ortho*-C-H activation of aryl tetrazines could be performed under mild reaction conditions, and allow the introduction of various functional groups (e.g., F, Br, Cl, I and OAc) (**Scheme 19**). Efficient electrophilic mono- and poly-*ortho*-fluorination of aryl tetrazines were demonstrated with good selectivity. This synthetic methodology provides an easy way to prepare *ortho*-functionalized aryl tetrazines, which were previously difficult to obtain.

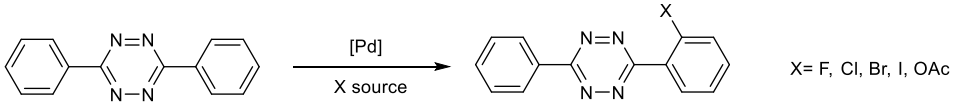

Scheme 19: C-H monofunctionalization of 3,6-diphenyl-1,2,4,5-tetrazine.

Another recently published report showed Friedel–Crafts alkylation could be employed for the preparation of red tetrazine-rhodamine and tetrazine-Si-rhodamine fluorophores, using aldehydes and diarylether or diarylsilane compounds (**Scheme 20**), which were not accessible by metal-catalyzed cross coupling reactions.[70]

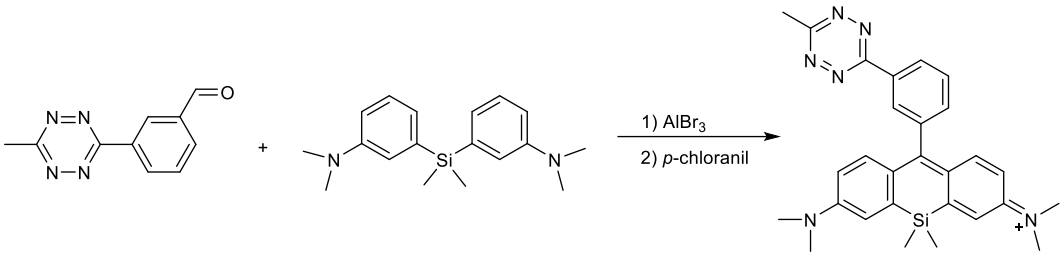

Scheme 20: Synthesis of a tetrazine-Si-rhodamine derivative by Friedel–Crafts alkylation.

1.1.3 Photophysical properties of 1,2,4,5-tetrazines

1,2,4,5-Tetrazines possess beautiful colors ranging from purple to orange to red due to the weak n-π* transition located in the visible. The absorption maxima for 1,2,4,5-tetrazine derivatives are usually observed between 510 and 530 nm with a low molar extinction coefficient around 1000 $L \cdot mol^{-1} \cdot cm^{-1}$. It was reported that the position of the absorption band corresponding to the n-π* transition is almost not affected by the nature of the substituents attached to the tetrazine core and was shown not to be solvatochromic.[76] On the contrary, the absorption band corresponding to the π-π* transition which appears in the UV region is quite intense, and its position strongly depends on the substituents nature. It correlates linearly with the electron donating or withdrawing ability of the substituents.[1,77]

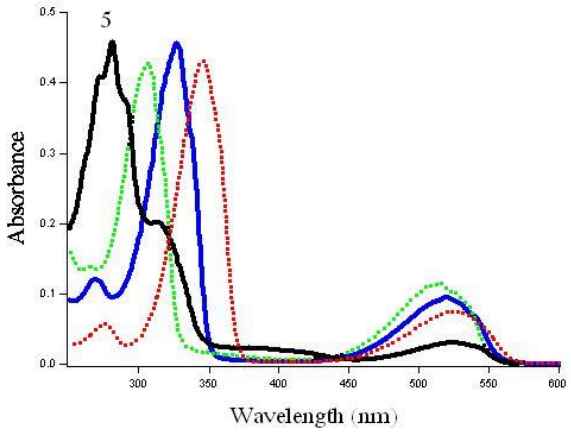

Figure 3: Absorption spectra of dichloro-tetrazine (green), chloro-methoxy-tetrazine (blue), dimethoxy-tetrazine (red), and 1,4-bis(chloro-tetrazinyloxo)butane (black) in dichloromethane.[77]

Our group has demonstrated that some tetrazines substituted by heteroatoms were highly fluorescent, while others were weakly or non-emissive (e.g., those directly linked to aromatics).[1] It was reported that the fluorescence spectra of tetrazines are usually broad in solution, with the emission maxima ranging from 550 to 590 nm (**Figure 4**). The photoluminescence quantum yields (PLQYs) are highly dependent on the nature of the substituents. In addition, the lifetime of the fluorescence for tetrazine molecules typically range from 10 to 160 ns, which is also highly dependent on the nature of the substituents.[1,64,77]

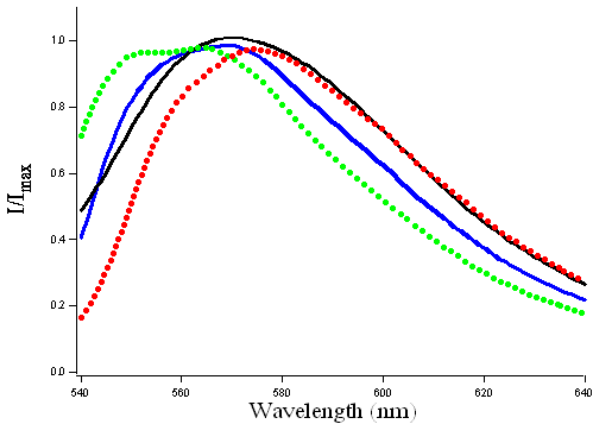

Figure 4: Fluorescence spectra of dichloro-tetrazine (green), chloro-methoxy-tetrazine (blue), dimethoxy-tetrazine (red), and 1,4-bis(chloro-tetrazinyloxo)butane (black) in dichloromethane.[77]

1.1.4 Electrochemistry of 1,2,4,5-tetrazines

Generally, 1,2,4,5-Tetrazines can be reversibly reduced in aprotic organic solvents. Due to the electron-deficient character of tetrazine molecules, they can accept one electron to give an anion radical, which is stable in the absence of acids (**Figure 5**).[1,77] The differences in $E_{1/2}$ values for the reversible reduction to the corresponding anion radicals reflect the electronic influence of the substituents. However, in the presence of a proton donor, the anion radical can be protonated and destroy the electrochemical reversibility. The loss of reversibility depends on the acidity of the proton donor and its amount.

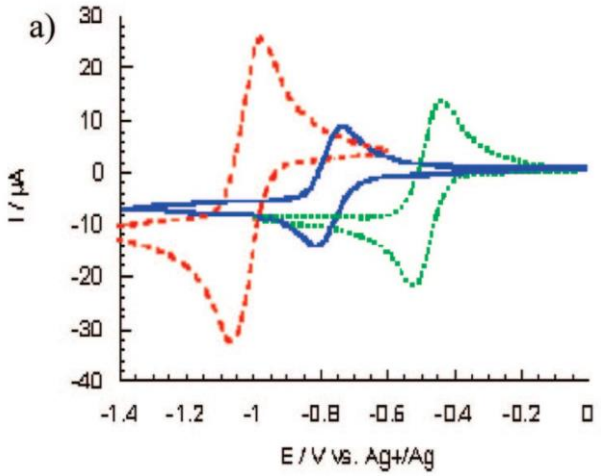

Figure 5: Cyclic voltammograms of dichloro-tetrazine (green), chloro-methoxy-tetrazine (blue), and dimethoxy-tetrazine (red) in dichloromethane.[77]

Most of the tetrazine derivatives are able to accept a second electron, although this process is not electrochemically reversible (**Figure 6**).[1,48] However, it is interesting to mention that this latter process is chemically reversible (except for dichlorotetrazine). The second electron transfer does not give a stable dianion, which is probably because it is very basic and thus reacts with traces of water or protic impurities.

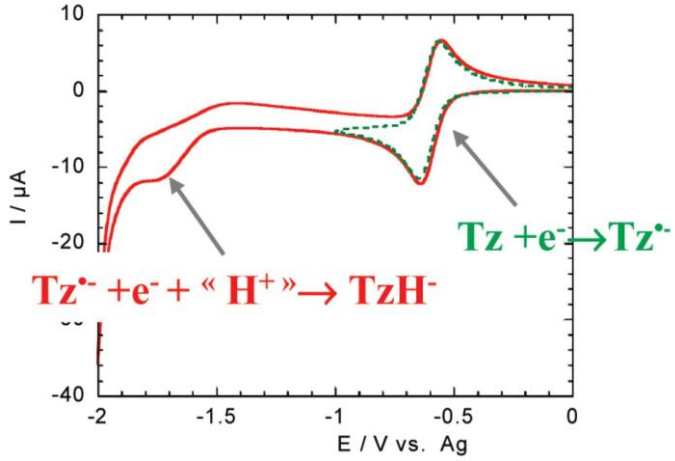

Figure 6: Cyclic voltammograms of 3,6-di([2,2'-bithiophen]-5-yl)-1,2,4,5-tetrazine showing the first and second reductions.

1.1.5 Applications of 1,2,4,5-tetrazines

1.1.5.1 Inverse Electron Demand Diels–Alder (iEDDA) reaction

One of the most important application of 1,2,4,5-tetrazines nowadays has to be the recently emerged tetrazine click chemistry by Inverse Electron Demand Diels–Alder (iEDDA) reaction. The importance of this field has significantly driven the development of tetrazine

synthetic chemistry. As a result, this chemistry has become a hot topic and several recent reviews regarding this field are available.[2,14–16]

Mechanism

Diels–Alder reaction describes a [4+2] cycloaddition between a conjugated diene and a substituted dienophile (alkene or alkyne) to form a (hetero-)cyclohexene system, via suprafacial/suprafacial interaction of the 4π-electrons of the diene with the 2π-electrons of the dienophile (**Figure 7**). Based on the electronic effects of the substituents on the diene and dienophile, Diels–Alder reactions can be classified into two types: a normal electron-demand Diels–Alder reaction, where an electron-rich diene reacts with an electron-deficient dienophile, or an inverse electron-demand Diels–Alder (iEDDA) reaction, where an electron-deficient diene reacts with an electron-rich dienophile.

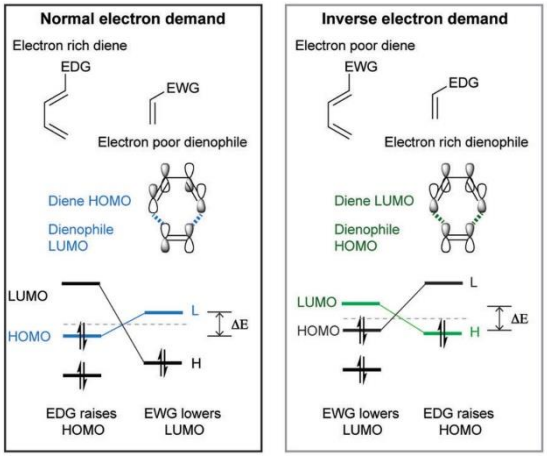

Figure 7: Frontier molecular orbital of normal and inverse electron demand Diels–Alder reaction. EDG = electron donating group, EWG = electron withdrawing group.[2]

In 1959, Carboni and Lindsey first demonstrated the ability of 1,2,4,5-tetrazine to react with unsaturated compounds to give dihydropyridazines or pyridazines.[6] The Carboni-Lindsey reaction starts with the 1,4-cycloaddition of the –C=N–N=C– diene system of the tetrazine to an appropriate alkene, giving a highly strained bicyclic intermediate. Then the adduct undergoes a retro-Diels–Alder reaction to yield the corresponding 4,5-dihydropyridazine accompanying the release of one equivalent of nitrogen. The 4,5-dihydropyridazine then either isomerizes to its 1,4-dihydro-isomers or is oxidized to a pyridazine product (**Scheme 21**). It is important to note that when alkyne dienophiles are employed, the respective pyridazines are directly obtained instead of the dihydropyridazine intermediates, and no oxidation step is needed.

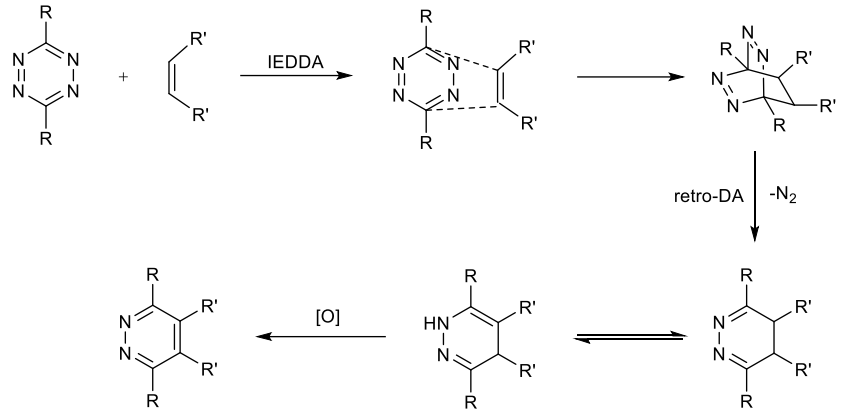

Scheme 21: Schematic representation of the reaction between a tetrazine and a dienophile (alkene).

Reactivity of diene and dienophile

The kinetics of iEDDA reaction is in principle determined by the energy gap between the HOMO and LUMO of the reactants according to the frontier molecular orbital theory (FMO) (**Figure 7**). That is to say, the smaller $HOMO_{dienophile}$–$LUMO_{diene}$ energy difference, the faster iEDDA reaction should be. In 1990s, Sauer and Boger have performed many studies on kinetics of iEDDA reaction in organic solvents. Recently, more studies have been performed to tune the tetrazine and dienophile pairs and enhance the iEDDA reaction rate and bioorthogonality. Generally, there are several important factors to determine the reactivity of diene and dienophile in iEDDA reaction.

Firstly, the electronic effects of the substituents on both diene and dienophile are important. Because electron donating groups (EDG) raise the HOMO and LUMO energy, while electron withdrawing groups (EWG) decrease the energy of those same orbitals, the $HOMO_{dienophile}$–$LUMO_{diene}$ energy difference can be controlled by changing the substituents, thus enhancing the reaction rate. Therefore for tetrazine diene, electron withdrawing groups lower the $LUMO_{diene}$ energy, and accelerate the reaction. For example, tetrazines bearing carboxylate groups show faster kinetics than tetrazines with methoxy groups.[78,79] While for dienophiles, electron donating substituents help increase the reaction rate (**Figure 8**). Many reports have discussed the reactivity of different substituted unstrained dienophiles and general rules have been demonstrated.[45,79,80] Generally, olefins react faster than acetylenes, because of the increased electron withdrawing ability of the triple bond, which lowers the energy of its HOMO (**Figure 8**). In addition, dienophiles bearing EDGs (e.g., dialkylamino) indeed have a higher reactivity.

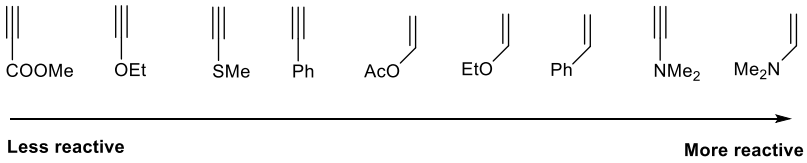

Figure 8: Electronic effects on dienophiles (olefins and acetylenes) in iEDDA reaction.

Secondly, the ring strain effect is regarded as the most important factor in the kinetics of iEDDA reaction. It was reported that the reaction rate increases with increasing ring strain, which means: cyclopropene > cyclobutene > cyclopentene > cyclohexene > cyclooctene. More importantly, it was demonstrated that *trans*-cyclooctene (TCO) as a dienophile showed a surprisingly higher reaction rate (around 6 orders of magnitude higher) compared to *cis*-cyclooctene. This higher reactivity is attributed to a 'crown' conformation adopted by TCO, which is lower in energy than the 'half-chair' conformation of *cis*-cyclooctene as predicted by *ab initio* calculations (**Figure 9**).[2]

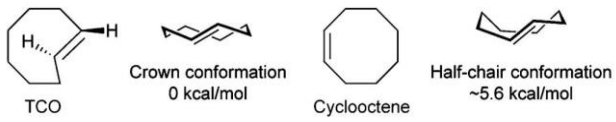

Figure 9: The 'crown' conformation of TCO and 'half-chair' conformation of *cis*-cyclooctene.

Houk and co-workers have revealed through computational studies that strained dienophiles are more reactive because of their pre-distorted conformation towards the transition state structure, which makes them require less distortion energies in the reaction.[81,82] Interestingly, one report demonstrated the design of more reactive dienophiles with the help of computational calculation. According to the *ab initio* calculations, the fusion of a cyclopropane ring with *trans*-cyclooctene to form s-TCO was proposed, as this should induce the formation of a non-crown conformer, and increase the reactivity towards tetrazines (**Figure 10**). Indeed, the resulting more strained, fused s-TCO ring was observed to make the reaction much faster (160 times) than TCO.[83]

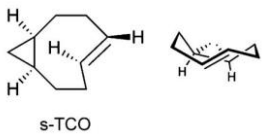

Figure 10: Fused cyclopropane and *trans*-cyclooctene ring s-TCO.

Thirdly, the stereochemistry of strained dienophiles has recently been found to be an important factor influencing the iEDDA reaction kinetic. For example, the functionalized

TCO (RO-TCO) in axial form showed a higher reactivity (4 times) than its equatorial isomer (**Figure 11**).[84–86]

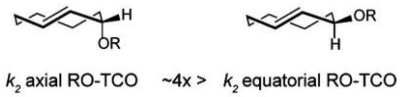

Figure 11: TCO (RO-TCO) in axial form and its equatorial isomer.

Fourthly, steric effect of both the dienophile and diene has a large effect on the iEDDA reaction rate. Generally, terminal alkenes and alkynes are more reactive than those with steric substituents. Although introducing EDGs into dienophiles may help increase the reaction rate, one has to notice the impeding steric effect could lead to only comparable or even lower reactivity.[13] The impeding steric effect also applies to the tetrazine diene. Therefore monosubstituted tetrazines show faster kinetics than disubstituted tetrazines (even those with strong EWGs).[49,84,87]

Lastly, solvent also has an influence on the iEDDA reaction rate. It was reported that using protic solvents (e.g., water) usually give a faster reaction rate. This is because of stabilizing interactions between the activated complex and water, as well as an enhanced hydrophobic interaction between cycloaddends.[88] In addition, hydrogen-bonding with tetrazines can induce polarity, lower the $HOMO_{dienophile}$–$LUMO_{diene}$ energy gap and thus enhance the reaction rate.[89,90]

Applications of iEDDA reaction

In 2008, two groups almost independently discovered that iEDDA reaction can be a perfect candidate for fast bioconjugation.[41,91] Since then, tetrazine bioorthogonal click chemistry has emerged as a powerful tool for decryption of biological messages from organisms, including applications spanning biological imaging and detection, cancer targeting, drug delivery and biomaterials science.[85,90,92–105] Tetrazine click chemistry stands out from other bioorthogonal reactions because of its superfast kinetics (10 000 times faster than CuAAC (copper(I)-catalyzed azide alkyne cycloaddition)), metal-free and physiological pH conditions, excellent orthogonality and biocompatibility.

For example, a series of conjugated BODIPY-tetrazine profluorescent probe were reported by Weissleder and co-workers, which show an excellent fluorescence turn-on ratio up to 1600-fold, via a postulated through-bond energy transfer (TBET) mechanism. These tetrazine derivatives were prepared by the recently developed metal-catalyzed synthetic approach, and an example is shown in **Scheme 22**. These extraordinarily efficient bioorthogonal turn-on probes were validated to exhibit excellent performance in biological imaging.[103]

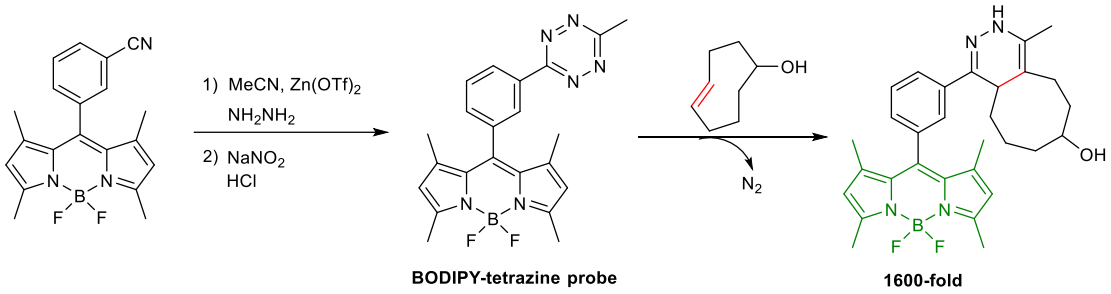

Scheme 22: An example of BODIPY-tetrazine fluorescent probe, showing a 1600-fold fluorescence turn-on ratio after addition of TCO.

Another report published by Wombacher and co-workers showed the synthesis of a palette of fluorogenic tetrazine dyes derived from the widely used fluorophores, which cover the entire emission range from green to far-red. The application of these fluorogenic probes in fixed and live cell labeling experiments were demonstrated. The tetrazine probes were also used for intracellular live cell protein imaging under no-wash conditions.[70]

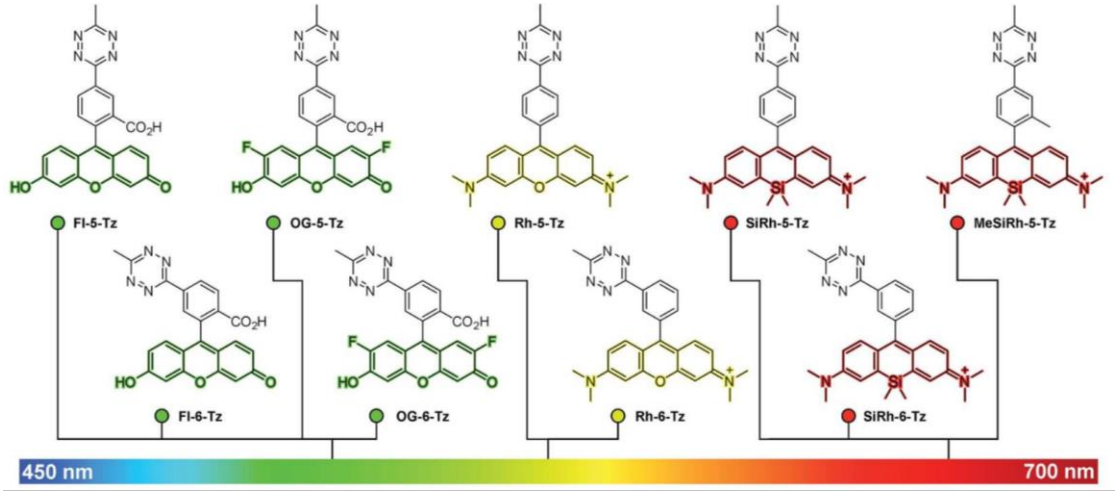

Figure 12: Presentation of green to far-red tetrazine fluorogenic probes.[70]

Another type of interesting application is the recently emerged iEDDA triggered ‘‘click-to-release’’ reaction. With the combination of advantages of bioorthogonal ligation reaction and the triggered bond cleavage under physiological conditions afterwards, this type of reactions can be highly useful for site-specific drug delivery for example.[85,97–100] **Scheme 23** shows an example reported by Bernardes and co-workers. They used vinyl ethers as protecting groups for alcohol-containing molecules and as reagents for bioorthogonal bond-cleavage reactions. The prodrug **A** reacted with tetrazine to form the intermediate **B**, which undergoes a Winstein spirocyclization to give the active drug **C**.

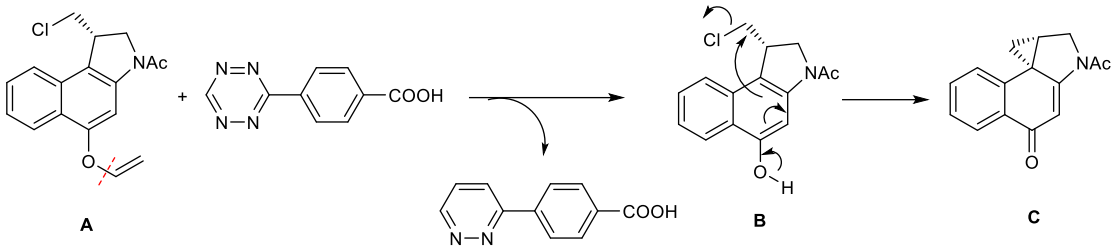

Scheme 22: An example of iEDDA triggered ‘‘click-to-release’’ reaction for drug delivery.

There are numerous reports to date related to tetrazine bioorthogonal click chemistry by iEDDA reaction, and new results are emerging rapidly and vastly. However, it is important to mention that applications using tetrazine iEEDA reaction go far beyond this. For example, it has also been successfully employed in the synthesis of numerous natural products.[3,7,8] Moreover, it was reported that new functional nanomaterials can be prepared by iEDDA reaction of tetrazines with C_{60} or carbon nanotubes.[106–108]

1.1.5.2 Functional molecules and molecular materials

We have discussed in the previous section, that 1,2,4,5-tetazine derivatives prepared by coupling reactions have successfully used for efficient organic solar cells and OFETs.[32,33,73,74] In fact, many more applications for 1,2,4,5-tetrazines regarding functional molecules and molecular materials have been reported.

For example, 1,2,4,5-tetrazine derivatives can be suitable candidates for nonlinear optics (NLO) due to the strong electron affinity of tetrazine, which could enhance the charge transfer in conjugated molecules. Zyss and co-workers proposed that the tetrazine moiety can either serve as the attractor for a classical dipolar push-pull molecule or more interestingly contribute to the formation of a linear octupole.[109] In addition, the tetrazine ring can be the attractive center of purely symmetrical quadrupolar molecules, with enhanced third-order γ values.[1] Based on these, our group has demonstrated the third-order NLO activity of some quadrupolar tetrazine derivatives with ferrocenyl or thienyl substituents displaying a high charge transfer in the fundamental state (**Figure 7**).[31]

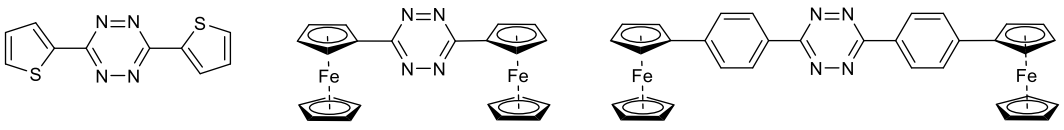

Figure 7: Some examples of quadrupolar tetrazine derivatives with NLO activity.

Another example is the application of 1,2,4,5-tetarzines for the elaboration of electrofluorochromic devices. Many reports regarding this field have been published by our group and others.[27–30,110] For example, our group was the first to demonstrate the modulation of fluorescence with the redox state of the tetrazine molecule.[28] By incorporating chloromethoxytetrazine and a polymeric electrolyte into a sandwich cell, the fluorescence of the tetrazine can be reversibly modulated according to its redox state. The device is highly fluorescent when the tetrazine is in its neutral state, and weakly emissive upon reduction (**Figure 8**). This type of passive fluorescent displays (essentially different from active LEDs) could find applications in fluorescent tunable panels, for example for decoration purposes.

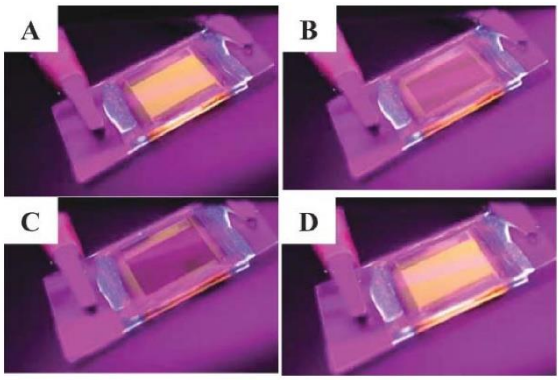

Figure 8: On and off switching by electrochemistry of a fluorescent panel display: (A) initial 0 V, (B) -1 V, (C) -2 V, (D) +1 V.

Another important application of 1,2,4,5-tetrazines is energetic materials. Many important synthetic works on tetrazines have been reported for this purpose. For example, the improved synthesis of dihydrazino-1,2,4,5-tetrazine by Hiskey and co-workers, which led to the easy synthesis of dichlorotetrazine.[23–25] Several 1,2,4,5-tetrazine derivatives that display particularly interesting properties for explosives or pyrotechnics have been reported, some examples are shown in **Figure 9**.[111–115]

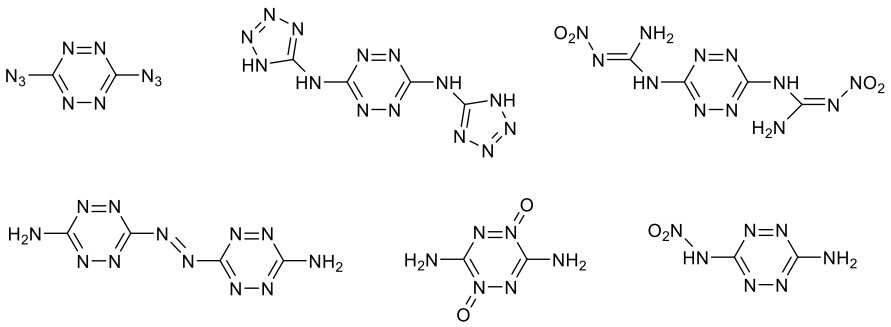

Figure 9: Some examples of high-nitrogen content 1,2,4,5-tetrazine derivatives for energetic material applications.

In addition, 1,2,4,5-tetrazines have been widely used in coordination chemistry. Upon complexation with various first-row transition metals (Ni, Zn, Mn, Fe, Cu) they form cyclic products, for supramolecular materials, as well as for organometallic fluorophores.[4,116–118] Interestingly, the use of anion-π interaction controlling the supramolecular arrangement of metallic complexes through the interaction of tetraizines with the counteranion was also demonstrated.[119,120]

Moreover, during the last decades, 1,2,4,5-tetrazines have also find applications in photocatalysis,[121,122] fluorescent nanoparticles,[123,124] biologically-active compounds,[125–127] and so on.

In the above section, we have presented a brief introduction of the main research field in this thesis, the chemistry of 1,2,4,5-tetrazines. In particular, the tetrazine Pinner synthesis as well as reactions involving tetrazines such as metal-catalyzed cross-coupling reactions, and inverse electron-demand Diels–Alder (iEDDA) reactions are introduced in detail, which are closely related to the results in this thesis. In the next section, a brief introduction of another main research field, thermally activated delayed fluorescence (TADF) will be presented, which is the major application aimed for the molecules in this work.

1.2 Thermally-Activated Delayed Fluorescence (TADF)

1.2.1 Introduction of TADF phenomenon

The thermally-activated delayed fluorescence (TADF) phenomenon was first discovered in 1961 by Parker and Hatchard with the organic molecule Eosin, and subsequently named after “E-type delayed fluorescence”.[128] In 1980, Blasse and co-workers first reported TADF phenomenon in organic metal complexes.[129] In the late 1990s, the TADF phenomenon was also observed in fullerene derivatives by Berberan-Santos and co-workers.[130] However, there was almost no application of TADF materials until 2009 due to the lack of rational molecular design for efficient TADF emitters.

In 2009, the concept of using TADF in organic light-emitting diodes (OLEDs) for harvesting both singlet and triplet was reported by Adachi and co-workers, using a Sn(IV)–porphyrin complex, although the devices only showed low efficiencies (**Figure 10**).[131] In the following year, highly emissive TADF OLED was achieved by Peters and co-workers using a copper(I) complex.[132]

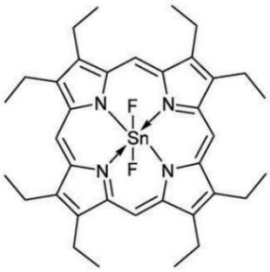

Adv. Mater. **2009**, *21*, 4802–4806

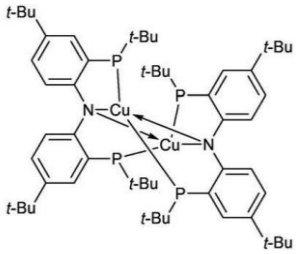

J. Am. Chem. Soc. **2010**, *132*, 9499–9508

Figure 10: Examples of TADF organometallic complexes initially used in OLED devices.

The breakthrough regarding TADF phenomenon was in 2011, when Adachi and co-workers reported the use of pure organic molecules for fabrication of OLEDs. They prepared the first purely organic TADF OLED with an EQE of 5.3%, which is approaching the theoretical limitation of OLEDs (5%, assuming a light out-coupling efficiency of 20%) using conventional fluorescent molecules.[133] Importantly, they found out that separating the spatial distributions of the highest occupied molecular orbital (HOMO) and the lowest unoccupied molecular orbital (LUMO) can effectively minimize the ΔE_{ST} to achieve efficient TADF. Therefore, a molecular design strategy was proposed, based on the introduction of electron donor and acceptor units in a way that the π-conjugation is highly distorted by steric hindrance introduced from the bulky substituents.[133] Shortly afterwards in 2012, the same groups reported a series of groundbreaking organic TADF emitters based on carbazolyl dicyanobenzene, which showed high photoluminescence (PL) efficiency and various emission colors from sky-blue to orange (**Figure 11**). The best OLED device using

these TADF emitters provided a promising EQE of 19.3%, which far surpasses the theoretical maximum of OLEDs employing conventional fluorescent emitters.[134] In addition, another breakthrough for TADF emitters was reported in the same year by the same group. They demonstrated that an exciplex formed between a donor molecule and an acceptor one (**Figure 11**) gave efficient an OLED device with an EQE of 10.0%.[135] Since these pioneering works, preparing organic TADF materials for electroluminescent (EL), as well as other applications have become a hot topic in the research community.[136–141]

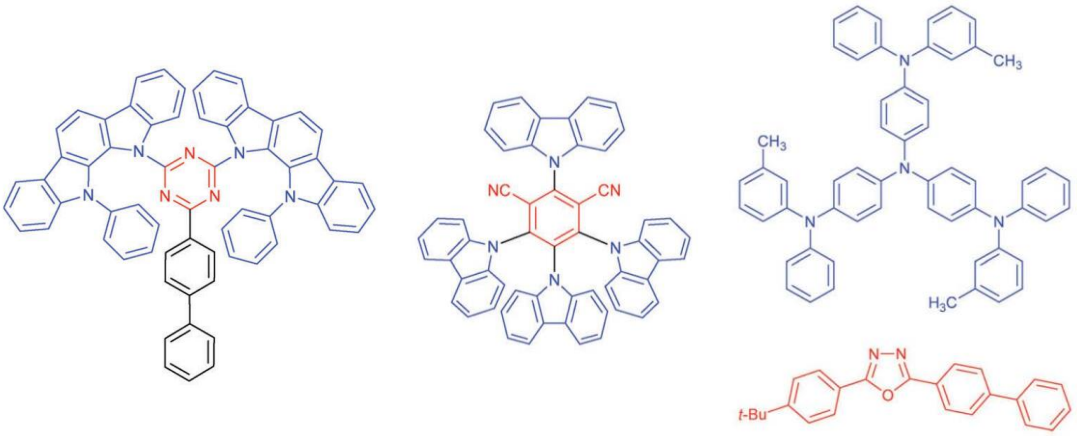

Appl. Phys. Lett. **2011**, *98*, 083302 *Nature* **2012**, *492*, 234–238 *Nat. Photonics* **2012**, *6*, 253–258

Figure 11: Examples of donor-acceptor type TADF molecules and exciplex.

1.2.2 TADF mechanism

In organic light emitting diodes (OLEDs), the recombination of electrons and holes in the emissive layer creates 25% singlet excitons and 75% triplet excitons, where the singlet excitons decay radiatively to yield fluorescence. Considerable efforts have been made to utilize the 75% non-radiative triplet excitons for obtaining high electroluminescence (EL) efficiency. Complexation of heavy metals into the organic aromatic frameworks has efficiently intermixed singlet and triplet states via an effective heavy atom spin-orbit coupling, which facilitates the transition from the lowest triplet excited state (T_1) to the ground state (S_0) accompanied with phosphorescence emission, yielding nearly 100% internal luminescent efficiency.[142] On the other hand, delayed fluorescence can be achieved by triplet-triplet annihilation (TTA) which converts two triplet excitons into one singlet exciton. This additional singlet exciton provides enhancement in the luminescent efficiency from 15% to 37.5% depending on the up-conversion mechanism.[143] A more promising pathway to harvest triplet excitons is thermally-activated delayed fluorescence (TADF). In this process, the triplet excitons can be converted to emissive singlet excitons via efficient reverse intersystem crossing (RISC) from the lowest triplet excited state (T_1) to the lowest singlet excited state (S_1) by thermal activation (**Figure 12**). The RISC rate

largely depends on the energy difference between S_1 and T_1 (ΔE_{ST}), and a small ΔE_{ST} efficiently facilitates the RISC process. An exceptionally high internal quantum efficiency (nearly 100%) can be achieved by carefully designing the organic molecules with a small energy gap (ΔE_{ST}).[136–141]

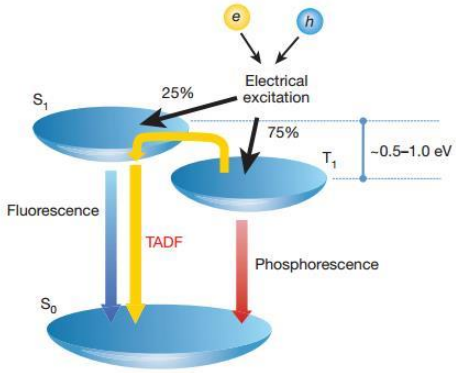

Figure 12: Energy diagram of TADF process.[134]

For achieving efficient TADF, the key process is the thermally activated RISC, which is temperature sensitive. A small ΔE_{ST} is critical because it governs the rate constant of RISC (k_{RISC}) according to the Boltzmann distribution:

$$k_{\mathrm{RISC}} \propto exp \frac{\Delta E_{\mathrm{ST}}}{k_{\mathrm{B}} T}$$

where k_B is the Boltzmann constant and T is the temperature. The ΔE_{ST} is the difference between the E_S and E_T, which can be defined as follows:

$$E_S = E_{orb} + K + J$$

$$E_T = E_{orb} + K - J$$

$$\Delta E_{ST} = E_S - E_T = 2J$$

where E_{orb} is the orbital energy, K is the electron repulsion energy and J is the exchange energy. Therefore the energy difference between singlet and triplet state (ΔE_{ST}) is 2J.[144] The ΔE_{ST} is generally high (0.5-1.0 eV) for organic molecules because the exchange energy between the two levels is high. An effective way to minimize the ΔE_{ST} is to separate the spatial distributions of the highest occupied molecular orbital (HOMO) and the lowest unoccupied molecular orbital (LUMO). However, a small overlap between HOMO and LUMO provides a small radiative decay rate constant (k_r), which is directly related to the photoluminescence quantum yield (PLQY) the of molecule. Therefore there is a trade-off between these two contradictions when designing a TADF molecule.[140]

1.2.3 Molecular designs to TADF molecules

As mentioned above, Adachi and co-workers has proposed a rational molecular design strategy in 2011, based on the introduction of electron donor and acceptor units in a way that the π-conjugation is highly distorted by steric hindrance introduced from the bulky substituents. The idea is to reduce the overlap of the HOMO and LUMO of the molecules, so that the ΔE_{ST} can be minimized. However, as large k_r and small ΔE_{ST} are conflicting, fine molecular design is usually required to realize them simultaneously for efficient TADF.[133]

To date, donor−acceptor (D−A) system exhibiting a charge-transfer (CT) transition is still the most successful design strategy for TADF materials. These TADF materials can be either a single organic D−A molecule (intramolecular D−A system), or organic exciplexes with two individual donor and acceptor molecules (intermolecular D−A system). Such molecular systems have achieved promising OLED performance by simultaneously realizing efficient RISC and high PLQY.[134,135,145–155] New molecular design strategies (intramolecular D−A system) such as using spiro-linker, through-space charge transfer effect, multiple resonance effect, asymmetric structures with two different donors, polymeric structures, etc. have been reported.[156–162] Electron donors such as phenoxazine, phenothiazine, dimethylacridine, carbazole and its derivatives are usually employed because of their high electron-donating abilities and easy inclusion into twisted TADF molecules. On the other hand, the choice of electron acceptors is more diverse. Various electron acceptors have been successfully used for preparing efficient TADF materials, including nitrogen heterocycle-based acceptors (such as triazine, diazine, heptazine, oxadiazole and triazole), cyano-based acceptors, diphenyl sulfoxide-based acceptors, diphenyl ketone-based acceptors, etc.[136–141]

It is interesting to mention that recently, Adachi and co-workers presented a novel molecular design strategy which takes advantage of the excited-state intramolecular proton transfer (ESIPT) to achieve highly efficient TADF materials without relying on the commonly used donor−acceptor system.[163]

1.2.4 Photophysics of TADF molecules

The increasing interests in application of TADF materials for OLEDs and other fields, has made the study of the photophysical properties of TADF molecules and the understanding of the TADF mechanism critical for the development of this research area. Generally, there are several important experiments that can be performed to determine the efficiency of a TADF molecule.[137,144]

Solvatochromism

Because most of the TADF molecules are designed through a donor-acceptor molecular system, the charge transfer (CT) excited state and its energy is very important for the TADF property. The experimental evidence for proving the CT excited state formed in an organic molecule is the solvatochromic effect in their emission.[137] Usually, polar media (e.g., ethanol) favor the CT state and lower its energy. Therefore the CT emission spectrum tends to red-shift with increasing solvent polarity. It can also be observed that the CT emission is usually broad and featureless in polar solvent, while it tends to become narrow (and resolved in some cases) in non-polar media. The energy of the CT state is strongly environment-dependent, therefore it is possible to tune the CT emission and the lowest singlet state energy of a TADF molecule by employing media with different polarity.[164,165]

Oxygen quenching

Since TADF is a process to harvest triplets, oxygen from air can severely quench the TADF process. Therefore it is important to mind the oxygen quenching effect when performing photophysical characterization of a TADF molecule. In other words, all the experiments should be performed in oxygen-free conditions in order to obtain reliable characteristics of a TADF molecule.[144]

Generally, there are two ways to maintain oxygen-free conditions for photophysical measurements: pump degassing and nitrogen/argon bubbling. For solid samples (neat film, sample dispersed in a host matrix, etc.), air can be removed easily by pump degassing or nitrogen/argon flushing. While for solution samples, it is easier to perform nitrogen/argon bubbling, although pump degassing is possible with several freeze/thaw cycles in a special spectroscopic cuvette. The difference in fluorescence intensity between air-equilibrated and degassed conditions is an indication of delayed fluorescence. Normally, a large difference means a higher contribution of delayed fluorescence to the overall emission.[165]

Fluorescence decay

As mentioned above, oxygen quenching is an indication of delayed fluorescence. To further confirm the delayed fluorescence existence in a molecule, it is important to measure its fluorescence decay in solution or solid film in oxygen-free conditions. The fluorescence decay of a TADF molecule usually consists of two parts: prompt and delayed fluorescence. The lifetime of prompt fluorescence is usually in the range of 1-100 ns as for normal fluorescence, the delayed fluorescence has a lifetime of typically 1 μs to 100 ms. The ratio of the delayed fluorescence component to the prompt fluorescence one (DF/PF) can also be determined from the fluorescence decay.[137,165]

Temperature dependence of TADF

Normally, the prompt fluorescence lifetime and intensity does not change too much upon changing temperature. Slightly longer lifetime and higher intensity at low temperatures

could be observed due to the limitation of non-radiative decay processes. However, delayed fluorescence lifetime and intensity are strongly dependent upon temperature because TADF is a thermally activated process.[144] Normally in a TADF molecule, a strong delayed fluorescence and no phosphorescence should be observed at room temperature. When decreasing the temperature, the amount of TADF should decrease and the phosphorescence starts to appear. When the temperature is low enough (e.g., 77K, liquid N_2), the TADF process should be deactivated and become very weak or not observed, and strong phosphorescence should be observed. However, in some cases, due to the very small ΔE_{ST} of the molecule, the TADF process is still quite good at 77K because very small thermal energy is needed in those cases to promote the TADF process. The temperature dependence of the delayed fluorescence is fundamental to prove that the delayed fluorescence is due to a TADF mechanism.[137,165]

Time-resolved spectra

In principle, the spectra of prompt and delayed fluorescence of a TADF molecule should be identical because the emission arises from the same singlet excited state. However, in some cases, red-shifting or blue-shifting of emission in time-resolved spectra may be observed, which can be explained by the presence of conformers that have slightly different energy levels.[144] The phosphorescence of a TADF molecule could also be determined from the time-resolved spectra at 77 K or even lower when the molecule possess a small ΔE_{ST}. Therefore, the ΔE_{ST} of a TADF molecule could be determined from prompt fluorescence and phosphorescence spectra as the energy of the lowest singlet (E_S) and triplet (E_T) excited states respectively. However, in some cases, the TADF molecule possess a very small ΔE_{ST}, as a result the fluorescence and phosphorescence spectra are almost indistinguishable. Interestingly, it was reported in many cases, that the phosphorescence of a TADF molecule originates from the donor's or acceptor's triplet level (depending on which triplet level is the lowest). As a result, the phosphorescence spectrum is identical to that of a single donor or acceptor molecule in the same conditions.[165]

Power dependence of TADF

Power dependence experiment is a convenient way to reliably distinguish between TADF and TTA phenomena.[137] TADF is an unimolecular process, therefore it is linearly dependent upon excitation power. While TTA is a bimolecular process which requires contact of two molecules in a triplet excited state, so its intensity is quadratically dependent upon excitation power.[143] However, in some cases, TTA and TADF can compete with each other, therefore the power law is in between 1 and 2.[144]

1.2.5 Application of TADF materials

The most important application field for TADF material is by far organic light emitting diodes (OLEDs).[134,135] TADF molecules are potential replacements for metal complex phosphors to facilitate up to 100% triplet exciton harvesting. With no need of expensive noble metals (e.g., iridium and platinum), pure organic TADF materials are indeed more appealing for OLED applications. In addition, due to the flexible molecular design, the emission wavelength of TADF materials can cover the whole visible spectrum, which is ideal for display and lighting applications. Therefore TADF materials have been regarded as the new generation of OLED materials over the last few years.[136–141]

Additionally, the use of purely organic TADF materials goes far beyond their application in electroluminescent devices. They can supersede metal complex emitters by acting as triplet sensitizers,[166] or bio-imaging dyes.[167,168] These molecules provide either sufficient spin-orbit coupling (SOC) to generate high triplet populations, yet they are able to provide conditions for efficient reverse intersystem crossing (RISC) and these parameters can be tunable.[169] As a result these molecules are widely represented among mechanochromic materials with many switchable parameters, such as emission color,[170–172] TADF on/off[173] or interplay of TADF and prompt fluorescence originating from different parts of the molecule.[174]

1.3 PhD project

The aim of this PhD project is the synthesis of novel electron-acceptor derivatives for the application of TADF emitters. It will be focused on the synthesis of new 1,2,4,5-tetrazine derivatives, including the exploration of synthetic methodologies for 1,2,4,5-tetrazines (e.g., tetrazine Pinner synthesis). Therefore, benzonitrile derivatives which are the typical precursors in the tetrazine Pinner synthesis will also be investigated. In addition, reactions involving tetrazines such as metal-catalyzed cross-coupling reactions, and inverse electron-demand Diels–Alder (iEDDA) reactions are of particular interest in this thesis in order to prepare novel donor-acceptor tetrazine and pyridazine derivatives. Moreover, 1,2,3,4-thiatriazole derivatives, as unpredicted products from modified Pinner synthesis, will also be investigated. The photophysical and electrochemical properties of all the prepared electron-acceptor derivatives will be studied. In particular, the novel donor-acceptor benzonitrile and thiatriazole derivatives which exhibit TADF phenomenon will be elaborately investigated for their potential applications as efficient TADF emitters.

1.4 Reference

[1] G. Clavier, P. Audebert, *Chem. Rev.* **2010**, *110*, 3299–3314.

[2] B. L. Oliveira, Z. Guo, G. J. L. Bernardes, *Chem. Soc. Rev.* **2017**, *46*, 4895–4950.

[3] N. Saracoglu, *Tetrahedron* **2007**, *63*, 4199–4236.

[4] W. Kaim, *Coord. Chem. Rev.* **2002**, *230*, 127–139.

[5] A. Pinner, *Chem. Ber.* **1893**, *26*, 2126.

[6] R. A. Carboni, R. V. Lindsey, *J. Am. Chem. Soc.* **1959**, *81*, 4342–4346.

[7] D. L. Boger, J. Hong, *J. Am. Chem. Soc.* **2001**, *123*, 8515–8519.

[8] A. Hamasaki, J. M. Zimpleman, I. Hwang, D. L. Boger, *J. Am. Chem. Soc.* **2005**, *127*, 10767–10770.

[9] D. L. Boger, *Chem. Rev.* **1986**, *86*, 781–793.

[10] Y. Li, F. Miomandre, G. Clavier, L. Galmiche, V. Alain-Rizzo, P. Audebert, *ChemElectroChem* **2017**, *4*, 430–435.

[11] S. M. Sakya, T. W. Strohmeyer, S. A. Lang, Y.-I. Lin, *Tetrahedron Lett.* **1997**, *38*, 5913–5916.

[12] D. Che, T. Wegge, M. T. Stubbs, G. Seitz, H. Meier, C. Methfessel, *J. Med. Chem.* **2001**, *44*, 47–57.

[13] J. Sauer, D. K. Heldmann, J. Hetzenegger, J. Krauthan, H. Sichert, J. Schuster, *European J. Org. Chem.* **1998**, 2885–2896.

[14] A. C. Knall, C. Slugovc, *Chem. Soc. Rev.* **2013**, *42*, 5131–5142.

[15] H. Wu, N. K. Devaraj, *Top. Curr. Chem.* **2016**, *374*, 1–22.

[16] H. Wu, N. K. Devaraj, *Acc. Chem. Res.* **2018**, *51*, 1249–1259.

[17] E.Cuellar, G.Castro, *Chem. Phys.* **1981**, *54*, 217–225.

[18] H. De Vries, D. A. Wiersma, *J. Chem. Phys.* **1980**, *72*, 1851–1863.

[19] H. De Vries, D. A. Wiersma, *Chem. Phys. Lett.* **1977**, *51*, 565–567.

[20] R. M. Hochstrasser, D. S. King, A. B. Smith, *J. Am. Chem. Soc.* **1977**, *99*, 3923–3933.

[21] M. Paczkowski, R. Pierce, A. B. Smith, R. M. Hochstrasser, *Chem. Phys. Lett.* **1980**, *72*, 5–9.

[22] U.Boesl, H.J.Neusser, E.W.Schlag, *Chem. Phys. Lett.* **1979**, *61*, 62–66.

[23] M. D. Coburn, G. A. Buntain, B. W. Harris, M. A. Hiskey, K.-Y. Lee, D. G. Ott, *J. Heterocycl. Chem.* **1991**, *28*, 2049–2050.

[24] D. E. Chavez, M. A. Hiskey, *J. Heterocycl. Chem.* **1998**, *35*, 1329–1332.

[25] D. E. Chavez, M. A. Hiskey, *J. Energ. Mater.* **1999**, *17*, 357–377.

[26] Z. Novak, A. Kotschy, *Org. Lett.* **2003**, *5*, 3495–3497.

[27] C. Quinton, V. Alain-Rizzo, C. Dumas-Verdes, G. Clavier, F. Miomandre, P. Audebert, *European J. Org. Chem.* **2012**, *2012*, 1394–1403.

[28] Y. Kim, E. Kim, G. Clavier, P. Audebert, *Chem. Commun.* **2006**, 3612–3614.

[29] P. Audebert, F. Miomandre, *Chem. Sci.* **2013**, *4*, 575–584.

[30] F. Miomandre, R. Meallet-Renault, J.-J. Vachon, R. B. Pansu, P. Audebert, *Chem. Commun.* **2008**, 1913–1915.

[31] I. Janowska, F. Miomandre, G. Clavier, P. Audebert, J. Zakrzewski, K. H. Thi, I. Ledoux-rak, **2006**, *11*, 12971–12975.

[32] Z. Li, J. Ding, N. Song, J. Lu, Y. Tao, *J. Am. Chem. Soc.* **2010**, 8–9.

[33] Z. Li, J. Ding, N. Song, X. Du, J. Zhou, J. Lu, Y. Tao, *Chem. Mater.* **2011**, *23*, 1977–1984.

[34] K. A. Hofmann, O. Ehrhart, *Berichte der Dtsch. Chem. Gesellschaft* **1912**, *45*, 2731–2740.

[35] N. O. Abdel, M. A. Kira, M. N. Tolba, *Tetrahedron Lett.* **1968**, 3871–3872.

[36] J. Yang, M. R. Karver, W. Li, S. Sahu, N. K. Devaraj, *Angew. Chemie - Int. Ed.* **2012**, *51*, 5222–5225.

[37] R. Stolle, *J. Prakt. Chem.* **1906**, *73*, 277–287.

[38] D. Wang, W. Chen, Y. Zheng, C. Dai, L. Wang, B. Wang, *Heterocycl. Commun.* **2013**, *19*, 171–177.

[39] Z. Fang, W. L. Hu, D. Y. Liu, C. Y. Yu, X. G. Hu, *Green Chem.* **2017**, *19*, 1299–1302.

[40] A. Pinner, *Berichte der Dtsch. Chem. Gesellschaft* **1897**, *30*, 1871–1890.

[41] M. L. Blackman, M. Royzen, J. M. Fox, *J. Am. Chem. Soc.* **2008**, *130*, 13518–13519.

[42] R. Selvaraj, J. M. Fox, *Tetrahedron Lett.* **2014**, *55*, 4795–4797.

[43] D. Nhu, S. Duffy, V. M. Avery, A. Hughes, J. B. Baell, *Bioorganic Med. Chem. Lett.* **2010**, *20*, 4496–4498.

[44] J. Sauer, G. R. Pabst, U. Holland, H. S. Kim, S. Loebbecke, *European J. Org. Chem.* **2001**, 697–706.

[45] D. R. Soenen, J. M. Zimpleman, D. L. Boger, *J. Org. Chem.* **2003**, *68*, 3593–3598.

[46] H. Zhang, W. S. Trout, S. Liu, G. A. Andrade, D. A. Hudson, S. L. Scinto, K. T. Dicker, Y. Li, N. Lazouski, J. Rosenthal, et al., *J. Am. Chem. Soc.* **2016**, *138*, 5978–5983.

[47] M. Savastano, C. Bazzicalupi, C. Giorgi, C. García-Gallarín, M. D. López De La Torre, F. Pichierri, A. Bianchi, M. Melguizo, *Inorg. Chem.* **2016**, *55*, 8013–8024.

[48] P. Audebert, S. Sadki, F. Miomandre, G. Clavier, M. C. Vernieres, M. Saoud, P. Hapiot, *New J. Chem.* **2004**, *28*, 387–392.

[49] M. Karver, R. Weissleder, S. A. Hilderbrand, *Bioconjug. Chem.* **2011**, *22*, 2263–2270.

[50] S. A. Lang Jr., B. D. Johnson, E. Cohen, *J. Heterocycl. Chem.* **1975**, *12*, 1143–1153.

[51] K. Wajda-hermanowicz, D. Pienia, A. Zatajska, Z. Ciunik, S. Berski, *J. Mol. Struct.* **2016**, *1114*, 108–122.

[52] F. Bentiss, M. Lagrenee, M. Traisnel, B. Mernari, H. Elattari, *J. Heterocycl. Chem.* **1999**, *36*, 149–152.

[53] F. Bentiss, M. Lagrenée, D. Barbry, *Tetrahedron Lett.* **2000**, *41*, 1539–1541.

[54] D. L. Alge, D. F. Donohue, K. S. Anseth, *Tetrahedron Lett.* **2013**, *54*, 5639–5641.

[55] H. Wu, J. Yang, J. Seckute, N. K. Devaraj, *Angew. Chemie - Int. Ed.* **2014**, *53*, 5805–5809.

[56] D. S. Liu, A. Tangpeerachaikul, R. Selvaraj, M. T. Taylor, J. M. Fox, A. Y. Ting, *J. Am. Chem. Soc.* **2012**, *134*, 792–795.

[57] D. Wang, W. Chen, Y. Zheng, C. Dai, K. Wang, B. Ke, B. Wang, *Org. Biomol. Chem.* **2014**, *12*, 3950–3955.

[58] R. A. Carboni, R. V Lindsey, *J. Am. Chem. Soc.* **1958**, *80*, 5793–5795.

[59] W. Skorianetz, E. S. Kováts, *Helv. Chim. Acta* **1972**, *55*, 1404–1414.

[60] W. Skorianetz, E. S. Kováts, *Helv. Chim. Acta* **1971**, *54*, 1922–1939.

[61] D. Boger, S. Sakya, *J. Org. Chem.* **1988**, *209*, 1415–1423.

[62] M. D. Helm, A. Plant, J. P. A. Harrity, *Org. Biomol. Chem.* **2006**, *4*, 4278–4280.

[63] Z. Novák, B. Bostai, M. Csékei, K. Lorincz, A. Kotschy, *Heterocycles* **2003**, *60*, 2653–2668.

[64] Y. H. Gong, F. Miomandre, R. Méallet-Renault, S. Badré, L. Galmiche, J. Tang, P. Audebert, G. Clavier, *European J. Org. Chem.* **2009**, 6121–6128.

[65] B. Venkateswara Rao, S. Dhokale, P. R. Rajamohanan, S. Hotha, *Chem. Commun.* **2013**, *49*, 10808–10810.

[66] J. Faragó, Z. Novák, G. Schlosser, A. Csámpai, A. Kotschy, *Tetrahedron* **2004**, *60*, 1991–1996.

[67] Q. Zhou, P. Audebert, G. Clavier, F. Miomandre, J. Tang, *RSC Adv.* **2014**, *4*, 7193–7195.

[68] N. Leconte, A. Keromnes-Wuillaume, F. Suzenet, G. Guillaumet, *Synlett* **2007**, 204–210.

[69] A. M. Bender, T. C. Chopko, T. M. Bridges, C. W. Lindsley, *Org. Lett.* **2017**, *19*, 5693–5696.

[70] A. Wieczorek, P. Werther, J. Euchner, R. Wombacher, *Chem. Sci.* **2017**, *8*, 1506–1510.

[71] G. Knorr, E. Kozma, A. Herner, E. A. Lemke, P. Kele, *Chem. - A Eur. J.* **2016**, *22*, 8972–8979.

[72] A. Wieczorek, T. Buckup, R. Wombacher, *Org. Biomol. Chem.* **2014**, *12*, 4177–4185.

[73] C. Quinton, V. Alain-Rizzo, C. Dumas-Verdes, G. Clavier, L. Vignau, P. Audebert, *New J. Chem.* **2015**, *39*, 9700–9713.

[74] D. K. Hwang, R. R. Dasari, M. Fenoll, V. Alain-Rizzo, A. Dindar, J. W. Shim, N. Deb, C. Fuentes-Hernandez, S. Barlow, D. G. Bucknall, et al., *Adv. Mater.* **2012**, *24*, 4445–4450.

[75] C. Testa, É. Gigot, S. Genc, R. Decréau, J. Roger, J. C. Hierso, *Angew. Chemie - Int. Ed.* **2016**, *55*, 5555–5559.

[76] S. F. MASON, *J. Chem. Soc.* **1959**, 1240–1246.

[77] P. Audebert, F. Miomandre, G. Clavier, M. C. Verniéres, S. Badré, R. Méallet-Renault, *Chem. - A Eur. J.* **2005**, *11*, 5667–5673.

[78] A. Hamasaki, R. Ducray, D. L. Boger, *J. Org. Chem.* **2006**, *71*, 185–193.

[79] D. L. Boger, R. P. Schaum, R. M. Garbaccio, *J. Org. Chem.* **1998**, *63*, 6329–6337.

[80] F. Thalhammer, U. Wallfahrer, J. Sauer, *Tetrahedron Lett.* **1990**, *31*, 6851–6854.

[81] F. Liu, Y. Liang, K. N. Houk, *J. Am. Chem. Soc.* **2014**, *136*, 11483–11493.

[82] F. Liu, R. S. Paton, S. Kim, Y. Liang, K. N. Houk, *J. Am. Chem. Soc.* **2013**, *135*, 15642–15649.

[83] M. T. Taylor, M. L. Blackman, O. Dmitrenko, J. M. Fox, T. Ligation, *J. Am. Chem. Soc.* **2011**, *133*, 9646–9649.

[84] J. A. Wagner, D. Mercadante, I. Nikic, E. A. Lemke, F. Gräter, *Chem. - A Eur. J.* **2015**, *21*, 12431–12435.

[85] R. M. Versteegen, R. Rossin, W. Ten Hoeve, H. M. Janssen, M. S. Robillard, *Angew. Chemie - Int. Ed.* **2013**, *52*, 14112–14116.

[86] J. Li, S. Jia, P. R. Chen, *Nat. Chem. Biol.* **2014**, *10*, 1003–1005.

[87] J. Balcar, G. Chrisam, F. X. Huber, J. Sauer, *Tetrahedron Lett.* **1983**, *24*, 1481–1484.

[88] A. Meijer, S. Otto, J. B. F. N. Engberts, *J. Org. Chem.* **1998**, *63*, 8989–8994.

[89] J. W. Wijnen, S. Zavarise, J. B. F. N. Engberts, M. Charton, *J. Org. Chem.* **1996**, *61*, 2001–2005.

[90] K. Lang, L. Davis, J. Torres-Kolbus, C. Chou, A. Deiters, J. W. Chin, *Nat. Chem.* **2012**, *4*, 298–304.

[91] N. K. Devaraj, R. Weissleder, S. A. Hilderbrand, *Bioconjug. Chem.* **2008**, *19*, 2297–2299.

[92] H. Wu, S. C. Alexander, S. Jin, N. K. Devaraj, *J. Am. Chem. Soc.* **2016**, *138*, 11429–11432.

[93] I. Nikić, G. Estrada Girona, J. H. Kang, G. Paci, S. Mikhaleva, C. Koehler, N. V. Shymanska, C. Ventura Santos, D. Spitz, E. A. Lemke, *Angew. Chemie - Int. Ed.* **2016**, *55*, 16172–16176.

[94] E. Jiménez-Moreno, Z. Guo, B. L. Oliveira, I. S. Albuquerque, A. Kitowski, A. Guerreiro, O. Boutureira, T. Rodrigues, G. Jiménez-Osés, G. J. L. Bernardes, *Angew. Chemie - Int. Ed.* **2017**, *56*, 243–247.

[95] C. P. Ramil, M. Dong, P. An, T. M. Lewandowski, Z. Yu, L. J. Miller, Q. Lin, *J. Am. Chem. Soc.* **2017**, *139*, 13376–13386.

[96] Y. Lee, W. Cho, J. Sung, E. Kim, S. B. Park, *J. Am. Chem. Soc.* **2018**, *140*, 974–983.

[97] I. Khan, P. F. Agris, M. V. Yigit, M. Royzen, *Chem. Commun.* **2016**, *52*, 6174–6177.

[98] J. M. M. Oneto, I. Khan, L. Seebald, M. Royzen, *ACS Cent. Sci.* **2016**, *2*, 476–482.

[99] K. Neumann, S. Jain, A. Gambardella, S. E. Walker, E. Valero, A. Lilienkampf, M. Bradley, *ChemBioChem* **2017**, *18*, 91–95.

[100] E. Jiménez-Moreno, Z. Guo, B. L. Oliveira, I. S. Albuquerque, A. Kitowski, A. Guerreiro, O. Boutureira, T. Rodrigues, G. Jiménez-Osés, G. J. L. Bernardes, *Angew. Chemie - Int. Ed.* **2017**, *56*, 243–247.

[101] N. K. Devaraj, S. Hilderbrand, R. Upadhyay, R. Mazitschek, R. Weissleder, *Angew. Chemie - Int. Ed.* **2010**, *49*, 2869–2872.

[102] J. B. Haun, N. K. Devaraj, S. A. Hilderbrand, H. Lee, R. Weissleder, *Nat. Nanotechnol.* **2010**, *5*, 660.

[103] J. C. T. Carlson, L. G. Meimetis, S. A. Hilderbrand, R. Weissleder, *Angew. Chemie - Int. Ed.* **2013**, *52*, 6917–6920.

[104] L. G. Meimetis, J. C. T. Carlson, R. J. Giedt, R. H. Kohler, R. Weissleder, *Angew. Chemie - Int. Ed.* **2014**, *53*, 7531–7534.

[105] C. Uttamapinant, J. D. Howe, K. Lang, V. Beránek, L. Davis, M. Mahesh, N. P. Barry, J. W. Chin, *J. Am. Chem. Soc.* **2015**, *137*, 4602–4605.

[106] Y. Murata, M. Suzuki, Y. Rubin, K. Komatsu, *Bull. Chem. Soc. Jpn.* **2003**, *76*, 1669–1672.

[107] H. Hayden, Y. K. Gun'ko, T. S. Perova, *Chem. Phys. Lett.* **2007**, *435*, 84–89.

[108] Y. Li, V. Alain-Rizzo, L. Galmiche, P. Audebert, F. Miomandre, G. Louarn, M. Bozlar, M. A. Pope, D. M. Dabbs, I. A. Aksay, *Chem. Mater.* **2015**, *27*, 4298–4310.

[109] J. Zyss, *Molecular Nonlinear Optics: Materials, Physics, and Devices*, **2013**.

[110] F. Miomandre, E. Lépicier, S. Munteanu, O. Galangau, J. F. Audibert, R. Méallet-Renault, P. Audebert, R. B. Pansu, *ACS Appl. Mater. Interfaces* **2011**, *3*, 690–696.

[111] D. E. Chavez, M. a. Hiskey, *J. Energ. Mater.* **1999**, *17*, 357–377.

[112] D. E. Chavez, M. A. Hiskey, R. D. Gilardi, *Angew. Chemie - Int. Ed.* **2000**, *39*, 1791–1793.

[113] H. Gao, R. Wang, B. Twamley, M. A. Hiskey, J. M. Shreeve, *Chem. Commun.* **2006**, 4007–4009.

[114] D. E. Chavez, D. A. Parrish, L. Mitchell, G. H. Imler, *Angew. Chemie - Int. Ed.* **2017**, *56*, 3575–3578.

[115] M. H. V Huynh, M. A. Hiskey, D. E. Chavez, D. L. Naud, R. D. Gilardi, *J. Am. Chem. Soc.* **2005**, *127*, 12537–12543.

[116] T. S. M. Tang, H. W. Liu, K. K. W. Lo, *Chem. Commun.* **2017**, *53*, 3299–3302.

[117] M. Marin, V. Lhiaubet-Vallet, C. Paris, M. Yamaji, M. A. Miranda, *Photochem. Photobiol. Sci.* **2011**, *10*, 1474–1479.

[118] J. Yuasa, A. Mitsui, T. Kawai, *Chem. Commun.* **2011**, *47*, 5807–5809.

[119] C. S. Campos-Fernández, R. Clerac, J. M. Koomen, D. H. Russell, K. R. Dunbar, *J. Am. Chem. Soc.* **2001**, *1*, 773–774.

[120] C. S. Campos-Fernández, B. L. Schottel, H. T. Chifotides, J. K. Bera, J. Bacsa, J. M. Koomen, D. H. Russell, K. R. Dunbar, *J. Am. Chem. Soc.* **2005**, *127*, 12909–12923.

[121] S. Samanta, S. Das, P. Biswas, *J. Org. Chem.* **2013**, *78*, 11184–11193.

[122] E. Jullien-Macchi, C. Allain, V. Alain-Rizzo, C. Dumas-Verdes, L. Galmiche, J. F. Audibert, M. Berhe Desta, R. B. Pansu, P. Audebert, *New J. Chem.* **2014**, *38*, 3401–3407.

[123] J. Malinge, C. Allain, L. Galmiche, F. Miomandre, P. Audebert, *Chem. Mater.* **2011**, *23*, 4599–4605.

[124] J. Malinge, C. Allain, A. Brosseau, P. Audebert, *Angew. Chemie - Int. Ed.* **2012**, *51*, 8534–8537.

[125] L. M. Werbel, D. J. Mcnamara, N. L. Colbry, J. L. Johnson, M. J. Degnan, B. Whitney, *J. Heterocycl. Chem.* **1979**, *16*, 881–894.

[126] W. X. Hu, G. W. Rao, Y. Q. Sun, *Bioorganic Med. Chem. Lett.* **2004**, *14*, 1177–1181.

[127] G. W. Rao, W. X. Hu, *Bioorganic Med. Chem. Lett.* **2006**, *16*, 3702–3705.

[128] C. A. Parker, C. G. Hatchard, *Trans. Faraday Soc.* **1961**, *57*, 1894–1904.

[129] G. Blasse, D. R. McMillin, *Chem. Phys. Lett.* **1980**, *70*, 1–3.

[130] M. N. Berberan-Santos, J. M. M. Garcia, *J. Am. Chem. Soc.* **1996**, *118*, 9391–9394.

[131] A. Endo, M. Ogasawara, A. Takahashi, D. Yokoyama, Y. Kato, C. Adachi, *Adv. Mater.* **2009**, *21*, 4802–4806.

[132] J. C. Deaton, S. C. Switalski, D. Y. Kondakov, R. H. Young, T. D. Pawlik, D. J. Giesen, S. B. Harkins, A. J. M. Miller, S. F. Mickenberg, J. C. Peters, *J. Am. Chem. Soc.* **2010**, *132*, 9499–9508.

[133] A. Endo, K. Sato, K. Yoshimura, T. Kai, A. Kawada, H. Miyazaki, C. Adachi, *Appl. Phys. Lett.* **2011**, *98*, 083302.

[134] H. Uoyama, K. Goushi, K. Shizu, H. Nomura, C. Adachi, *Nature* **2012**, *492*, 234–238.

[135] K. Goushi, K. Yoshida, K. Sato, C. Adachi, *Nat. Photonics* **2012**, *6*, 253–258.

[136] Y. Tao, K. Yuan, T. Chen, P. Xu, H. Li, R. Chen, C. Zheng, L. Zhang, W. Huang, *Adv. Mater.* **2014**, *26*, 7931–7958.

[137] F. B. Dias, T. J. Penfold, A. P. Monkman, *Methods Appl. Fluoresc.* **2017**, *5*, 012001.

[138] M. Y. Wong, E. Zysman-Colman, *Adv. Mater.* **2017**, *29*, 1605444.

[139] Y. Im, M. Kim, Y. J. Cho, J. A. Seo, K. S. Yook, J. Y. Lee, *Chem. Mater.* **2017**, *29*, 1946–1963.

[140] Z. Yang, Z. Mao, Z. Xie, Y. Zhang, S. Liu, J. Zhao, J. Xu, Z. Chi, M. P. Aldred, *Chem. Soc. Rev.* **2017**, *46*, 915–1016.

[141] X. Cao, D. Zhang, S. Zhang, Y. Tao, W. Huang, *J. Mater. Chem. C* **2017**, 7699–7714.

[142] M. A. Baldo, D. F. O'Brien, Y. You, A. Shoustikov, S. Sibley, M. E. Thompson, S. R. Forrest, *Nature* **1998**, *395*, 151–154.

[143] D. Y. Kondakov, T. D. Pawlik, T. K. Hatwar, J. P. Spindler, *J. Appl. Phys.* **2009**, *106*, 124510.

[144] P. Pander, F. B. Dias, *Disp. Imaging* **2017**, *2*, 249–263.

[145] S. I. Kato, Y. Yamada, H. Hiyoshi, K. Umezu, Y. Nakamura, *J. Org. Chem.* **2015**, *80*, 9076–9090.

[146] S. Hirata, Y. Sakai, K. Masui, H. Tanaka, S. Y. Lee, H. Nomura, N. Nakamura, M. Yasumatsu, H. Nakanotani, Q. Zhang, et al., *Nat. Mater.* **2015**, *14*, 330–336.

[147] S. Feuillastre, M. Pauton, L. Gao, A. Desmarchelier, A. J. Riives, D. Prim, D. Tondelier, B. Geffroy, G. Muller, G. Clavier, et al., *J. Am. Chem. Soc.* **2016**, *138*, 3990–3993.

[148] Y. J. Cho, B. D. Chin, S. K. Jeon, J. Y. Lee, *Adv. Funct. Mater.* **2015**, *25*, 6786–6792.

[149] I. S. Park, S. Y. Lee, C. Adachi, T. Yasuda, *Adv. Funct. Mater.* **2016**, *26*, 1813–1821.

[150] Y. J. Cho, K. S. Yook, J. Y. Lee, *Adv. Mater.* **2014**, *26*, 6642–6646.

[151] Y. J. Cho, S. K. Jeon, J. Y. Lee, *Adv. Opt. Mater.* **2016**, *4*, 688–693.

[152] D. Zhang, M. Cai, Y. Zhang, D. Zhang, L. Duan, *Mater. Horizons* **2016**, *3*, 145–151.

[153] Y. J. Cho, S. K. Jeon, B. D. Chin, E. Yu, J. Y. Lee, *Angew. Chemie - Int. Ed.* **2015**, *54*, 5201–5204.

[154] Y. Xiang, S. Gong, Y. Zhao, X. Yin, J. Luo, K. Wu, Z. H. Lu, C. Yang, *J. Mater. Chem. C* **2016**, *4*, 9998–10004.

[155] H. Tanaka, K. Shizu, H. Miyazaki, C. Adachi, *Chem. Commun.* **2012**, *48*, 11392–11394.

[156] T. Nakagawa, S. Y. Ku, K. T. Wong, C. Adachi, *Chem. Commun.* **2012**, *48*, 9580–9582.

[157] K. Kawasumi, T. Wu, T. Zhu, H. S. Chae, T. Van Voorhis, M. A. Baldo, T. M. Swager, *J. Am. Chem. Soc.* **2015**, *137*, 11908–11911.

[158] H. Tsujimoto, D.-G. Ha, G. Markopoulos, H. S. Chae, M. A. Baldo, T. M. Swager, *J. Am. Chem. Soc.* **2017**, *139*, 4894–4900.

[159] S. Shao, J. Hu, X. Wang, L. Wang, X. Jing, F. Wang, *J. Am. Chem. Soc.* **2017**, *139*, 17739–17742.

[160] S. Xu, T. Liu, Y. Mu, Y. F. Wang, Z. Chi, C. C. Lo, S. Liu, Y. Zhang, A. Lien, J. Xu, *Angew. Chemie - Int. Ed.* **2015**, *54*, 874–878.

[161] Z. Xie, C. Chen, S. Xu, J. Li, Y. Zhang, S. Liu, J. Xu, Z. Chi, *Angew. Chemie - Int. Ed.* **2015**, *54*, 7181–7184.

[162] T. Hatakeyama, K. Shiren, K. Nakajima, S. Nomura, S. Nakatsuka, K. Kinoshita, J. Ni, Y. Ono, T. Ikuta, *Adv. Mater.* **2016**, *28*, 2777–2781.

[163] M. Mamada, K. Inada, T. Komino, W. J. Potscavage, H. Nakanotani, C. Adachi, *ACS Cent. Sci.* **2017**, *3*, 769–777.

[164] F. B. Dias, K. N. Bourdakos, V. Jankus, K. C. Moss, T. Kamtekar, V. Bhalla, J. Santos, M. R. Bryce, A. P. Monkman, *Adv. Mater.* **2013**, *25*, 3707–3714.

[165] F. B. Dias, J. Santos, D. R. Graves, P. Data, R. S. Nobuyasu, M. A. Fox, A. S. Batsanov, T. Palmeira, M. N. Berberan-Santos, M. R. Bryce, et al., *Adv. Sci.* **2016**, *3*, 1600080.

[166] T. C. Wu, D. N. Congreve, M. A. Baldo, T. C. Wu, D. N. Congreve, M. A. Baldo, *Appl. Phys. Lett.* **2015**, *107*, 031103.

[167] T. Li, D. Yang, L. Zhai, S. Wang, B. Zhao, N. Fu, L. Wang, Y. Tao, W. Huang, *Adv. Sci.* **2017**, *4*, 1600166.

[168] X. Xiong, F. Song, J. Wang, Y. Zhang, Y. Xue, L. Sun, N. Jiang, P. Gao, L. Tian, X. Peng, *J. Am. Chem. Soc.* **2014**, *136*, 9590–9597.

[169] J. S. Ward, R. S. Nobuyasu, A. S. Batsanov, P. Data, A. P. Monkman, F. B. Dias, M. R. Bryce, *Chem. Commun.* **2016**, *52*, 2612–2615.

[170] Y. Zhang, H. Ma, S. Wang, Z. Li, K. Ye, J. Zhang, Y. Liu, Q. Peng, Y. Wang, *J. Phys. Chem. C* **2016**, *120*, 19759–19767.

[171] M. Okazaki, Y. Takeda, P. Data, P. Pander, H. Higginbotham, A. P. Monkman, S. Minakata, *Chem. Sci.* **2017**, *8*, 2677–2686.

[172] P. Rajamalli, N. Senthilkumar, P. Gandeepan, *J. Mater. Chem. C* **2016**, *4*, 900–904.

[173] R. Pashazadeh, P. Pander, A. Lazauskas, F. B. Dias, J. V. Grazulevicius, *J. Phys. Chem. Lett.* **2018**, *9*, 1172–1177.

[174] B. Xu, Y. Mu, Z. Mao, Z. Xie, H. Wu, Y. Zhang, C. Jin, Z. Chi, S. Liu, J. Xu, et al., *Chem. Sci.* **2016**, *7*, 2201–2206.

Chapter 2

Metal-free synthetic approach to 3-monosubstituted unsymmetrical 1,2,4,5-tetrazines

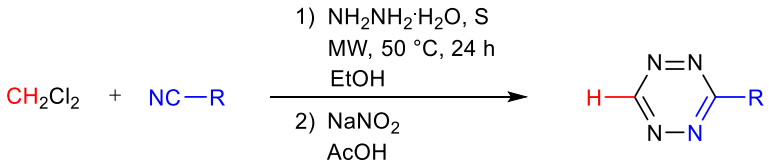

Y. Qu, F.-X. Sauvage, G. Clavier, F. Miomandre, P. Audebert, *Angew. Chem. Int. Ed.* **2018**, *57*, 12057–12061.

2.1 Introduction

In the first chapter, we have already discussed the prominent potential applications of 1,2,4,5-tetrazines. As a well-known electron-deficient heterocycle,[1] 1,2,4,5-tetrazines have been widely used in various application fields for many decades, such as organic electronics (e.g., OPVs, OFETs),[2–4] energetic materials,[5–7] coordination chemistry,[8–10] electrofluorochromism[11–14] and total synthesis of natural products.[15,16] More recently, tetrazine based click chemistry (also called inverse Electron Demand Diels–Alder reaction or iEDDA reaction) has become a powerful tool for decryption of biological messages from organisms,[17,18] including applications spanning biological imaging and detection, cancer targeting, drug delivery and biomaterials science.[19–30] As a result, the synthesis of reactive tetrazine reagents has recently attracted significant interest to the research community worldwide.

Despite the promising application potential of 1,2,4,5-tetrazines, the synthesis of some tetrazine molecules (e.g., unsymmetrical 1,2,4,5-tetrazines) which are useful for bio-orthogonal click chemistry is still challenging.[1,31] Therefore, in addition to designing new tetrazine reagents, developing synthetic routes that improve access to those broadly useful tetrazine molecules has recently become more and more valuable, because it not only eases the way to existing tetrazine applications but also facilitates the development of new applications.

The classical approach to prepare 1,2,4,5-tetrazines is a two-step procedure starting from the addition of hydrazine to nitrile precursors, followed by oxidation of the resulting 1,2-dihydrotetrazine.[1] However, this approach is usually not efficient for unsymmetrical tetrazines. 3-monosubstituted unsymmetrical 1,2,4,5-tetrazines were conventionally prepared from aromatic or alkyl nitrile precursors and formamidine salts, but yields are typically low, between 10% to 20%.[32] Recently, Devaraj et al. demonstrated an effective metal-catalyzed one-pot procedure to prepare 3-monosubstituted unsymmetrical 1,2,4,5-tetrazines.[33] This approach is currently intensively employed by scientists to prepare tetrazines useful for bio-orthogonal conjugation. However, the limitations of this approach are also obvious because it requires excess anhydrous hydrazine as the solvent (usually 50 equivalents to the nitrile precursors). Anhydrous hydrazine is an oily, highly toxic and hazardous reagent, which is commercially limited in several parts of the world, including Europe and China due to safety regulations. As a result, this synthetic procedure is limited to certain labs or companies. In addition, it also requires excess formamidine salts (usually 10 equiv.) and a non-neglectable amount of expensive metal catalysts (0.5 equiv.) (Therefore explaining the high prices of commercial clickable tetrazines, usually in the 1,000 $/g range). Moreover, the harsh conditions are not compatible with several functional

groups such as carbonyls and alkyl halides, which are susceptible to give either nucleophilic addition or reduction.[26]

In this chapter, a facile and efficient synthetic approach to 3-monosubstituted unsymmetrical 1,2,4,5-tetrazines which are very useful for bio-orthogonal reactions is presented. In this approach, 3-monosubstituted unsymmetrical 1,2,4,5-tetrazines are conveniently prepared in high yields using dichloromethane (DCM) as an initial reactant. To the best of our knowledge, this is the first time that DCM is recognized as a novel reactant in the chemistry of tetrazine synthesis. 11 unsymmetrical 1,2,4,5-tetrazine examples were synthesized with excellent yields (up to 75%) through this novel approach. The synthetic approach presented here readily offers an improved access to both 3-aryl and 3-alkyl unsymmetrical 1,2,4,5-tetrazines, which are expected to be widely utilized in various applications, particularly in tetrazine based click chemistry. Moreover, it opens the possibility that DCM could be utilized as a novel reagent in the synthesis of other heterocycles.

2.2 Synthesis

The reaction is shown in **Scheme 1**. DCM was selected as a novel starting material instead of the commonly used formamidine salts. Interestingly, DCM was found to exhibit a surprisingly good reactivity and selectivity in this reaction. As a result, only mild reaction conditions are required. Anhydrous hydrazine, which is highly dangerous, can be replaced by the much more stable hydrazine hydrate. In addition, ethanol was used as the solvent, along with 2 equivalents of sulfur. In this reaction, only 1 equivalent of DCM is required rather than excess amount (10 equiv.) of formamidine salts. It is also important to mention no metal catalyst is required in this novel approach.

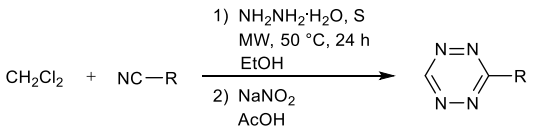

Scheme 1: Synthetic approach for 3-monosubstituted unsymmetrical 1,2,4,5-tetrazines.

The reaction conditions were firstly optimized by using 4-cyanophenylacetic acid as the nitrile precursor (**Table 1**), in particular because the resulting tetrazine **T1** is a well-known specifically useful tetrazine for bio-orthogonal applications.[17] It was found that the reaction temperature is very important to the outcome of this reaction. At 80 °C, the reaction was completed quickly within 6 hours, as most of the nitrile precursor was consumed as indicated by ^{1}H NMR (**Entry 1**). However, a large amount of unwanted side products was also formed, which led to a tedious purification procedure, and the product yield was

relatively low (38%). Interestingly, it was observed that the yield of the reaction increased significantly when decreasing the temperature. The best temperature was found to be 50 °C, leading to an excellent yield of product (72%, **Entry 3**). Moreover, almost no side product was formed in this case which makes the purification quite easy. It is noteworthy that further decreasing the temperature to 40 °C decreased the product yield again (**Entry 4**). In addition, sulfur addition was found to be very important in this reaction, as historically noticed in the Pinner reaction.[34,35] Acting as an inducer, 1 equivalent of sulfur led to a good yield, while slight excesses of sulfur still improved the yield of the reaction. Finally, addition of 2 equivalents of sulfur was found to give the best yield (72%). When no sulfur was used in the reaction, the nitrile precursor was mostly recovered and only a very low amount of product was observed (3%, **Entry 5**). However, addition of a larger excess of sulfur (4 equiv.) also lowered the product yield because of increased unwanted side reactions (**Entry 9**). It is important to note that the amount of sulfur added was also found to be important when elucidating the mechanism of the reaction (see **2.3 Mechanism**). Microwave heating was employed for all the reactions, but heating in a sealed tube also worked well, with only minor changes to the product yield.

Table 1: Optimization of the reaction conditions[(a)].

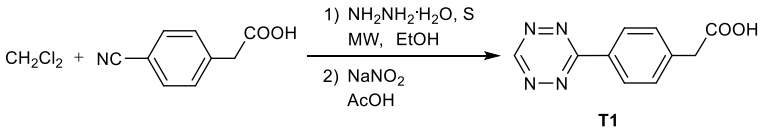

T1

Entry	Temp., time	S	Yield [%][(b)]
1	80 °C, 6 h	2 equiv.	38
2	60°C, 24 h	2 equiv.	61
3	50 °C, 24 h	2 equiv.	72
4	40 °C, 24 h	2 equiv.	40
5	50 °C, 24 h	0 equiv.	3
6	50 °C, 24 h	1 equiv.	45
7	50 °C, 24 h	1.2 equiv.	62
8	50 °C, 24 h	1.5 equiv.	70
9	50 °C, 24 h	4 equiv.	55

(a) All reactions were carried out on a 0.5 mmol scale in 0.5 ml EtOH. 1 equiv. DCM, 1 equiv. nitrile precursor and 8 equiv. hydrazine hydrate (MW = microwave, equiv. = equivalents). (b) Yields (isolated) based on the nitrile precursor.

In order to extend the scope of this synthetic approach, we started to apply this approach to various benzonitrile substrates, and therefore a series of 3-monosubstituted unsymmetrical 1,2,4,5-tetrazines were successfully prepared (**Table 2**). At first, four unsymmetrical tetrazines **T1-T4** which are useful for bio-orthogonal conjugation were successfully prepared in good to high yields (40%-72%). One interesting result to mention is tetrazine **T3** with hydroxyl group, which could be prepared by using 4-(aminomethyl)benzonitrile hydrochloride as the nitrile precursor in a high yield (71%, **Scheme 2**). It is likely that the nitrous acid (HNO_2) used in the oxidation step could also react with the primary amine to give the alcohol. The product yield is higher than the yield of the reaction when employing the "normal" nitrile precursor 4-(hydroxymethyl) benzonitrile (64%). Furthermore, the price of 4-(hydroxymethyl)benzonitrile price is much higher than the one of 4-(aminomethyl)benzonitrile hydrochloride. Therefore, this last substrate offers a more efficient and cheaper pathway to tetrazine **T3**. On the other hand, when the amine is protected with a Boc group, the transformation to the alcohol is not observed affording a convenient way to obtain the amine functionalized derivative **T4**.

Table 2: Synthesis of 3-monosubstituted unsymmetrical tetrazines **T1**-**T11**[(a)].

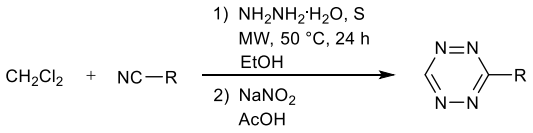

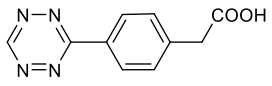

T1, 72%

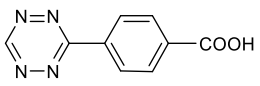

T2, 70%

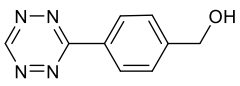

T3, 64%, 71%[(b)]

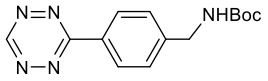

T4, 40%

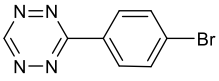

T5, 38%[(c)]

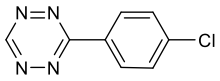

T6, 54%

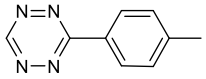

T7, 56%

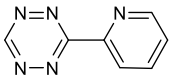

T8, 43%

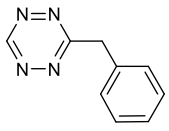

T9, 45%

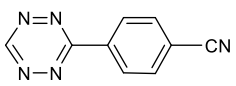

T10, 61%

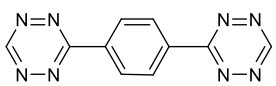

T11, 75%[(d)]

(a) Reactions were carried out on a 1 mmol scale in 1 ml EtOH. Yields (isolated) based on the starting nitrile. 1 equiv. DCM, 1 equiv. nitrile precursor, 2 equiv. sulfur and 8 equiv. hydrazine hydrate (except **T11**).
(b) **T3** was alternatively prepared using 4-(aminomethyl)benzonitrile hydrochloride as the nitrile precursor.

(c) 0.2 ml DMF as co-solvent. (d) 2 equiv. DCM, 1 equiv. nitrile precursor, 4 equiv. sulfur and 16 equiv. hydrazine hydrate.

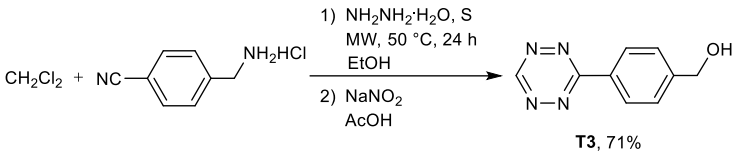

Scheme 2: Synthesis of **T3** using 4-(aminomethyl)benzonitrile hydrochloride as the nitrile precursor.

Monosubstituted Tetrazines **T5**-**T8** were also readily synthesized through our novel synthetic approach in good to high yields. It is important to mention that **T5** and **T6** are useful materials for further preparation of new photo and/or electroactive molecular materials through coupling reactions, and some results will be presented in **Chapter 4**. Another important result we observed is that unsymmetrical alkyl tetrazines could also be readily prepared through this approach. Tetrazine **T9** was directly prepared from the respective alkyl nitrile precursor (benzyl cyanide) and DCM in a good yield (45%).

Remarkably, when using 1,4-dicyanobenzene as the nitrile precursor, the two cyano groups could be sequentially converted to tetrazine groups. As a result, both tetrazine **T10** and **T11** were synthesized in high yields (61%-75%). Notably, **T11** is a di-tetrazine molecule which has two functional sites adapted for click reactions, which could potentially serve as a bifunctional bio-orthogonal tetrazine reagent.

It is worth mentioning, however, that the reaction did not work in a few trials with other chloro-reagent, such as dichloroethane (CH_3CHCl_2) or chloroform ($CHCl_3$) (**Scheme 3**), and is probably limited to DCM (CH_2Cl_2) as a synthon.

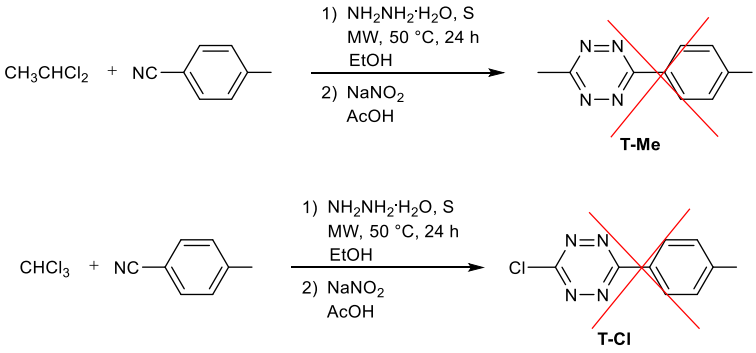

Scheme 3: Attempts to synthesize **T-Me** and **T-Cl** using dichloroethane (CH_3CHCl_2) or chloroform ($CHCl_3$) as reactants.

2.3 Mechanism

To study the mechanism of this new reaction, the participation of DCM (CH_2Cl_2) in the tetrazine ring formation was firstly confirmed by employing ^{13}C labelled DCM ($^{13}CH_2Cl_2$) as a reactant (**Scheme 4**). The doublet signal at 10.17 ppm ($^1J_{CH}$ = 212.04 Hz) in the ^1H NMR spectrum and the super high intensity of singlet signal at 157.73 ppm in the ^{13}C NMR spectrum (**Figure 1**), which could be assigned respectively to the proton and carbon of H-^{13}C group, clearly indicate the incorporation of ^{13}C into the tetrazine ring. Additionally, the C-3 carbon which shows a doublet signal at 166.61 ppm ($^3J_{CC}$ = 29.20 Hz) in the ^{13}C NMR spectrum also supports the incorporation of ^{13}C into the tetrazine ring of **T12**.

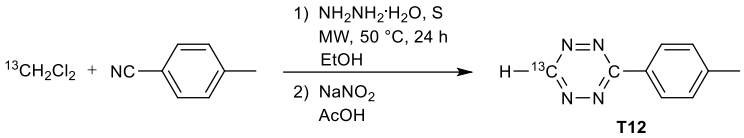

Scheme 4: Synthesis of **T12** employing $^{13}CH_2Cl_2$ as a reactant.

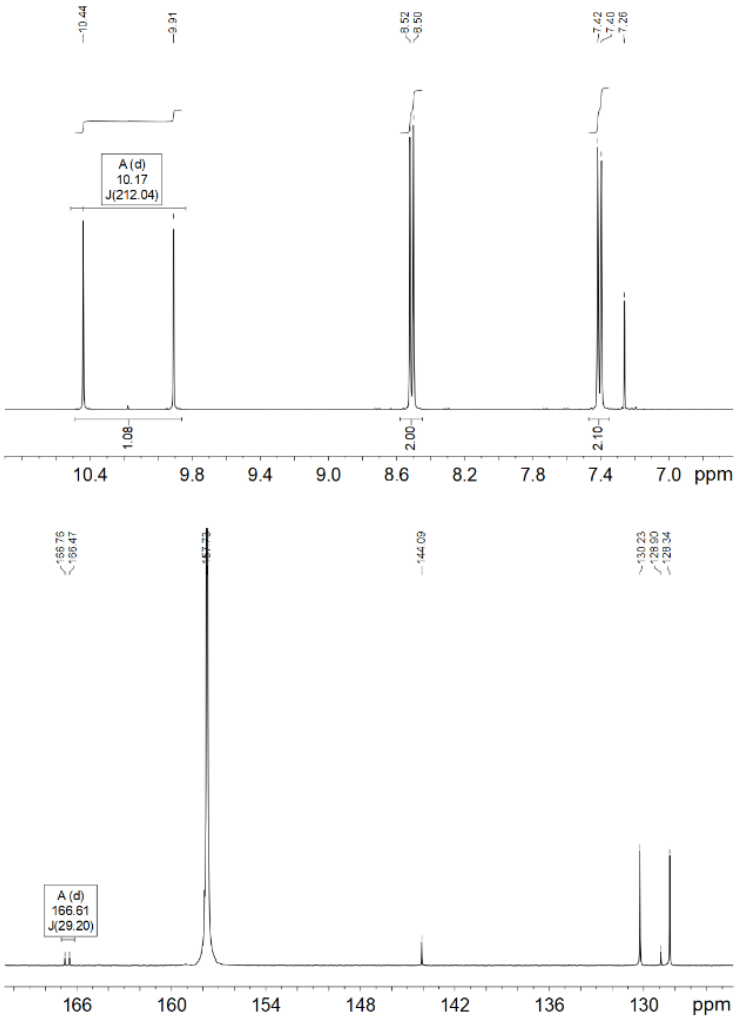

Figure 1: ^{1}H NMR ((**upper**, 400 MHz, $CDCl_3$) and ^{13}C NMR (**lower**, 100 MHz, $CDCl_3$) spectra of **T12**. Only downfield parts of the spectra are shown here for clarity sake.

It is commonly agreed that the formation of 1,2,4,5-tetrazine is a two-step synthetic sequence starting from the nucleophilic attack of nitrile precursor by sulfur activated hydrazine, followed by oxidation of the resulting 1,2-dihydrotetrazine.[1] Due to the fact that no standard “Pinner” product is formed with only 1 equivalent of DCM added, the first step is likely to be the addition of the sulfur-activated hydrazine on DCM. Then a second substitution step follows on the second chlorine, rendered more reactive because of the first addition. As a noticeable amount of product is formed with as little as 1 equivalent of sulfur (despite 2 equivalents improved the yields), and that the dihydrotetrazine is formed before the oxidant addition, it is proposed that hydrazine alone reacts in this second addition step. Afterwards, addition on the nitrile likely occurs, it does not matter which terminal nitrogen attacks at the cyano group, because the following cyclization step leads to the same ring. Finally, a double elimination occurs, before the final oxidative aromatization step. Following this reasoning, a possible mechanism for the tetrazine ring formation using CH_2Cl_2 as a reactant is proposed and presented in **Scheme 5**.

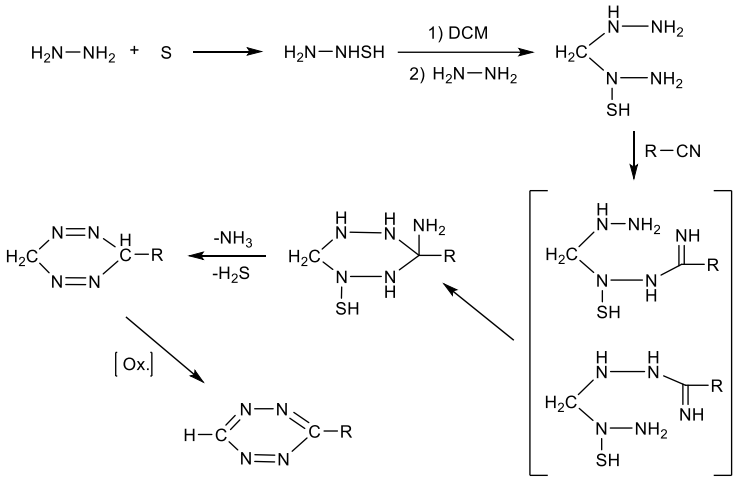

Scheme 5: Proposed mechanism for tetrazine ring formation using CH_2Cl_2 as a reactant.

In order to support the proposed mechanism, we have investigated the influence of amounts of sulfur in this reaction (**Table 1**) to support the idea that the activated hydrazine was only implicated in the first addition step, and not further. It turned out that 1.2 equivalents of sulfur already leads to a very good yield, and 1.5 equivalents give almost the same high yield as 2 equivalents. This indicates that addition of sulfur amount in moderate excess to 1 equivalent is sufficient for the reaction to proceed. The excess amount probably serves to compensate for a non-quantitative formation of the sulfur-hydrazine activated nucleophile due to the heterogenous reaction. These results strongly

suggest that only 1 equivalent of activated sulfur-hydrazine is required in the first step of the reaction process, and 1 equivalent of hydrazine alone is involved afterwards in the following step, as proposed in **Scheme 5**.

2.4 Photophysical properties

The photophysical data of tetrazine derivatives **T1-T9** are given in **Table 3**. All the tetrazines present an absorption band in the visible with a maximum located around 535 nm and a rather low extinction coefficient, which is typical of tetrazine derivatives. Unfortunately, all the tetrazines show a very weak emission (only **T5** shows a PLQY over 1%). The low PLQYs for these tetrazines were expected as it is known that only tetrazines substituted with heteroatoms are highly emissive.[1]

Table 3: Photophysical data of **T1-T9**.

	λ_{Abs} (nm)[(a)]	λ_{FL} (nm)[(b)]	Φ_{PL}(%)[(c)]
T1	536 (300)	595	0.2%
T2	534 (270)	/	/
T3	535 (750)	581	0.2%
T4	535 (500)	598	0.2%
T5	533 (580)	577	1.4%
T6	533 (880)	575	0.1%
T7	535 (930)	578	0.2%
T9	535 (400)	587	0.2%

(a) Absorption maxima measured in acetonitrile (1×10^{-5} M) at room temperature. Values in brackets are extinction coefficients. (b) Emission maxima measured in acetonitrile (1×10^{-5} M) at room temperature (c) Photoluminescence quantum yields of compounds in acetonitrile at room temperature.

2.5 Electrochemistry

The electrochemistry of tetrazine derivatives **T1-T9** was studied in solution in acetonitrile. Two types of cyclic voltammetries (CV) are observed:

I. For non-acidic compounds a nicely reversible CV is observed (**Figure 2**, full green line).

II. For acidic compounds (**T1-T2**), a fully irreversible reduction peak can be seen (**Figure 2**, dotted red line)

All CVs have been compared to a standard (chloroethoxytetrazine) to assess the number of electrons exchanged on one hand and the standard potential on the other hand. Using a standard allows one to get rid of electrode surface issues for the relation between peak current and number of electrons and of reference drift for the determination of standard potential.

The results are summarized in **Table 4**. All compounds behaving reversibly shows a one-electron reduction as expected, leading to the anion radical which is thus stable at the timescale of cyclic voltammetry. Moreover, the standard potentials for the redox couples formed by the tetrazines and their anion radicals all lie around -1.35 V vs. Fc which is similar to tetrazines substituted by donating aromatic groups like pyrrole or thiophene.[1] It can be noticed that **T5-T6** have a more positive reduction potential of ca. +0.1 V in agreement with the withdrawing character of the halogen substituents borne by the tetrazine core. This demonstrates that the redox potentials of these tetrazine derivatives are actually sensitive to the electronic properties of the substituent.

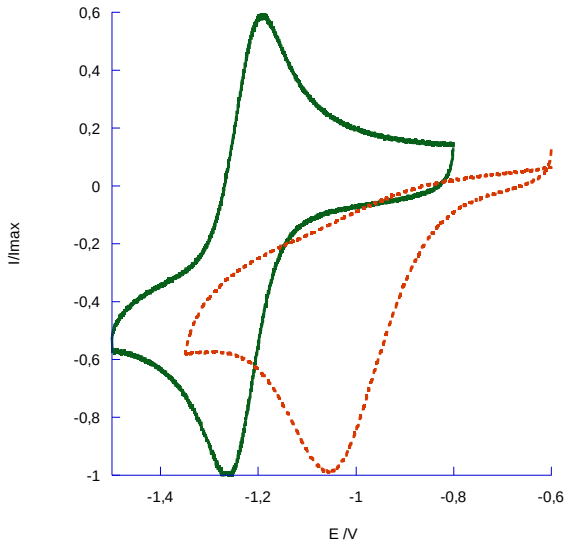

Figure 2: CVs of **T7** (full green line) and **T1** (dotted red line) in acetonitrile (+$TBAPF_6$) on glassy carbon electrode at 0.1 V/s. Currents are normalized vs. the peak cathodic value for clarity sake.

The two compounds substituted with acidic functions show a non-reversible electrochemical behavior assigned to the rapid protonation of the anion radical. This leads to more positive reduction potential (typically -1.14 V for the peak reduction potential of **T1**) in agreement with an internal 'EC' mechanism. Besides the number of electrons exchanged which has been found close to 2 is in agreement with a '$2H^+ + 2e^-$' mechanism

similar to quinone reduction. Typically after the one-electron first reduction and fast protonation, the generated radical is further reduced even faster, and the anion protonated again.

Table 4: Electrochemical data for **T1-T9**[(a)]

	Standard potential /V vs. Fc^+/Fc	**Exp. det. number of electrons exchanged**
T1	n.d.	2.25
T2	n.d.	1.88
T3	-1.33	0.97
T4	-1.35	0.98
T5	-1.23	0.89
T6	-1.24	1.12
T7	-1.32	0.95
T9	-1.35	0.97

(a) In acetonitrile (+$TBAPF_6$) on glassy carbon electrode. n.d. = not defined.

***Note**: The photophysics and electrochemistry in this chapter were studied by an internship student Francois-Xavier Sauvage from our group PPSM.

2.6 Conclusion

In this chapter, we have presented a facile, efficient and metal-free synthetic approach to 3-monosubstituted unsymmetrical 1,2,4,5-tetrazines. DCM has been demonstrated to be a novel alternative reagent to formamidine salts in the unsymmetrical tetrazine synthesis. It exhibits an excellent reactivity and selectivity in the process of tetrazine ring formation, resulting in high product yields and mild reaction conditions. This is the first time that DCM is recognized as a novel reactant useful for tetrazine synthesis, and it opens the possibility that it could be utilized as a novel reagent in the synthesis of other heterocycles. Eleven 3-monosubstituted unsymmetrical 1,2,4,5-tetrazine derivatives were therefore readily prepared employing this novel synthetic approach, among which some tetrazines are already used in bio-orthogonal reactions, as well as other application fields (e.g., photo and/or electroactive molecular materials).

2.7 Experimental details

General Methods:

Synthesis. All chemicals were received from commercial sources and used without further purification. Microwave reactions were performed on a microwave synthesis reactor (Anton Paar Monowave 300). Thin layer chromatography (TLC) analysis were performed on silica gel. Column chromatography purifications were performed with SDS 0.040–0.063 mm silica gel. All mixtures of solvents are given in v/v ratio. NMR spectra were recorded on a JEOL ECS (400 MHz) spectrometer. ^{13}C NMR spectra were proton decoupled. HRMS spectra were measured either on an UPLC/ESI-HRMS device (an Acquity Waters UPLC system coupled to a Waters LCT Premier XE mass spectrometer equipped with an electrospray ion source), or a Q-TOF mass spectrometer (Q-TOF 6540, Agilent) equipped with an APPI ion source. Melting points (m.p.) were determined on a Heizbank System Kofler type WME (Wagner & Munz).

Photophysics. Fluorescence spectra were measured on a Fluorolog3 spectrofluorimeter (Horiba) in quartz cuvettes using solutions of tetrazines 6.10^{-4} M in acetonitrile (Spectroscopic grade). Before each measurement UV-vis spectra were recorded on a Cary 4000 spectrophotometer (Agilent) to determine the maximum absorption wavelength and check that the corresponding absorbance is lower than 0.1. Quantum yields were determined using chloroethoxytetrazine (Φ_{PL} = 0.4) as the standard.

Electrochemistry. Cyclic voltammetry was performed with a potentiostat Versastat4 (Ametek) in small volume electrochemical cells (2-3 mL) on solutions of tetrazine (ca. 1 mM) in acetonitrile (HPLC grade) with tetrabutylammonium tetrafluoroborate (0.1 M) as the supporting electrolyte. Glassy carbon (1 mm diameter) was used as the working electrode after polishing on a 1 µm diamond slurry. Platinum wire was used as the counter electrode. $Ag|Ag^+(10^{-2}$ M) in acetonitrile was used as the reference electrode and calibrated vs. chloroethoxytetrazine as the standard.

General procedure for synthesis of T1-T10.

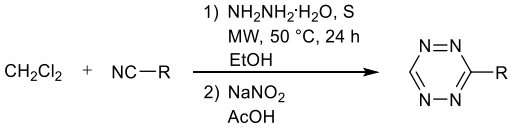

Nitrile substrate (1 mmol), CH_2Cl_2 (1 mmol, 63.70 µl), sulfur (2 mmol, 64 mg) and ethanol (1 ml) were mixed together in a 30 ml microwave reaction tube. Hydrazine monohydrate (8 mmol, 0.4 ml) was added slowly with stirring afterwards. The vessel was sealed and the reaction mixture was heated at 50 °C for 24 hours. (Caution should be exercised due to

the elevated pressure in the sealed reaction vessel when heating, particularly attempting scale up). Then 3 ml of CH_2Cl_2 and sodium nitrite (10 mmol, 0.69 g) in 10 ml of H_2O were added to the mixture. Excess acetic acid (60 mmol, 3.42 ml) was then added slowly at 0 °C, during which the solution turned bright red in color. The reaction mixture was extracted with dichloromethane. The organic phase was dried over anhydrous magnesium sulfate ($MgSO_4$), filtered and concentrated under reduced pressure. The resulting residue was purified using silica gel chromatography.

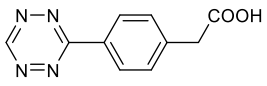

T1

T1: A red crystalline solid was obtained after column chromatography (CH_2Cl_2:acetic acid = 50:1) (155 mg, yield: 72%). ^{1}H NMR (400 MHz, $CDCl_3$, δ): 10.22 (s, 1H), 8.62 (d, *J* = 8.24 Hz, 2H), 7.55 (d, *J* = 8.24 Hz, 2H), 3.80 (s, 2H) ppm; ^{13}C NMR (100 MHz, $CDCl_3$, δ): 175.09, 166.38, 157.99, 138.79, 130.89, 130.65, 128.76, 40.81 ppm; HRMS $[M+H]^+$ m/z calcd. for $[C_{10}H_9N_4O_2]^+$ 217.0726, found 217.0722; m.p. 183 °C.

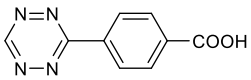

T2

T2: The reaction mixture was extracted with ethyl acetate instead of dichloromethane due to the low solubility of the crude mixture in dichloromethane. A red solid was obtained after column chromatography (Petroleum ether:EtOAc:acetic acid = 50:50:1) (141 mg, yield: 70%). ^{1}H NMR (400 MHz, DMSO-d_6, δ): 10.66 (s, 1H), 8.62 (d, *J* = 8.24 Hz, 2H), 8.22 (d, *J* = 8.24 Hz, 2H) ppm; ^{13}C NMR (100 MHz, DMSO-d_6, δ): 166.73, 165.11, 158.29, 135.73, 134.37, 130.25, 128.01 ppm; HRMS $[M-H]^-$ m/z calcd. for $[C_9H_5N_4O_2]^-$ 201.0413, found 201.0412; m.p. 199 °C.

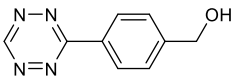

T3

T3: A red crystalline solid was obtained after column chromatography (Petroleum ether:EtOAc = 3:1) (120 mg, yield: 64%; 133mg, yield: 71% when using 4-(aminomethyl)-benzonitrile hydrochloride as nitrile precursor). ^{1}H NMR (400 MHz, $CDCl_3$, δ): 10.22 (s, 1H), 8.62 (d, *J* = 8.24 Hz, 2H), 7.61 (d, *J* = 8.24 Hz, 2H), 4.86 (d, *J* = 5.80 Hz, 2H), 1.93 (d, *J* = 5.80 Hz, 1H) ppm; ^{13}C NMR (100 MHz, $CDCl_3$, δ): 166.47, 157.94, 146.43, 130.88, 128.67,

127.59, 64.83 ppm; HRMS $[M+H]^+$ m/z calcd. for $[C_9H_9N_4O]^+$ 189.0776, found 189.0773; m.p. 105 °C.

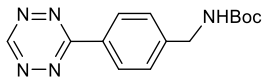

T4

T4: A pink solid was obtained after column chromatography (Petroleum ether:EtOAc = 5:1 and CH_2Cl_2:EtOAc = 100:1) (114 mg, yield: 40%). ^1H NMR (400 MHz, $CDCl_3$, δ): 10.21 (s, 1H), 8.60 (d, *J* = 8.24 Hz, 2H), 7.52 (d, *J* = 8.24 Hz, 2H), 4.99 (s, br, 1H), 4.45 (d, *J* = 5.95 Hz, 2H), 1.48 (s, 9H) ppm; ^{13}C NMR (100 MHz, $CDCl_3$, δ): 166.43, 157.93, 156.07, 144.79, 130.67, 128.73, 128.28, 80.06, 44.48, 28.53 ppm; HRMS $[M+H]^+$ m/z calcd. for $[C_{14}H_{17}N_5O_2]^+$ 288.1461, found 288.1469; m.p. 123 °C.

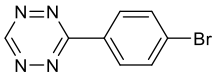

T5

T5: 0.2 ml DMF was added as co-solvent. A red solid was obtained after column chromatography (Petroleum ether:CH_2Cl_2 = 2:1) (90 mg, yield: 38%). ^1H NMR (400 MHz, $CDCl_3$, δ): 10.25 (s, 1H), 8.51 (d, *J* = 8.70 Hz, 2H), 7.76 (d, *J* = 8.70 Hz, 2H) ppm; ^{13}C NMR (100 MHz, $CDCl_3$, δ): 166.12, 158.04, 132.89, 130.62, 129.82, 128.64 ppm; HRMS $[M]^+$ m/z calcd. for $[C_8H_5BrN_4]^+$ 235.9704, found 235.9692; m.p. 176±2 °C (lit.[36] m.p. 182-184 °C).

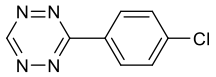

T6

T6: A red solid was obtained after column chromatography (Petroleum ether:CH_2Cl_2 = 2:1) (103 mg, yield: 54%). ^1H NMR (400 MHz, $CDCl_3$, δ): 10.24 (s, 1H), 8.58 (d, *J* = 8.70 Hz, 2H), 7.59 (d, *J* = 8.70 Hz, 2H) ppm; ^{13}C NMR (100 MHz, $CDCl_3$, δ): 165.98, 157.99, 139.98, 130.16, 129.91, 129.69 ppm; HRMS $[M+H]^+$ m/z calcd. for $[C_8H_7ClN_4]^+$ 194.0358, found 194.0354; m.p. 166 °C (lit.[36] m.p. 164-167 °C).

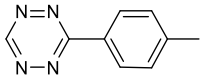

T7

T7: A red solid was obtained after column chromatography (Petroleum ether:CH_2Cl_2 = 2:1) (96 mg, yield: 56%). ^{1}H NMR (400 MHz, $CDCl_3$, δ): 10.19 (s, 1H), 8.52 (d, *J* = 8.24 Hz, 2H), 7.42 (d, *J* = 8.24 Hz, 2H), 2.49 (s, 3H) ppm; ^{13}C NMR (100 MHz, $CDCl_3$, δ): 166.65, 157.80, 144.15, 130.29, 128.96, 128.41, 21.89 ppm; HRMS $[M+H]^+$ m/z calcd. for $[C_9H_9N_4]^+$ 173.0819, found 173.0822; m.p. 88 °C (lit.[36] m.p. 86-88 °C).

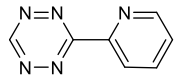

T8

T8: A red crystalline solid was obtained silica column chromatography (Petroleum ether:EtOAc = 1:1) (68 mg, yield: 43%). ^{1}H NMR (400 MHz, $CDCl_3$, δ): 10.35 (s, 1H), 8.96 (d, *J* = 4.58 Hz, 1H), 8.67 (d, *J* = 7.79 Hz, 1H), 7.99 (t, *J* = 7.79 Hz, 1H), 7.58 (dd, *J* = 7.79 Hz, *J* = 4.58 Hz, 1H) ppm; ^{13}C NMR (100 MHz, $CDCl_3$, δ): 165.92, 158.50, 151.18, 150.07, 137.67, 126.90, 124.46 ppm; HRMS $[M+H]^+$ m/z calcd. for $[C_7H_6N_5]^+$ 160.0623, found 160.0625; m.p. 116 °C.

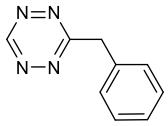

T9

T9: A red oil was obtained after column chromatography (Petroleum ether:CH_2Cl_2 = 2:1) (77 mg, yield: 45%). ^{1}H NMR (400 MHz, $CDCl_3$, δ): 10.19 (s, 1H), 7.43 (d, *J* = 8.24 Hz, 2H), 7.34 (dd, *J* = 8.24 Hz, *J* = 7.33 Hz, 2H), 7.28 (d, *J* = 7.33 Hz, 1H), 4.67 (s, 2H) ppm; ^{13}C NMR (100 MHz, $CDCl_3$, δ): 171.99, 158.12, 135.61, 129.35, 129.08, 127.61, 41.87 ppm; HRMS $[M]^+$ m/z calcd. for $[C_{10}H_8N_4]^+$ 172.0750, found 172.0743.

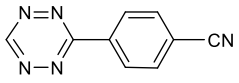

T10

T10: A red crystalline solid was obtained after column chromatography (Petroleum ether:CH_2Cl_2 = 1:1) (111 mg, yield: 61%). ^{1}H NMR (400 MHz, $CDCl_3$, δ): 10.32 (s, 1H), 8.78 (d, *J* = 8.70 Hz, 2H), 7.92 (d, *J* = 8.70 Hz, 2H) ppm; ^{13}C NMR (100 MHz, $CDCl_3$, δ): 165.47, 158.28, 135.65, 133.21, 128.82, 118.11, 116.71 ppm; m.p. 166 °C.

Synthesis of T11

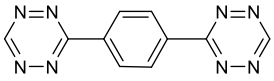

T11

1,4-Dicyanobenzene (1 mmol, 130 mg), CH_2Cl_2 (2 mmol, 127.50 µl), sulfur (4 mmol, 128 mg) and ethanol (1 ml) were mixed together in a 30 ml microwave reaction tube. Hydrazine monohydrate (16 mmol, 0.8 ml) was added slowly with stirring afterwards. The vessel was sealed and the reaction mixture was heated at 50 °C for 24 hours. (Caution should be exercised due to the elevated pressure in the sealed reaction vessel when heating, particularly attempting scale up). Then 3 ml of CH_2Cl_2 and sodium nitrite (20 mmol, 1.38 g) in 10 ml of H_2O were added to the mixture. Excess acetic acid (120 mmol, 6.84 ml) was then added slowly at 0 °C, during which the solution turned bright red in color. The reaction mixture was extracted with dichloromethane. The organic phase was dried over anhydrous magnesium sulfate ($MgSO_4$), filtered and concentrated under reduced pressure. The resulting residue was purified by column chromatography on silica gel.

A red crystalline solid was obtained after column chromatography (Petroleum ether: CH_2Cl_2 = 1:3) (178 mg, yield: 75%). ^{1}H NMR (400 MHz, DMSO-d_6, δ): 10.65 (s, 2H), 8.79 (s, 4H) ppm; ^{13}C NMR (100 MHz, DMSO-d_6, δ): 165.74, 158.74, 136.23, 129.29 ppm; m.p. 263±2 °C.

Synthesis of T12

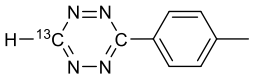

T12

4-Methylbenzonitrile (1 mmol, 118 mg), $^{13}CH_2Cl_2$ (1 mmol, 63.70 µl), sulfur (2 mmol, 64 mg) and ethanol (1 ml) were mixed together in a 30 ml microwave reaction tube. Hydrazine monohydrate (8 mmol, 0.4 ml) was added slowly with stirring afterwards. The vessel was sealed and the reaction mixture was heated at 50 °C for 24 hours. (Caution should be exercised due to the elevated pressure in the sealed reaction vessel when heating, particularly attempting scale up). Then 3 ml of CH_2Cl_2 and sodium nitrite (10 mmol, 0.69 g) in 10 ml of H_2O were added to the mixture. Excess acetic acid (60 mmol, 3.42 ml) was then added slowly at 0 °C, during which the solution turned bright red in color. The reaction mixture was extracted with dichloromethane. The organic phase was dried over anhydrous magnesium sulfate ($MgSO_4$), filtered and concentrated under reduced pressure. The resulting residue was purified by column chromatography on silica gel.

A red solid was obtained after column chromatography (Petroleum ether:CH_2Cl_2 = 2:1) (88 mg, yield: 51%). ^{1}H NMR (400 MHz, $CDCl_3$, δ): 10.17 (d, $^1J_{CH}$ = 212.04 Hz, 1H), 8.51 (d, $^3J_{HH}$ = 8.24 Hz, 2H), 7.41 (d, $^3J_{HH}$ = 8.24 Hz, 2H), 2.48 (s, 3H) ppm; ^{13}C NMR (100 MHz,

$CDCl_3$, δ): 166.61 (d, $^3J_{CC}$ = 29.20 Hz), 157.73, 144.09, 130.23, 128.89, 128.34, 21.82 ppm; HRMS $[M+H]^+$ m/z calcd. for $[C_8{}^{13}CH_9N_4]^+$ 174.0855, found 174.0857.

Synthesis of T1 using a sealed pressure tube

4-Cyanophenylacetic acid (1 mmol, 161 mg), CH_2Cl_2 (1 mmol, 63.70 µl), sulfur (2 mmol, 64 mg) and ethanol (1 ml) were mixed together in a pressure tube reactor. Hydrazine monohydrate (8 mmol, 0.4 ml) was added slowly with stirring afterwards. The tube was sealed and the reaction mixture was heated at 50 °C for 24 hours. (Caution should be exercised due to the elevated pressure in the sealed reaction vessel when heating, particularly attempting scale up). Then 3 ml of CH_2Cl_2 and sodium nitrite (10 mmol, 0.69 g) in 10 ml of H_2O were added to the mixture. Excess acetic acid (60 mmol, 3.42 ml) was then added slowly at 0 °C, during which the solution turned bright red in color. The reaction mixture was extracted with dichloromethane. The organic phase was dried over anhydrous magnesium sulfate ($MgSO_4$), filtered and concentrated under reduced pressure. The resulting residue was purified by column chromatography on silica gel (CH_2Cl_2:acetic acid = 50:1) to give 147 mg of **T1**. (Yield: 68%).

Inverse electron demand Diels–Alder reaction (iEDDA) of T10 and T11

To further confirm the structures of tetrazines we have obtained, **T10** and **T11** were subjected to iEDDA reaction with cyclooctyne. Cyclooctyne was prepared according to published procedure.[37] Both reactions proceeded at room temperature in dichloromethane (DCM), and completed quickly within a few minutes. This is in accordance with the known high reactivity of 3-monosubstituted unsymmetrical 1,2,4,5-tetrazines.

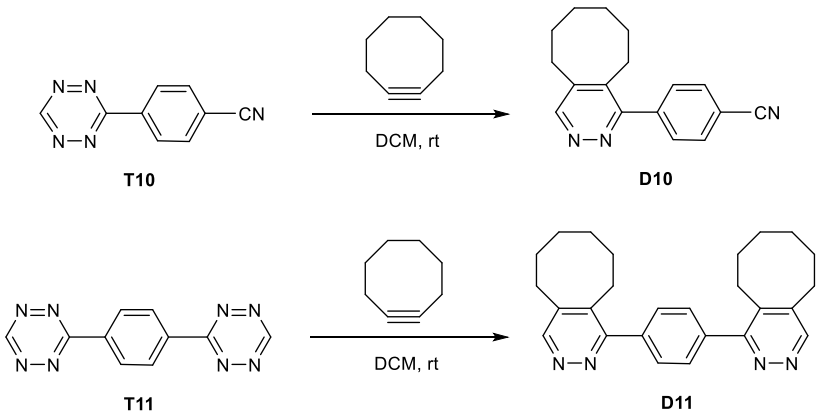

To a 10 mL round bottom flask equipped with a stir bar, 0.05 mmol of **T10** or **T11** (9.2 mg or 11.9 mg), and 4 mL of DCM were added. Then 0.2 mmol of cyclooctyne (25 µL) was added with stirring at room temperature. The color of the solution turned from bright red to colorless immediately and N_2 gas evolved. The reaction mixture was allowed to stir for

another 10 min, and then all the volatiles were evaporated under vacuum. The products were subjected to characterization without further purification required.

D10 (13 mg, white solid, yield: 99%)

^{1}H NMR (400 MHz, $CDCl_3$, δ): 8.94 (s, 1H), 7.79 (d, *J* = 8.4 Hz, 2H), 7.61 (d, *J* = 8.4 Hz, 2H), 2.89-2.80 (m, 2H), 2.77-2.67 (m, 2H), 1.86-1.76 (m, 2H), 1.59-1.51 (m, 2H), 1.49-1.42 (m, 2H), 1.41-1.33 (m, 2H) ppm; ^{13}C NMR (100 MHz, $CDCl_3$, δ): 160.34, 152.01, 142.53, 141.77, 138.60, 132.29, 130.07, 118.65, 112,74, 31.20, 30.38, 29.62, 26.54, 25.99, 25.41 ppm; HRMS $[M+H]^+$ m/z calcd. for $[C_{17}H_{18}N_3]^+$ 264.1495, found 264.1494; m.p. 170 °C.

D11 (19.8 mg, white solid, yield: 99%)

^{1}H NMR (400 MHz, $CDCl_3$, δ): 8.93 (s, 2H), 7.60 (s, 4H), 2.88-2.82 (m, 4H), 2.82-2.76 (m, 4H), 1.87-1.77 (m, 4H), 1.64-1.54 (m, 4H), 1.52-1.43 (m, 4H), 1.43-1.34 (m, 4H) ppm; ^{13}C NMR (100 MHz, $CDCl_3$, δ): 161.73, 151.74, 141.55, 139.09, 138.21, 129.17, 31.29, 30.49, 29.67, 26.60, 26.06, 25.54 ppm; HRMS $[M+H]^+$ m/z calcd. for $[C_{26}H_{31}N_4]^+$ 399.2543, found 399.2541.

2.8 Reference

[1] G. Clavier, P. Audebert, *Chem. Rev.* **2010**, *110*, 3299–3314.

[2] D. K. Hwang, R. R. Dasari, M. Fenoll, V. Alain-Rizzo, A. Dindar, J. W. Shim, N. Deb, C. Fuentes-Hernandez, S. Barlow, D. G. Bucknall, et al., *Adv. Mater.* **2012**, *24*, 4445–4450.

[3] Z. Li, J. Ding, N. Song, J. Lu, Y. Tao, *J. Am. Chem. Soc.* **2010**, 8–9.

[4] Z. Li, J. Ding, N. Song, X. Du, J. Zhou, J. Lu, Y. Tao, *Chem. Mater.* **2011**, *23*, 1977–1984.

[5] D. E. Chavez, D. A. Parrish, L. Mitchell, G. H. Imler, *Angew. Chemie - Int. Ed.* **2017**, *56*, 3575–3578.

[6] M. Marin, V. Lhiaubet-Vallet, C. Paris, M. Yamaji, M. A. Miranda, *Photochem. Photobiol. Sci.* **2011**, *10*, 1474–1479.

[7] M. H. V Huynh, M. A. Hiskey, D. E. Chavez, D. L. Naud, R. D. Gilardi, *J. Am. Chem. Soc.* **2005**, *127*, 12537–12543.

[8] T. S. M. Tang, H. W. Liu, K. K. W. Lo, *Chem. Commun.* **2017**, *53*, 3299–3302.

[9] W. Kaim, *Coord. Chem. Rev.* **2002**, *230*, 127–139.

[10] J. Yuasa, A. Mitsui, T. Kawai, *Chem. Commun.* **2011**, *47*, 5807–5809.

[11] C. Quinton, V. Alain-Rizzo, C. Dumas-Verdes, G. Clavier, F. Miomandre, P. Audebert, *European J. Org. Chem.* **2012**, *2012*, 1394–1403.

[12] Y. Kim, E. Kim, G. Clavier, P. Audebert, *Chem. Commun.* **2006**, 3612–3614.

[13] P. Audebert, F. Miomandre, *Chem. Sci.* **2013**, *4*, 575–584.

[14] F. Miomandre, R. Meallet-Renault, J.-J. Vachon, R. B. Pansu, P. Audebert, *Chem. Commun.* **2008**, 1913–1915.

[15] D. L. Boger, J. Hong, *J. Am. Chem. Soc.* **2001**, *123*, 8515–8519.

[16] A. Hamasaki, J. M. Zimpleman, I. Hwang, D. L. Boger, *J. Am. Chem. Soc.* **2005**, *127*, 10767–10770.

[17] B. L. Oliveira, Z. Guo, G. J. L. Bernardes, *Chem. Soc. Rev.* **2017**, *46*, 4895–4950.

[18] A. C. Knall, C. Slugovc, *Chem. Soc. Rev.* **2013**, *42*, 5131–5142.

[19] N. K. Devaraj, S. Hilderbrand, R. Upadhyay, R. Mazitschek, R. Weissleder, *Angew. Chemie - Int. Ed.* **2010**, *49*, 2869–2872.

[20] J. B. Haun, N. K. Devaraj, S. A. Hilderbrand, H. Lee, R. Weissleder, *Nat. Nanotechnol.* **2010**, *5*, 660.

[21] C. P. Ramil, M. Dong, P. An, T. M. Lewandowski, Z. Yu, L. J. Miller, Q. Lin, *J. Am. Chem. Soc.* **2017**, *139*, 13376–13386.

[22] Y. Lee, W. Cho, J. Sung, E. Kim, S. B. Park, *J. Am. Chem. Soc.* **2018**, *140*, 974–983.

[23] K. Lang, L. Davis, J. Torres-Kolbus, C. Chou, A. Deiters, J. W. Chin, *Nat. Chem.* **2012**, *4*, 298–304.

[24] J. C. T. Carlson, L. G. Meimetis, S. A. Hilderbrand, R. Weissleder, *Angew. Chemie - Int. Ed.* **2013**, *52*, 6917–6920.

[25] L. G. Meimetis, J. C. T. Carlson, R. J. Giedt, R. H. Kohler, R. Weissleder, *Angew. Chemie - Int. Ed.* **2014**, *53*, 7531–7534.

[26] H. Wu, J. Yang, J. Seckute, N. K. Devaraj, *Angew. Chemie - Int. Ed.* **2014**, *53*, 5805–5809.

[27] C. Uttamapinant, J. D. Howe, K. Lang, V. Beránek, L. Davis, M. Mahesh, N. P. Barry, J. W. Chin, *J. Am. Chem. Soc.* **2015**, *137*, 4602–4605.

[28] I. Nikić, G. Estrada Girona, J. H. Kang, G. Paci, S. Mikhaleva, C. Koehler, N. V. Shymanska, C. Ventura Santos, D. Spitz, E. A. Lemke, *Angew. Chemie - Int. Ed.* **2016**, *55*, 16172–16176.

[29] H. Wu, S. C. Alexander, S. Jin, N. K. Devaraj, *J. Am. Chem. Soc.* **2016**, *138*, 11429–11432.

[30] E. Jiménez-Moreno, Z. Guo, B. L. Oliveira, I. S. Albuquerque, A. Kitowski, A. Guerreiro, O. Boutureira, T. Rodrigues, G. Jiménez-Osés, G. J. L. Bernardes, *Angew. Chemie - Int. Ed.* **2017**, *56*, 243–247.

[31] H. Wu, N. K. Devaraj, *Acc. Chem. Res.* **2018**, *51*, 1249–1259.

[32] M. Karver, R. Weissleder, S. A. Hilderbrand, *Bioconjug. Chem.* **2011**, *22*, 2263–2270.

[33] J. Yang, M. R. Karver, W. Li, S. Sahu, N. K. Devaraj, *Angew. Chemie - Int. Ed.* **2012**, *51*, 5222–5225.

[34] P. Audebert, S. Sadki, F. Miomandre, G. Clavier, M. C. Vernieres, M. Saoud, P. Hapiot, *New J. Chem.* **2004**, *28*, 387–392.

[35] N. O. Abdel, M. A. Kira, M. N. Tolba, *Tetrahedron Lett.* **1968**, 3871–3872.

[36] S. A. Lang Jr., B. D. Johnson, E. Cohen, *J. Heterocycl. Chem.* **1975**, *12*, 1143–1153.

[37] L. Brandsma, H. D. Verkruijsse, *Synthesis (Stuttg).* **1978**, *4*, 290–290.

Chapter 3

Novel donor-acceptor benzonitrile derivatives exhibiting TADF, AIE and mechanochromism

3.1 Introduction

Benzonitrile derivatives are of particular interest in this thesis for two reasons. Firstly, they are useful precursors to prepare 1,2,4,5-tetrazine molecules. Indeed, as described in the first and second chapters, various 1,2,4,5-tetrazine materials with different applications can be prepared from their benzonitrile precursors by the classical Pinner synthesis or its modified versions.[1–3] Secondly, electron deficient benzonitrile core has been regarded as one of the most popular electron-acceptors for constructing TADF molecules since the introduction of this field,[4–11] due to their easy preparation and excellent photophysical properties. Therefore, preparing novel donor-acceptor benzonitrile materials which exhibit superior photophysical properties are of particular interest to the research community.

In this chapter, we will firstly describe the synthesis of three simple donor-acceptor benzonitrile compounds, and their subsequent reactions to prepare several novel symmetrical and unsymmetrical 1,2,4,5-tetrazine derivatives. Then, a molecular design for novel donor-acceptor benzonitrile derivatives will be introduced. Several series of new donor-acceptor benzonitrile compounds were conveniently prepared, which interestingly exhibit TADF, AIE and mechanochromic properties.

3.2 Donor-acceptor benzonitriles for tetrazine synthesis

Three simple donor-acceptor benzonitrile compounds **N1-N3** were firstly designed and prepared for the later synthesis of donor-acceptor 1,2,4,5-tetrazines (**Scheme 1**). **N1** and **N2** were prepared by a convenient nucleophilic substitution reaction in high yields (82% and 75%) while attempts to prepare **N3** with the same method was unsuccessful. Instead it was synthesized by Buchwald-Hartwig cross-coupling reaction in a high yield (73%). **N1-N3** have been previously reported by different synthetic methods.[12,13]

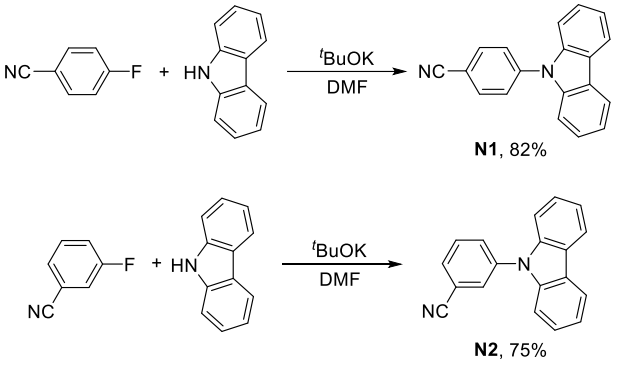

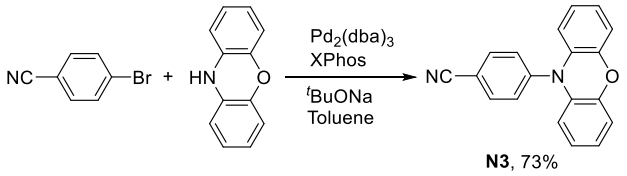

Scheme 1: Preparation of donor-acceptor benzonitrile compounds **N1-N3**.

Two types of tetrazine synthetic methods were attempted for preparing both symmetrical and unsymmetrical 1,2,4,5-tetrazines. Firstly, the classical Pinner synthesis was used on the benzonitrile precursors **N1-N3**. New symmetrical donor-acceptor 1,2,4,5-tetrazine **Tz1** and **Tz3** were successfully prepared, although in low yields, due to the low solubility of the benzonitrile substrates. Addition of a small amount of DMF as co-solvent improved the yield a bit in the case of **Tz1**, however, a competition reaction process was interestingly observed which will be described in detail in **Chapter 6**. In addition, **Tz2** was isolated as a red solid which is completely insoluble in any organic solvents, and thus it was not possible to characterize it by common analytical methods.

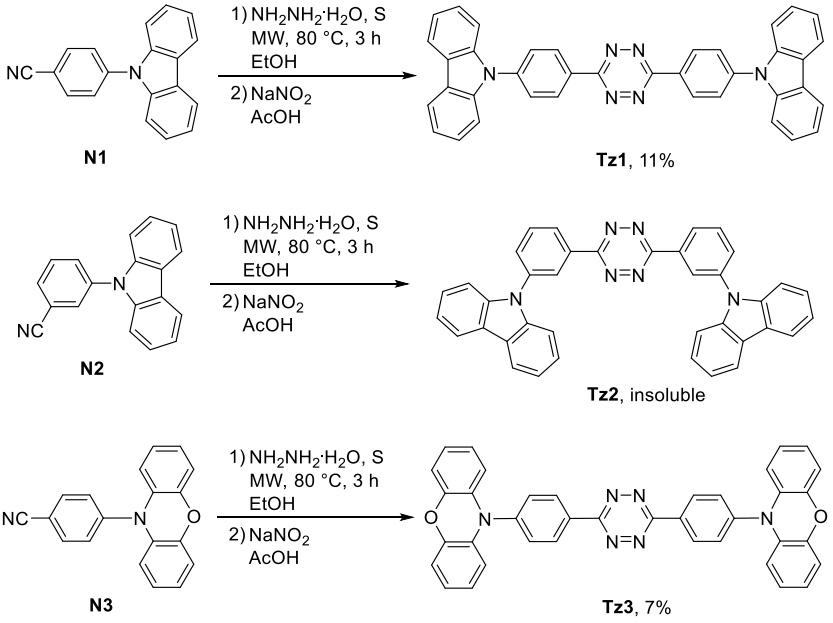

Scheme 2: Preparation of symmetrical donor-acceptor 1,2,4,5-tetrazines **Tz1-Tz3**.

Next, we intended to employ our metal-free approach to 3-monosubstituted unsymmetrical 1,2,4,5-tetrazines (described in **Chapter 2**) on the benzonitrile precursors **N1-N3**. **TA1**, **TA1'** and **TA2** were successfully prepared, however in low yields, also due to the low solubility of the benzonitrile substrates.

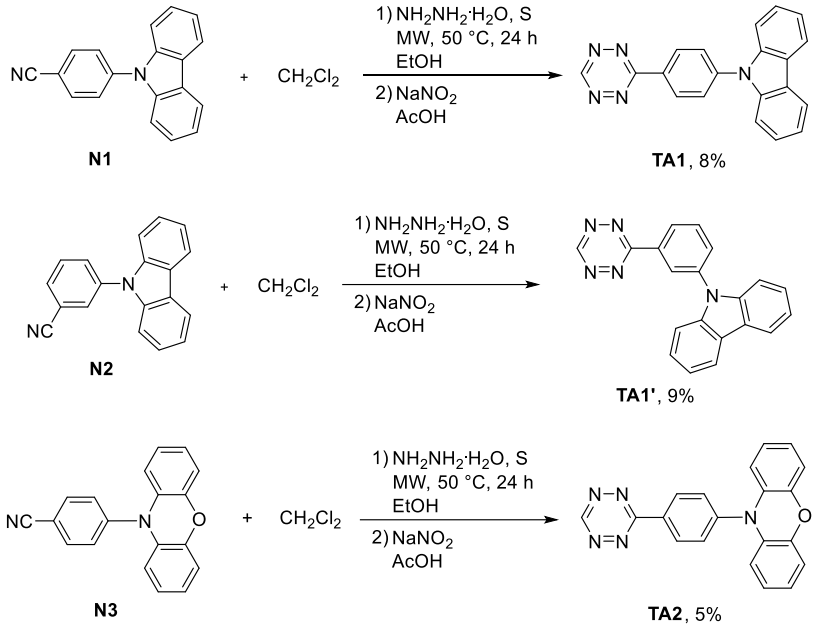

Scheme 3: Preparation of 3-monosubstituted unsymmetrical donor-acceptor 1,2,4,5-tetrazines **TA1**, **TA1'** and **TA3**.

Although several interesting donor-acceptor 1,2,4,5-tetrazine derivatives have been successfully prepared, the Pinner synthesis and its modified version was of limited interest because of the yields of the products. An alternative synthetic strategy to prepare these molecules in high yields would thus be desirable and work toward this goal will be presented in **Chapter 4**.

3.3 Molecular design of novel donor-acceptor benzonitriles

When preparing donor-acceptor benzonitrile compounds for tetrazine synthesis, we found that nucleophilic substitution reaction is a convenient and versatile synthetic method for preparing new benzonitrile derivatives. The reaction can be easily performed in a one-pot synthesis procedure, and importantly, there are a large variety of fluorobenzonitriles which are commercially available.

In this study, we found that 2,3,4,5,6-pentafluorobenzonitrile (PFBN) is an interesting starting material in the preparation of functionalized benzonitrile derivatives. The different reactivity of the five fluorine atoms of 2,3,4,5,6-pentafluorobenzonitrile (PFBN) towards nucleophilic substitution (**Figure1**) offers us a special advantage to prepare various differently substituted benzonitrile derivatives in a facile and efficient manner.[14,15]

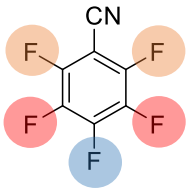

Figure 1: 2,3,4,5,6-pentafluorobenzonitrile (PFBN) with color showing the difference of reactivity of the fluorine atoms toward nucleophilic substitution: blue: most reactive, orange: medium reactivity, red: least reactive.

The para fluorine atom of PFBN readily undergoes nucleophilic substitution first in the presence of a weak base (e.g., K_2CO_3) at room temperature or even lower (0 °C). Then the fluorine atoms at ortho and ortho' positions can be displaced subsequently by nucleophiles at room temperature or a slightly higher temperature also using a weak base (e.g., K_2CO_3). Eventually, the meta and meta' fluorine atoms could be substituted by nucleophiles using a stronger base (e.g., Cs_2CO_3, ^{t}BuOK) at a higher temperature (60 °C-80 °C).[14,15]

Through this unique synthetic methodology, a series of donor-acceptor benzonitrile derivatives with different number of substitutions by carbazole donors (**N4-N8**) were first conveniently prepared (**Scheme 4**). As long as the reaction conditions were carefully controlled by using the appropriate base and temperature, the fluorine atoms on the PFBN can be displaced by carbazoles sequentially, giving the target substituted compound as the main product, with only slight amount of side compounds featuring other substitutions. For example, when one equivalent of carbazole to PFBN was used, **N4** was obtained in a high yield at 0 °C in the presence of K_2CO_3. When 2, 3, 4 or 5 equivalents of carbazoles per PFBN were used, **N5-N8** were obtained in high yields using the appropriate base and temperature (see **3.8 Experimental details**). The formation of the respective benzonitrile derivatives can be easily observed by the change of signals in the ^{19}F NMR spectra (**Figure 2**). Although benzonitries **N6-N8** have already been reported by other groups as efficient TADF materials,[5–7,9] no one has studied the chemistry of reactivity of fluorine atoms on PFBN to prepare TADF molecules in a stepwise manner. Two new blue TADF materials (**N4** and **N5**) were therefore prepared and studied. In these two molecules, the fluorine unit plays a role of weak electron acceptor, and it improves the solubility of the molecules compared to the H or CN unit, which is an important character for solution-processable OLEDs. **N4** and **N5** are easily crystalized from a petroleum ether and DCM (3:1) mixture. X-ray single crystal structures of both **N4** and **N5** are shown in **Scheme 4**.

All the benzonitrile derivatives were prepared in high yields (71%-95%) by one-step nucleophilic substitution reactions which are metal-catalyst free and cost effective. This

methodology provided a facile and convenient way to prepare efficient TADF emitters in a selective manner.

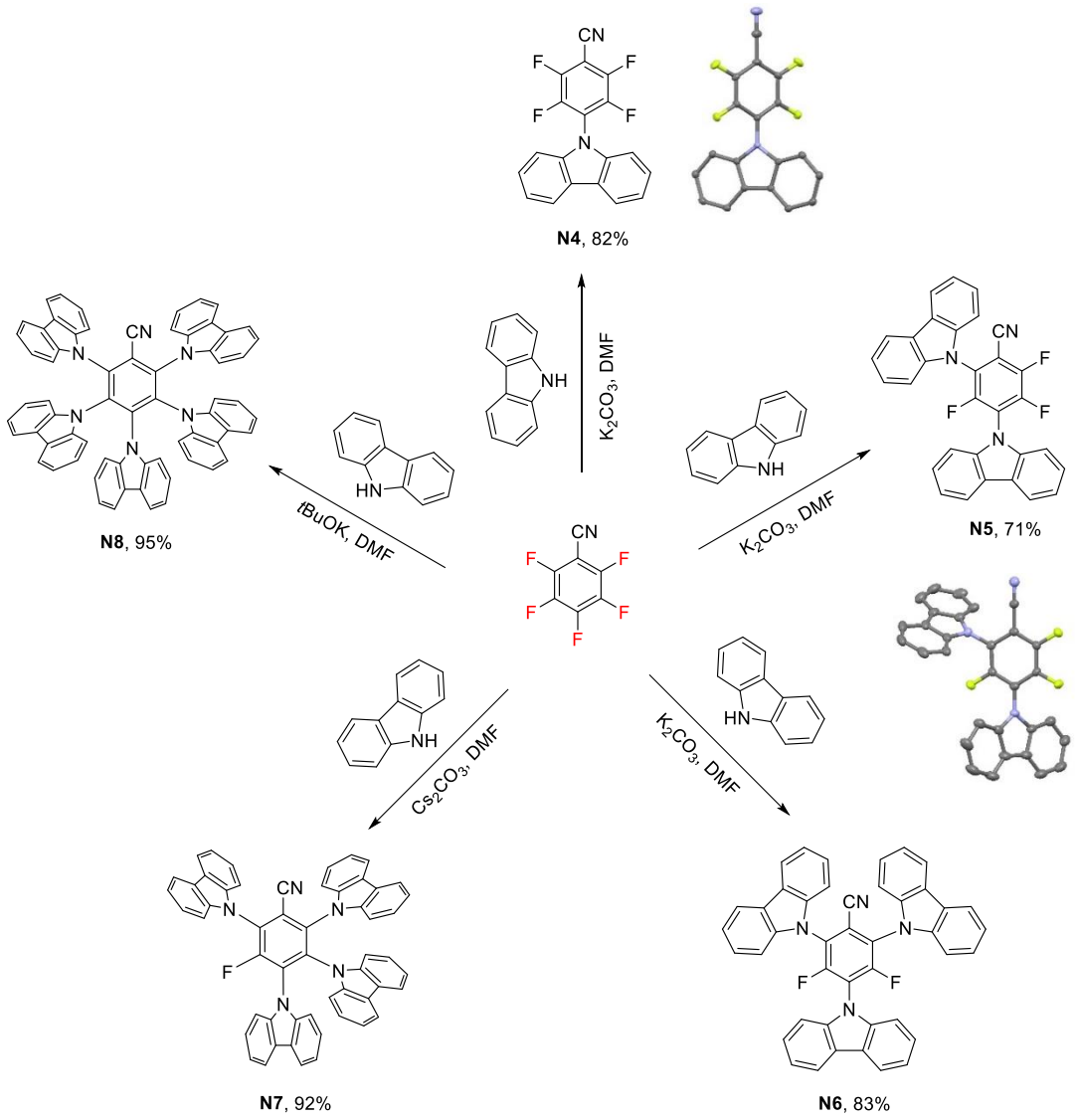

Scheme 4: Preparation of donor-acceptor benzonitrile compounds **N4-N8**, along with the X-ray crystallographic structure of **N4** and **N5**.

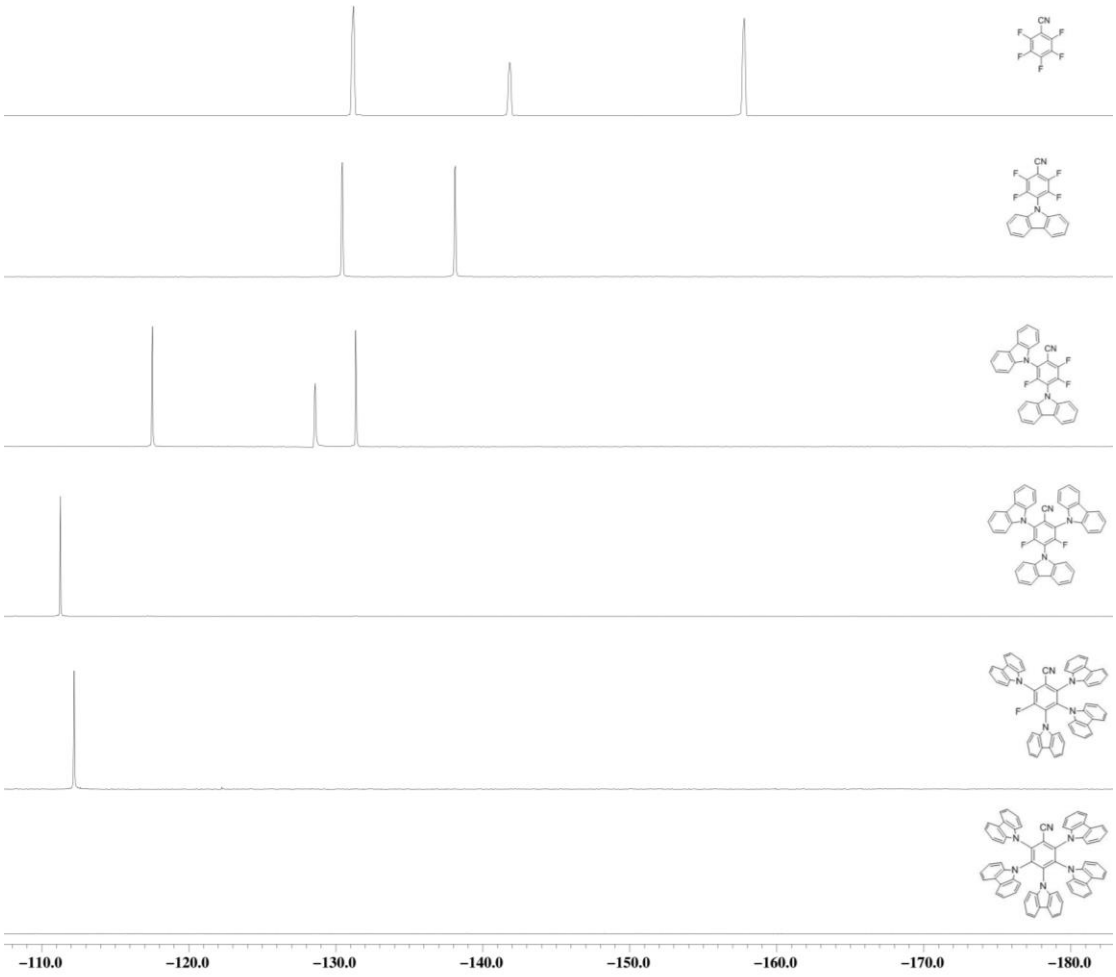

Figure 2: Comparison of ^{19}F NMR (376 MHz, $CDCl_3$) spectra of PFBN and **N4-N8**.

Next, we intended to prepare new donor-acceptor benzonitrile derivatives substituted by donors of different nature. Six different donor molecules were employed in this study, and the results are summarized in **Table 1**. In addition to **N4** which was described above, three more donor-acceptor benzonitrile derivatives **N9-N11** bearing only one donor moiety (phenoxazine, phenothiazine or 3,6-di-*tert*-butyl-*9H*-carbazole) were prepared in high yields (80%-86%). Compared to **N1** and **N3** which have no fluorine atoms, the four fluorine atoms in **N4** and **N9** act as weak electron acceptors in the molecules which make these molecules exhibit excellent TADF characteristics, while **N1** and **N3** don't. **N10** and **N11** also exhibit excellent TADF characteristics. Additionally, **N10** shows a prominent AIE effect which will be described in detail in paragraph **3.6 Photophysical properties**. **N9** and **N10** form crystals easily from a petroleum ether and DCM (3:1) mixture. The X-ray single crystal structures of **N4**, **N9** and **N10** are also shown in **Table 1**. Unfortunately, the nucleophilic substitution reaction didn't work when using 9,9-dimethyl-9,10-dihydroacridine or 10,11-dihydro-*5H*-dibenzo[*b,f*]azepine as donors.

Table 1: Synthesis of donor-acceptor benzonitrile derivatives which has only one donor moiety [(a)].

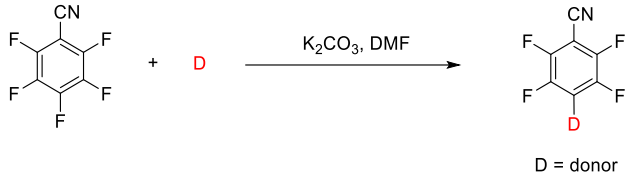

D = donor

Entry	D	Product	Yield (%)	Crystal structure
1	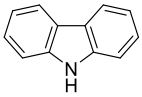	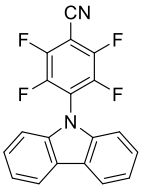 **N4**	82	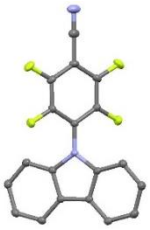
2	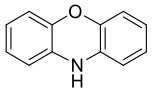	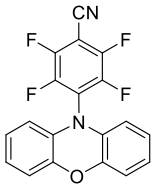 **N9**	85	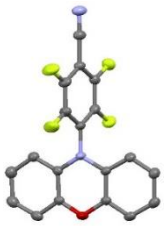
3	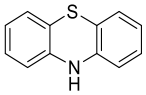	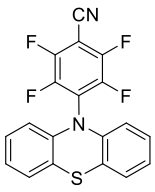 **N10**	80	
4	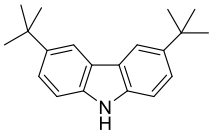	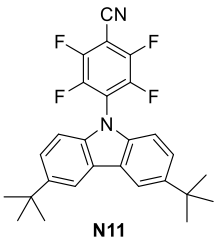 **N11**	86	Not obtained
5	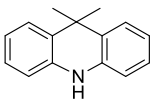	No product	/	/

6	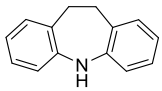	No product	/	/

(a) All reactions were carried out on a 1 mmol scale. Yields (isolated) based on PFBN.

3.4 Novel benzonitrile compounds with mixed carbazole and phenoxazine substituents

Previously, we have described an elaborative synthetic strategy to prepare new donor-acceptor benzonitrile compounds in a stepwise manner from one single benzonitrile precursor (PFBN). However, all the benzonitriles prepared previously only have one type of donor in each molecule. With the clear different reactivity of fluorine atoms on PFBN, it is expected that it should be easy to introduce two or more different donor moieties on one single molecule. Indeed, it would be very interesting if we could introduce two different donors on one single molecule, because these type of molecules have been proved to possess interesting photophysical properties due to the different charge transfer (CT) states induced in one single molecule.[16–18]

Therefore, we started to expand the scope of this synthetic methodology by introducing two different donors on one PFBN. Benzonitrile derivatives **N9**, **N12** and **N13** were first synthesized by sequential nucleophilic displacement of the para, ortho and ortho' fluorine atoms on PFBN with one, two and three equivalents of phenoxazine (**Scheme 5)**. The reactions were high yields, however, unlike with carbazole, further substitution of the meta and meta' fluorine atoms on the molecule using phenoxazine was found impossible. It is likely due to the increased steric hindrance on the molecule when the para, ortho and ortho' positions are already functionalized with phenoxazine moieties, and the phenoxazine anion is not strong enough to displace the meta and meta' fluorine on the molecule. **N9** and **N12** form orange crystals from a petroleum ether and DCM (3:1) mixture. The X-ray single crystal structures of **N9** and **N12** are also shown in **Scheme 5**.

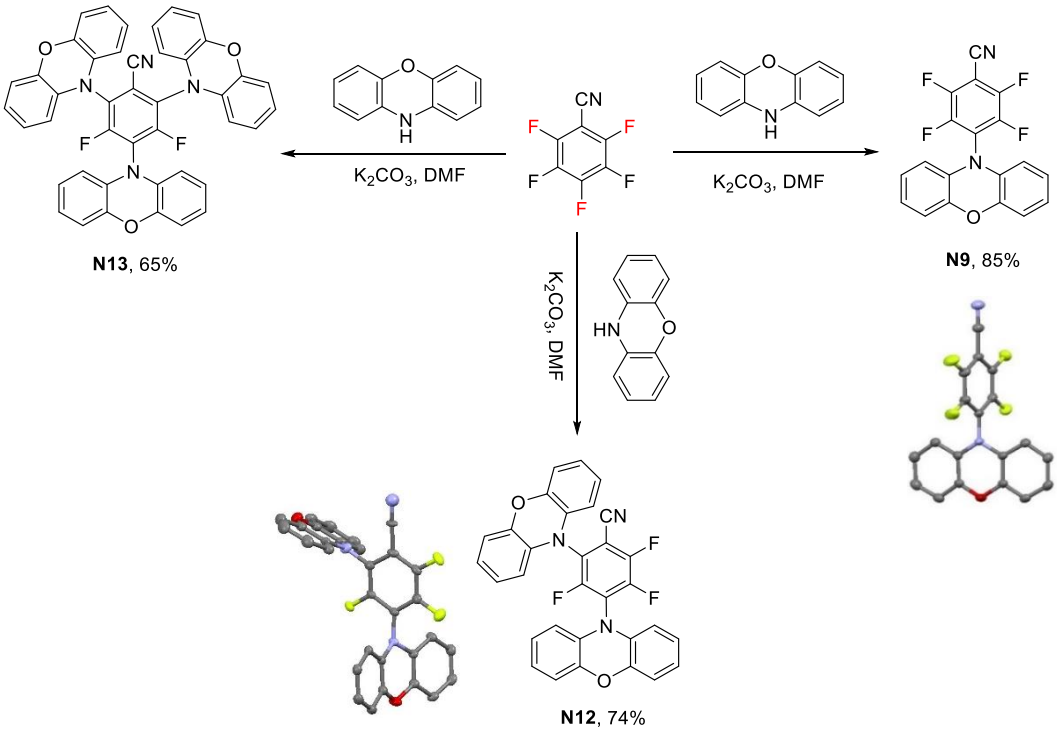

Scheme 5: Preparation of donor-acceptor benzonitrile compounds **N9**, **N12** and **N13**, along with the X-ray crystallographic structures of **N9** and **N12**.

Then the hetero-substituted benzonitrile derivatives **N14**-**N22** were successfully prepared by further functionalization on benzonitriles **N9**, **N12** and **N13** (**Table 2**). The remaining fluorine atoms on **N9**, **N12** and **N13** were displaced sequentially with various equivalents of carbazoles in the presence of K_2CO_3 or Cs_2CO_3 at room temperature or higher (60 °C-80 °C), according to the reactivity of the compounds. When the reaction conditions were carefully controlled, the sequential substitution reactions proceeded smoothly resulting in the target substituted compound as main product, with only small amount of differently substituted compounds. The formation of the respective benzonitrile derivatives were easily determined by the changes of signals in the ^{19}F NMR spectra, as exemplified for the series **N9** and **N14-N17** in **Figure 3**. However, it is important to note that benzonitrile derivative **N19a** was obtained always with around 10% amount of its structural isomer **N19b**. It was not possible to separate the two isomers by column chromatography due to their very close polarity. Interestingly, by simply changing the different combinations of donor moieties (phenoxazine, carbazole) and acceptor moieties (cyano, fluorine), the emission of the compounds could be modulated.

Table 2: Synthesis of hetero-substituted donor-acceptor benzonitrile compounds **N14-N22**[(a)].

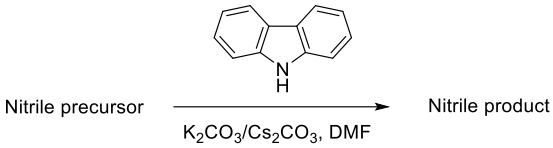

Entry	Nitrile precursor	Nitrile product	Yield (%)
1	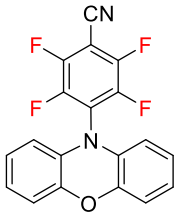 **N9**	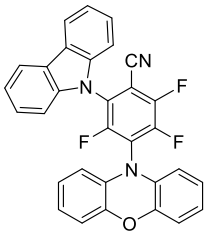 **N14**	69
2		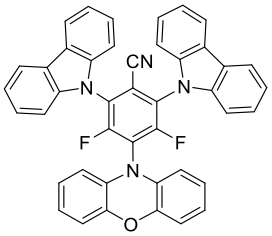 **N15**	74
3		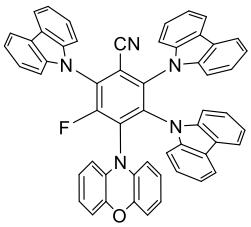 **N16**	90
4		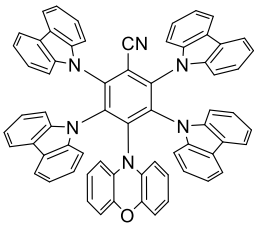 **N17**	98

5	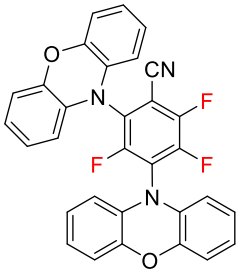 **N12**	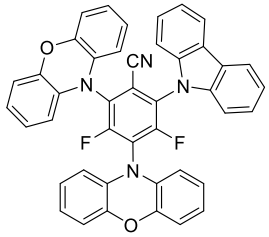 **N18**	83
6		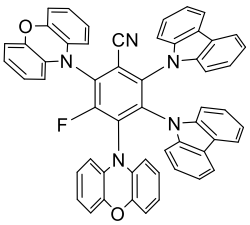 **N19a** 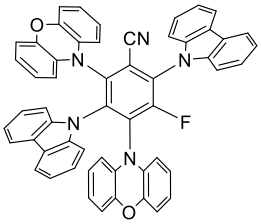 **N19b**	86[(b)]
7		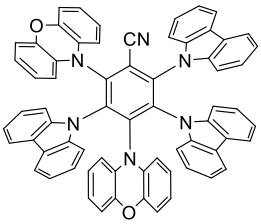 **N20**	97
8	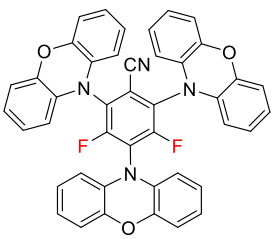 **N13**	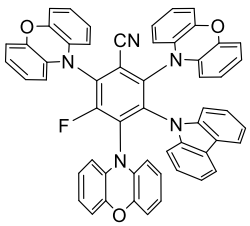 **N21**	86
9		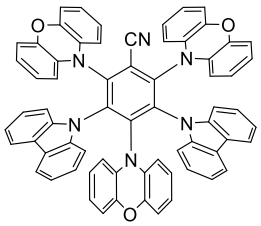 **N22**	97

(a) All reactions were carried out on a 1 mmol scale. Yields (isolated) based on nitrile precursor. (b) Total yield: 86% (the ratio between **N19a** and **N19b** is 9:1 determined by ^{1}H and ^{19}F NMR).

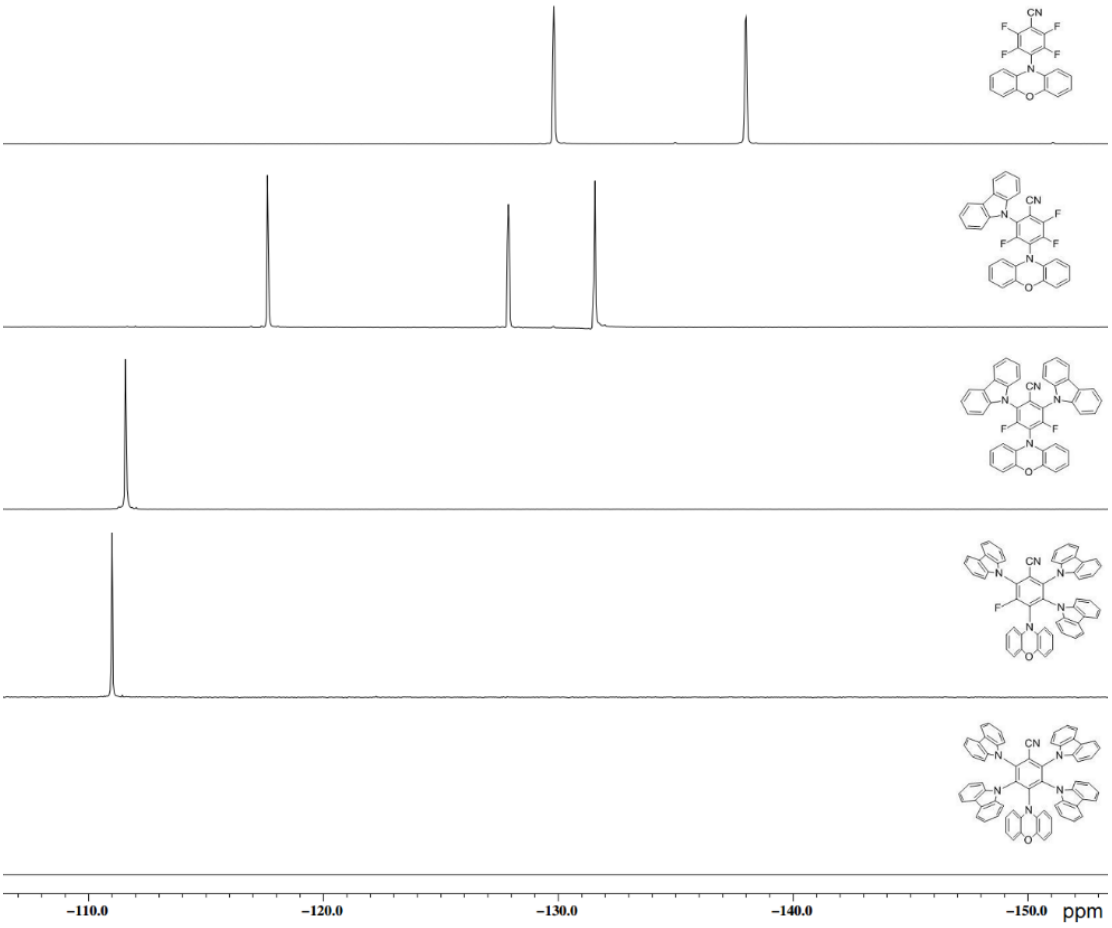

Figure 3: Comparison of ^{19}F NMR (376 MHz, $CDCl_3$) spectra of **N9** and **N14-N17**.

In order to study the structure-property relationship, some selected benzonitrile derivatives were studied by single crystal X-ray diffraction (XRD). Notably, the crystal structures of the **N9, N14-N17** series of compounds were obtained and are presented here (**Table 3**). All the molecules possess large twisting angles between the donor and acceptor, which should facilitate the spatial separation of the HOMO and LUMO, leading to a small ΔE_{ST} and efficient TADF characteristics. The dihedral angles decrease with the increasing number of donor moieties on the molecules, and the dihedral angle between the phenoxazine moiety and the acceptor are always larger than those between the carbazole moiety and the acceptor in each molecule. In the molecular packing of all molecules, no close π–π stacking are found due to the twisted structure, which is beneficial to avoid aggregation-caused quenching (ACQ).

Table 3: X-ray crystallographic structures of **N9** and **N14-N17**, along with their molecular packing and the dihedral angles between the donor (PXZ = phenoxazine, CBZ = carbazole) and acceptor.

	Molecular structure	Molecular packing	Dihedral angles (°)
N9	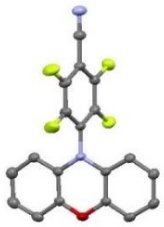	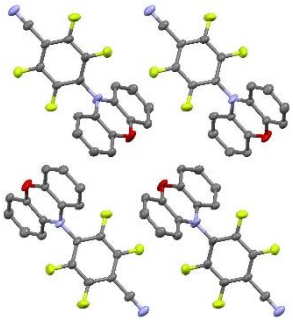	77.83 (PXZ)
N14		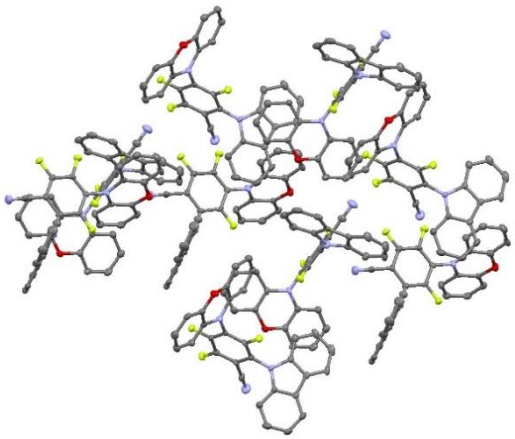	69.45 (CBZ), 73.37 (PXZ)
N15	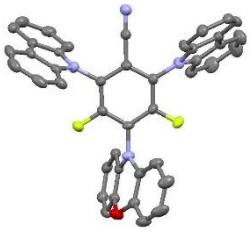	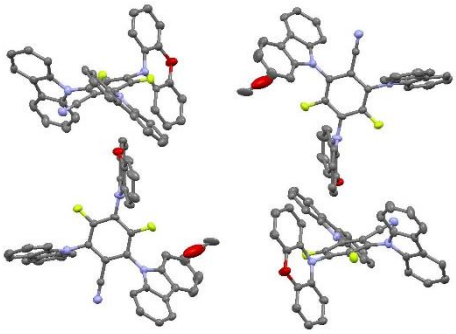	68.28 (CBZ), 70.37 (CBZ), 75.37 (PXZ)

N16	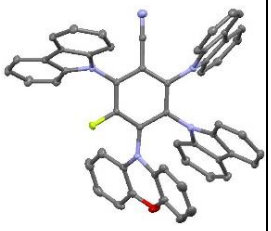	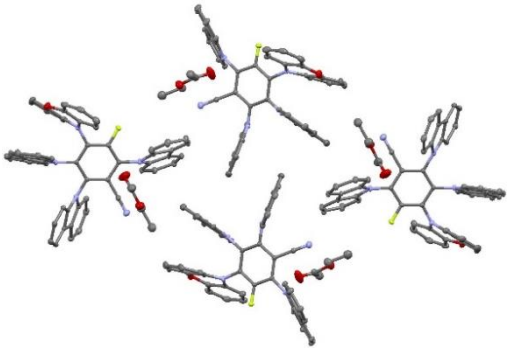	58.20 (CBZ), 65.16 (CBZ), 66.45 (CBZ), 68.05 (PXZ)
N17	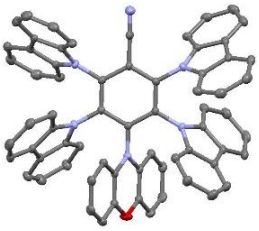	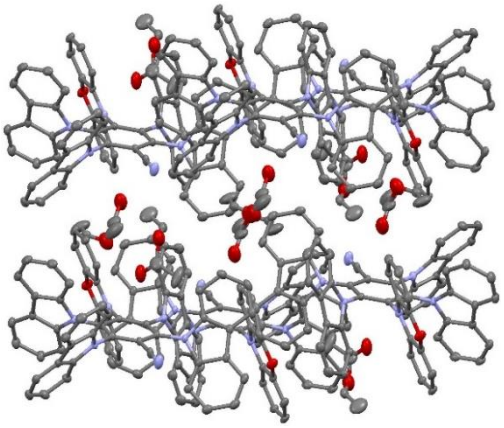	62.15 (CBZ), 62.15 (CBZ), 64.17 (CBZ), 64.17 (CBZ), 65.53 (PXZ)

3.5 Electrochemistry

The electrochemical properties of the new donor-acceptor benzonitrile derivatives **N4, N5** and **N9-N22** were collaboratively studied by the electrochemist Marharyta Vasylieva from EXCILIGHT project. The detailed electrochemical properties for all the compounds will not be discussed in this thesis but only the general trends.

The cyclic voltammograms (CV) of all the donor-acceptor benzonitrile derivatives feature a reversible reduction peak which can be assigned to the benzonitrile core reduction and one or more oxidation peaks which can be assigned to the peripheral donor moieties. It is important to note that the phenoxazine and phenothiazine moieties are reversibly oxidized, while the oxidation of the carbazole moieties is irreversible as already known. In addition, for the hetero-substituted benzonitrile compounds, it is interesting to mention that the phenoxazines moieties are always oxidized before the carbazoles as expected based on its stronger electron donating strength. The CV of **N17** is given as a representative example in **Figure 4**.

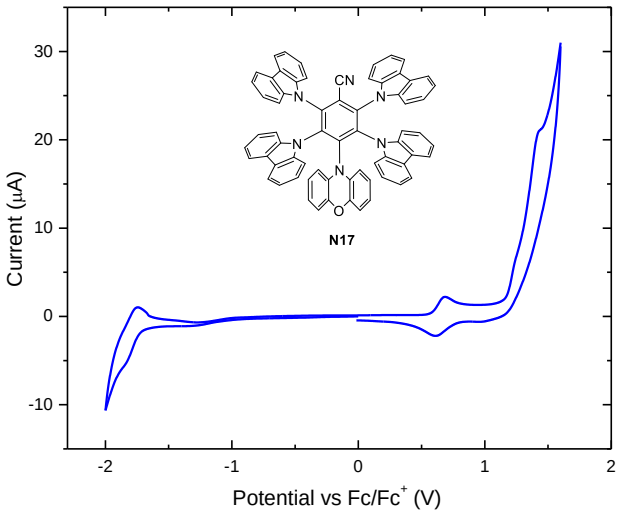

Figure 4: Cyclic voltammetry of **N17** in DCM at room temperature.

The redox potentials for all the new benzonitrile derivatives, along with the estimated HOMO and LUMO values are given in **Table 4**.

Table 4: Electrochemical properties of **N4, N5 and N9-N22**.

	E_{ox} vs Fc/Fc^+ (V)[a]	E_{red} vs Fc/Fc^+ (V)[a]	HOMO (eV)[b]	LUMO (eV)[c]
N4	1.13	-1.97	6.23	3.13
N5	1.05	-1.87	6.15	3.23
N9	0.56	-1.95	5.66	3.15
N10	0.49	-1.93	5.59	3.17
N11	1.01	-1.93	6.11	3.17
N12	0.56	-1.85	5.66	3.25
N13	0.57	-1.80	5.67	3.30
N14	0.56	-1.87	5.66	3.23
N15	0.57	-1.83	5.67	3.27
N16	0.52	-1.78	5.62	3.32
N17	0.40	-1.89	5.5	3.21
N18	0.58	-1.81	5.68	3.29

N19	0.51	-1.84	5.61	3.26
N20	0.42	-1.87	5.52	3.23
N21	0.49	-1.81	5.59	3.29
N22	0.39	-1.83	5.49	3.27

(a) Measured in DCM at room temperature by cyclic voltammetry. (b) Estimated from the oxidation potential in DCM, HOMO = E_{ox} + 5.1. (c) Estimated from the reduction potential in DCM, LUMO = E_{red} + 5.1.

3.6 Photophysical properties

The photophysical properties of the new donor-acceptor benzonitrile derivatives **N4, N5** and **N9-N22** were collaboratively studied by the photophysicist Antonio Maggiore which belongs to our group PPSM and EXCILIGHT project. All the benzonitriles exhibit TADF characteristics. In addition, some of them feature prominent AIE effect (e.g., **N10**), and some of them show excellent mechanochromism effect (e.g., **N14-N17**). Some photophysical properties of these compounds are summarized in **Table 5**, which clearly show the TADF characteristics of these benzonitrile derivatives. This thesis does not intend to discuss the details of the photophysical properties of all these derivatives. Nevertheless, the photophysical properties of one example **N10**, which I have performed the characterizations by myself in University of Durham, will be demonstrated here to highlight the interesting photophysical properties of these donor-acceptor benzonitrile derivatives. Additionally, the mechanochromism effect of one example **N17** is also presented in this thesis.

Table 5: Photophysical properties of **N4**, **N5**, **N9** and **N11-N22** in PMMA 0.1% (w/w) film.

	λ_{PL} (nm)[(a)]	$\Phi_{PL}^{air}/\Phi_{PL}^{degas}$ (%)[(b)]	τ_{PF} (ns)[(c)]	τ_{DF} (µs)[(d)]
N4	424	28.8/37.4	9.5	300
N5	438	18.7/n.d.	12.7	750
N9	524	4.5/5	9.7	2.1
N11	442	38/53	8.5	150
N12	555	3.3/4.3	17.8	2.5
N13	586	1.5/1.8	7.3	1.6
N14	533	4.2/5.2	9.8	8.8
N15	548	4.0/4.9	9.3	59.5

N16	552	13.6/15.9	17.4	4.3
N17	565	15.1/18.1	12.5	13.8
N18	570	3.7/4.9	10.3	2.3
N19	574	6.5/7.7	20.9	3.6
N20	584	8.5/11.4	30.4	2.2
N21	590	3.8/4.3	10.0	2.5
N22	596	6.4/7.9	11.8	1.3

(a) Emission maxima. (b) PLQY in air-equilibrated and degassed atmosphere. n.d. = not defined (c) Prompt fluorescence lifetime determined from PL decay. (d) Delayed fluorescence lifetime determined from PL decay.

N10 display an unusual emission phenomenon which was observed during the synthesis. When irradiated at 365 nm with a UV lamp, the crystal of **N10** exhibits super bright green emission, while almost no emission could be observed from the solution of **N10** in methylcyclohexane (MCH, **Figure 5**) and it is completely non-emissive in any other solvent.

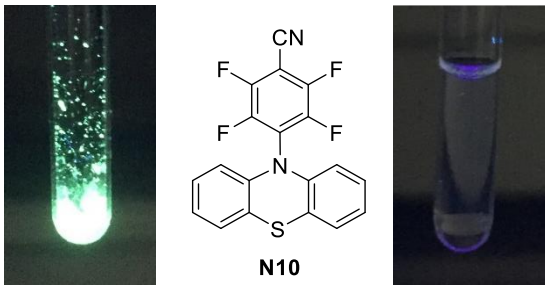

Figure 5: Photos of crystal (left) and MCH solution (right) of **N10** under 365 nm UV-irradiation, along with the chemical structure of **N10** (middle).

This phenomenon can be regarded as a type of aggregation-induced emission (AIE), which has attracted intensive interest from researchers since the introduction of this field in 2001.[19–21] Molecules with AIE phenomenon have found applications in various fields, ranging from bioimaging, chemosensing or optoelectronics to stimuli-responsive systems.[22–27] More importantly, molecules exhibiting both AIE and TADF characteristics have recently become a hot topic because such molecules show a prominent application potential when combining the advantages of both phenomena.[17,18,28–34]

The photophysical data of **N10** are depicted in **Table 6** and **Figure 6**. As mentioned earlier, **N10** only emit weakly in MCH (Φ_{PL} = 0.2%), and is completely non-emissive in any other solvents. Moreover, the emission intensity does not change in air-equilibrated or degassed MCH solutions (**Figure 7**), indicating that no sizeable TADF characteristics could be

observed for this molecule in solution. This is probably due to the very weak emission of **N10** in solution.

Table 6: Photophysical properties of **N10**.

	λ_{PL} (nm)[a]	$\Phi_{PL}^{air}/\Phi_{PL}^{degas}$ (%)	τ_{PF} (ns)[e]	τ_{DF} (µs)[f]	DF/PF[g]
MCH	602	0.20/0.20[b]	/	/	/
Crystal	500	39	8.5 ± 0.4	2.3 ± 0.06	5.0
Crystal_80K	/	92[c]	12.0 ± 0.2	1187 ± 98	7.3
Neat film	507	7.7/7.9[d]	7.5 ± 0.9	0.64 ± 0.01	2.2
Zeonex film	541	1.7/2.1[d]	7.3 ± 0.4	0.60 ± 0.02	0.61

(a) Emission maxima. (b) PLQY in air-equilibrated and degassed MCH solution. (c) Estimated from the change of emission intensity. (d) PLQY in air and N_2 atmosphere. (e) Prompt fluorescence lifetime determined from PL decay. (f) Delayed fluorescence lifetime determined from PL decay. (g) Ratio of delayed fluorescence component to prompt fluorescence component.

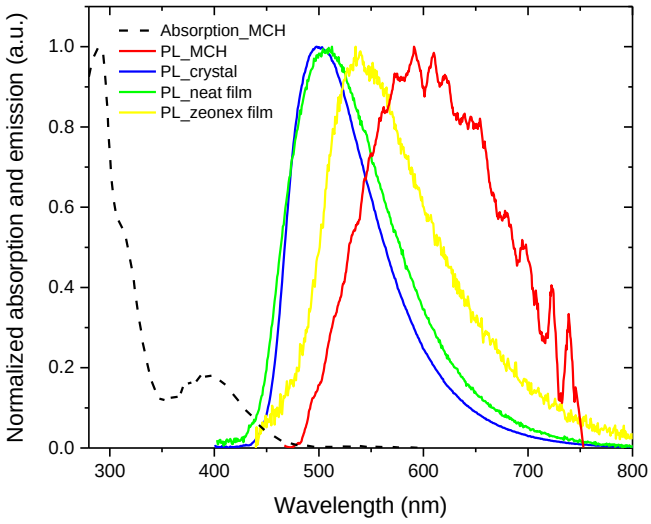

Figure 6: Normalized fluorescence spectra of **N10** in MCH, crystal, neat film and zeonex 1% (w/w) film, and normalized absorption spectrum in MCH. Note: the fluorescence spectrum in MCH was smoothed computationally.

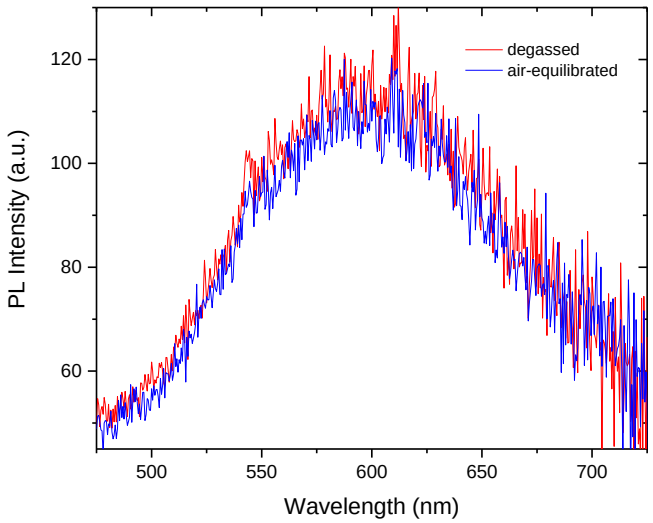

Figure 7: PL spectra of **N10** in degassed and air-equilibrated MCH at room temperature.

Surprisingly, the intensity of emission of **N10** shows a 200-times increase when going from MCH solution ($\boldsymbol{\Phi}_{\mathbf{PL}}$ = 0.2%) to crystal ($\boldsymbol{\Phi}_{\mathbf{PL}}$ = 39 %) and subsequently, a prominent TADF component was turned on (**Figure 8**). The ratio of the delayed fluorescence component to the prompt fluorescence one (DF/PF) was determined to be 5 from the PL decay of **N10**, which is a very high ratio for delayed fluorescence. Moreover, the TADF characteristic of **N10** in crystal form at 80 K remains prominent, showing a surprisingly high DF/PF ratio of 7.3 (**Figure 9**), and a very high PLQY ($\boldsymbol{\Phi}_{\mathbf{PL}}$ = 92 %) was estimated from the emission intensity in this form at 80 K. In addition, at 80 K the intensity of TADF is still substantial and thus phosphorescence is hardly distinguishable from delayed fluorescence (**Figure 9** and **10**). This clearly indicates that the difference between singlet and triplet energy levels ($\Delta E_{S\text{-}T}$) is approaching zero, which explains the prominent TADF characteristic of **N10** crystal. It is also important to note that the PL decays of **N10** crystal in degassed and air-equilibrated atmosphere has almost no difference (**Figure 11**), indicating oxygen does not affect the TADF property of the crystal. This is because oxygen could not permeate the crystal due to its close molecular packing, as a result no quenching of the triplet states happened. This is highly desirable as TADF molecules in most cases (e.g., solution and film) suffer from a significant oxygen quenching, while **N10** crystal exhibit excellent TADF characteristic in air.

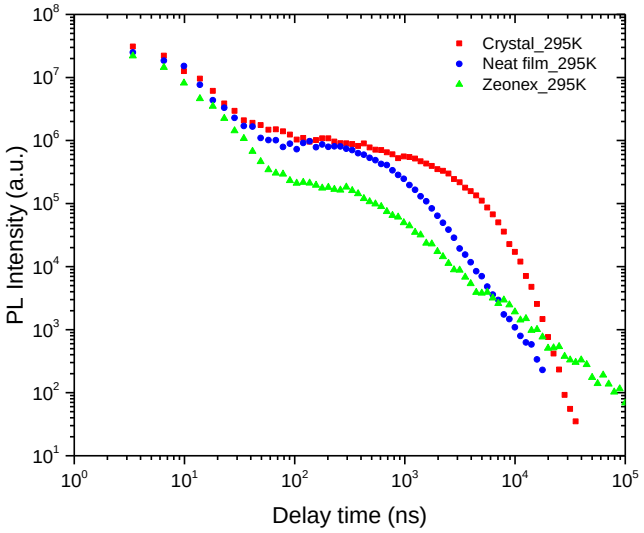

Figure 8: PL decay of **N10** crystal, neat film and zeonex 1% (w/w) film at room temperature.

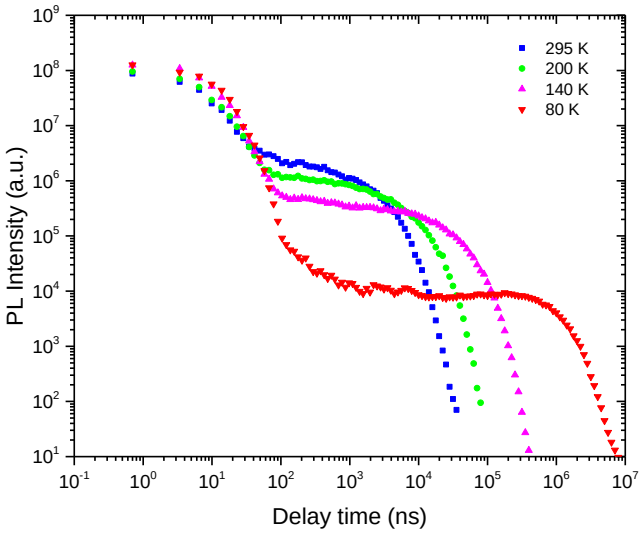

Figure 9: PL decays of **N10** crystal at various temperatures.

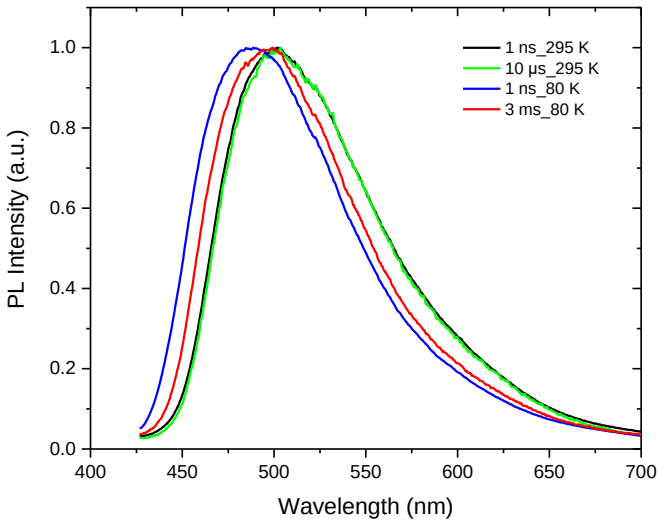

Figure 10: Time-resolved spectra of a **N10** crystal.

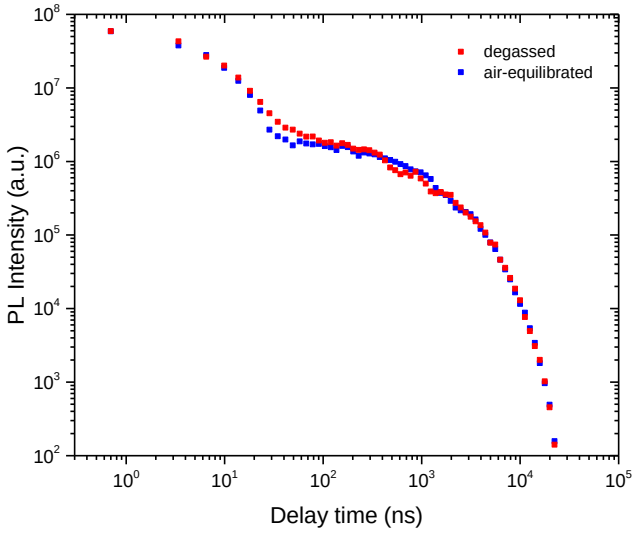

Figure 11: PL decays of **N10** crystal in degassed and air-equilibrated atmosphere at room temperature.

In comparison with the crystal form, the neat film of **N10** still has a good TADF characteristics, however much weaker than the crystal form (**Figure 8** and **12**). The PLQY decreased to 7.9%, and the DF/PF ratio decreased to a value of 2.2 at room temperature (**Table 6**). This probably comes from the fact that some molecules form microcrystals when preparing the neat film, which lead to good TADF characteristics, while the others are in an amorphous state which weakens the TADF characteristic. Very weak TADF performance was measured in the zeonex film of **N10** (**Figure 8** and **13**) because the molecules are well dispersed and no crystals/microcrystals could be formed. As a result,

the TADF performance dramatically decreased. The PLQY in this case decreased to only 2.1% and the DF/PF ratio decreased to a small value of 0.61 at room temperature (**Table 6**). Time-resolved spectroscopic studies for both neat film and zeonex film of **N10** were also performed at 80 K, but no clear sign of phosphorescence could be observed.

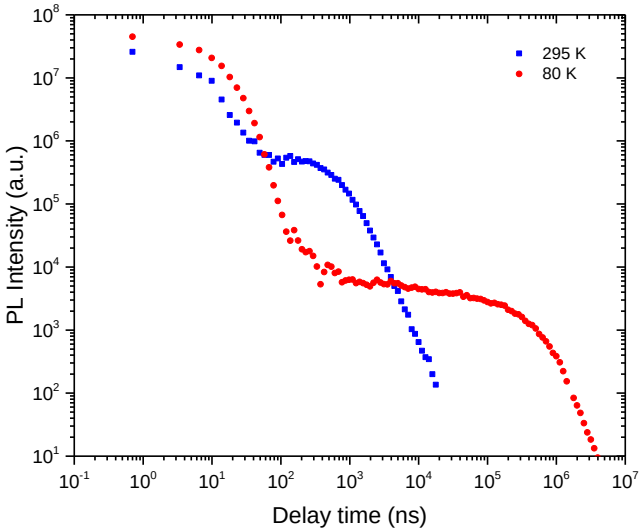

Figure 12: PL decays of **N10** in neat film at 295 K and 80 K.

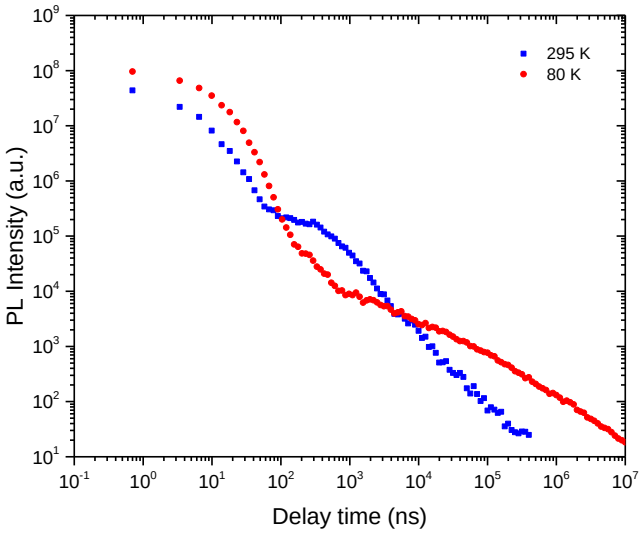

Figure 13: PL decays of **N10** in zeonex 1% (w/w) at 295 K and 80 K.

In addition, in order to differentiate the TADF from the TTA delayed fluorescence, power dependence of delayed fluorescence intensity of **N10** crystal, neat film and zeonex film were measured (**Figure 14-16**). The results clearly indicate that the delayed fluorescence in all cases originates from the TADF mechanism.

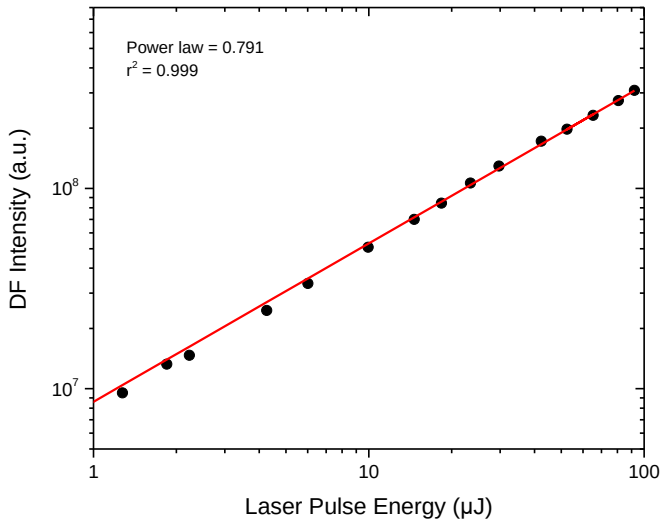

Figure 14: Power dependence of delayed fluorescence of a **N10** crystal at room temperature.

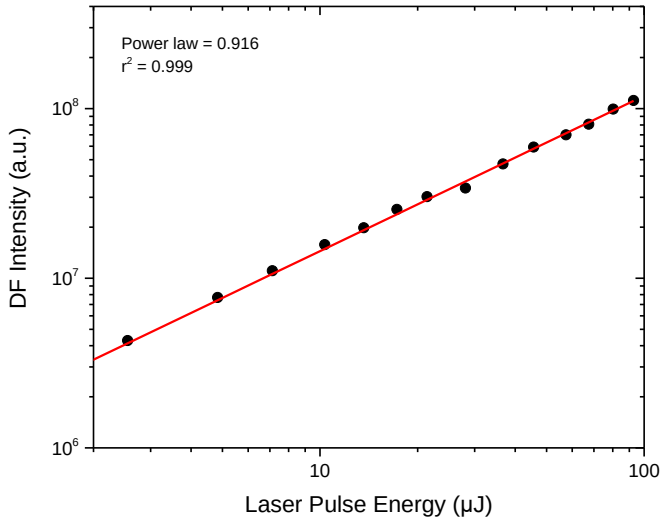

Figure 15: Power dependence of delayed fluorescence of a **N10** neat film at room temperature.

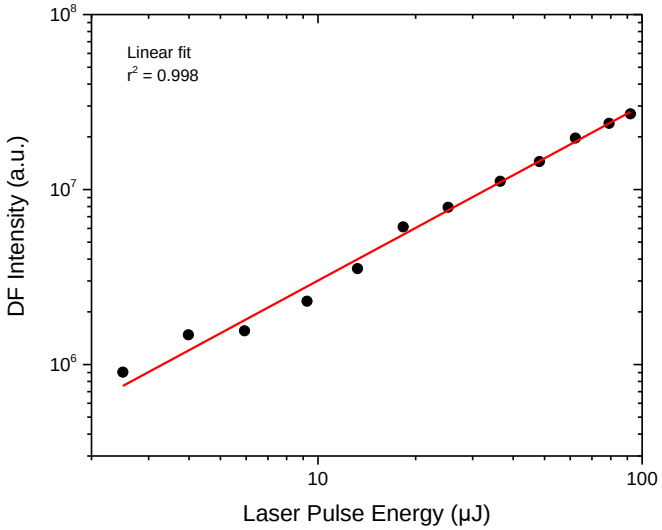

Figure 16: Power dependence of delayed fluorescence of **N10** zeonex film at room temperature.

The mechanochromism effect of the new donor-acceptor benzonitrile derivatives is exemplified by **N17** (**Figure 17**). Mechanochromic luminescent (MCL) materials have recently received considerable attention due to the possibilities to achieve tuning and switching on/off of their luminescence by using external stimuli.[35-36] They have found many applications in optoelectronic devices, sensors, probes, optical data storage devices, and security inks.[37-40] The mechanochromic behavior is generally observed upon applying an external stress, such as grinding, milling, shearing, heating, and solvent fuming. It is usually induced by either conformational changes that alter dipole−dipole interactions or changes in the intermolecular interaction between adjacent molecules.[35-36]

Therefore, the initial powder of **N17** shows an orange emission under 365 nm UV-irradiation (**Figure 17a**). Upon grinding, the emission shifts to red (**Figure 17b**), while after addition of toluene and drying the sample leading to a yellow/orange emission (**Figure 17c**). The red emission can be then restored after grinding the sample again (**Figure 17d**). The emission spectra of different forms of **N17** are shown in **Figure 18**.

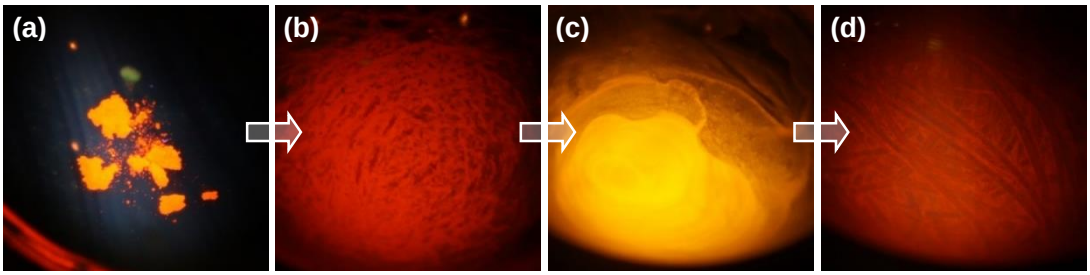

Figure 17: Photos of **N17** under 365 nm UV-irradiation, (a) initial powder, (b) after grinding, (c) after addition of toluene and drying, (d) after grinding.

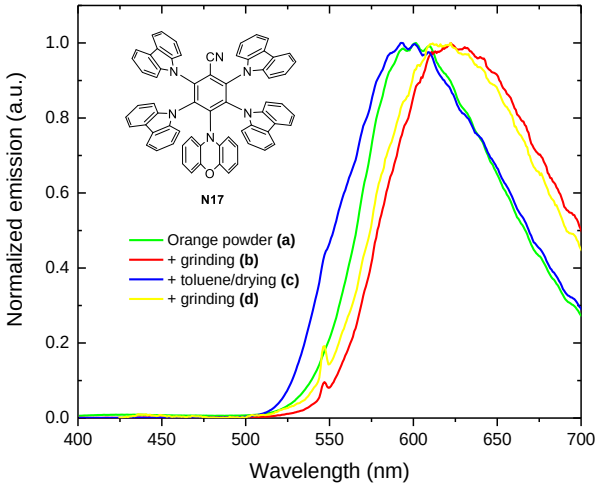

Figure 18: Normalized fluorescence spectra of **N17**, (a) initial powder, (b) after grinding, (c) after addition of toluene and drying, (d) after grinding.

3.7 Conclusion

In this chapter, three simple donor-acceptor benzonitrile derivatives have been firstly prepared. They have been successfully used for the preparation of 6 novel symmetrical and unsymmetrical 1,2,4,5-tetrazine derivatives, although yields are low. Then, an elaborative synthetic strategy to prepare novel donor-acceptor benzonitrile derivatives in a stepwise manner is introduced using the versatile precursor PFBN. Several series of new donor-acceptor benzonitrile derivatives were thus conveniently prepared. All the products were prepared by a one or two-step procedure in high yields. The X-ray single crystal structure of some compounds were presented and discussed to understand the structure-property relationship. The electrochemical properties of all the new benzonitrile derivatives are also presented and briefly discussed.

All the donor-acceptor benzonitrile derivatives exhibit TADF characteristics as expected. In addition, some of the compounds show interesting AIE or/and mechanochromism effect. The photophysics of **N10** is exemplified in this thesis which interestingly exhibit both TADF and AIE characteristics.

3.8 Experimental details

General Methods:

Synthesis. All chemicals were received from commercial sources and used without further purification. Thin layer chromatography (TLC) was performed on silica gel. Column chromatography was performed with SDS 0.040–0.063 mm silica gel. All mixtures of solvents are given in v/v ratio. NMR spectra were recorded on a JEOL ECS (400 MHz) spectrometer. ^{13}C NMR spectra were proton decoupled. HRMS spectra were measured either on an UPLC/ESI-HRMS device (an Acquity Waters UPLC system coupled to a Waters LCT Premier XE mass spectrometer equipped with an electrospray ion source), or a Q-TOF mass spectrometer (Q-TOF 6540, Agilent) equipped with an APPI ion source.

Photophysics. Zeonex ® 480 blends were prepared from toluene solutions by the drop-cast method and dried in vacuum. All solutions were investigated at 10^{-5} mol dm^{-3} concentration and were degassed using five freeze/pump cycles. Absorption and emission spectra were collected using a UV-3600 double beam spectrophotometer (Shimadzu), and a Fluoromax fluorescence spectrometer (Horiba) or QePro fluorescence spectrometer (Ocean Optics). Photoluminescence quantum yields of crystal and films were measured using an integrating sphere (Labsphere) coupled with a 365 nm LED light source (Ocean Optics) and a QePro fluorescence spectrometer (Ocean Optics). Photoluminescence quantum yield in MCH solution was measured using tetraphenylporphyrin (Φ_{PL} = 0.07) as the standard.

Phosphorescence, prompt fluorescence (PF), and delayed fluorescence (DF) spectra and decays were recorded using nanosecond gated luminescence and lifetime measurements (from 400 ps to 1 s) using either third harmonics of a high-energy, pulsed Nd:YAG laser emitting at 355 nm (EKSPLA) or a N2 laser emitting at 337 nm. Emission was focused onto a spectrograph and detected on a sensitive gated iCCD camera (Stanford Computer Optics) of sub-nanosecond resolution. PF/DF time-resolved measurements were performed by exponentially increasing gate and delay times.

Electrochemistry. The electrochemical cell comprised a platinum electrode with a 1 mm diameter of working area as a working electrode, an Ag electrode as a reference electrode and a platinum coil as an auxiliary electrode. Cyclic voltammetry measurements were conducted at room temperature at a potential rate of 50 mV/s and were calibrated against the ferrocene/ferrocenium redox couple. All voltammograms were recorded on a CHInstruments Electrochemical Analyzer model 660 potentiostat. Electrochemical measurements were conducted at 1.0 mM concentration in molecules, in 0.1 M solutions of Bu_4NPF_6 (99%) in DCM at room temperature.

Synthesis of N1-N3

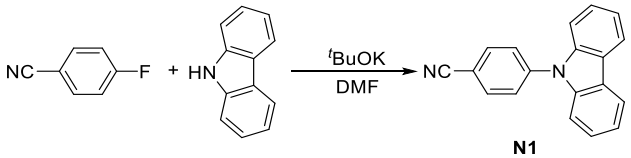

N1

To a 50 mL two-neck round bottom flask equipped with a stir bar, 5 mmol of carbazole (0.84 g), 5.5 mmol of potassium *tert*-butoxide (^{t}BuOK) (0.62 g) and 10 mL of dry DMF were added under inert atmosphere. Then 5 mmol of 4-fluorobenzonitrile (0.6 g) was added and the reaction mixture was allowed to stir at room temperature overnight. The reaction mixture was then neutralized with acidified water, extracted with dichloromethane, and dried over anhydrous magnesium sulfate ($MgSO_4$). The product was purified using silica gel chromatography (Petroleum ether:CH_2Cl_2= 3:1) to give 1.1 g of **N1** as a white solid (yield: 82%).

^{1}H NMR (400 MHz, $CDCl_3$, δ): 8.15 (d, *J* = 7.79 Hz, 2H), 7.92 (d, *J* = 8.60 Hz, 2H), 7.75 (d *J* = 8.60 Hz, 2H), 7.49–7.41 (m, 4H), 7.38–7.31 (m, 2H) ppm; ^{13}C NMR (100 MHz, $CDCl_3$, δ): 142.22, 140.02, 134.08, 127.26, 126.52, 124.14, 121.14, 120.73, 118.53, 110.60, 109.67 ppm.[13]

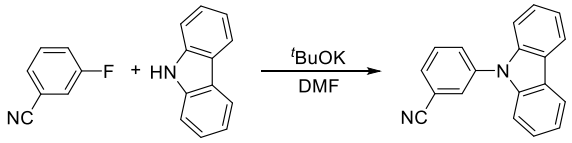

N2

To a 50 mL two-neck round bottom flask equipped with a stir bar, 5 mmol of carbazole (0.84 g), 5.5 mmol of ^{t}BuOK (0.62 g) and 10 mL of dry DMF were added under inert atmosphere. Then 5 mmol of 3-fluorobenzonitrile (0.6 g) was added and the reaction mixture was allowed to stir at room temperature overnight. After the reaction mixture was neutralized with acidified water, extracted with dichloromethane, and dried over anhydrous magnesium sulfate ($MgSO_4$). The product was purified using silica gel chromatography (Petroleum ether:CH_2Cl_2= 3:1) to give 1.0 g of **N2** as a white solid (yield: 75%).

^{1}H NMR (400 MHz, $CDCl_3$, δ): 8.16 (d, *J* = 7.79 Hz, 2H), 7.90 (s, 1H), 7.88–7.83 (m, 1H), 7.79–7.71 (m, 2H), 7.50–7.32 (m, 6H) ppm; ^{13}C NMR (100 MHz, $CDCl_3$, δ): 140.30, 138.96, 131.59, 131.09, 130.85, 130.40, 126.44, 123.83, 120.88, 120.68, 118.06, 114.29, 109.38 ppm.

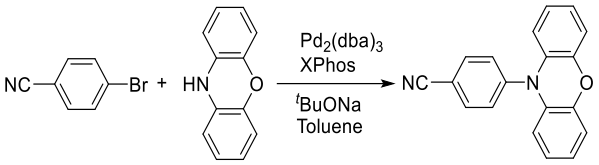

N3

To a 250 mL two-neck round bottom flask equipped with a stir bar, 4-bromobenzonitrile (5 mmol, 0.91 g), phenoxazine (5.5 mmol, 1.0 g), sodium *tert*-butoxide (^{t}BuONa) (5.5 mmol, 0.53 g) and 100 ml of anhydrous toluene were added. The reaction mixture was degassed by bubbling through nitrogen for 15 min under vigorous stirring. Then $Pd_2(dba)_3$ (0.1 mmol, 92 mg) and XPhos (0.25 mmol, 119 mg) were added and degassed for another 15 min. The reaction mixture was heated to 110 °C under a nitrogen atmosphere for 15 h. The reaction mixture was then cooled down to room temperature, extracted with dichloromethane, and dried over anhydrous magnesium sulfate ($MgSO_4$). The product was purified using silica gel chromatography (Petroleum ether:CH_2Cl_2= 3:1) to give 1.03 g of **N3** as an orange solid (yield: 73%).

^{1}H NMR (400 MHz, $CDCl_3$, δ): 7.89 (d, *J* = 8.20 Hz, 2H), 7.50 (d, *J* = 8.20 Hz, 2H), 6.76–6.56 (m, 6H), 5.91 (d, *J* = 7.80 Hz, 2H) ppm.[12]

Synthesis of Tz1-Tz3

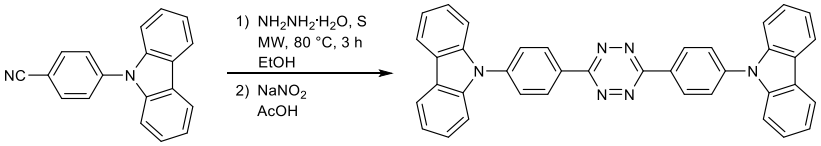

N1 **Tz1**, 11%

Procedure A: Nitrile precursor-**N1** (1 mmol, 0.268 g), sulfur (0.6 mmol, 19.2 mg) and ethanol (2 ml) were mixed together in a 30 ml microwave reaction tube. Hydrazine monohydrate (4 mmol, 0.2 ml) was added slowly with stirring afterwards. The vessel was sealed and the reaction mixture was heated to 80 °C for 3 hours. Then 3 ml of CH_2Cl_2 and sodium nitrite (5 mmol, 0.35 g) in 10 ml of H_2O were added to the mixture. Excess acetic acid (30 mmol, 1.71 ml) was then added slowly at 0 °C. The reaction mixture was extracted with dichloromethane. The organic phase was dried over anhydrous magnesium sulfate ($MgSO_4$), filtered and concentrated under reduced pressure. The product was purified using silica gel chromatography (Petroleum ether:CH_2Cl_2= 3:1) to give 31 mg of **Tz1** as an orange solid (yield: 11%).

^{1}H NMR (400 MHz, $CDCl_3$, δ): 8.95 (d, *J* = 8.60 Hz, 4H), 8.19 (d, *J* = 7.80 Hz, 4H), 7.91 (d *J* = 8.60 Hz, 4H), 7.60 (d, *J* = 7.80 Hz, 4H), 7.48 (t, *J* = 7.80 Hz, 4H), 7.36 (t, *J* = 7.80 Hz, 4H) ppm; ^{13}C NMR (100 MHz, $CDCl_3$, δ): 163.61, 142.22, 140.37, 130.27, 129.80, 127.46, 126.41, 124.05, 120.81, 120.66, 110.04 ppm.

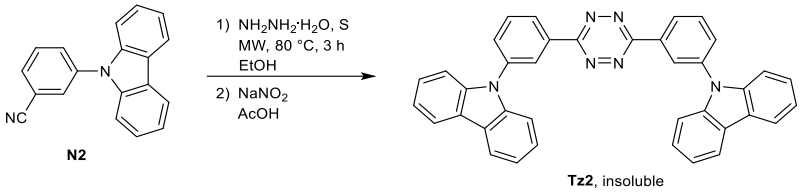

Tz2 was prepared following **Procedure A** using **N2** as a nitrile precursor. It was purified using silica gel chromatography (Petroleum ether:CH_2Cl_2= 3:1) to give a red solution. However, the product quickly precipitated from the solution afterwards and became insoluble in any organic solvents. Therefore it was not possible to characterize it by common characterization methods.

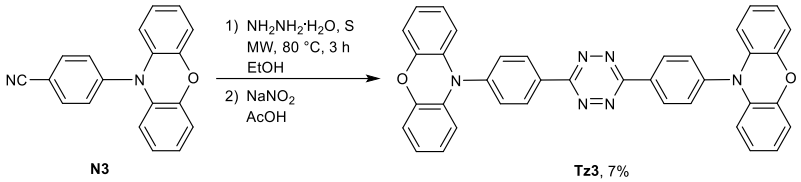

Tz3 was prepared following **Procedure A** using **N3** as a nitrile precursor. It was obtained as a purple solid after silica gel chromatography (Petroleum ether:CH_2Cl_2= 3:1) (20 mg, yield: 7%).

^{1}H NMR (400 MHz, $CDCl_3$, δ): 8.90 (d, *J* = 8.60 Hz, 4H), 7.64 (d, *J* = 8.60 Hz, 4H), 6.77–6.60 (m, 12H), 6.06 (d, *J* = 7.80 Hz, 4H) ppm.

Synthesis of TA1, TA1' and TA2

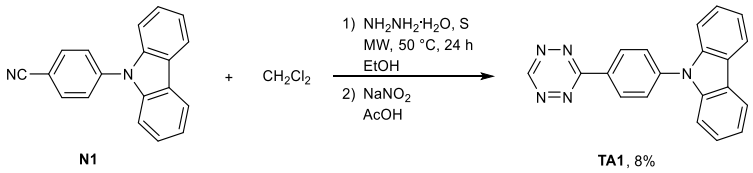

Procedure B: Nitrile precursor-**N1** (1 mmol, 0.268 g), CH_2Cl_2 (1 mmol, 63.70 µl), sulfur (2 mmol, 64 mg) and ethanol (2 ml) were mixed together in a 30 ml microwave reaction tube. Hydrazine monohydrate (8 mmol, 0.4 ml) was added slowly with stirring afterwards. The vessel was sealed and the reaction mixture was heated to 50 °C for 24 hours. Then 3 ml of CH_2Cl_2 and sodium nitrite (10 mmol, 0.69 g) in 10 ml of H_2O were added to the mixture. Excess acetic acid (60 mmol, 3.42 ml) was then added slowly at 0 °C. The reaction mixture was extracted with dichloromethane. The organic phase was dried over anhydrous magnesium sulfate ($MgSO_4$), filtered and concentrated under reduced pressure. The

product was purified using silica gel chromatography (Petroleum ether:CH_2Cl_2= 1:1) to give 25 mg of **TA1** as a red solid (yield: 8%).

^{1}H NMR (400 MHz, $CDCl_3$, δ): 10.27 (s, 1H), 8.89 (d, *J* = 8.24 Hz, 2H), 8.17 (d, *J* = 7.80 Hz, 2H), 7.88 (d, *J* = 8.24 Hz, 2H), 7.56 (d, *J* = 7.80 Hz, 2H), 7.46 (t, *J* = 7.80 Hz, 2H), 7.34 (t, *J* = 7.80 Hz, 2H) ppm; ^{13}C NMR (100 MHz, $CDCl_3$, δ): 166.11, 157.96, 142.56, 140.29, 130.10, 130.06, 127.40, 126.41, 124.05, 120.84, 120.65, 109.99 ppm; HRMS $[M+H]^+$ m/z calcd. for $[C_{20}H_{14}N_5]^+$ 324.1249, found 324.1253.

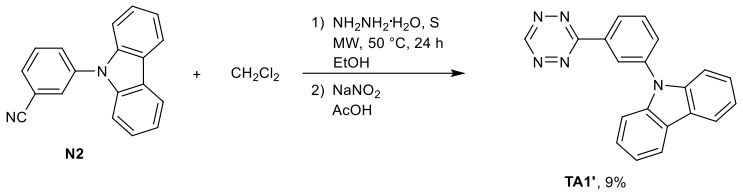

TA1' was prepared following **Procedure B** using **N2** as a nitrile precursor. It was obtained as a red solid after silica gel chromatography (Petroleum ether:CH_2Cl_2= 1:1) (29 mg, yield: 9%).

^{1}H NMR (400 MHz, $CDCl_3$, δ): 10.27 (s, 1H), 8.89 (t, *J* = 1.70 Hz, 1H), 8.73 (dt, *J* = 7.80 Hz, *J* = 1.70 Hz, 1H), 8.17 (d, *J* = 7.80 Hz, 2H), 7.94–7.82 (m, 2H), 7.52–7.41 (m, 4H), 7.36–7.30 (m, 2H) ppm; ^{13}C NMR (100 MHz, $CDCl_3$, δ): 166.14, 158.19, 140.68, 139.20, 133.74, 131.65, 131.17, 127.13, 126.83, 126.33, 123.76, 120.60, 120.53, 109.76 ppm.

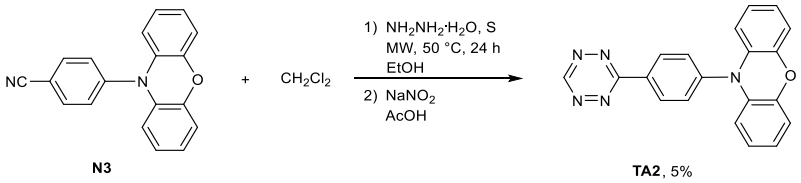

TA2 was prepared following **Procedure B** using **N3** as a nitrile precursor. It was obtained as a deep red solid after silica gel chromatography (Petroleum ether:CH_2Cl_2= 1:1) (16 mg, yield: 5%).

^{1}H NMR (400 MHz, $CDCl_3$, δ): 10.28 (s, 1H), 8.87 (d, *J* = 8.24 Hz, 2H), 7.63 (d, *J* = 8.24 Hz, 2H), 6.79–6.59 (m, 6H), 6.05 (dd, *J* = 7.80 Hz, *J* = 1.50 Hz, 2H) ppm; ^{13}C NMR (100 MHz, $CDCl_3$, δ): 166.08, 158.04, 144.18, 144.06, 133.78, 132.01, 131.62, 131.16, 123.47, 122.08, 115.92, 113.53 ppm; HRMS $[M+H]^+$ m/z calcd. for $[C_{20}H_{14}N_5O]^+$ 340.1198, found 340.1192.

Synthesis of N4-N22

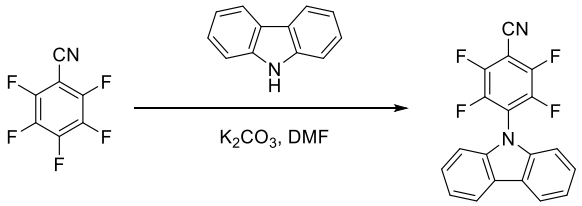

N4

To a 50 mL two-neck round bottom flask equipped with a stir bar, 1 mmol of carbazole (0.167 g), 1.2 mmol of potassium carbonate (K_2CO_3) (0.166 g) and 6 mL of dry DMF were added under inert atmosphere. Then 1 mmol of 2,3,4,5,6-pentafluorobenzonitrile (PFBN) (0.125 mL) was added at 0 °C and the reaction mixture was allowed to stir at room temperature overnight. After the reaction mixture was neutralized with acidified water, extracted with dichloromethane, and dried over anhydrous magnesium sulfate ($MgSO_4$). The product first was purified by recrystallization from CH_2Cl_2 to afford 0.192 g white crystals **N4**. The residue was purified using silica gel chromatography (Petroleum ether:CH_2Cl_2= 3:1) to give 0.08 g of **N4** as a white solid (total yield: 82%).

^{1}H NMR (400 MHz, $CDCl_3$, δ): 8.13 (dd, *J* = 7.79 Hz, *J* = 1.37 Hz, 2H), 7.48 (ddd, *J* = 8.24 Hz, *J* = 7.33 Hz, *J* = 1.37 Hz, 2H), 7.38 (ddd, *J* = 7.79 Hz, *J* = 7.33 Hz, *J* = 0.92 Hz, 2H), 7.13 (d, *J* = 8.24 Hz, 2H) ppm; ^{13}C NMR (100 MHz, $CDCl_3$, δ): 148.09 (dd, $^1J_{CF}$ = 264.06 Hz, $^2J_{CF}$ = 14.38 Hz), 143.70 (dd, $^1J_{CF}$ = 258.79 Hz, $^2J_{CF}$ = 12.46 Hz), 139.14, 126.90, 124.64, 122.87 (t, $^2J_{CF}$ = 14.38 Hz), 122.15, 120.82, 110.02, 107.22 (t, $^3J_{CF}$ = 4.79 Hz), 93.58 (t, $^2J_{CF}$ = 17.25 Hz) ppm; ^{19}F NMR (376 MHz, $CDCl_3$, δ): -130.45 (s, 2F), -138.09 (s, 2F) ppm; HRMS $[M]^+$ m/z calcd. for $[C_{19}H_8N_2F_4]^+$ 340.0642, found 340.0614.

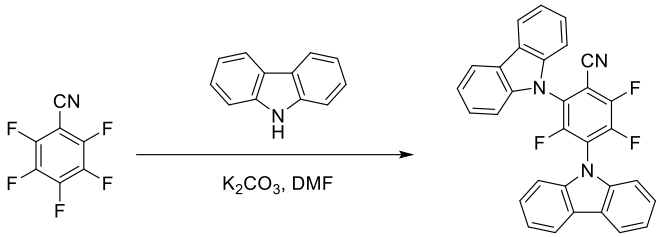

N5

To a 50 mL two-neck round bottom flask equipped with a stir bar, 2 mmol of carbazole (0.334 g), 2.4 mmol of K_2CO_3 (0.332 g) and 6 mL of dry DMF were added under inert atmosphere. Then 1 mmol of PFBN (0.125 mL) was added at 0 °C and the reaction mixture was allowed to stir at room temperature overnight. After the reaction mixture was neutralized with acidified water, extracted with dichloromethane, and dried over anhydrous $MgSO_4$. The product was purified using silica gel chromatography (Petroleum ether:CH_2Cl_2= 3:1) to give 0.346 g of **N5** as a white solid (yield: 71%).

^{1}H NMR (400 MHz, $CDCl_3$, δ): 8.16-8.12 (m, 4H), 7.53-7.47 (m, 4H), 7.40-7.36 (m, 4H), 7.25-7.21 (m, 4H) ppm; ^{13}C NMR (100 MHz, $CDCl_3$, δ): 151.83 (d, $^{1}J_{CF}$ = 262.62 Hz), 149.74 (dd, $^{1}J_{CF}$ = 260.70 Hz, $^{2}J_{CF}$ = 18.21 Hz), 146.95 (dd, $^{1}J_{CF}$ = 263.10 Hz, $^{2}J_{CF}$ = 13.42 Hz), 139.97, 139.25, 126.87, 126.80, 125.28 (d, $^{2}J_{CF}$ = 18.21 Hz), 124.64, 124.46, 122.65 (t, $^{2}J_{CF}$ = 16.29 Hz), 122.08, 121.90, 121.02, 120.84, 110.03, 109.51, 109.27 (t, $^{3}J_{CF}$ = 4.79 Hz), 103.38 (d, $^{2}J_{CF}$ = 15.34 Hz) ppm; ^{19}F NMR (376 MHz, $CDCl_3$, δ): -117.53 (s, 1F), -128.60 (s, 1F), -131.38 (s, 1F)) ppm; HRMS $[M+H]^+$ m/z calcd. for $[C_{31}H_{17}N_3F_3]^+$ 488.1375, found 488.1368.

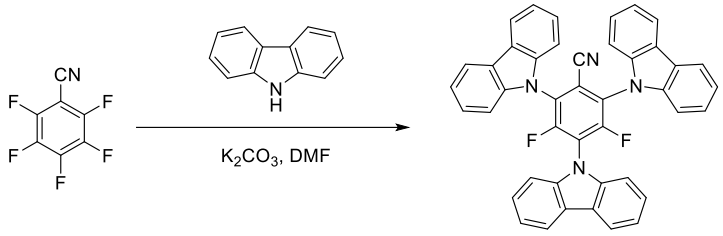

N6

To a 50 mL two-neck round bottom flask equipped with a stir bar, 3 mmol of carbazole (0.501 g), 3.6 mmol of K_2CO_3 (0.497 g) and 6 mL of dry DMF were added under inert atmosphere. Then 1 mmol of PFBN (0.125 mL) was added at 0 °C and the reaction mixture was allowed to stir at room temperature overnight. Afterwards the reaction mixture was neutralized with acidified water, extracted with dichloromethane, and dried over anhydrous $MgSO_4$. The product was purified using silica gel chromatography (Petroleum ether:CH_2Cl_2= 2:1) to give 0.527 g of **N6** as a white solid (yield: 83%).

^{1}H NMR (400 MHz, $CDCl_3$, δ): 8.17 (d, *J* = 7.79 Hz, 4H), 8.12 (d, *J* = 7.79 Hz, 2H), 7.57 (ddd, *J* = 7.98 Hz, *J* = 7.33 Hz, *J* = 1.37 Hz, 4H), 7.51 (ddd, *J* = 8.24 Hz, *J* = 7.33 Hz, *J* = 1.37 Hz, 2H), 7.42-7.35 (m, 10H), 7.29 (d, *J* = 8.24 Hz, 2H) ppm; ^{13}C NMR (100 MHz, $CDCl_3$, δ): 155.30 (dd, $^{1}J_{CF}$ = 266.45 Hz, $^{3}J_{CF}$ = 4.79 Hz), 140.15, 139.31, 127.22 (dd, $^{2}J_{CF}$ = 14.38 Hz, $^{4}J_{CF}$ = 5.75 Hz), 126.87, 126.85, 124.65, 124.52, 122.35 (t, $^{2}J_{CF}$ = 15.34 Hz), 122.03, 121.89, 121.13, 120.88, 114.85, 111.36 (t, $^{3}J_{CF}$ = 4.79 Hz), 110.01, 109.42 ppm; ^{19}F NMR (376 MHz, $CDCl_3$, δ): -111.26 (s, 2F) ppm; HRMS $[M+H]^+$ m/z calcd. for $[C_{43}H_{25}N_4F_2]^+$ 635.2047, found 635.2040.[9]

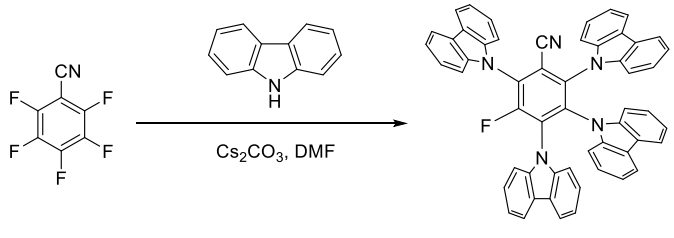

N7

To a 50 mL two-neck round bottom flask equipped with a stir bar, 4 mmol of carbazole (0.668 g), 4.8 mmol of cesium carbonate (Cs_2CO_3) (1.564 g) and 8 mL of dry DMF were added under inert atmosphere. Then 1 mmol of PFBN (0.125 mL) was added and the reaction mixture was stirred at 60 °C overnight. Afterwards the reaction mixture was neutralized with acidified water, extracted with dichloromethane, and dried over anhydrous $MgSO_4$. The product was purified using silica gel chromatography (Petroleum ether:CH_2Cl_2= 2:1) to give 0.719 g of **N7** as a light yellow solid (yield: 92%).

^{1}H NMR (400 MHz, $CDCl_3$, δ): 8.20 (d, *J* = 7.79 Hz, 2H), 7.73-7.71 (m, 4H), 7.67-7.60 (m, 4H), 7.44 (ddd, *J* = 7.79 Hz, *J* = 6.87 Hz, *J* = 1.37 Hz, 2H), 7.34 (d, *J* = 7.79 Hz, 2H), 7.23-7.17 (m, 4H), 7.11-7.03 (m, 8H), 6.94 (d, *J* = 8.24 Hz, 2H), 6.81 (ddd, *J* = 7.79 Hz, *J* = 6.87 Hz, *J* = 0.92 Hz, 2H), 6.65 (ddd, *J* = 8.24 Hz, *J* = 7.33 Hz, *J* = 1.37 Hz, 2H) ppm; ^{13}C NMR (100 MHz, $CDCl_3$, δ): 155.47 (d, $^1J_{CF}$ = 263.58 Hz), 140.19, 138.87, 138.59, 137.55, 137.28 (d, $^3J_{CF}$ = 3.83 Hz), 135.31, 131.62 (d, $^2J_{CF}$ = 13.42 Hz), 129.70 (d, $^2J_{CF}$ = 13.42 Hz), 126.91, 125.86, 125.72, 124.84, 124.74, 124.33, 124.24, 123.91, 121.98, 121.46, 121.35, 121.20, 120.89, 120.45, 120.31, 119.70, 115.81 (d, $^4J_{CF}$ = 2.88 Hz), 112.26 (d, $^3J_{CF}$ = 3.83 Hz), 110.09, 109.90, 109.85, 109.81 ppm; ^{19}F NMR (376 MHz, $CDCl_3$, δ): -112.20 (s, 1F) ppm; HRMS $[M+H]^+$ m/z calcd. for $[C_{55}H_{33}N_5F]^+$ 782.2720, found 782.2729.[9]

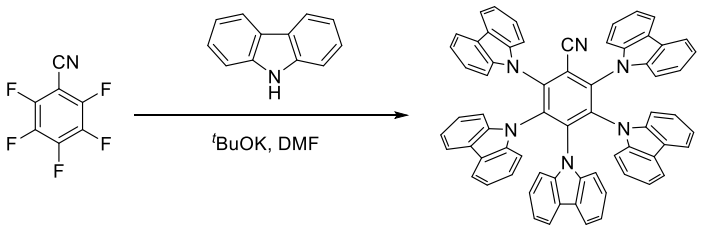

N8

To a 50 mL two-neck round bottom flask equipped with a stir bar, 5 mmol of carbazole (0.835 g), 5 mmol of potassium *tert*-butoxide (^{t}BuOK) (0.561 g) and 8 mL of dry DMF were added under inert atmosphere. The solution was allowed to stir at room temperature for 1 h. Then 1 mmol of PFBN (0.125 mL) was added and the reaction mixture was stirred at 80 °C overnight. Afterwards the reaction mixture was neutralized with acidified water, extracted with dichloromethane, and dried over anhydrous $MgSO_4$. The product was purified using silica gel chromatography (Petroleum ether:CH_2Cl_2= 3:2) to give 0.883 g of **N8** as a light yellow solid (yield: 95%).

^{1}H NMR (400 MHz, DMSO-d_6, δ): 7.83-7.80 (m, 8H), 7.71 (d, *J* = 8.24 Hz, 2H), 7.68 (d, *J* = 8.24 Hz, 4H), 7.35 (d, *J* = 7.79 Hz, 4H), 7.29 (d, *J* = 7.79 Hz, 2H), 7.10 (ddd, *J* = 7.79 Hz, *J* = 7.33 Hz, *J* = 0.92 Hz, 4H), 7.03 (ddd, *J* = 7.79 Hz, *J* = 7.33 Hz, *J* = 0.92 Hz, 4H), 6.72-6.60 (m, 10H), 6.55 (ddd, *J* = 8.24 Hz, *J* = 7.33 Hz, *J* = 0.92 Hz, 2H) ppm; ^{13}C NMR (100 MHz, DMSO-d_6, δ): 143.01, 141.66, 139.84, 138.80, 138.59, 125.49, 124.10, 123.30,

123.04, 122.98, 121.09, 120.55, 120.45, 119.62, 119.52, 117.72, 113.65, 112.62, 112.34, 112.14 ppm; HRMS $[M]^+$ m/z calcd. for $[C_{67}H_{40}N_6]^+$ 928.3, found 928.3.[5–7]

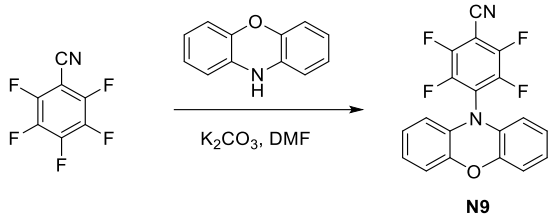

N9

To a 50 mL two-neck round bottom flask equipped with a stir bar, 1 mmol of phenoxazine (0.183 g), 1.2 mmol of potassium carbonate (K_2CO_3) (0.166 g) and 6 mL of dry DMF were added under inert atmosphere. Then 1 mmol of 2,3,4,5,6-pentafluorobenzonitrile (PFBN) (0.125 mL) was added at 0°C and the reaction mixture was allowed to stir at room temperature overnight. Afterwards the reaction mixture was neutralized with acidified water, extracted with dichloromethane, and dried over anhydrous magnesium sulfate ($MgSO_4$). The product was purified using silica gel chromatography (Petroleum ether:CH_2Cl_2= 3:1) to give 0.303 g of **N9** as an orange solid (yield: 85%). Single crystal of **N9** was grown from slow evaporation of petroleum ether/dichloromethane (3:1) mixture.

^{1}H NMR (400 MHz, $CDCl_3$, δ): 6.86-6.81 (m, 4H), 6.77-6.72 (m, 2H), 6.01 (d, *J* = 7.33 Hz, 2H) ppm; ^{13}C NMR (100 MHz, $CDCl_3$, δ): 148.42 (dd, $^1J_{CF}$ = 265.50 Hz, $^2J_{CF}$ = 15.34 Hz), 146.41 (dd, $^1J_{CF}$ = 259.91 Hz, $^2J_{CF}$ = 13.42 Hz), 144.08, 130.31, 123.97, 123.84, 123.77 (t, $^2J_{CF}$ = 14.38 Hz), 116.80, 112.91, 107.06 (t, $^3J_{CF}$ = 3.83 Hz), 95.09 (t, $^2J_{CF}$ = 17.25 Hz) ppm; ^{19}F NMR (376 MHz, $CDCl_3$, δ): -129.80 (s, 2F), -138.00 (s, 2F) ppm; HRMS $[M]^+$ m/z calcd. for $[C_{19}H_8N_2OF_4]^+$ 356.0573, found 356.0587.

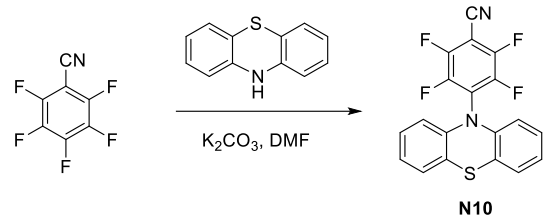

N10

To a 50 mL two-neck round bottom flask equipped with a stir bar, 1 mmol of phenothiazine (0.199 g), 1.2 mmol of potassium carbonate (K_2CO_3) (0.166 g) and 6 mL of dry DMF were added under inert atmosphere. Then 1 mmol of 2,3,4,5,6-pentafluorobenzonitrile (PFBN) (0.125 mL) was added at 0°C and the reaction mixture was allowed to stir at room temperature overnight. After the reaction mixture was neutralized with acidified water, extracted with dichloromethane, and dried over anhydrous magnesium sulfate ($MgSO_4$). The product was purified using silica gel chromatography (Petroleum ether:CH_2Cl_2= 3:1)

to give 0.298 g of **N10** as a green solid (yield: 80%). Single crystal of **N10** was grown from slow evaporation of petroleum ether/dichloromethane (3:1) mixture.

^{1}H NMR (400 MHz, $CDCl_3$, δ): 7.13-7.10 (m, 2H), 7.01-6.94 (m, 4H), 6.25 (dd, *J* = 7.79 Hz, *J* = 1.37 Hz, 2H) ppm; ^{13}C NMR (100 MHz, $CDCl_3$, δ): 148.31 (dd, $^{1}J_{CF}$ = 265.50 Hz, $^{2}J_{CF}$ = 15.34 Hz), 146.53 (dd, $^{1}J_{CF}$ = 258.79 Hz, $^{2}J_{CF}$ = 13.42 Hz), 140.96, 127.56, 127.54, 126.85 (t, $^{2}J_{CF}$ = 15.34 Hz), 124.67, 123.04, 115.72, 107.07 (t, $^{3}J_{CF}$ = 4.79 Hz), 95.38 (t, $^{2}J_{CF}$ = 17.25 Hz) ppm; ^{19}F NMR (376 MHz, $CDCl_3$, δ): -129.98 (s, 2F), -138.22 (s, 2F) ppm; HRMS $[M]^+$ m/z calcd. for $[C_{19}H_8N_2SF_4]^+$ 372.0344, found 372.0345.

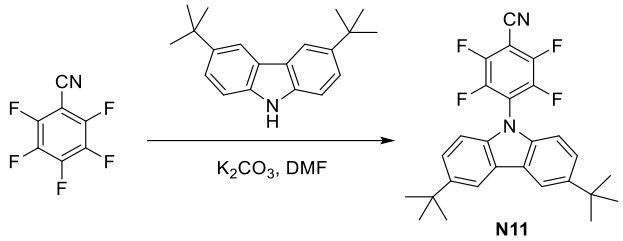

N11

To a 50 mL two-neck round bottom flask equipped with a stir bar, 1 mmol of 3,6-di-*tert*-butyl-*9H*-carbazole (0.279 g), 1.2 mmol of potassium carbonate (K_2CO_3) (0.166 g) and 6 mL of dry DMF were added under inert atmosphere. Then 1 mmol of 2,3,4,5,6-pentafluorobenzonitrile (PFBN) (0.125 mL) was added at 0°C and the reaction mixture was allowed to stir at room temperature overnight. After the reaction mixture was neutralized with acidified water, extracted with dichloromethane, and dried over anhydrous magnesium sulfate ($MgSO_4$). The product was purified using silica gel chromatography (Petroleum ether:CH_2Cl_2= 3:1) to give 0.389 g of **N11** as a white solid (yield: 86%).

^{1}H NMR (400 MHz, $CDCl_3$, δ): 8.12 (d, *J* = 1.80 Hz, 2H), 7.51 (dd, *J* = 8.24 Hz, *J* = 1.80 Hz, 2H), 7.05 (dt, *J* = 8.24 Hz, *J* = 1.80 Hz, 2H), 1.46 (s, 18H) ppm; ^{13}C NMR (100 MHz, $CDCl_3$, δ): 148.05 (d, $^{1}J_{CF}$ = 262.77 Hz), 145.31, 143.62 (d, $^{1}J_{CF}$ = 260.22 Hz), 137.57, 124.74, 124.51, 123.36, 116.92, 109.64, 107.42, 93.00, 35.00, 32.03 ppm; ^{19}F NMR (376 MHz, $CDCl_3$, δ): -130.86 (s, 2F), -138.43 (s, 2F) ppm; HRMS $[M]^+$ m/z calcd. for $[C_{27}H_{24}N_2F_4]^+$ 452.1876, found 452.1869.

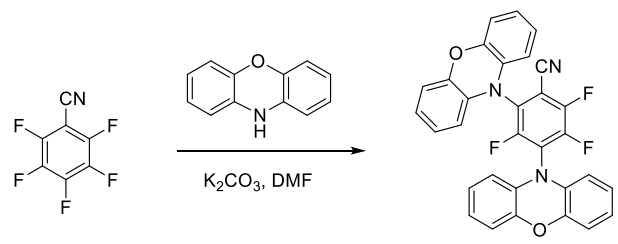

N12

To a 50 mL two-neck round bottom flask equipped with a stir bar, 2 mmol of phenoxazine (0.366 g), 2.4 mmol of K_2CO_3 (0.332 g) and 6 mL of dry DMF were added under inert atmosphere. Then 1 mmol of PFBN (0.125 mL) was added at 0°C and the reaction mixture was allowed to stir at room temperature overnight. Afterwards the reaction mixture was neutralized with acidified water, extracted with dichloromethane, and dried over anhydrous $MgSO_4$. The product was purified using silica gel chromatography (Petroleum ether:CH_2Cl_2= 3:1) to give 0.384 g of **N12** as an orange solid (yield: 74%). Single crystal of **N12** was grown from slow evaporation of petroleum ether/dichloromethane (3:1) mixture.

^{1}H NMR (400 MHz, $CDCl_3$, δ): 6.85-6.80 (m, 8H), 6.78-6.72 (m, 4H), 6.03 (d, *J* = 7.33 Hz, 2H), 5.97 (d, *J* = 7.33 Hz, 2H) ppm; ^{13}C NMR (100 MHz, $CDCl_3$, δ): 158.33 (d, $^1J_{CF}$ = 263.58 Hz), 150.60 (d, $^1J_{CF}$ = 265.50 Hz), 150.47 (d, $^1J_{CF}$ = 263.58 Hz), 144.16, 131.14, 130.46, 126.96 (d, $^2J_{CF}$ = 15.34 Hz), 124.35 (t, $^2J_{CF}$ = 15.34 Hz), 123.94, 123.85, 123.81, 116.90, 116.86, 112.73, 109.03, 108.07 (d, $^2J_{CF}$ = 11.50 Hz) ppm; ^{19}F NMR (376 MHz, $CDCl_3$, δ): -117.08 (s, 1F), -126.73 (s, 1F), -129.80 (s, 1F) ppm; HRMS $[M]^+$ m/z calcd. for $[C_{31}H_{16}N_3O_2F_3]^+$ 519.1195, found 519.1198.

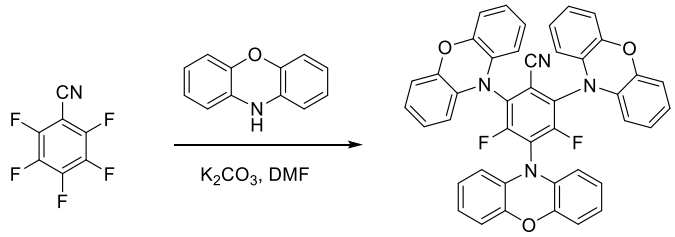

N13

To a 50 mL two-neck round bottom flask equipped with a stir bar, 3 mmol of phenoxazine (0.550 g), 3.6 mmol of K_2CO_3 (0.497 g) and 6 mL of dry DMF were added under inert atmosphere. Then 1 mmol of PFBN (0.125 mL) was added at 0°C and the reaction mixture was allowed to stir at room temperature overnight. Afterwards the reaction mixture was neutralized with acidified water, extracted with dichloromethane, and dried over anhydrous $MgSO_4$. The product was purified using silica gel chromatography (Petroleum ether:CH_2Cl_2= 2:1) to give 0.444 g of **N13** as a red solid (yield: 65%).

^{1}H NMR (400 MHz, $CDCl_3$, δ): 6.85-6.76 (m, 18H), 6.03-5.99 (m, 6H) ppm; ^{13}C NMR (100 MHz, $CDCl_3$, δ): 161.08 (dd, $^1J_{CF}$ = 267.41 Hz, $^3J_{CF}$ = 4.79 Hz), 144.24, 144.19, 131.21, 130.49, 129.41 (dd, $^2J_{CF}$ = 13.42 Hz, $^4J_{CF}$ = 5.75 Hz), 124.96 (t, $^2J_{CF}$ = 16.29 Hz), 123.87, 123.85, 123.83, 123.81, 123.28, 116.96, 116.88, 112.47, 112.40, 111.12 ppm; ^{19}F NMR (376 MHz, $CDCl_3$, δ): -109.33 (s, 2F) ppm; HRMS $[M+H]^+$ m/z calcd. for $[C_{43}H_{25}N_4O_3F_2]^+$ 683.1895, found 683.1893.

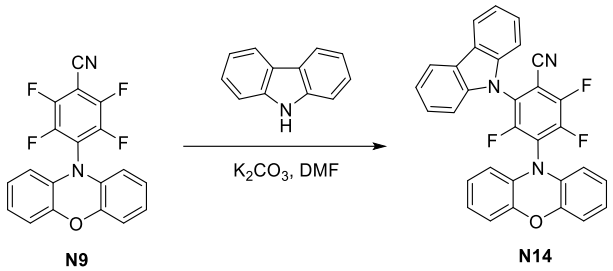

N9 **N14**

To a 50 mL two-neck round bottom flask equipped with a stir bar, 1 mmol of carbazole (0.167 g), 1.2 mmol of potassium carbonate (K_2CO_3) (0.166 g) and 6 mL of dry DMF were added under inert atmosphere. Then 1 mmol of **N9** (0.356 g) was added at 0 °C and the reaction mixture was allowed to stir at room temperature overnight. Afterwards the reaction mixture was neutralized with acidified water, extracted with dichloromethane, and dried over anhydrous magnesium sulfate ($MgSO_4$). The product was purified using silica gel chromatography (Petroleum ether:CH_2Cl_2= 3:1) to give 0.347 g of **N14** as a yellow solid (yield: 69%). A single crystal of **N14** was grown from slow evaporation of petroleum ether/dichloromethane (3:1) mixture.

^{1}H NMR (400 MHz, $CDCl_3$, δ): 8.14 (d, *J* = 7.79 Hz, 2H), 7.48 (ddd, *J* = 8.24 Hz, *J* = 7.33 Hz, *J* = 1.37 Hz, 2H), 7.38 (ddd, *J* = 7.79 Hz, *J* = 7.33 Hz, *J* = 1.37 Hz, 2H), 7.13 (d, *J* = 8.24 Hz, 2H), 6.84-6.77 (m, 6H), 6.14 (d, *J* = 7.79 Hz, 2H) ppm; ^{13}C NMR (100 MHz, $CDCl_3$, δ): 154.57 (d, $^1J_{CF}$ = 262.62 Hz), 150.07 (ddd, $^1J_{CF}$ = 265.50 Hz, $^2J_{CF}$ = 14.38 Hz, $^3J_{CF}$ = 3.83 Hz), 149.79 (ddd, $^1J_{CF}$ = 262.62 Hz, $^2J_{CF}$ = 11.50 Hz, $^3J_{CF}$ = 3.83 Hz), 144.15, 139.84, 130.53, 126.83, 125.71 (d, $^2J_{CF}$ = 17.25 Hz), 124.51, 123.92, 123.89, 123.51 (t, $^2J_{CF}$ = 16.29 Hz), 121.97, 121.07, 116.84, 112.78, 109.49, 109.15, 104.75 (d, $^2J_{CF}$ = 14.38 Hz) ppm; ^{19}F NMR (376 MHz, $CDCl_3$, δ): -117.61 (s, 1F), -127.87 (s, 1F), -131.61 (s, 1F) ppm; HRMS $[M]^+$ m/z calcd. for $[C_{31}H_{16}N_3OF_3]^+$ 503.1245, found 503.1246.

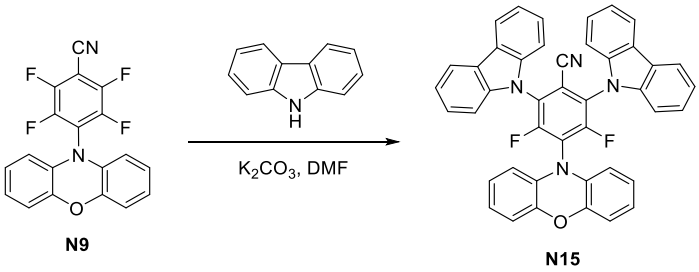

N9 **N15**

To a 50 mL two-neck round bottom flask equipped with a stir bar, 2 mmol of carbazole (0.334 g), 2.4 mmol of K_2CO_3 (0.332 g) and 6 mL of dry DMF were added under inert atmosphere. Then 1 mmol of **N9** (0.356 g) was added at 0 °C and the reaction mixture was allowed to stir at room temperature overnight. Afterwards the reaction mixture was neutralized with acidified water, extracted with dichloromethane, and dried over anhydrous magnesium sulfate ($MgSO_4$). The product was purified using silica gel chromatography

(Petroleum ether:CH_2Cl_2= 2:1) to give 0.482 g of **N15** as a yellow solid (yield: 74%). A single crystal of **N15** was grown from slow evaporation of methanol/dichloromethane (1:1) mixture.

^{1}H NMR (400 MHz, $CDCl_3$, δ): 8.16 (d, *J* = 7.79 Hz, 4H), 7.56-7.52 (m, 4H), 7.41-7.37 (m, 4H), 7.27-7.24 (m, 4H), 6.88-6.79 (m, 6H), 6.26-6.23 (m, 2H) ppm; ^{13}C NMR (100 MHz, $CDCl_3$, δ): 158.18 (dd, $^1J_{CF}$ = 262.62 Hz, $^3J_{CF}$ = 4.79 Hz), 144.22, 140.00, 130.74, 127.59 (dd, $^2J_{CF}$ = 14.38 Hz, $^4J_{CF}$ = 5.75 Hz), 126.89, 124.57, 123.95, 123.89, 123.22 (t, $^2J_{CF}$ = 15.34 Hz), 121.96, 121.16, 116.89, 116.12 (t, $^4J_{CF}$ = 2.88 Hz), 112.58, 111.28 (t, $^3J_{CF}$ = 3.83 Hz), 109.40 ppm; ^{19}F NMR (376 MHz, $CDCl_3$, δ): -111.56 (s, 2F) ppm; HRMS $[M+H]^+$ m/z calcd. for $[C_{43}H_{25}N_4OF_2]^+$ 651.1983, found 651.1987.

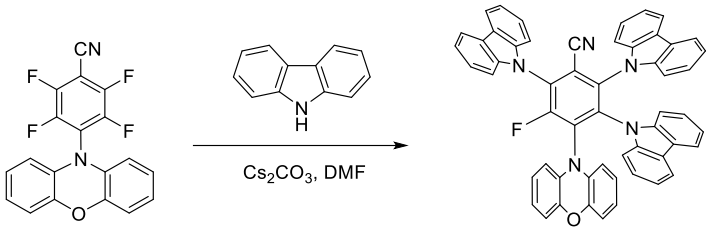

N9 **N16**

To a 50 mL two-neck round bottom flask equipped with a stir bar, 3 mmol of carbazole (0.501 g), 3.6 mmol of Cs_2CO_3 (1.173 g) and 8 mL of dry DMF were added under inert atmosphere. Then 1 mmol of **N9** (0.356 g) was added and the reaction mixture was stirred at 60 °C overnight. Afterwards the reaction mixture was neutralized with acidified water, extracted with dichloromethane, and dried over anhydrous $MgSO_4$. The product was purified using silica gel chromatography (Petroleum ether:CH_2Cl_2= 2:1) to give 0.718 g of **N16** as an orange solid (yield: 90%). A single crystal of **N16** was grown from slow evaporation of ethyl acetate/dichloromethane (1:1) mixture.

^{1}H NMR (400 MHz, $CDCl_3$, δ): 8.21 (d, *J* = 7.79 Hz, 2H), 7.73 (d, *J* = 7.79 Hz, 2H), 7.66-7.62 (m, 2H), 7.55-7.52 (m, 4H), 7.47-7.43 (m, 2H), 7.30 (d, *J* = 7.79 Hz, 2H), 7.17-7.13 (m, 2H), 7.10-7.06 (m, 2H), 6.94-6.89 (m, 4H), 6.77-6.73 (m, 2H), 6.56-6.51 (m, 4H), 6.38-6.33 (m, 4H) ppm; ^{13}C NMR (100 MHz, $CDCl_3$, δ): 158.64 (d, $^1J_{CF}$ = 262.62 Hz), 144.91, 140.14, 139.02, 138.22, 138.05, 137.73, 133.45 (d, $^2J_{CF}$ = 12.46 Hz), 130.02, 130.00 (d, $^2J_{CF}$ = 11.50 Hz), 126.90, 125.72, 124.78, 124.72, 124.19, 124.08, 123.48, 122.95, 121.99, 121.35, 121.21, 120.88, 120.45, 119.82, 116.11, 116.04 (d, $^3J_{CF}$ = 6.71 Hz), 113.77, 112.14 (d, $^4J_{CF}$ = 4.79 Hz), 110.34, 109.95, 109.63 ppm; ^{19}F NMR (376 MHz, $CDCl_3$, δ): -111.00 (s, 1F) ppm; HRMS $[M+H]^+$ m/z calcd. for $[C_{55}H_{33}N_5OF]^+$ 798.2669, found 798.2690.

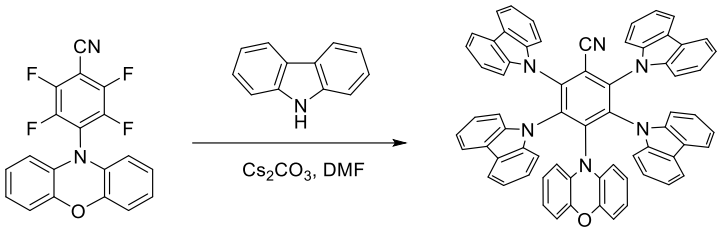

N9 **N17**

To a 50 mL two-neck round bottom flask equipped with a stir bar, 4 mmol of carbazole (0.668 g), 4.8 mmol of cesium carbonate (Cs_2CO_3) (1.564 g) and 8 mL of dry DMF were added under inert atmosphere. Then 1 mmol of **N9** (0.356 g) was added and the reaction mixture was stirred at 80 °C overnight. Afterwards the reaction mixture was neutralized with acidified water, extracted with dichloromethane, and dried over anhydrous $MgSO_4$. The product was purified using silica gel chromatography (Petroleum ether:CH_2Cl_2= 3:2) to give 0.926 g of **N17** as an orange solid (yield: 98%). A single crystal of **N17** was grown from slow evaporation of ethyl acetate/dichloromethane (1:1) mixture.

^{1}H NMR (400 MHz, DMSO-d_6, δ): 7.87 (d, *J* = 8.24 Hz, 4H), 7.82 (d, *J* = 7.79 Hz, 4H), 7.60 (d, *J* = 8.24 Hz, 4H), 7.56 (d, *J* = 7.79 Hz, 4H), 7.29 (d, *J* = 7.79 Hz, 2H), 7.12 (dd, *J* = 8.24 Hz, *J* = 7.33 Hz, 4H), 7.05 (dd, *J* = 8.24 Hz, *J* = 7.33 Hz, 4H), 6.85 (dd, *J* = 7.79 Hz, *J* = 7.33 Hz, 4H), 6.72 (dd, *J* = 7.79 Hz, *J* = 7.33 Hz, 4H), 6.19 (dd, *J* = 7.79 Hz, *J* = 7.33 Hz, 2H), 6.01 (dd, *J* = 8.24 Hz, *J* = 7.33 Hz, 2H), 5.94 (d, *J* = 8.24 Hz, 2H) ppm; ^{13}C NMR (100 MHz, DMSO-d_6, δ): 142.49, 141.38, 139.21, 138.91, 138.47, 127.10, 124.78, 123.67, 122.81, 122.78, 122.26, 120.96, 120.63, 120.20, 119.86, 119.37, 116.69, 116.65, 114.30, 113.38, 112.17, 111.92 ppm; HRMS $[M]^+$ m/z calcd. for $[C_{67}H_{40}N_6O]^+$ 944.3264, found 944.3276.

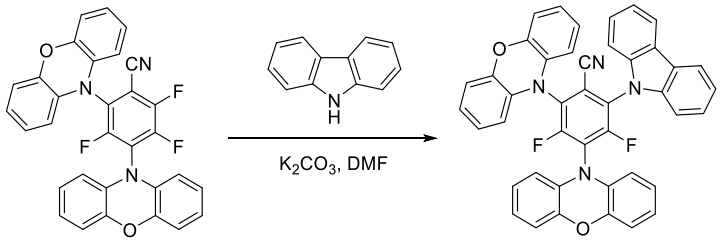

N12 **N18**

To a 50 mL two-neck round bottom flask equipped with a stir bar, 1 mmol of carbazole (0.167 g), 1.2 mmol of potassium carbonate (K_2CO_3) (0.166 g) and 6 mL of dry DMF were added under inert atmosphere. Then 1 mmol of **N12** (0.520 g) was added and the reaction mixture was stirred at 40 °C overnight. Afterwards the reaction mixture was neutralized with acidified water, extracted with dichloromethane, and dried over anhydrous magnesium sulfate ($MgSO_4$). The product was purified using silica gel chromatography (Petroleum ether:CH_2Cl_2= 3:1) to give 0.554 g of **N18** as an orange solid (yield: 83%).

^{1}H NMR (400 MHz, $CDCl_3$, δ): 8.15 (d, *J* = 7.79 Hz, 2H), 7.50 (ddd, *J* = 8.24 Hz, *J* = 7.33 Hz, *J* = 1.37 Hz, 2H), 7.38 (ddd, *J* = 7.79 Hz, *J* = 7.33 Hz, *J* = 1.37 Hz, 2H), 7.15 (d, *J* = 8.24 Hz, 2H), 6.86-6.78 (m, 12H), 6.14-6.09 (m, 4H) ppm; ^{13}C NMR (100 MHz, $CDCl_3$, δ): 160.43 (dd, $^{1}J_{CF}$ = 265.50 Hz, $^{3}J_{CF}$ = 4.79 Hz), 158.68 (dd, $^{1}J_{CF}$ = 266.45 Hz, $^{3}J_{CF}$ = 4.79 Hz), 144.24, 144.18, 139.74, 131.36, 130.61, 128.71 (dd, $^{2}J_{CF}$ = 15.34 Hz, $^{4}J_{CF}$ = 4.79 Hz), 128.23 (dd, $^{2}J_{CF}$ = 15.34 Hz, $^{4}J_{CF}$ = 4.79 Hz), 126.79, 124.51, 124.06 (t, $^{2}J_{CF}$ = 15.34 Hz), 123.88, 123.86, 123.84, 123.79, 121.95, 121.09, 119.38 (t, $^{4}J_{CF}$ = 4.79 Hz), 116.95, 116.87, 112.48, 112.41, 111.20 (t, $^{3}J_{CF}$ = 4.79 Hz), 109.36 ppm; ^{19}F NMR (376 MHz, $CDCl_3$, δ): -109.84 (s, 1F), -111.17 (s, 1F) ppm; HRMS $[M]^+$ m/z calcd. for $[C_{43}H_{24}N_4O_2F_2]^+$ 666.1867, found 666.1874.

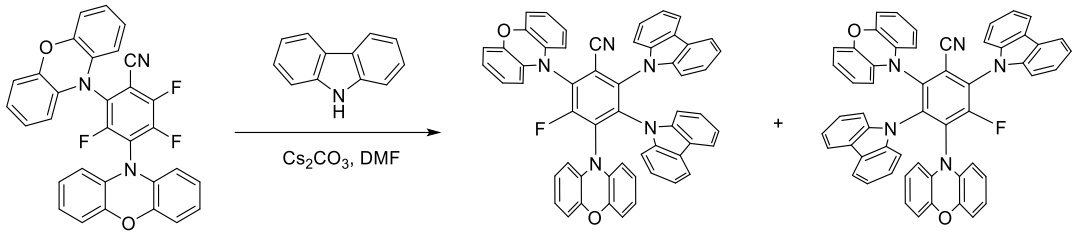

N12 **N19a** **N19b**

To a 50 mL two-neck round bottom flask equipped with a stir bar, 2 mmol of carbazole (0.334 g), 2.4 mmol of Cs_2CO_3 (0.782 g) and 8 mL of dry DMF were added under inert atmosphere. Then 1 mmol of **N12** (0.520 g) was added and the reaction mixture was stirred at 60 °C overnight. Afterwards the reaction mixture was neutralized with acidified water, extracted with dichloromethane, and dried over anhydrous $MgSO_4$. The product was purified using silica gel chromatography (Petroleum ether:CH_2Cl_2= 2:1) to give 0.702 g of **N19a+N19b** as an orange solid (total yield: 86%, the ratio between **N19a** and **N19b** is 9:1 determined by ^{1}H and ^{19}F NMR).

The ^{1}H NMR and ^{13}C NMR data represent the signals for **N19a**, regardless of the small signals which are ascribed to **N19b**. ^{1}H NMR (400 MHz, $CDCl_3$, δ): 7.72 (d, *J* = 7.79 Hz, 2H), 7.51 (d, *J* = 7.33 Hz, 2H), 7.16 (d, *J* = 7.33 Hz, 2H), 7.11-7.05 (m, 4H), 7.00-6.96 (m, 2H), 6.94-6.88 (m, 6H), 6.81 (d, *J* = 8.24 Hz, 2H), 6.74-6.70 (m, 2H), 6.54-6.50 (m, 2H), 6.48-6.43 (m, 2H), 6.40 (d, *J* = 7.79 Hz, 2H), 6.33 (d, *J* = 7.79 Hz, 2H), 6.19 (d, *J* = 7.79 Hz, 2H) ppm; ^{13}C NMR (100 MHz, $CDCl_3$, δ): 160.64 (d, $^{1}J_{CF}$ = 263.58 Hz), 144.89, 144.34, 138.83, 138.31, 138.36, 138.02, 134.14 (d, $^{2}J_{CF}$ = 12.93 Hz), 131.55, 131.14 (d, $^{2}J_{CF}$ = 16.29 Hz), 129.82, 125.71, 124.78, 124.16, 124.07, 123.96, 123.87, 123.47, 122.91, 121.37, 120.92, 120.44, 119.82, 119.44 (d, $^{3}J_{CF}$ = 4.79 Hz), 117.06, 116.08, 113.66, 112.62, 112.09 (d, $^{4}J_{CF}$ = 4.79 Hz), 110.23, 109.83 ppm; ^{19}F NMR (376 MHz, $CDCl_3$, δ): -110.39 (s, 1F, **N19a**), -111.47 (**N19b**) ppm; HRMS $[M+H]^+$ m/z calcd. for $[C_{55}H_{33}N_5O_2F]^+$ 814.2620, found 814.2618.

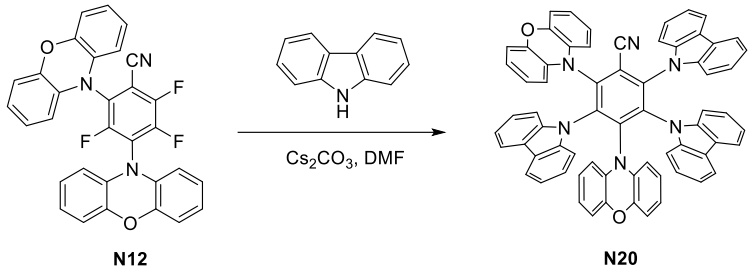

N12 **N20**

To a 50 mL two-neck round bottom flask equipped with a stir bar, 3 mmol of carbazole (0.501 g), 3.6 mmol of Cs_2CO_3 (1.173 g) and 8 mL of dry DMF were added under inert atmosphere. Then 1 mmol of **N12** (0.520 g) was added and the reaction mixture was stirred at 80 °C overnight. Afterwards the reaction mixture was neutralized with acidified water, extracted with dichloromethane, and dried over anhydrous $MgSO_4$. The product was purified using silica gel chromatography (Petroleum ether:CH_2Cl_2= 3:2) to give 0.932 g of **N20** as an orange solid (yield: 97%).

^{1}H NMR (400 MHz, DMSO-d_6, δ): 7.79 (d, *J* = 8.24 Hz, 4H), 7.74 (d, *J* = 7.79 Hz, 2H), 7.62 (d, *J* = 8.24 Hz, 2H), 7.51 (d, *J* = 7.79 Hz, 2H), 7.35 (d, *J* = 8.24 Hz, 2H), 7.20 (dd, *J* = 8.24 Hz, *J* = 1.37 Hz, 2H), 7.14-7.04 (m, 6H), 6.94 (dd, *J* = 8.24 Hz, *J* = 7.33 Hz, 2H), 6.83 (dd, *J* = 7.79 Hz, *J* = 7.33 Hz, 2H), 6.77-6.65 (m, 6H), 6.57 (ddd, *J* = 7.79 Hz, *J* = 7.33 Hz, *J* = 1.37 Hz, 2H), 6.36 (dd, *J* = 8.24 Hz, *J* = 1.37 Hz, 2H), 6.20 (ddd, *J* = 8.24 Hz, *J* = 7.33 Hz, *J* = 1.37 Hz, 2H), 6.08 (ddd, *J* = 8.24 Hz, *J* = 7.33 Hz, *J* = 1.37 Hz, 2H), 5.92 (dd, *J* = 7.79 Hz, *J* = 7.33 Hz, 2H) ppm; ^{13}C NMR (100 MHz, DMSO-d_6, δ): 143.72, 143.08, 141.90, 141.61, 141.20, 140.90, 139.05, 138.80, 138.78, 138.09, 130.34, 126.94, 124.49, 123.37, 123.31, 122.97, 122.68, 122.54, 122.28, 121.89, 120.72, 120.29, 119.84, 119.79, 119.32., 118.94, 118.69, 116.32, 114.99, 114.79, 113.93, 112.87, 112.04, 112.01, 111.45 ppm; HRMS $[M+H]^+$ m/z calcd. for $[C_{67}H_{41}N_6O_2]^+$ 961.3291, found 961.3287.

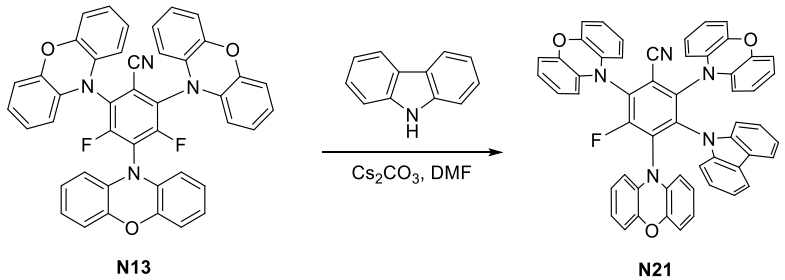

N13 **N21**

To a 50 mL two-neck round bottom flask equipped with a stir bar, 1 mmol of carbazole (0.167 g), 1.2 mmol of Cs_2CO_3 (0.391 g) and 8 mL of dry DMF were added under inert atmosphere. Then 1 mmol of **N13** (0.683 g) was added and the reaction mixture was stirred at 60 °C overnight. Afterwards the reaction mixture was neutralized with acidified water,

extracted with dichloromethane, and dried over anhydrous $MgSO_4$. The product was purified using silica gel chromatography (Petroleum ether:CH_2Cl_2= 2:1) to give 0.714 g of **N21** as an orange solid (yield: 86%).

^{1}H NMR (400 MHz, DMSO-d_6, δ): 7.81 (d, *J* = 7.79 Hz, 2H), 7.11 (d, *J* = 8.24 Hz, 2H), 7.07-7.03 (m, 2H), 6.98-6.92 (m, 8H), 6.81-6.56 (m, 14H), 6.43-6.39 (m, 4H) ppm; ^{13}C NMR (100 MHz, DMSO-d_6, δ): 160.80 (d, $^1J_{CF}$ = 262.62 Hz), 143.71, 143.66, 143.51, 142.12 (d, $^3J_{CF}$ = 4.79 Hz), 140.65 (d, $^4J_{CF}$ = 4.79 Hz), 139.29, 135.25 (d, $^2J_{CF}$ = 12.46 Hz), 131.96 (d, $^2J_{CF}$ = 15.34 Hz), 131.37, 130.85, 130.43, 125.11, 124.85, 124.35, 123.89, 123.87, 123.77, 123.71, 123.61, 122.70 (d, $^3J_{CF}$ = 4.79 Hz), 121.02, 120.26, 116.89, 116.06, 116.01, 115.25, 115.15, 114.46, 113.14 (d, $^4J_{CF}$ = 4.79 Hz), 111.82 ppm; ^{19}F NMR (376 MHz, DMSO-d_6, δ): -112.89 (s, 1F) ppm; HRMS $[M+H]^+$ m/z calcd. for $[C_{55}H_{33}N_5O_3F]^+$ 830.2567, found 830.2567.

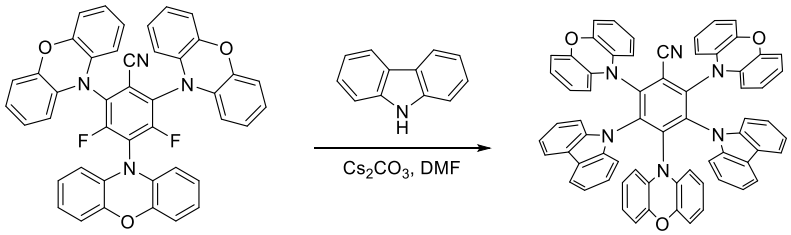

N13 **N22**

To a 50 mL two-neck round bottom flask equipped with a stir bar, 2 mmol of carbazole (0.334 g), 2.4 mmol of Cs_2CO_3 (0.782 g) and 8 mL of dry DMF were added under inert atmosphere. Then 1 mmol of **N13** (0.683 g) was added and the reaction mixture was stirred at 80 °C overnight. Afterwards the reaction mixture was neutralized with acidified water, extracted with dichloromethane, and dried over anhydrous $MgSO_4$. The product was purified using silica gel chromatography (Petroleum ether:CH_2Cl_2= 3:2) to give 0.948 g of **N22** as a deep orange solid (yield: 97%).

^{1}H NMR (400 MHz, $CDCl_3$, δ): 7.73 (d, *J* = 7.79 Hz, 4H), 7.03-6.99 (m, 8H), 6.80 (ddd, *J* = 7.79 Hz, *J* = 7.33 Hz, *J* = 0.92 Hz, 4H), 6.67-6.56 (m, 10H), 6.41-6.34 (m, 8H), 6.26 (ddd, *J* = 7.79 Hz, *J* = 7.33 Hz, *J* = 1.37 Hz, 2H), 6.18 (ddd, *J* = 8.24 Hz, *J* = 7.33 Hz, *J* = 1.37 Hz, 2H), 6.00 (dd, *J* = 8.24 Hz, *J* = 1.37 Hz, 2H) ppm; ^{13}C NMR (100 MHz, $CDCl_3$, δ): 146.10, 144.82, 142.99, 142.91, 141.36, 139.00, 130.47, 127.71, 124.75, 124.54, 124.48, 123.36, 123.10, 122.98, 121.46, 120.86, 119.91, 116.31, 115.93, 115.32, 114.07, 113.53, 111.55 ppm; HRMS $[M]^+$ m/z calcd. for $[C_{67}H_{40}N_6O_3]^+$ 976.3162, found 976.3185.

3.9 Reference

[1] G. Clavier, P. Audebert, *Chem. Rev.* **2010**, *110*, 3299–3314.

[2] H. Wu, N. K. Devaraj, *Acc. Chem. Res.* **2018**, *51*, 1249–1259.

[3] Y. Qu, F.-X. Sauvage, G. Clavier, F. Miomandre, P. Audebert, *Angew. Chemie - Int. Ed.* **2018**, *57*, 12057–12061.

[4] H. Uoyama, K. Goushi, K. Shizu, H. Nomura, C. Adachi, *Nature* **2012**, *492*, 234–238.

[5] D. Zhang, M. Cai, Y. Zhang, D. Zhang, L. Duan, *Mater. Horizons* **2016**, *3*, 145–151.

[6] S. Tanimoto, T. Suzuki, H. Nakanotani, C. Adachi, *Chem. Lett.* **2016**, *45*, 770–772.

[7] Y. J. Cho, S. K. Jeon, J. Y. Lee, *Adv. Opt. Mater.* **2016**, *4*, 688–693.

[8] I. S. Park, S. Y. Lee, C. Adachi, T. Yasuda, *Adv. Funct. Mater.* **2016**, *26*, 1813–1821.

[9] Y. J. Cho, B. D. Chin, S. K. Jeon, J. Y. Lee, *Adv. Funct. Mater.* **2015**, *25*, 6786–6792.

[10] Y. J. Cho, S. K. Jeon, B. D. Chin, E. Yu, J. Y. Lee, *Angew. Chemie - Int. Ed.* **2015**, *54*, 5201–5204.

[11] Y. J. Cho, K. S. Yook, J. Y. Lee, *Adv. Mater.* **2014**, *26*, 6642–6646.

[12] N. Liu, B. Wang, W. Chen, C. Liu, X. Wang, Y. Hu, *RSC Adv.* **2014**, *4*, 51133–51139.

[13] M. Guan, Z. Q. Bian, Y. F. Zhou, F. Y. Li, Z. J. Li, C. H. Huang, **2003**, 2708–2709.

[14] R. Krishnan, A. Parthiban, *J. Fluor. Chem.* **2014**, *162*, 17–25.

[15] M. R. Cargill, K. E. Linton, G. Sandford, D. S. Yufit, J. A. K. Howard, *Tetrahedron* **2010**, *66*, 2356–2362.

[16] M. Aydemir, S. Xu, C. Chen, M. R. Bryce, Z. Chi, A. P. Monkman, *J. Phys. Chem. C* **2017**, *121*, 17764–17772.

[17] S. Xu, T. Liu, Y. Mu, Y. F. Wang, Z. Chi, C. C. Lo, S. Liu, Y. Zhang, A. Lien, J. Xu, *Angew. Chemie - Int. Ed.* **2015**, *54*, 874–878.

[18] Z. Xie, C. Chen, S. Xu, J. Li, Y. Zhang, S. Liu, J. Xu, Z. Chi, *Angew. Chemie - Int. Ed.* **2015**, *54*, 7181–7184.

[19] J. Mei, N. L. C. Leung, R. T. K. Kwok, J. W. Y. Lam, B. Z. Tang, *Chem. Rev.* **2015**, *115*, 11718–11940.

[20] Y. Hong, J. W. Y. Lam, B. Z. Tang, *Chem. Soc. Rev.* **2011**, *40*, 5361.

[21] Y. Hong, J. W. Y. Lam, B. Z. Tang, *Chem. Commun.* **2009**, 4332–4353.

[22] R. T. K. Kwok, C. W. T. Leung, J. W. Y. Lam, B. Z. Tang, *Chem. Soc. Rev.* **2015**, *44*, 4228–4238.

[23] R. Hu, N. L. C. Leung, B. Z. Tang, *Chem. Soc. Rev.* **2014**, *43*, 4494–4562.

[24] D. Ding, K. Li, B. Liu, B. Z. Tang, *Acc. Chem. Res.* **2013**, *46*, 2441–2453.

[25] Z. Zhao, J. W. Y. Lam, B. Z. Tang, *J. Mater. Chem.* **2012**, *22*, 23726–23740.

[26] Z. Chi, X. Zhang, B. Xu, X. Zhou, C. Ma, Y. Zhang, S. Liu, J. Xu, *Chem. Soc. Rev.* **2012**, *41*, 3878–3896.

[27] J. Liu, J. W. Y. Lam, B. Z. Tang, *J. Inorg. Organomet. Polym. Mater.* **2009**, *19*, 249–285.

[28] J. Guo, X. L. Li, H. Nie, W. Luo, S. Gan, S. Hu, R. Hu, A. Qin, Z. Zhao, S. J. Su, et al., *Adv. Funct. Mater.* **2017**, *27*, 1606458.

[29] S. Shao, J. Hu, X. Wang, L. Wang, X. Jing, F. Wang, *J. Am. Chem. Soc.* **2017**, *139*, 17739–17742.

[30] I. Ho, W. Song, J. Yeob, *Org. Electron.* **2016**, *29*, 22–26.

[31] R. Furue, T. Nishimoto, I. S. Park, J. Lee, T. Yasuda, *Angew. Chemie - Int. Ed.* **2016**, *55*, 7171–7175.

[32] K. Sun, W. Jiang, X. Ban, B. Huang, Z. Zhang, M. Ye, Y. Sun, *RSC Adv.* **2016**, *6*, 22137–22143.

[33] L. Q. Yan, Z. N. Kong, Y. Xia, Z. J. Qi, *New J. Chem.* **2016**, *40*, 7061–7067.

[34] S. Gan, W. Luo, B. He, L. Chen, H. Nie, R. Hu, A. Qin, Z. Zhao, B. Z. Tang, *J. Mater. Chem. C* **2016**, *4*, 3705–3708.

[35] Y. Sagara, S. Yamane, M. Mitani, C. Weder, T. Kato, Adv. Mater., 2016, 28, 1073–1095.

[36] Y. Sagara, T. Kato, Nat. Chem. 2009, 1, 605–610.

[37] A. Pucci, R. Bizzarri, R. Giacomo, Soft Matter, 2011, 7, 3689–3700.

[38] Z. Chi, X. Zhang, B. Xu, X. Zhou, C. Ma, Y. Zhang, S. Liu, J. Xu, Chem. Soc. Rev., 2012, 41, 3878–3896.

[39] X. Zhang, Z. Chi, Y. Zhang, S. Liu, J. Xu, J. Mater. Chem. C, 2013, 1, 3376–3390.

[40] S. Yagai, T. Seki, H. Aonuma, K. Kawaguchi, T. Karatsu, T. Okura, A. Sakon, H. Uekusa, H. Ito, Chem. Mater. 2016, 28, 234–241.

Chapter 4

Novel donor-acceptor tetrazine derivatives prepared by Buchwald-Hartwig cross-coupling reaction

4.1 Introduction

The importance of development of novel synthetic routes that improve access to 1,2,4,5-tetrazine derivatives with various functional groups has been described in the first and second chapters. In the first chapter, we have explored a novel modified Pinner synthesis approach to 1,2,4,5-tetrazines. In this chapter a novel synthetic approach based on post-modification on simple tetrazine precursors to prepare functionalized tetrazine derivatives will be presented.

Post-modification on a simple tetrazine building block is widely used to prepare tetrazines with reactive functional groups or complex functional groups, including commonly used fluorophores for bio-imaging application.[1–3] As mentioned before, nucleophilic aromatic substitution (S_NAr) of a conventional 1,2,4,5-tetrazine precursor, commonly dichlorotetrazine, dipyrazolyltetrazine or dithiomethyltetrazine, has long been regarded as one of the most powerful methods to prepare functionalized 1,2,4,5-tetrazines for various applications.[1] However, to prepare π-conjugated 1,2,4,5-tetrazine derivatives, metal-catalyzed cross-coupling reaction on a simple tertrazine precursor is more useful. Although several examples of metal-catalyzed cross-coupling reactions have been reported on tetrazine, most of them still suffer from low yields and a limited scope regarding the tetrazine substrates.[4–8] This can be explained by the fact that the nitrogen atoms in the tetrazine ring can act as ligands for a metal and deactivate their catalytic activity or the tetrazine core can be reduced by metals followed by the decomposition of the ring.[9,10]

Herein we report an important synthetic tool, Buchwald-Hartwig cross-coupling reaction, in the synthesis and functionalization of tetrazine compounds. Buchwald-Hartwig cross-coupling reaction is of considerable importance in modern synthetic chemistry, as numerous pharmaceuticals, natural products and novel materials have been synthesized by this methodology.[11,12] However, there is no detailed study of Buchwald-Hartwig coupling reaction in the tetrazine chemistry to date. The only report describing Buchwald-Hartwig reaction on tetrazine molecules came from our group, however the scope was limited to only two examples. In addition, the reaction conditions were not optimized, only moderate yields (40% and 47%) were observed with long time of heating (36 hours and 6 days).[13] In this work, we systematically studied Buchwald-Hartwig coupling reaction on tetrazine molecules, and successfully prepared a series of novel donor-acceptor 1,2,4,5-tetrazine molecules in high yields (61%-72%). The important factors of Buchwald-Hartwig cross-coupling reaction for tetrazine functionalization are well discussed, which could be of practical importance for researchers performing Buchwald-Hartwig coupling reaction on difficult substrates, as well as other cross-coupling reactions with tetrazines. Although some of the donor-acceptor 1,2,4,5-tetrazine molecules have already been successfully prepared by the modified Pinner synthesis in **Chapter 3**, yields are particularly low. The

methodology provided here not only offers a facile and efficient pathway to prepare new donor-acceptor 1,2,4,5-tetrazine molecules, but is also expected to facilitate the future applications of 1,2,4,5-tetrazine as electron-deficient component in organic electronic or valuable intermediate for the synthesis of natural products.

4.2 Synthesis

We initially chose 3-(4-bromophenyl)-1,2,4,5-tetrazine **1** as the tetrazine substrate, because 3-monosubstituted unsymmetrical tetrazines are very useful in the bio-orthogonal click chemistry due to their fast cycloaddition reaction rate. Tetrazine **1** was conveniently prepared by the novel metal-free synthetic approach recently developed in our group[14] (see chapter 2). Molecules with strong electron donating abilities (e.g. carbazole, phenoxazine, phenothiazine and 9,10-Dihydro-9,9-dimethylacridine) have been chosen for this study, because donor-acceptor molecules are of particular interest in organic electronics, due to the charge transfer (CT) excited states induced by the electron donor-acceptor system.[15–17] The reaction conditions were optimized by using **1** and carbazole as the starting materials (**Table 1**). Firstly, the choice of the base was crucial for the outcome of this reaction. When strong bases such as ^{t}BuONa (pK_a = 17) or lithium hexamethyldisilamide (LHMDS, pK_a = 26) were applied, the tetrazine precursor **1** quickly degraded resulting in no target product (entries 1 and 2). However, when weak base NEt_3 (pK_a = 11) was applied, it did not tend to promote the hydrogen bromide elimination, resulting no reaction at all (entry 5). Fortunately, weak inorganic base carbonates (pK_a = 10) which could react heterogeneously in non-polar solvent were found to promote the hydrogen bromide elimination successfully (entries 3 and 4), and cesium carbonate (Cs_2CO_3) was found to be the most reactive base resulting in a high yield of the expected product (72%, entry 3). Secondly, the choice of the catalyst and ligand played an important role on the reaction yield. We found out that tris(dibenzylideneacetone)dipalladium(0) ($Pd_2(dba)_3$) was the most effective catalyst tested and 2-dicyclohexylphosphino-2',4',6'-triisopropylbiphenyl (XPhos) gave much better results than other ligands tested ($P(^{t}Bu)_3$, 1,1'-Bis(diphenylphosphino)ferrocene (DPPF), entries 6 and 7).

Table 1: Optimization of the Buchwald-Hartwig reaction conditions on tetrazine **1** [(a)].

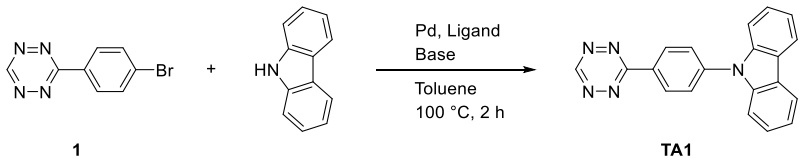

1 TA1

Entry	Pd, Ligand	Base	Yield (%)[(b)]

1	$Pd_2(dba)_3$, Xphos	^tBuONa	0
2	$Pd_2(dba)_3$, Xphos	LHMDS	0
3	$Pd_2(dba)_3$, Xphos	Cs_2CO_3	72
4	$Pd_2(dba)_3$, Xphos	K_2CO_3	35
5	$Pd_2(dba)_3$, Xphos	NEt_3	0
6	$Pd_2(dba)_3$, $P(^tBu)_3$	Cs_2CO_3	15
7	$Pd_2(dba)_3$, DPPF	Cs_2CO_3	10
8	$Pd(OAc)_2$, Xphos	Cs_2CO_3	56

(a) All reactions were carried out on a 0.2 mmol scale in 10 ml toluene. Pd = palladium catalyst. (b) Yields (isolated) based on the tetrazine precursor **1**.

The optimization of the amount of the palladium catalyst and ligand loading is summarized in **Table 2**. It is important to note that excess amount of XPhos relative to $Pd_2(dba)_3$ was necessary to achieve a high yield, and 4 equivalents XPhos to $Pd_2(dba)_3$ was found to give the best yield. This is probably because excess amount of ligand can well stabilize the palladium catalyst and prevent the binding of catalyst to the nitrogen atoms on tetrazine which could deactivate the palladium catalyst. The amount of $Pd_2(dba)_3$ and XPhos loading was finally optimized to 3% and 12%, respectively, to give the best yield (72%). Additionally, the influence of the reaction temperature and time was also examined. It was found that both a high temperature and a prolonged reaction time are not preferable for this reaction, so heating at 100 °C for 2 hours was found to give the best result (**Table 3**), although the temperature seems to be a less relevant parameter than the base choice.

Table 2: Optimization of the palladium catalyst and ligand loading [(a)].

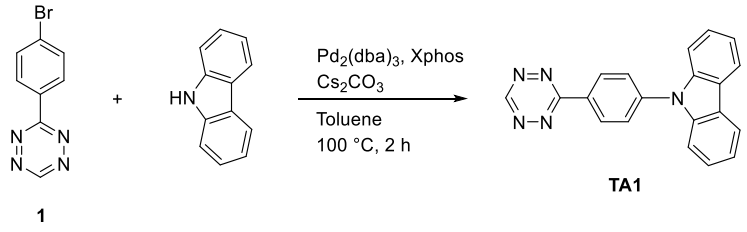

Entry	$Pd_2(dba)_3$ (%)[(b)]	Xphos (%)[(b)]	Yield (%)[(c)]
1	10	0	0
2	10	20	51
3	10	40	71

4	5	20	69
5	3	12	72
6	1	4	40

(a) All reactions were carried out on a 0.2 mmol scale in 10 ml toluene. (b) Percentage amount relative to the tetrazine precursor **1**. (c) Yields (isolated) based on the tetrazine precursor **1**.

Table 3: Optimization of the reaction temperature and time [(a)].

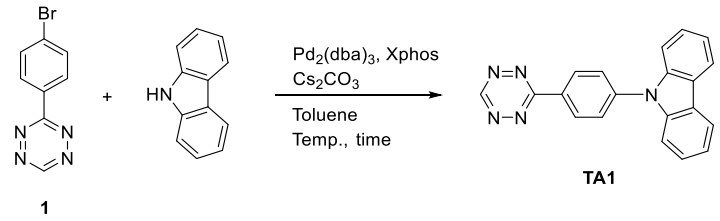

Entry	Temp. (°C)	Time (h)	Yield (%)[(b)]
1	110	1	62
2	100	2	72
3	90	3	70
4	80	4	59
5	70	6	55

(a) All reactions were carried out on a 0.2 mmol scale in 10 ml toluene. Temp. = temperature. (b) Yields (isolated) based on the tetrazine precursor **1**.

With these optimized parameters in hand, we then intended to extend the scope of this synthetic strategy with other electron rich amines. Three new donor-acceptor 3-monosubstituted unsymmetrical tetrazines **TA2-TA4** were successfully prepared in high yields (61%-71%) using phenoxazine, phenothiazine or 9,10-Dihydro-9,9-dimethylacridine as a donor instead of carbazole, employing the optimized conditions above (**Scheme 1**).

The product yields for **TA1** and **TA2** were significantly increased to 72% and 71% respectively (23 and 27 % in two steps) using the Buchwald-Hartwig cross-coupling reaction in this study as compared to the very low yields for the same products when using the modified Pinner synthesis (6% and 4% in two steps) shown in chapter 2.

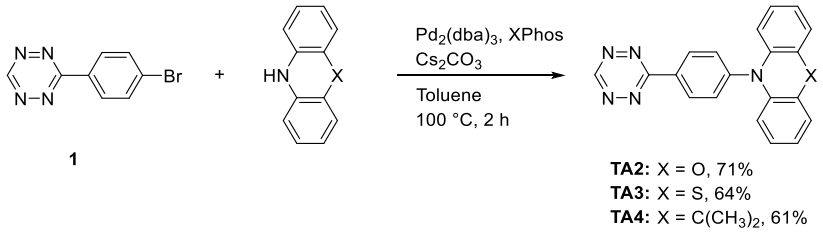

Scheme 1: Synthesis of 3-monosubstituted unsymmetrical tetrazines **TA2-TA4**.

Moreover, donor-acceptor 3,6-disubstituted symmetrical tetrazines **TA5-TA7** were also prepared in high yields (61%-69%) by Buchwald-Hartwig coupling reaction using bifunctional tetrazine precursor **2** (**Scheme 2**). In this case, it was initially found that using the above optimized conditions only led to a low yield of product (less than 10%), while a large amount of tetrazine precursor **2** was recovered. This suggests that the tetrazine precursor **2** is less reactive than tetrazine **1**, therefore the stronger base ^{t}BuONa was attempted to increase the product yields. It was found that tetrazine precursor **2** is more chemically stable to bases compared to tetrazine **1** (tetrazine **2** only degrades slowly in the presence of ^{t}BuONa), which is important to obtain a reasonable yield of product. As expected, the yield of the reaction significantly increased (up to 69%) using ^{t}BuONa as a base, along with 6 hours of heating time (necessary to reach the completion of tetrazine precursor **2**).

The reaction of tetrazine **2** with carbazole gave a red solid which is insoluble in any organic solvents. Thus, it was not possible to characterize it by common analytical methods as already observed when the same molecule was prepared using the Pinner synthesis (molecule **Tz2** in **Chapter 3**).

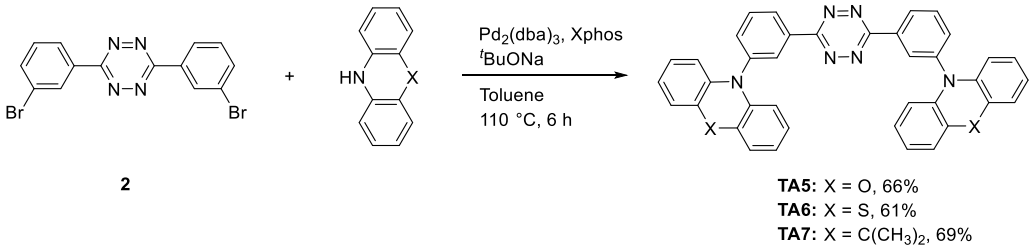

Scheme 2: Synthesis of 3, 6-disubstituted symmetrical tetrazines **TA5-TA7**.

All the obtained donor-acceptor tetrazine derivatives **TA1-TA7** were characterized by ^{1}H, ^{13}C NMR and HRMS. The structure of **TA2** and **TA3** were further confirmed by single crystal X-ray diffraction (XRD) (**Table 4**). From the crystal structure, it can be observed that the phenyl ring and the tetrazine acceptor are coplanar in both cases. For **TA2**, the phenoxazine is orthogonal to the phenyl-tetrazine moiety, while in **TA3**, the phenothiazine

is rather distorted. The molecular packing of both **TA2** and **TA3** shows a clear π–π stacking of the donor moieties. In both molecules, the phenyl-tetrazine moieties are arranged head to tail in the unit cell.

Table 4: X-ray crystallographic structures of **TA2** and **TA3**, along with their molecular packing.

	Molecular structure	**Molecular packing**
TA2	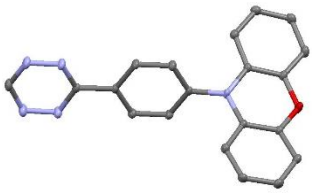	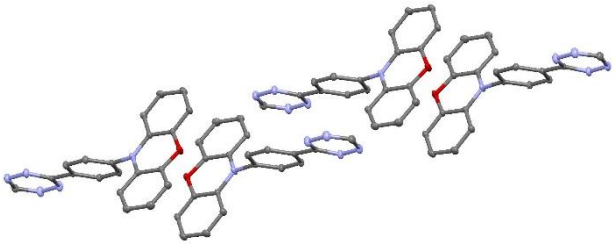
TA3		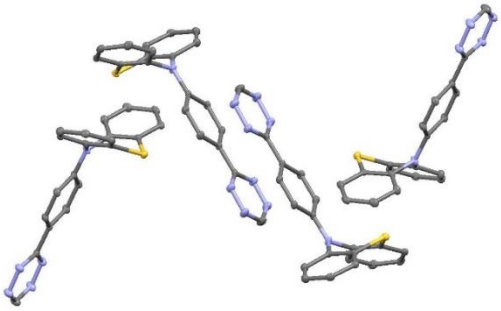

4.3 Photophysical characterizations

The photophysical properties of **TA1-TA7** are given in **Table 5** and **Figure 1-2**. All the **TA** molecules show an absorption band in the visible with a maximum located near 550 nm and a rather low extinction coefficient (540-700 $L \cdot mol^{-1} \cdot cm^{-1}$), which is typical of tetrazine derivatives.[1] Unfortunately, all the **TA** molecules are non-emissive, likely due to the through-bond energy transfer (TBET) or photoinduced electron transfer (PET) according to the previous reports.[8,18,19] [1][20]

Table 5: Absorption maxima of **TA1-TA7** [(a)].

	λ_{Abs} **(nm)**
TA1	256, 310, 360, 561
TA2	241, 261, 323, 413, 541

TA3	276, 370, 561
TA4	270, 369, 542
TA5	240, 303, 546
TA6	257, 302, 547
TA7	291, 547

(a) Measured in DCM (1×10^{-5} M) at room temperature.

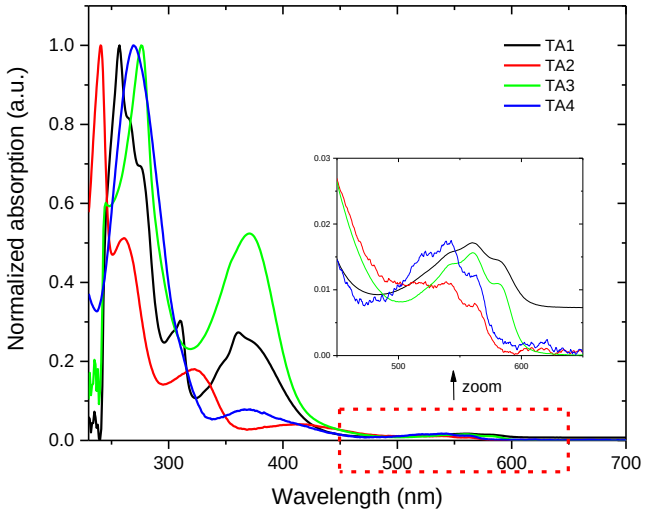

Figure 1: Absorption spectra of **TA1-TA4** in DCM at room temperature.

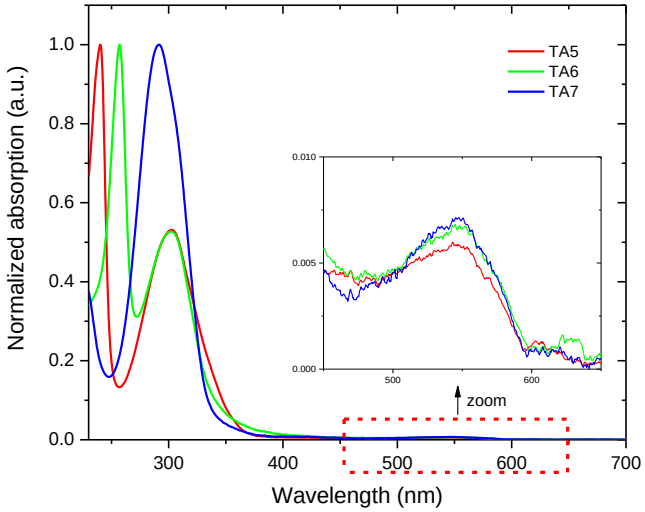

Figure 2: Absorption spectra of **TA5-TA7** in DCM at room temperature.

4.4 Electrochemistry

The electrochemical properties of **TA1-TA7** are depicted in **Table 6** and **Figure 3-4**. Two reversible peaks were found for molecules **TA2-TA7**, which can be ascribed to the oxidation of the donor moiety and the reduction of the tetrazine acceptor, respectively. However in the case of **TA1**, only the reduction peak of the tetrazine moiety is reversible. The oxidation peak is irreversible because the carbazole moiety is known to be irreversibly oxidized. Interestingly, the influence of the donor group on the redox potential of the tetrazine is quite weak, this being indicative of a weak conjugation between these two moieties. The HOMO and LUMO values were thus estimated from the oxidation and reduction potentials.

Table 6: Electrochemical properties of **TA1-TA7**.

	E_{ox} vs Fc/Fc^+ (V)[a]	E_{red} vs Fc/Fc^+ (V)[a]	HOMO (eV)[b]	LUMO (eV)[c]
TA1	0.86	-1.17	5.96	3.93
TA2	0.29	-1.17	5.39	3.93
TA3	0.24	-1.24	5.34	3.86
TA4	0.40	-1.21	5.50	3.89
TA5	0.27	-1.22	5.37	3.88
TA6	0.21	-1.2	5.31	3.90
TA7	0.45	-1.14	5.55	3.96

(a) Measured in DCM at room temperature by cyclic voltammetry. (b) Estimated from the oxidation potential in DCM, HOMO = E_{ox} + 5.1. (c) Estimated from the reduction potential in DCM, LUMO = E_{red} + 5.1.

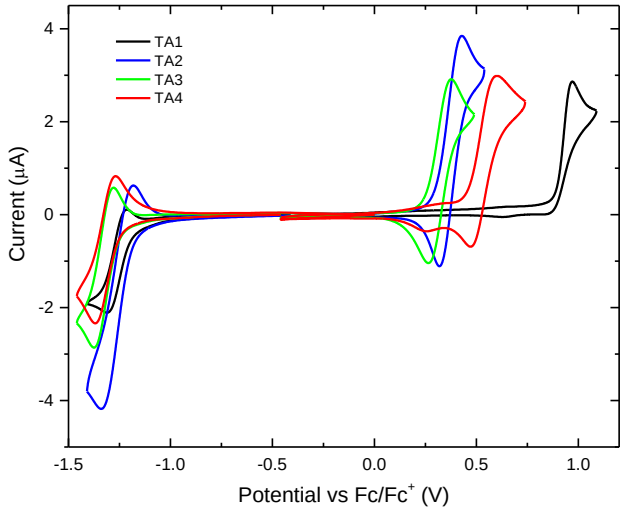

Figure 3: Cyclic voltammetry of **TA1-TA4** in DCM at room temperature.

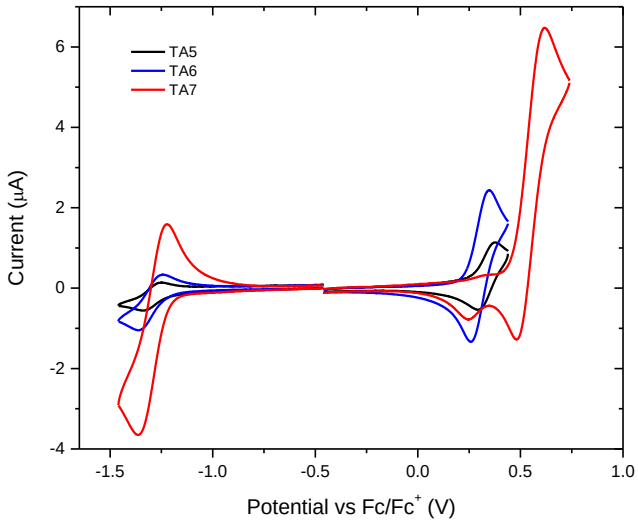

Figure 4: Cyclic voltammetry of **TA5-TA7** in DCM at room temperature.

4.5 Conclusion

In conclusion, we have extended the scope of a facile, efficient synthetic tool, Buchwald-Hartwig cross-coupling reaction, in the synthesis of 1,2,4,5-tetrazine derivatives. We have discovered the optimized working conditions through an unprecedented systematic study of Buchwald-Hartwig cross-coupling reaction applied to tetrazine molecules. Moreover, we have showed that this reaction can be used for the preparation of symmetrical and more importantly rather fragile unsymmetrical 3-monosubstituted tetrazines with various electron

rich aromatic secondary amines. Donor-acceptor 1,2,4,5-tetrazine molecules (**TA1-TA7**) were thus prepared in high yields (61%-72%). This synthetic methodology should largely improve the access to various functionalized 1,2,4,5-tetrazines and facilitate the application of 1,2,4,5-tetrazines as electron-deficient materials in organic electronics, as valuable intermediates for the synthesis of natural products or bioorthogonal reactions. Regarding this last aspect, we will demonstrate in the next chapter, that some of those new tetrazine are efficient fluorescent turn-on probes upon iEDDA reaction.

4.6 Experimental details

General Methods:

Synthesis. All chemicals were received from commercial sources and used without further purification. Thin layer chromatography (TLC) was performed on silica gel. Flash column chromatography purification was performed on a CombiFlash-Rf system with a variable wavelength UV detector. All mixtures of solvents are given in v/v ratio. NMR spectra were recorded on a JEOL ECS (400 MHz) spectrometer. ^{13}C NMR spectra were proton decoupled. HRMS spectra were measured either on an UPLC/ESI-HRMS device (an Acquity Waters UPLC system coupled to a Waters LCT Premier XE mass spectrometer equipped with an electrospray ion source), or a Q-TOF mass spectrometer (Q-TOF 6540, Agilent) equipped with an APPI ion source.

Tetrazine **1**,[14] **2**[21] and cyclooctyne[22] were prepared by according to published procedures.

Photophysics. All solutions were investigated at 10^{-5} mol dm^{-3} concentration. Absorption spectra were collected using a UV-3600 double beam spectrophotometer (Shimadzu).

Electrochemistry. The electrochemical cell comprised of platinum electrode with a 1 mm diameter of working area as a working electrode, an Ag electrode as a reference electrode and a platinum coil as an auxiliary electrode. Cyclic voltammetry measurements were conducted at room temperature at a potential rate of 50 mV/s and were calibrated against ferrocene/ferrocenium redox couple. All voltammograms were recorded on a CHInstruments Electrochemical Analyzer model 660 potentiostat. Electrochemical measurements were conducted in 1.0 mM concentrations for all cyclic voltammetry measurements. Electrochemical studies were undertaken in 0.1 M solutions of Bu_4NPF_6, 99% in dichloromethane (DCM) at room temperature.

Synthesis of TA1

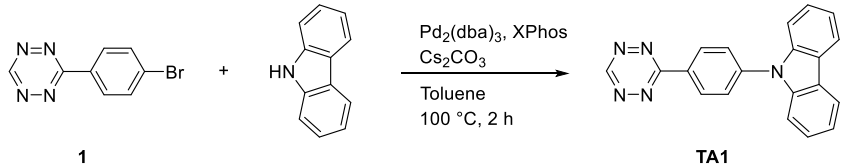

1 TA1

Procedure A: To a 100 ml two-neck round bottom flask equipped with a stir bar, tetrazine **1** (0.2 mmol, 47.6 mg), carbazole donor (0.24 mmol, 40.1 mg), cesium carbonate (0.4 mmol, 130 mg) and 10 ml of anhydrous toluene were added. The reaction mixture was degassed by bubbling through nitrogen for 15 min under vigorous stirring. Then $Pd_2(dba)_3$ (0.006 mmol, 5.5 mg) and XPhos (0.024 mmol, 11.5 mg) were added and degassed for another

15 min. The reaction mixture was heated to 100 °C under a nitrogen atmosphere for 2 h. The reaction mixture was then cooled down to room temperature, extracted with dichloromethane. The organic phase was dried over anhydrous magnesium sulfate ($MgSO_4$), filtered and concentrated under reduced pressure. The product was purified using flash column chromatography (Petroleum ether:CH_2Cl_2= 3:1) to give 46.5 mg of **TA1** as a red solid (yield: 72%).

^{1}H NMR (400 MHz, $CDCl_3$, δ): 10.27 (s, 1H), 8.89 (d, *J* = 8.24 Hz, 2H), 8.17 (d, *J* = 7.80 Hz, 2H), 7.88 (d, *J* = 8.24 Hz, 2H), 7.56 (d, *J* = 7.80 Hz, 2H), 7.46 (t, *J* = 7.80 Hz, 2H), 7.34 (t, *J* = 7.80 Hz, 2H) ppm; ^{13}C NMR (100 MHz, $CDCl_3$, δ): 166.11, 157.96, 142.56, 140.29, 130.10, 130.06, 127.40, 126.41, 124.05, 120.84, 120.65, 109.99 ppm; HRMS $[M+H]^+$ m/z calcd. for $[C_{20}H_{14}N_5]^+$ 324.1249, found 324.1253.

Synthesis of TA2

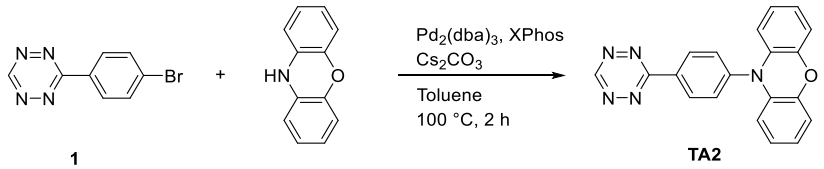

TA2 was prepared following **Procedure A** using phenoxazine as a donor. A deep red solid was obtained after flash column chromatography (Petroleum ether:CH_2Cl_2 = 3:1) (48.1 mg, yield: 71%). Single crystal of **TA2** was grown from slow evaporation of petroleum ether/CH_2Cl_2 (3:1) mixture.

^{1}H NMR (400 MHz, $CDCl_3$, δ): 10.28 (s, 1H), 8.87 (d, *J* = 8.24 Hz, 2H), 7.63 (d, *J* = 8.24 Hz, 2H), 6.79–6.59 (m, 6H), 6.05 (dd, *J* = 7.80 Hz, *J* = 1.50 Hz, 2H) ppm; ^{13}C NMR (100 MHz, $CDCl_3$, δ): 166.08, 158.04, 144.18, 144.06, 133.78, 132.01, 131.62, 131.16, 123.47, 122.08, 115.92, 113.53 ppm; HRMS $[M+H]^+$ m/z calcd. for $[C_{20}H_{14}N_5O]^+$ 340.1198, found 340.1192.

Synthesis of TA3

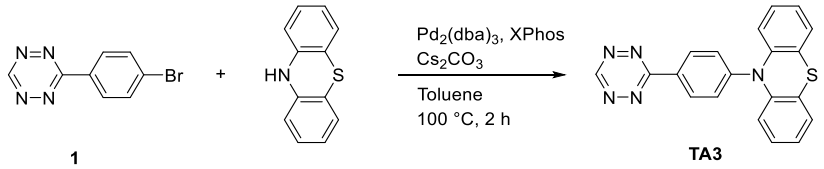

TA3 was prepared following **Procedure A** using phenothiazine as a donor. A deep red solid was obtained after flash column chromatography (Petroleum ether:CH_2Cl_2 = 3:1)

(45.4 mg, yield: 64%). Single crystal of **TA3** was grown from slow evaporation of petroleum ether/CH_2Cl_2 (3:1) mixture.

^{1}H NMR (400 MHz, $CDCl_3$, δ): 10.13 (s, 1H), 8.56 (d, *J* = 8.24 Hz, 2H), 7.37 (d, *J* = 7.80 Hz, 2H), 7.32 (d, *J* = 8.24 Hz, 2H), 7.24 (d, *J* = 7.80 Hz, 2H), 7.17–7.10 (m, 4H) ppm; ^{13}C NMR (100 MHz, $CDCl_3$, δ): 166.16, 157.47, 148.93, 141.92, 130.72, 130.17, 128.58, 127.40, 125.79, 125.55, 124.14, 120.14 ppm; HRMS $[M+H]^+$ m/z calcd. for $[C_{20}H_{14}N_5S]^+$ 356.0970, found 356.0977.

Synthesis of TA4

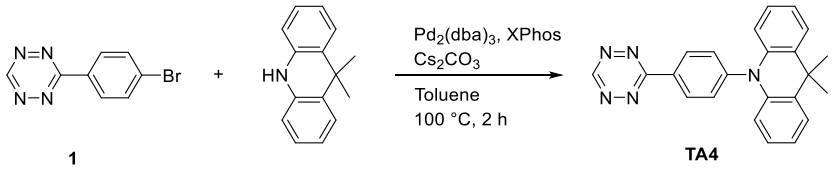

TA4 was prepared following **Procedure A** using 9,10-Dihydro-9,9-dimethylacridine as a donor. A red solid was obtained after flash column chromatography (Petroleum ether:CH_2Cl_2 = 3:1) (44.4 mg, yield: 61%).

^{1}H NMR (400 MHz, $CDCl_3$, δ): 10.28 (s, 1H), 8.89 (d, *J* = 8.24 Hz, 2H), 7.62 (d, *J* = 8.24 Hz, 2H), 7.49 (dd, *J* = 7.80 Hz, *J* = 1.80 Hz, 2H), 7.05–6.95 (m, 4H), 6.40 (dd, *J* = 7.80 Hz, *J* = 1.80 Hz, 2H) ppm; ^{13}C NMR (100 MHz, $CDCl_3$, δ): 166.22, 158.00, 146.42, 140.55, 131.94, 131.14, 131.00, 126.59, 125.52, 121.37, 114.61, 36.26, 31.18 ppm; HRMS $[M+H]^+$ m/z calcd. for $[C_{23}H_{20}N_5]^+$ 366.1719, found 366.1725.

Synthesis of TA5

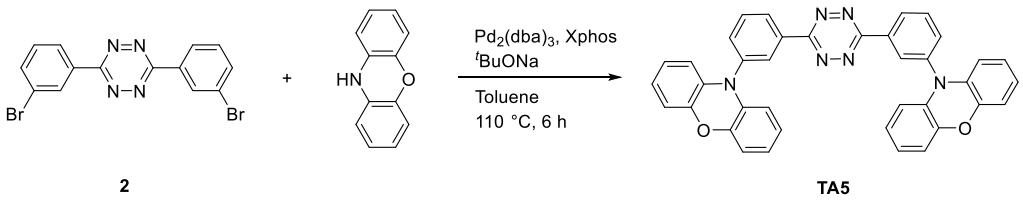

Procedure B: To a 100 ml two-neck round bottom flask equipped with a stir bar, tetrazine **2** (0.2 mmol, 78.4 mg), phenoxazine donor (0.48 mmol, 87.9 mg), sodium *tert*-butoxide (0.48 mmol, 46.1 mg) and 15 ml of anhydrous toluene were added. The reaction mixture was degassed by bubbling through nitrogen for 15 min under vigorous stirring. Then $Pd_2(dba)_3$ (0.012 mmol, 11 mg) and XPhos (0.048 mmol, 23 mg) were added and degassed for another 15 min. The reaction mixture was heated to 110 °C under a nitrogen atmosphere for 6 h. The reaction mixture was then cooled down to room temperature, extracted with dichloromethane. The organic phase was dried over anhydrous magnesium

sulfate ($MgSO_4$), filtered and concentrated under reduced pressure. The product was purified using flash column chromatography (Petroleum ether:CH_2Cl_2= 4:1) to give 78.3 mg of **TA5** as a purple solid (yield: 66%).

^{1}H NMR (400 MHz, $CDCl_3$, δ): 8.77 (d, *J* = 8.24 Hz, 2H), 8.69 (t, *J* = 1.80 Hz, 2H), 7.87 (t, *J* = 8.24 Hz, 2H), 7.67 (d, *J* = 8.24 Hz, 2H), 6.77–6.56 (m, 12H), 6.00 (dd, *J* = 7.80 Hz, *J* = 1.80 Hz, 4H) ppm; ^{13}C NMR (100 MHz, $CDCl_3$, δ): 163.61, 144.12, 140.55, 135.84, 135.04, 134.13, 132.37, 131.05, 128.16, 123.45, 121.87, 115.82, 113.44 ppm; HRMS $[M]^+$ m/z calcd. for $[C_{38}H_{24}N_6O_2]^+$ 596.1961, found 596.1947.

Synthesis of TA6

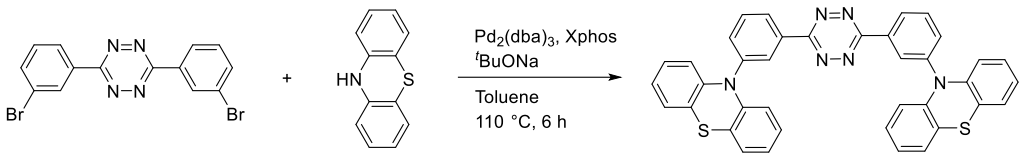

2 **TA6**

TA6 was prepared following **Procedure B** using phenothiazine as a donor. A red solid was obtained after flash column chromatography (Petroleum ether:CH_2Cl_2 = 4:1) (76.3 mg, yield: 61%).

^{1}H NMR (400 MHz, $CDCl_3$, δ): 8.74–8.67 (m, 4H), 7.81 (t, *J* = 8.24 Hz, 2H), 7.66 (d, *J* = 8.24 Hz, 2H), 7.11 (dd, *J* = 7.80 Hz, *J* = 1.80 Hz, 4H), 6.97–6.85 (m, 8H), 6.44 (dd, *J* = 7.80 Hz, *J* = 1.80 Hz, 4H) ppm; ^{13}C NMR (100 MHz, $CDCl_3$, δ): 163.74, 143.83, 143.02, 134.48, 133.95, 131.80, 129.07, 127.32, 127.15, 127.06, 123.35, 122.44, 117.59 ppm; HRMS $[M]^+$ m/z calcd. for $[C_{38}H_{24}N_6S_2]^+$ 628.1504, found 628.1500.

Synthesis of TA7

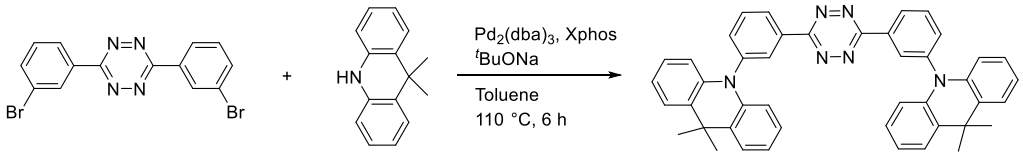

2 **TA7**

TA7 was prepared following **Procedure B** using 9,10-Dihydro-9,9-dimethylacridine as a donor. A red solid was obtained after flash column chromatography (Petroleum ether:CH_2Cl_2 = 4:1) (89.9 mg, yield: 69%).

^{1}H NMR (400 MHz, $CDCl_3$, δ): 8.81 (d, *J* = 8.24 Hz, 2H), 8.67 (t, *J* = 1.80 Hz, 2H), 7.90 (t, *J* = 8.24 Hz, 2H), 7.66 (d, *J* = 8.24 Hz, 2H), 7.49 (dd, *J* = 7.80 Hz, *J* = 1.80 Hz, 4H), 7.03–6.91 (m, 8H), 6.34 (dd, *J* = 7.80 Hz, *J* = 1.80 Hz, 4H), 1.72 (s, 12H) ppm; ^{13}C NMR (100

MHz, $CDCl_3$, δ): 163.68, 142.60, 140.79, 136.41, 134.89, 132.07, 131.43, 130.37, 127.92, 126.57, 125.46, 121.02, 114.14 ppm; HRMS $[M+H]^+$ m/z calcd. for $[C_{44}H_{37}N_6]^+$ 649.3080, found 649.3093.

4.7 Reference

[1] G. Clavier, P. Audebert, *Chem. Rev.* **2010**, *110*, 3299–3314.

[2] H. Wu, N. K. Devaraj, *Acc. Chem. Res.* **2018**, *51*, 1249–1259.

[3] B. L. Oliveira, Z. Guo, G. J. L. Bernardes, *Chem. Soc. Rev.* **2017**, *46*, 4895–4950.

[4] Z. Novak, A. Kotschy, *Org. Lett.* **2003**, *5*, 3495–3497.

[5] N. Leconte, A. Keromnes-Wuillaume, F. Suzenet, G. Guillaumet, *Synlett* **2007**, 204–210.

[6] A. M. Bender, T. C. Chopko, T. M. Bridges, C. W. Lindsley, *Org. Lett.* **2017**, *19*, 5693–5696.

[7] A. Wieczorek, T. Buckup, R. Wombacher, *Org. Biomol. Chem.* **2014**, *12*, 4177–4185.

[8] H. Wu, J. Yang, J. Seckute, N. K. Devaraj, *Angew. Chemie - Int. Ed.* **2014**, *53*, 5805–5809.

[9] W. Kaim, *Coord. Chem. Rev.* **2002**, *230*, 127–139.

[10] S. Maji, B. Sarkar, S. Patra, J. Fiedler, S. M. Mobin, V. G. Puranik, *Inorg. Chem.* **2006**, *45*, 1316–1325.

[11] P. Ruiz-Castillo, S. L. Buchwald, *Chem. Rev.* **2016**, *116*, 12564–12649.

[12] M. M. Heravi, Z. Kheilkordi, V. Zadsirjan, M. Heydari, M. Malmir, *J. Organomet. Chem.* **2018**, *861*, 17–104.

[13] C. Quinton, V. Alain-Rizzo, C. Dumas-Verdes, G. Clavier, L. Vignau, P. Audebert, *New J. Chem.* **2015**, *39*, 9700–9713.

[14] Y. Qu, F.-X. Sauvage, G. Clavier, F. Miomandre, P. Audebert, *Angew. Chemie - Int. Ed.* **2018**, *57*, 12057–12061.

[15] M. Y. Wong, E. Zysman-Colman, *Adv. Mater.* **2017**, *29*, 1605444.

[16] Z. Yang, Z. Mao, Z. Xie, Y. Zhang, S. Liu, J. Zhao, J. Xu, Z. Chi, M. P. Aldred, *Chem. Soc. Rev.* **2017**, *46*, 915–1016.

[17] F. B. Dias, T. J. Penfold, A. P. Monkman, *Methods Appl. Fluoresc.* **2017**, *5*, 012001.

[18] J. C. T. Carlson, L. G. Meimetis, S. A. Hilderbrand, R. Weissleder, *Angew. Chemie - Int. Ed.* **2013**, *52*, 6917–6920.

[19] L. G. Meimetis, J. C. T. Carlson, R. J. Giedt, R. H. Kohler, R. Weissleder, *Angew. Chemie - Int. Ed.* **2014**, *53*, 7531–7534.

[20] C. Dumas-Verdes, F. Miomandre, E. Lépicier, O. Galangau, T. T. Vu, G. Clavier, R. Méallet-Renault, P. Audebert, *European J. Org. Chem.* **2010**, 2525–2535.

[21] C. Quinton, S. H. Chi, C. Dumas-Verdes, P. Audebert, G. Clavier, J. W. Perry, V. Alain-Rizzo, *J. Mater. Chem. C* **2015**, *3*, 8351–8357.

[22] L. Brandsma, H. D. Verkruijsse, *Synthesis (Stuttg).* **1978**, *4*, 290–290.

Chapter 5

IEDDA reaction of 1,2,4,5-tetrazines: Synthesis of pyridazine derivatives

5.1 Introduction

In the last chapter, we have presented the synthesis of a series of interesting donor-acceptor 1,2,4,5-tetrazine derivatives. In this chapter, we will focus on the application of these molecules in the inverse Electron Demand Diels–Alder (iEDDA) reaction. The Diels-Alder cycloaddition of tetrazines with electron rich dienophiles was first reported in 1959 and was known as the Carboni−Lindsey reaction.[1] Since then, this chemistry has been utilized in a number of studies for preparing biologically active molecules, including a number of studies in total synthesis of natural products,[2–5] as well as the recently developed fast bioconjugation with e.g. strained cyclooctynes or trans-cyclooctene.

In this chapter, we will firstly focus the study on the ability of our donor-acceptor tetrazine derivatives in the iEDDA reaction, including fluorescence turn-on of the new donor-acceptor tetrazine derivatives. Then we will focus our interest on the electrochemical and photophysical properties of the donor-acceptor pyridazine derivatives prepared by the iEDDA reaction because pyridazine as an electron-deficient heterocycle and its substituted derivatives have recently attracted interest for their application potential in optoelectronic functional materials.[6–10]

5.2 Synthesis

As described in the first chapter, tetrazine acts as a diene in the iEDDA reaction to form a dihydropyridazine or pyridazine depending on the alkene or alkyne nature of the dienophile, respectively. A list of dienophiles and their reaction rates in iEDDA reaction can be found in literature.[11–13] In this study, cyclooctyne was chosen as the dienophile because the triple bond in cyclooctyne allowed us to obtain directly the pyridazine products in one step without the need for an additional oxidation step and tedious purifications. Therefore, the donor-acceptor tetrazine derivatives which we have presented in the last chapter (**TA1-TA7**) were employed to react with cyclooctyne. Interestingly, the very efficient reaction of cyclooctyne with tetrazines[13] allowed us to obtain molecules **DA1-DA7** in almost quantitative yields (**Scheme 1**). It was observed that compounds **TA1-TA4** react with cyclooctyne in dichloromethane (DCM) at room temperature within several minutes to give **DA1-DA4**, while the reactions of **TA5-TA7** with cyclooctyne were performed at 50 °C for 1 hour to give **DA5-DA7**. This is in accordance with the superior cycloaddition reaction rate of 3-monosubstituted unsymmetrical tetrazines compared to those of 3,6-disubstituted symmetrical ones as reported previously.[11,12]

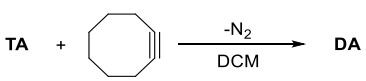

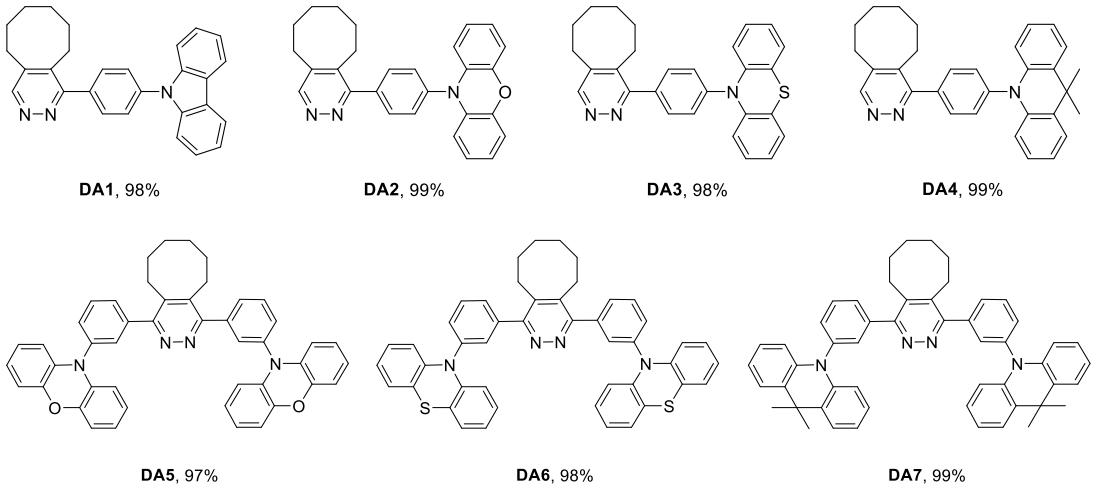

Scheme 1: Synthesis of **DA1-DA7.** All reactions were carried out on a 1 mmol scale in 10 ml DCM. Yields (isolated) based on the **TA** precursors.

As indicated in chapter 4, all the **TA** molecules are completely non-emissive, however the fluorescence can be readily turned on upon treating cyclooctyne in all cases, as the resulting pyridazines are emissive. The reaction of **TA2** with cyclooctyne is exemplified here to show the fluorescence turn-on ability of our donor-acceptor tetrazines (**Figure 1**)**.** The reaction proceeded quickly in DCM at room temperature. After the addition of cyclooctyne, the typical red color of the tetrazine solution quickly disappeared and nitrogen gas evolved, resulting in a colorless and highly emissive solution (**Figure 1c**). The X-ray single crystal structures of both **TA2** and **DA2** are also shown in **Figure 1b**.

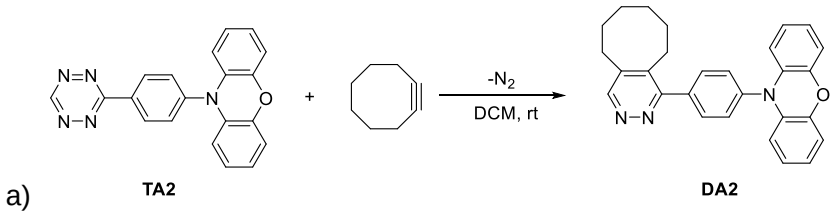

a)

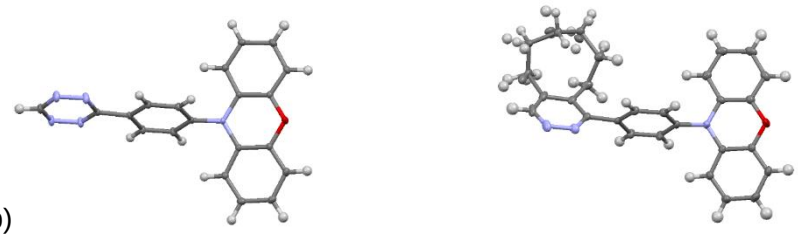

b)



c)

Figure 1: a) IEDDA reaction of **TA2** with cyclooctyne. b) X-ray crystallographic structure of the initial tetrazine (left) and product (right). c) Photos of the initial compound (left) and the adduct product (right) under 365 nm UV-irradiation.

The fluorescence turn-on property was studied by recording fluorescence spectra during the course of the reaction (**Figure 2**). The gradual increase in emission intensity indicates the formation of the pyridazine moiety. The reaction was completed when it reached a plateau approximately 15 minutes after the addition of cyclooctyne

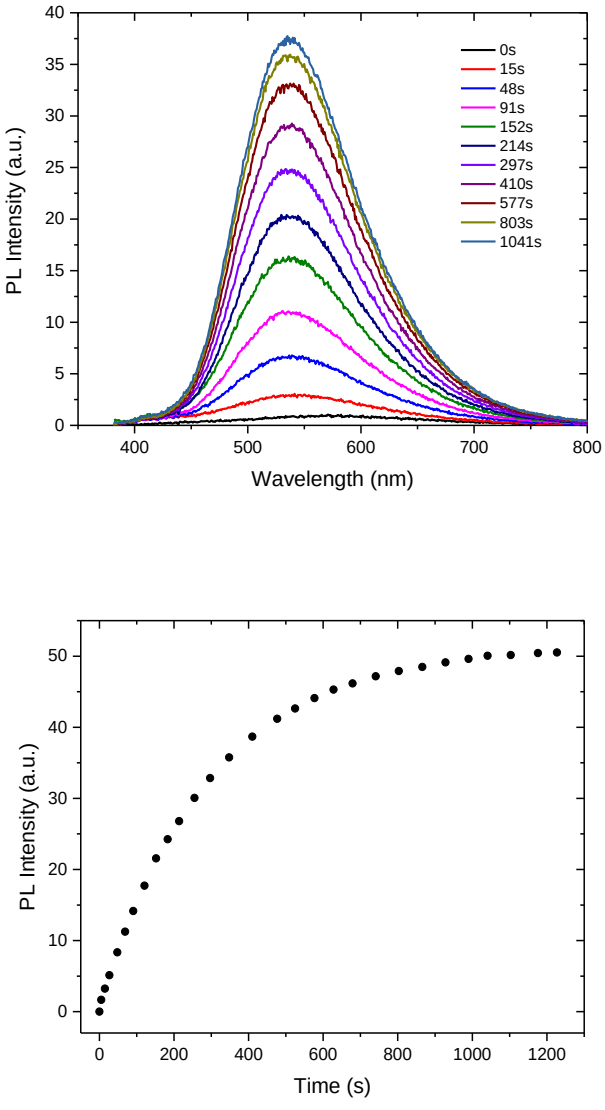

Figure 2: (top) Fluorescence spectra recorded during the course of the iEDDA reaction of **TA2** and cyclooctyne in DCM at room temperature and (bottom) plot of the variation of fluorescence emission (integration of the area of each spectrum) as a function of time.

5.3 Electrochemistry

The electrochemical properties of **DA1-DA7** are depicted in **Table 1** and **Figure 3, 4**. In contrast to the **TA** derivatives which show both oxidation and reduction peaks in cyclic voltammetry, only the oxidation peaks of the donor moieties were found for all **DA** derivatives. In the case of **DA2-DA7**, these oxidation peaks are fully reversible, while in the case of **DA1**, it is irreversible because carbazole moiety is known as irreversible. Therefore, the HOMO and LUMO values were estimated from the combination of the oxidation potentials and the optical gaps which are estimated from the onset of absorption spectra in DCM.

Table 1: Electrochemical properities of **DA1-DA7**.

	E_{ox} vs Fc/Fc^+ (V)[a]	E_g (eV)[b]	HOMO (eV)[c]	LUMO (eV)[d]
DA1	0.73	3.52	5.83	2.31
DA2	0.21	3.46	5.31	1.85
DA3	0.21	3.38	5.31	1.93
DA4	0.38	3.32	5.48	2.16
DA5	0.25	3.31	5.35	2.04
DA6	0.29	3.30	5.39	2.09
DA7	0.43	3.34	5.53	2.19

(a) Measured in DCM at room temperature by cyclic voltammetry. (b) Estimated from the onset of absorption spectra in DCM. (c) Estimated from the oxidation potential in DCM, HOMO = E_{ox} + 5.1. (d) Calculated from HOMO - E_g.

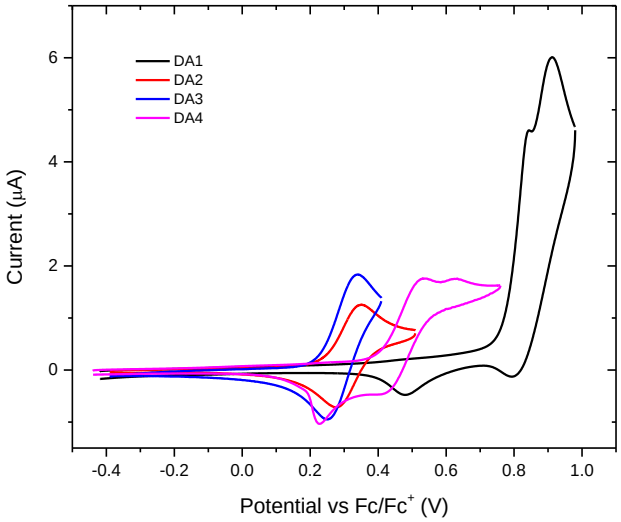

Figure 3: Cyclic voltammetry of **DA1-DA4** in DCM at room temperature.

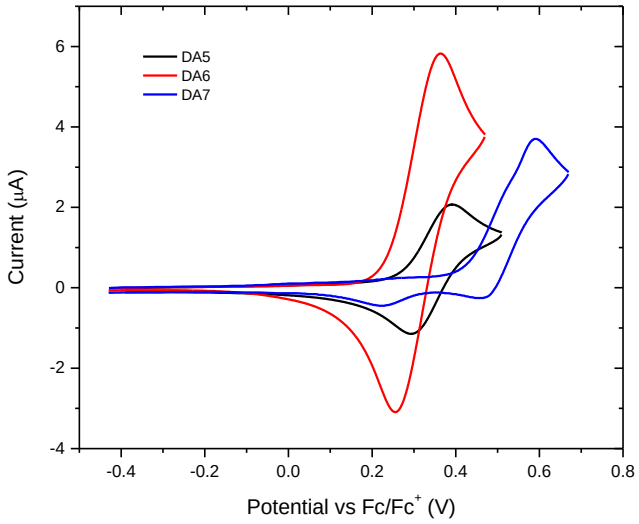

Figure 4: Cyclic voltammetry of **DA5-DA7** in DCM at room temperature.

5.4 Photophysical properties

The main photophysical properties of **DA1-DA7** are depicted in **Table 2** and **Figure 5, 7-21**.

Table 2: Photophysical properties of **DA1-DA7**.

	λ_{Abs} (nm)[(a)]	λ_{FL} (nm)[(b)]	λ_{Phos} (nm)[(c)]	Φ_{PL}(%)[(d)]
DA1	238, 292, 326, 340	346, 362	485	0.1
DA2	240, 324	536	455, 481	15.5
DA3	258, 314	558	500, 526	4.2
DA4	288	487	488	3.5
DA5	240, 323	577	482	1.6
DA6	258, 317	602	505, 532	0.9
DA7	286	522	478	0.6

(a) Absorption maxima measured in DCM (1×10^{-5} M) at room temperature. (b) Emission maxima measured in DCM (1×10^{-5} M) at room temperature. (c) Measured in Zeonex 1% (w/w) at 80 K after a delay of 10 ms. (d) Measured in DCM at room temperature.

The absorption and emission spectra of **DA2** (example in section 5.2 for exhibition of fluorescence turn-on property) are shown in **Figure 5**. The clear solvatochromic effect for **DA2** indicates that the emission originates from a charge transfer (CT) excited state. Except **DA2**, **DA3**, **DA5** and **DA6** also show a clear solvatochromic effect (**Figure 17, 19, 20**) which indicates that the emission comes from a charge transfer (CT) excited state. However, no clear solvatochromic effect was observed for **DA1**, **DA4** and **DA7** because the compounds are only emissive in DCM but very weakly or not emissive in other solvents (**Figure 15, 18, 21**). In addition, the phosphorescence emission of all the **DA** compounds were measured in Zeonex 1% (w/w) at 80 K after a delay of 10 ms (**Figure 15-21**), which are summarized in **Table 2**.

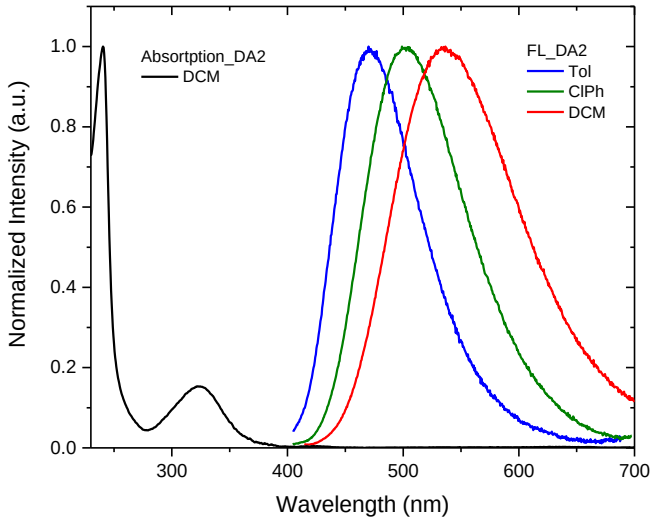

Figure 5: Absorption spectrum of **DA2** in DCM and photoluminescence spectra of **DA2** in various solvents at room temperature.

The reaction scheme of **TA3** with cyclooctyne to give **DA3** is shown in **Figure 6**, along with the X-ray single crystal structures of both **TA3** and **DA3**. Similarly to the reaction of **TA2** with cyclooctyne, the reaction of **TA3** with cyclooctyne proceeded quickly in DCM at room temperature. The red colored non-emissive tetrazine solution became colorless and emissive.

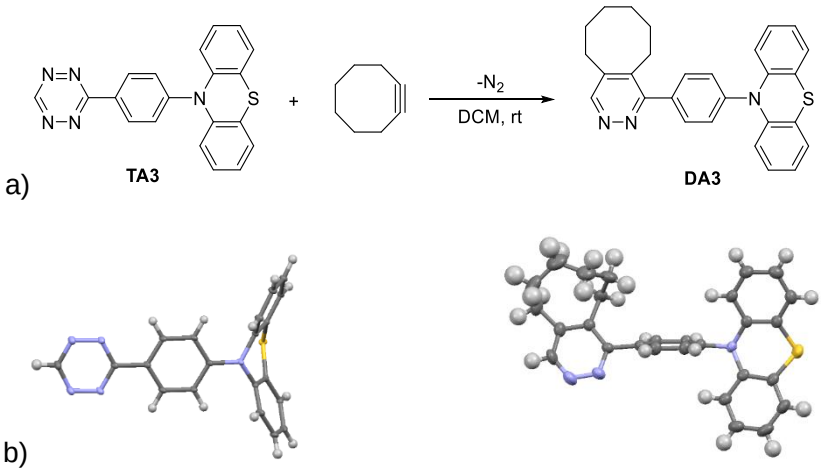

Figure 6: a) IEDDA reaction of **TA3** with cyclooctyne. b) X-ray crystallographic structure of the initial tetrazine (left) and the product (right).

The photoluminescence spectrum of **DA3** in Zeonex 1% (w/w) in degassed condition shows an additional signal (at around 550 nm) compared to the spectrum in air-equilibrated condition, which can be attributed to room temperature phosphorescence (RTP, **Figure 7**). The time resolved emission spectrum and photoluminescence decay of **DA3** indicate that this additional signal has a long lifetime which corresponds to the phosphorescence of the molecule (**Figure 8** and **9**). The ratio of the room temperature phosphorescence component to the fluorescence one was determined to be 0.68. In addition, the singlet and triplet energy levels were estimated to be 3.16 eV and 2.63 eV, respectively, from the onset of the fluorescence and phosphorescence spectra (**Figure 8**).

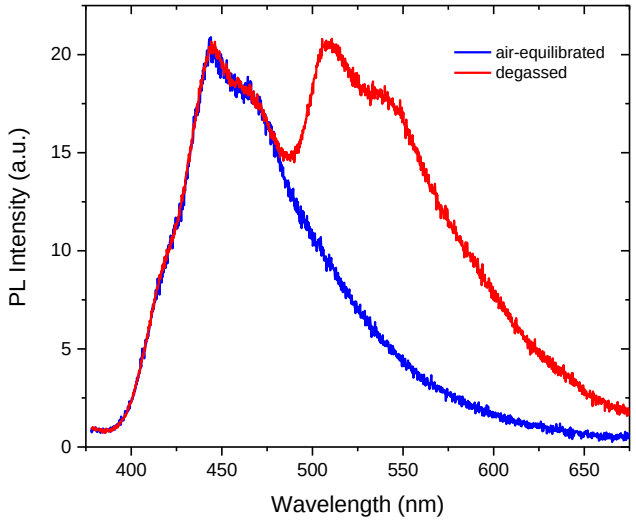

Figure 7: Photoluminescence spectra of **DA3** in Zeonex 1% (w/w) in degassed (red) and air-equilibrated (blue) conditions at room temperature.

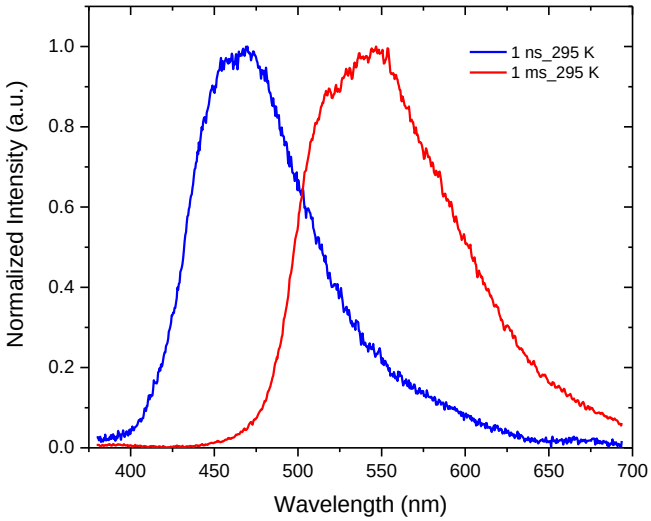

Figure 8: Time-resolved spectra of **DA3** in Zeonex 1% (w/w) at room temperature in degassed atmosphere. The blue spectrum corresponds to the fluorescence and the red one to the phosphorescence.

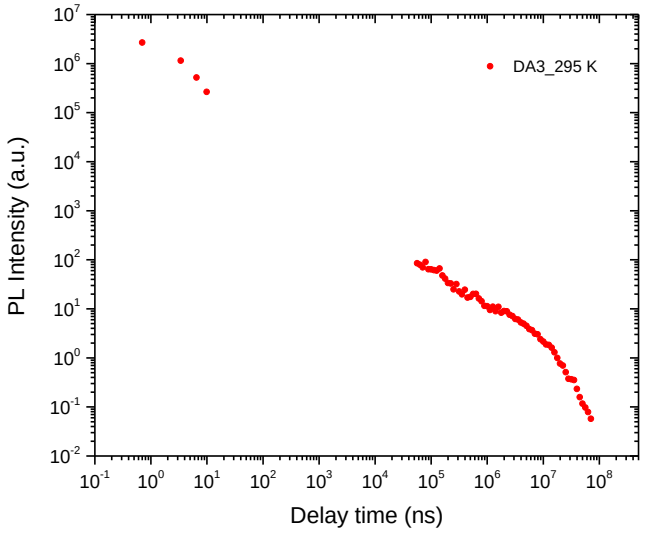

Figure 9: PL decay of **DA3** in Zeonex 1% (w/w) at room temperature in degassed atmosphere.

The photophysical properties of **DA6** are similar to those of **DA3**. It also exhibits clear RTP effect and the ratio of the RTP component to the fluorescence one was determined to be 0.48 (**Figure 10**). Additionally, the singlet and triplet energy levels were estimated to be 3.13 eV and 2.61 eV, respectively, from the onset of the fluorescence and phosphorescence spectra (**Figure 11**).

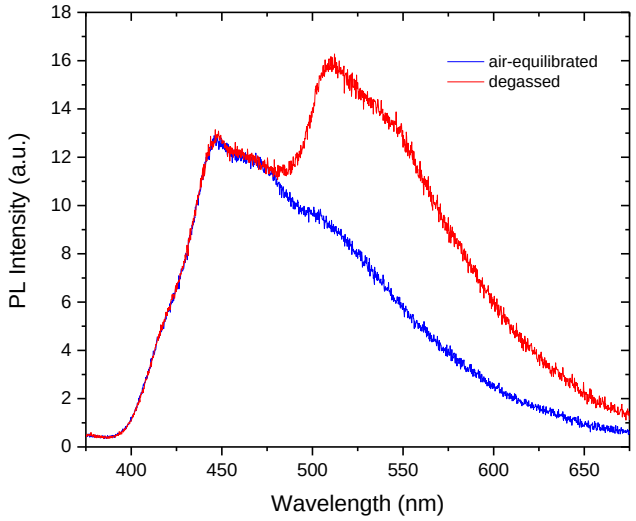

Figure 10: Photoluminescence spectra of **DA6** in Zeonex 1% (w/w) in degassed (red) and air-equilibrated (blue) conditions at room temperature.

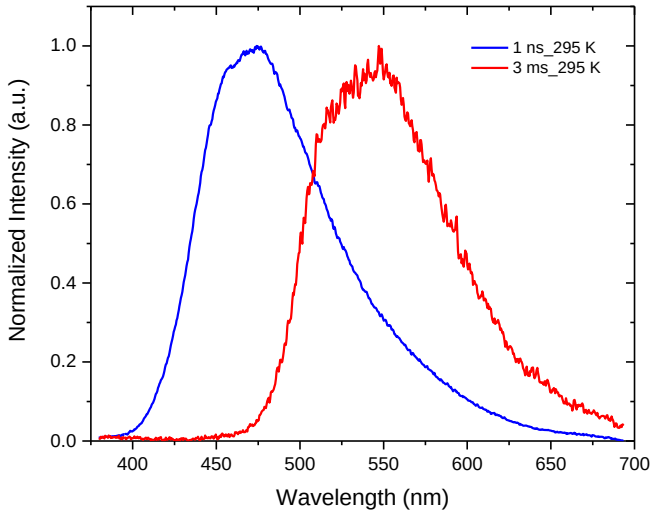

Figure 11: Time-resolved spectra of **DA6** in Zeonex 1% (w/w) at room temperature in degassed atmosphere. The blue spectrum corresponds to the fluorescence and the red one to the phosphorescence.

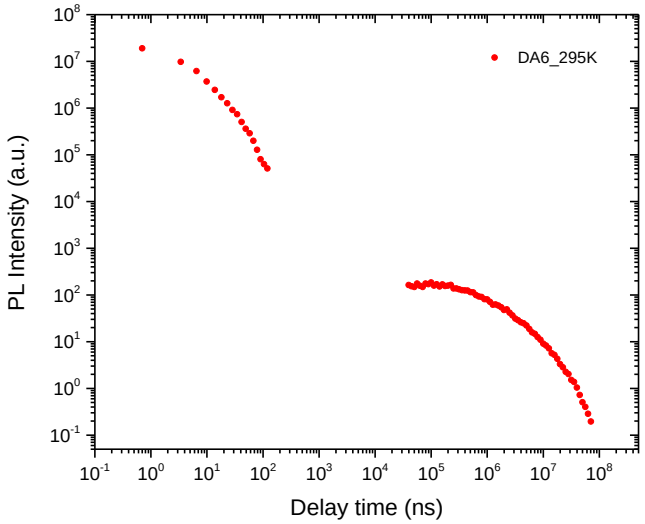

Figure 12: PL decay of **DA6** in Zeonex 1% (w/w) at room temperature in degassed atmosphere.

The room temperature phosphorescence emission exhibited by compounds **DA3** and **DA6** is most likely due to an efficient intersystem crossing to a long lived triplet excited state that is promoted by the phenothiazine donor attached to the pyridazine acceptor core. RTP materials have attracted intensive interests because of their relatively long decay lifetimes and large Stoke shift, which have already been reported to be useful in many fields such

as organic light-emitting diodes (OLEDs),[14,15] bioimaging and sensing[16] or organic photovoltaics (OPV).[17]

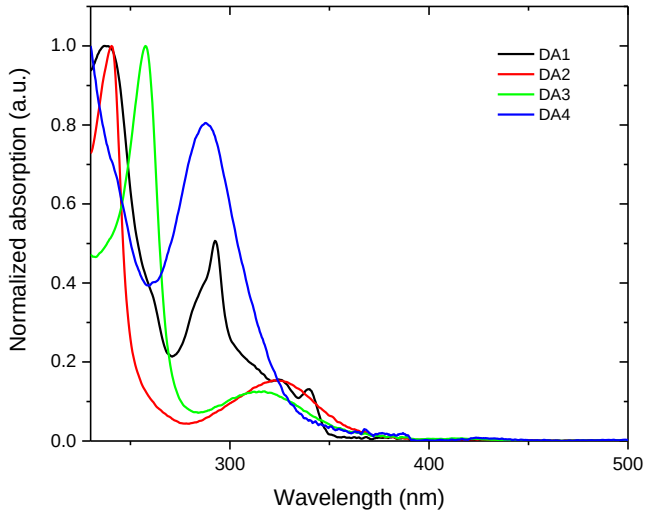

Figure 13: Absorption spectra of **DA1-DA4** in DCM at room temperature.

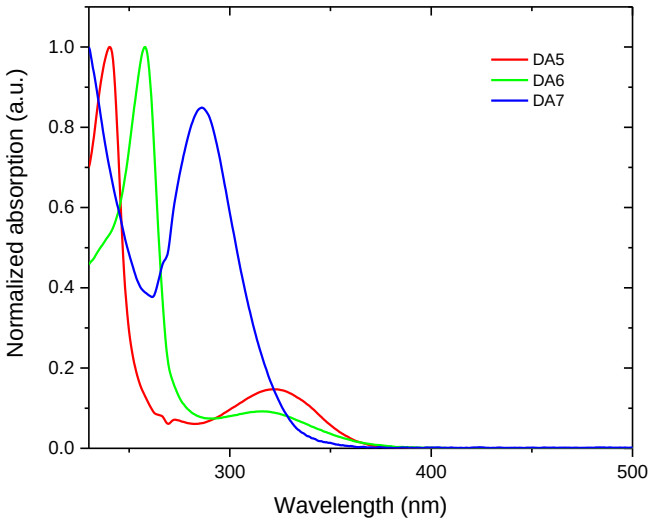

Figure 14: Absorption spectra of **DA5-DA7** in DCM at room temperature.

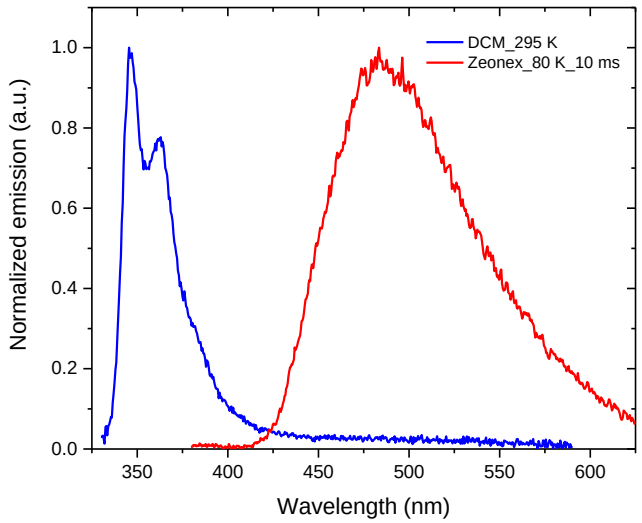

Figure 15: Normalized fluorescence spectrum of **DA1** in DCM at room temperature (blue) and normalized phosphorescence spectrum of **DA1** in Zeonex at 80 K (red).

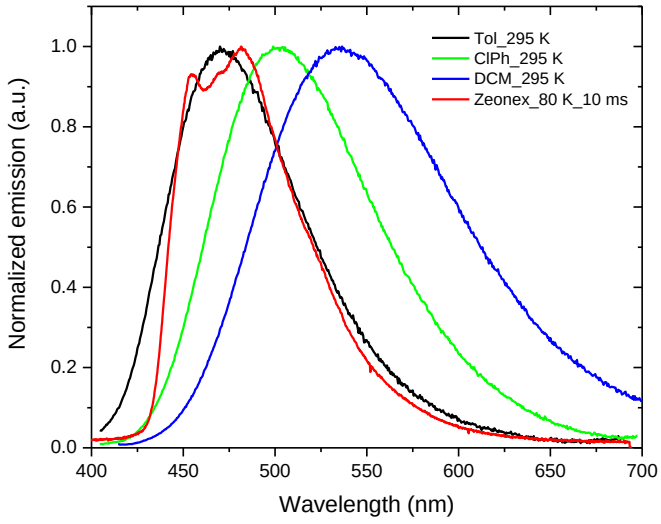

Figure 16: Normalized fluorescence spectra of **DA2** in toluene (black), chlorobenzene (green) and DCM (blue) at room temperature and normalized phosphorescence spectrum of **DA2** in Zeonex at 80 K (red).

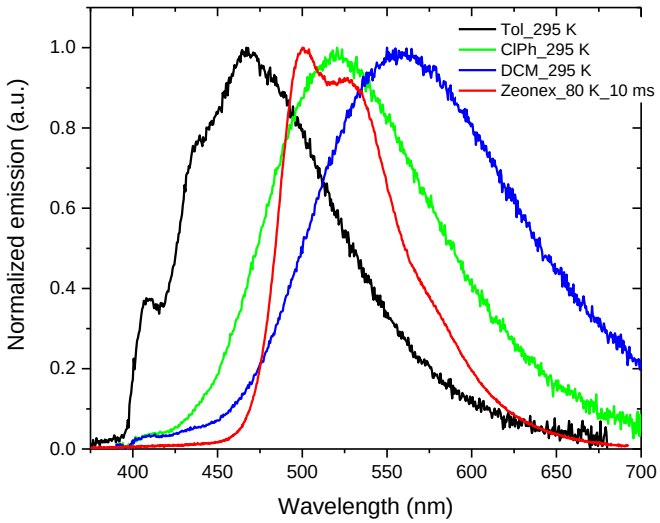

Figure 17: Normalized fluorescence spectra of **DA3** in toluene (black), chlorobenzene (green) and DCM (blue) at room temperature and normalized phosphorescence spectrum of **DA3** in Zeonex at 80 K (red).

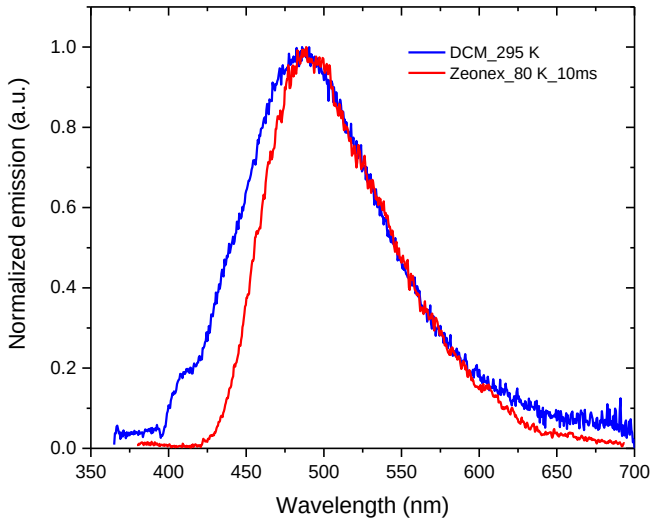

Figure 18: Normalized fluorescence spectrum of **DA4** in DCM at room temperature (blue) and normalized phosphorescence spectrum of **DA4** in Zeonex at 80 K (red).

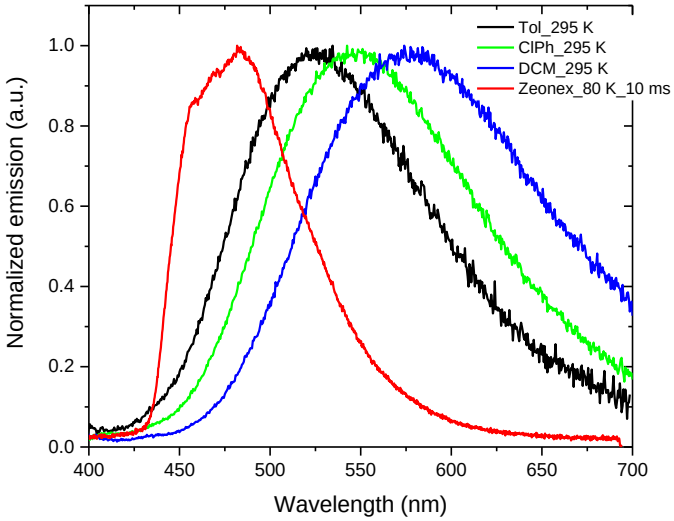

Figure 19: Normalized fluorescence spectra of **DA5** in toluene (black), chlorobenzene (green) and DCM (blue) at room temperature and normalized phosphorescence spectrum of **DA5** in Zeonex at 80 K (red).

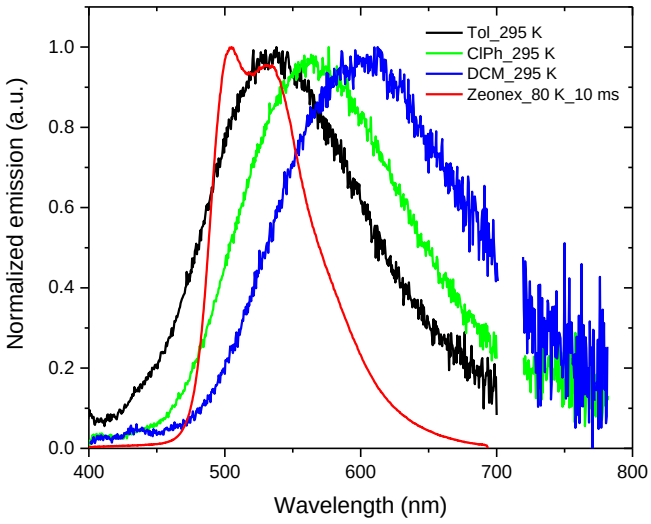

Figure 20: Normalized fluorescence spectra of **DA6** in toluene (black), chlorobenzene (green) and DCM (blue) at room temperature and normalized phosphorescence spectrum of **DA6** in Zeonex at 80 K (red).

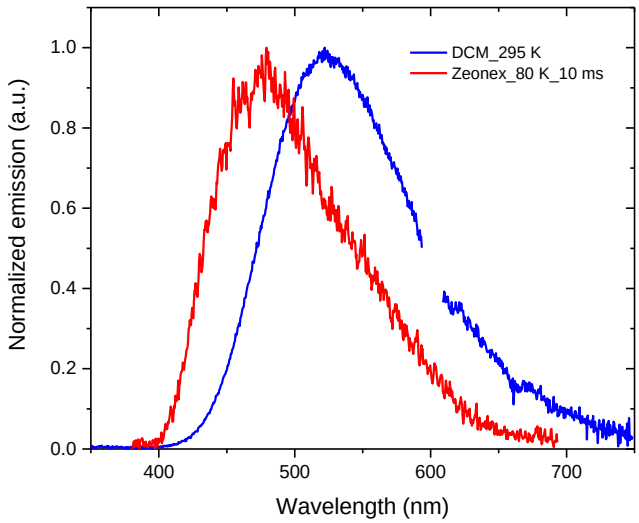

Figure 21: Normalized fluorescence spectra of **DA7** in DCM at room temperature (blue) and normalized phosphorescence spectrum of **DA7** in Zeonex at 80 K (red).

5.5 Conclusion

In this chapter, we have firstly studied the efficiency of our donor-acceptor tetrazine derivatives **TA1-TA7** in the inverse Electron Demand Diels–Alder (iEDDA) reaction. The fluorescence turn-on ability of the new donor-acceptor tetrazine derivatives was exemplified by the reaction of **TA2** and cyclooctyne, which shows a fast rate and a high fluorescence turn-on ratio.

Then we were interested in the study of the electrochemical and photophysical properties of all the donor-acceptor pyridazine derivatives **DA1-DA7** prepared by the iEDDA reaction. Interestingly, it was observed that **DA3** and **DA6** exhibit clear room temperature phosphorescence (RTP) emission which could find applications in various fields such as organic electronics (e.g. OLED, OPV), as well as bioimaging and sensing.

5.6 Experimental details

General Methods:

Synthesis. All chemicals were received from commercial sources and used without further purification. Thin layer chromatography (TLC) was performed on silica gel. Flash column chromatography purification was performed on a CombiFlash-Rf system with a variable wavelength UV detector. All mixtures of solvents are given in v/v ratio. NMR spectra were recorded on a JEOL ECS (400 MHz) spectrometer. ^{13}C NMR spectra were proton decoupled. HRMS spectra were measured either on an UPLC/ESI-HRMS device (an Acquity Waters UPLC system coupled to a Waters LCT Premier XE mass spectrometer equipped with an electrospray ion source), or a Q-TOF mass spectrometer (Q-TOF 6540, Agilent) equipped with an APPI ion source.

Cyclooctyne[18] was prepared according to published procedures.

Photophysic. Zeonex ® 480 blends were prepared from toluene solutions by the drop-cast method and dried in a vacuum. All solutions were investigated at 10^{-5} mol dm^{-3} concentration and were degassed using five freeze/pump cycles. Absorption and emission spectra were collected using a UV-3600 double beam spectrophotometer (Shimadzu), and a Fluoromax fluorescence spectrometer (Jobin Yvon) or QePro fluorescence spectrometer (Ocean Optics). Photoluminescence quantum yields in DCM solution were measured using 9,10-diphenylanthracene (Φ_{PL} = 0.684) as the standard.

Phosphorescence, prompt fluorescence (PF), and spectra and decays were recorded using nanosecond gated luminescence and lifetime measurements (from 400 ps to 1 s) using either third harmonics of a high-energy, pulsed Nd:YAG laser emitting at 355 nm (EKSPLA) or a N2 laser emitting at 337 nm. Emission was focused onto a spectrograph and detected on a sensitive gated iCCD camera (Stanford Computer Optics) of sub-nanosecond resolution. PF/DF time-resolved measurements were performed by exponentially increasing gate and delay times.

Electrochemistry. The electrochemical cell comprised of platinum electrode with a 1 mm diameter of working area as a working electrode, an Ag electrode as a reference electrode and a platinum coil as an auxiliary electrode. Cyclic voltammetry measurements were conducted at room temperature at a potential rate of 50 mV/s and were calibrated against ferrocene/ferrocenium redox couple. All voltammograms were recorded on a CHInstruments Electrochemical Analyzer model 660 potentiostat. Electrochemical measurements were conducted in 1.0 mM concentrations for all cyclic voltammetry measurements. Electrochemical studies were undertaken in 0.1 M solutions of Bu_4NPF_6, 99% in dichloromethane (DCM) at room temperature.

General procedure for synthesis of DA1-DA4

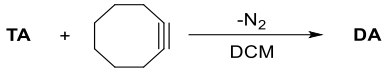

To a 50 mL round bottom flask equipped with a stir bar, 0.1 mmol of **TA1-TA4**, and 10 mL of DCM were added. Then 0.4 mmol of cyclooctyne (50 µL) was added with stirring at room temperature. The color of the solution turned from red to colorless after several minutes and N_2 gas evolved. The reaction mixture was allowed to stir for another 20 min. All the volatiles were evaporated under vacuum and the residue was purified using flash column chromatography.

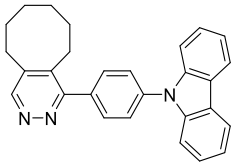

DA1

DA1: A white solid was obtained after flash column chromatography (Petroleum ether:EtOAc = 2:3) (39.6 mg, yield: 98%).

^{1}H NMR (400 MHz, $CDCl_3$, δ): 8.96 (s, 1H), 8.17 (d, *J* = 8.24 Hz, 2H), 7.78–7.68 (m, 4H), 7.51 (d, *J* = 7.80 Hz, 2H), 7.44 (t, *J* = 7.80 Hz, 2H), 7.32 (t, *J* = 7.80 Hz, 2H), 2.94–2.85 (m, 4H), 1.90–1.80 (m, 2H), 1.76–1.66 (m, 2H), 1.54–1.40 (m, 4H) ppm; ^{13}C NMR (100 MHz, $CDCl_3$, δ): 161.33, 151.75, 141.58, 140.82, 138.87, 138.25, 136.96, 130.84, 126.93, 126.19, 123.66, 120.51, 120.30, 109.94, 31.28, 30.56, 29.70, 26.77, 26.10, 25.57 ppm; HRMS $[M+H]^+$ m/z calcd. for $[C_{28}H_{26}N_3]^+$ 404.2127, found 404.2127.

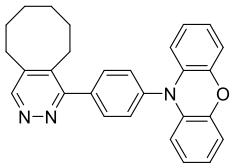

DA2

DA2: A white solid was obtained after flash column chromatography (Petroleum ether:EtOAc = 2:3) (41.5 mg, yield: 99%). A single crystal of **DA2** was grown from slow evaporation of petroleum ether/EtOAc (2:3) mixture.

^{1}H NMR (400 MHz, $CDCl_3$, δ): 8.97 (s, 1H), 7.73 (d, *J* = 8.24 Hz, 2H), 7.48 (d, *J* = 8.24 Hz, 2H), 6.76–6.57 (m, 6H), 6.01 (d, *J* = 7.80 Hz, 2H), 2.95–2.81 (m, 4H), 1.89–1.79 (m, 2H), 1.71–1.61 (m, 2H), 1.55–1.38 (m, 4H) ppm; ^{13}C NMR (100 MHz, $CDCl_3$, δ): 161.27, 151.32, 144.11, 142.19, 139.69, 139.62, 137.79, 134.29, 132.03, 131.01, 123.42, 121.67, 115.67,

113.50, 31.25, 30.47, 29.76, 26.87, 26.09, 25.53 ppm; HRMS $[M+H]^+$ m/z calcd. for $[C_{28}H_{26}N_3O]^+$ 420.2076, found 420.2090.

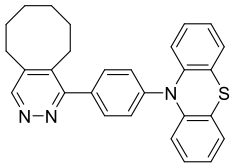

DA3

DA3: A light yellow solid was obtained after flash column chromatography (Petroleum ether:EtOAc = 2:3) (42.6 mg, yield: 98%). A single crystal of **DA3** was grown from slow evaporation of petroleum ether/EtOAc (2:3) mixture.

^{1}H NMR (400 MHz, $CDCl_3$, δ): 8.94 (s, 1H), 7.71 (d, *J* = 8.24 Hz, 2H), 7.49 (d, *J* = 8.24 Hz, 2H), 7.07 (d, *J* = 7.80 Hz, 2H), 6.96–6.82 (m, 4H), 6.38 (d, *J* = 7.80 Hz, 2H), 2.93–2.81 (m, 4H), 1.89–1.78 (m, 2H), 1.71–1.61 (m, 2H), 1.54–1.38 (m, 4H) ppm; ^{13}C NMR (100 MHz, $CDCl_3$, δ): 161.27, 151.72, 144.09, 141.87, 141.54, 138.79, 137.39, 131.61, 129.89, 127.08, 127.05, 123.01, 121.51, 117.10, 31.25, 30.48, 29.68, 26.79, 26.09, 25.56 ppm; HRMS $[M+H]^+$ m/z calcd. for $[C_{28}H_{26}N_3S]^+$ 436.1847, found 436.1855.

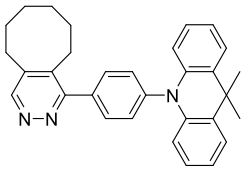

DA4

DA4: A white solid was obtained after flash column chromatography (Petroleum ether:EtOAc = 2:3) (44.1 mg, yield: 99%).

^{1}H NMR (400 MHz, $CDCl_3$, δ): 8.97 (s, 1H), 7.77 (d, *J* = 8.24 Hz, 2H), 7.54–7.44 (m, 4H), 7.05–6.91 (m, 4H), 6.37 (d, *J* = 7.80 Hz, 2H), 2.94–2.84 (m, 4H), 1.89–1.80 (m, 2H), 1.71 (s, 6H), 1.71–1.65 (m, 2H), 1.55–1.40 (m, 4H) ppm; ^{13}C NMR (100 MHz, $CDCl_3$, δ): 161.34, 151.76, 141.68, 141.54, 140.88, 138.82, 137.87, 131.80, 131.42, 130.20, 126.50, 125.35, 120.82, 114.23, 36.11, 31.29, 31.24, 30.43, 29.66, 26.80, 26.07, 25.54 ppm; HRMS $[M+H]^+$ m/z calcd. for $[C_{31}H_{32}N_3]^+$ 446.2596, found 446.2606.

General procedure for synthesis of DA5-DA7

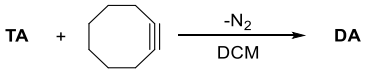

To a 50 mL round bottom flask equipped with a stir bar, 0.1 mmol of **TA5-TA7**, and 15 mL of DCM were added. Then 0.4 mmol of cyclooctyne (50 µL) was added with stirring at room temperature. The reaction mixture was heated to 50 °C and allowed to stir for 1 hour. The color of the solution turned from red to colorless indicating the completion of the reaction. The reaction mixture was then cooled down to room temperature. All the volatiles were evaporated under vacuum and the residue was purified using flash column chromatography.

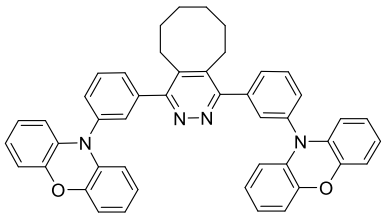

DA5

DA5: A light yellow solid was obtained after flash column chromatography (Petroleum ether:EtOAc = 2:1) (65.8 mg, yield: 97%).

^{1}H NMR (400 MHz, $CDCl_3$, δ): 7.75 (t, *J* = 8.24 Hz, 2H), 7.66 (d, *J* = 8.24 Hz, 2H), 7.52 (s, 2H), 7.48 (d, *J* = 8.24 Hz, 2H), 6.74–6.56 (m, 12H), 6.03 (d, *J* = 7.80 Hz, 4H), 2.84 (s, br, 4H), 1.60 (s, br, 4H), 1.41 (s, br, 4H) ppm; ^{13}C NMR (100 MHz, $CDCl_3$, δ): 160.39, 144.01, 141.04, 139.70, 139.01, 134.34, 131.66, 131.49, 131.24, 129.57, 123.44, 121.61, 115.62, 113.43, 30.37, 27.49, 25.91 ppm; HRMS $[M+H]^+$ m/z calcd. for $[C_{46}H_{37}N_4O_2]^+$ 677.2917, found 677.2923.

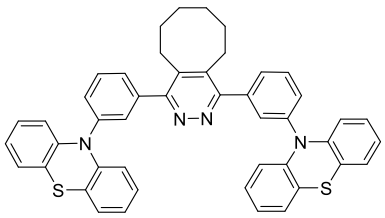

DA6

DA6: A light yellow solid was obtained after flash column chromatography (Petroleum ether:EtOAc = 2:1) (69.3 mg, yield: 98%).

^{1}H NMR (400 MHz, $CDCl_3$, δ): 7.73 (t, *J* = 8.24 Hz, 2H), 7.63 (d, *J* = 8.24 Hz, 2H), 7.54 (s, 2H), 7.51 (d, *J* = 8.24 Hz, 2H), 7.04 (dd, *J* = 7.80 Hz, *J* = 1.80 Hz, 4H), 6.93–6.79 (m, 8H), 6.36 (d, *J* = 7.80 Hz, 4H), 2.85 (s, br, 4H), 1.60 (s, br, 4H), 1.40 (s, br, 4H) ppm; ^{13}C NMR (100 MHz, $CDCl_3$, δ): 160.54, 144.11, 141.26, 140.61, 139.66, 131.21, 131.04, 130.39, 128.94, 127.08, 127.02, 122.92, 120.99, 116.76, 30.42, 27.51, 25.94 ppm; HRMS $[M+H]^+$ m/z calcd. for $[C_{46}H_{37}N_4S_2]^+$ 709.2460, found 709.2485.

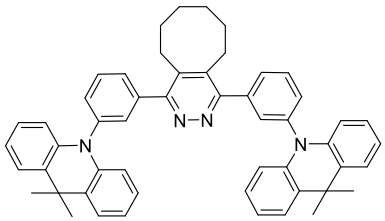

DA7

DA7: A white solid was obtained after flash column chromatography (Petroleum ether:EtOAc = 2:1) (72.1 mg, yield: 99%).

^{1}H NMR (400 MHz, $CDCl_3$, δ): 7.78 (t, *J* = 8.24 Hz, 2H), 7.70 (d, *J* = 8.24 Hz, 2H), 7.52 (t, *J* = 1.80 Hz, 2H), 7.50–7.43 (m, 6H), 7.03–6.90 (m, 8H), 6.39 (d, *J* = 7.80 Hz, *J* = 1.80 Hz, 4H), 2.94–2.82 (m, 4H), 1.70 (s, 12H), 1.60 (s, br, 4H), 1.38 (s, br, 4H) ppm; ^{13}C NMR (100 MHz, $CDCl_3$, δ): 160.54, 141.21, 141.02, 140.99, 139.43, 132.22, 131.57, 131.27, 130.19, 129.32, 126.55, 125.32, 120.82, 114.21, 36.14, 31.25, 30.33, 27.45, 25.93 ppm; HRMS $[M+H]^+$ m/z calcd. for $[C_{52}H_{49}N_4]^+$ 729.3957, found 729.3975.

5.7 Reference

[1] R. A. Carboni, R. V. Lindsey, *J. Am. Chem. Soc.* **1959**, *81*, 4342–4346.

[2] A. Hamasaki, J. M. Zimpleman, I. Hwang, D. L. Boger, *J. Am. Chem. Soc.* **2005**, *127*, 10767–10770.

[3] D. L. Boger, J. Hong, *J. Am. Chem. Soc.* **2001**, *123*, 8515–8519.

[4] S. M. Sakya, T. W. Strohmeyer, S. A. Lang, Y.-I. Lin, *Tetrahedron Lett.* **1997**, *38*, 5913–5916.

[5] D. Che, T. Wegge, M. T. Stubbs, G. Seitz, H. Meier, C. Methfessel, *J. Med. Chem.* **2001**, *44*, 47–57.

[6] J. G. Yu, S. H. Han, H. R. Jeon, H. K. Chung, J. Y. Lee, *J. Lumin.* **2018**, *194*, 33–39.

[7] B. X. Mi, P. F. Wang, Z. Q. Gao, C. S. Lee, S. J. Lee, H. L. Hong, X. M. Chen, M. S. Wong, P. F. Xia, K. W. Cheah, et al., *Adv. Mater.* **2009**, *21*, 339–343.

[8] Z. Q. Gao, B. X. Mi, H. L. Tam, K. W. Cheah, C. H. Chen, M. S. Wong, S. T. Lee, C. S. Lee, *Adv. Mater.* **2008**, *20*, 774–778.

[9] S. Liu, X. Zhang, C. Ou, S. Wang, X. Yang, X. Zhou, B. Mi, D. Cao, Z. Gao, *ACS Appl. Mater. Interfaces* **2017**, *9*, 26242–26251.

[10] M. Li, Y. Yuan, Y. Chen, *ACS Appl. Mater. Interfaces* **2018**, *10*, 1237–1243.

[11] B. L. Oliveira, Z. Guo, G. J. L. Bernardes, *Chem. Soc. Rev.* **2017**, *46*, 4895–4950.

[12] A. C. Knall, C. Slugovc, *Chem. Soc. Rev.* **2013**, *42*, 5131–5142.

[13] J. Sauer, D. K. Heldmann, J. Hetzenegger, J. Krauthan, H. Sichert, J. Schuster, *European J. Org. Chem.* **1998**, 2885–2896.

[14] M. A. Baldo, D. F. O'Brien, Y. You, A. Shoustikov, S. Sibley, M. E. Thompson, S. R. Forrest, *Nature* **1998**, *395*, 151–154.

[15] Y. Liu, G. Zhan, Z. W. Liu, Z. Q. Bian, C. H. Huang, *Chinese Chem. Lett.* **2016**, *27*, 1231–1240.

[16] Q. Zhao, C. Huang, F. Li, *Chem. Soc. Rev.* **2011**, *40*, 2508–2524.

[17] C. L. Lee, I. W. Hwang, C. C. Byeon, B. H. Kim, N. C. Greenham, *Adv. Funct. Mater.* **2010**, *20*, 2945–2950.

[18] L. Brandsma, H. D. Verkruijsse, *Synthesis (Stuttg).* **1978**, *4*, 290–290.

Chapter 6

Modified Pinner synthesis: New convenient one-pot synthesis of thiatriazole derivatives

6.1 Introduction

The 1,2,3,4-thiatriazole heterocycle was first reported in 1896 by Freund and co-workers[1–2] and its structural assignment was firmly established in 1950s by Lieber and co-workers.[3–4] A number of 1,2,3,4-thiatriazoles were then prepared and studied during that period.[5–14] However, the study was only limited to synthesis, structure characterization and investigations of their stability. The chemistry of 1,2,3,4-thiatriazoles has then been almost forgotten for many decades thereafter. As a strong electron-deficient heterocycle, 1,2,3,4-thiatriazole is potentially an excellent electron acceptor in organic donor-acceptor materials. Due to charge-transfer (CT) states introduced in the donor-acceptor system, these molecules can exhibit interesting photophysical and electrochemical properties, and therefore are of particular interest in organic electronics.[15–19] However, there have been no applications related to 1,2,3,4-thiatriazoles reported so far.

1,2,3,4-thiatriazoles are commonly prepared by diazotization of thiohydrazides, or reaction of dithioates with azide ion, in high yields (**Scheme 1**).[5–14] However, both methods require preparation of starting thioacylating agents, which in many cases are difficult to obtain. This highly increases the synthetic complexity of 1,2,3,4-thiatriazole derivatives, especially for those with complex functional groups. As a result, no 1,2,3,4-thiatriazole derivatives with complex functional groups have been prepared so far. Therefore, developing practical and convenient synthetic approaches for preparing functionalized 1,2,3,4-thiatriazole derivatives would be highly valuable to this field.

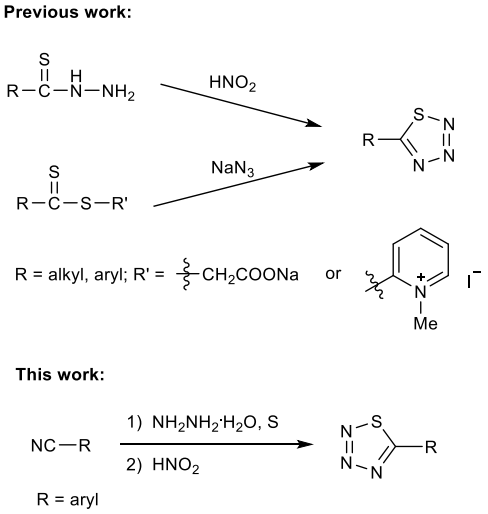

Scheme 1: Overview of the different synthetic approaches to 1,2,3,4-thiatriazoles.

In this study, we report a novel convenient one-pot synthesis of 1,2,3,4-thiatriazoles directly from commercially available nitrile compounds in high yields (51%-80%), with no need for isolating any thioacylating agents (**Scheme 1**). The access to the 1,2,3,4-thiatriazoles is

significantly improved since there is a large variety of commercially available nitrile starting materials. Using this approach we have designed and synthesized an example of a donor-acceptor thiatriazole derivative using phenoxazine as a donor, and achieved a high yield (70%). This molecule exhibits excellent thermally activated delayed fluorescence (TADF) characteristics both in solution and film. To the best of our knowledge, this is the first example of 1,2,3,4-thiatriazole used as an electron acceptor for the preparation of highly efficient TADF emitters.

6.2 Synthesis

Having a long experience in 1,2,4,5-tetrazine synthesis,[20–27] we have noticed that solvent plays an important role in the synthesis of tetrazines through the Pinner reaction. In the first chapter, we have discovered that dichloromethane (DCM) serves as a novel reagent in the synthesis of 3-monosubstituted unsymmetrical 1,2,4,5-tetrazines.[27] In this chapter a comprehensive study of solvent effect in the modified Pinner synthesis was performed, and we found out that the products obtained during the reaction are significantly influenced by the nature of the solvent employed.

The traditional Pinner synthesis is a two-step procedure starting with the formal addition of two nitrile precursors on hydrazine in ethanol, followed by cyclization to give 1,2-dihydrotetrazines which can be isolated. These intermediates are then oxidized to afford 1,2,4,5-tetrazines.[28–30] Here we used 4-bromobenzonitrile as a standard nitrile precursor to survey the effect of a range of solvents on the modified Pinner synthesis. The results are summarized in **Table 1**. When the traditional conditions with ethanol as a solvent in the first step was used followed by oxidation in one pot, 3,6-disubstituted symmetrical tetrazine **T1** was obtained in a good yield (43%) as expected. However, when the polar protic solvent ethanol was replaced by non-polar solvents (e.g., toluene or chloroform) or slightly polar aprotic solvents (e.g., tetrahydrofuran (THF) or acetone), the reactions did not work and the starting nitriles were fully recovered. When the highly polar aprotic solvent acetonitrile was used, we isolated 16% of unsymmetrical 3-(4-bromophenyl)-6-methyl-1,2,4,5-tetrazine **T2** because acetonitrile acts both as the solvent and second nitrile precursor in the reaction. In addition to the tetrazine, the 1,2,3,4-thiatriazole **TT1** was also obtained in 9% yield. More interestingly, when using dimethylformamide (DMF) as a solvent, the yield of **TT1** significantly increased to 41%. It is interesting to mention that 3-monosubstituted unsymmetrical 1,2,4,5-tetrazine **T3** was also obtained, with 8% yield, probably because DMF can also act as both a solvent and reactant involved in the tetrazine ring formation. Similar results have been previously reported by Weissleder and co-workers,[31] however the role of DMF in the reaction is not clear so far.

Finally, when the much more polar, and less electrophilic solvent dimethyl sulfoxide (DMSO) was employed, the yield of the 1,2,3,4-thiatriazole **TT1** was optimized to as high as 74%. These findings are remarkably interesting because this is the first time that a 1,2,3,4-thiatriazole has been isolated out of a Pinner-type synthesis. All the reactions were performed in a one-pot procedure without isolating any thioacylating agents. It is worth noting that in the case of all three solvents (acetonitrile, DMF and DMSO) a trace amount (yield below 1%) of symmetrical tetrazine **T1** could also be observed.

Table 1: Survey of solvent effect in the modified Pinner synthesis [(a)].

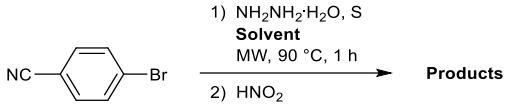

Solvent		Dielectric Constant	Products[(b)]
Polar protic solvent	Ethanol	25	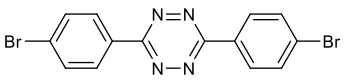 **T1, 43%**
Non-polar solvent	Toluene	2.3	SN[(c)]
	Chloroform	4.8	SN
Polar aprotic solvent	THF	7.5	SN
	Acetone	21	SN
	Acetonitrile	37	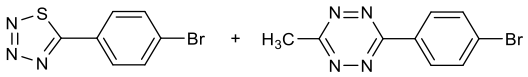 **TT1, 9%** **T2, 16%**
	DMF	38	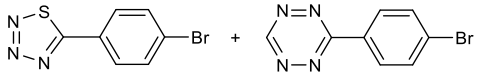 **TT1, 41%** **T3, 8%**
	DMSO	47	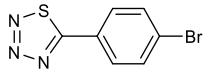 **TT1, 74%**

(a) All reactions were carried out on a 0.5 mmol scale in 2 ml solvent. MW = microwave. (b) Yields (isolated) based on the nitrile precursor. (c) SN = Starting Nitrile Precursors.

The reaction with DMSO as a solvent became the most interesting to us because it provides a novel, convenient pathway to 1,2,3,4-thiatriazoles directly from commercially available nitrile reagents in an excellent yield. The reaction conditions were optimized by

changing the amount of sulfur and reaction temperature. Acting as both an inducer and reactant in the reaction, the amount of sulfur is crucial in this reaction. Theoretically, one equivalent of sulfur should lead to one equivalent of thiatriazole product. Indeed, when using 1 equivalent of sulfur the reaction gave a reasonable yield (53%), while a slight excess of sulfur could further improve the yield and 1.5 equivalents of sulfur gave the best result (74%, **Table 2**). The reaction temperature and time were optimized at 90 °C for 1 hour because decreasing the reaction temperature only resulted in a prolonged reaction time to obtain similar yields (**Table 3**). We used microwave heating throughout, but we have verified that running the reaction in a sealed tube using conventional heating (90 °C, 1 h) worked fine as well, resulting in a similar yield (72%).

Table 2: Survey of the influence of sulfur amounts on the new 1,2,3,4-thiatriazoles synthesis [(a)].

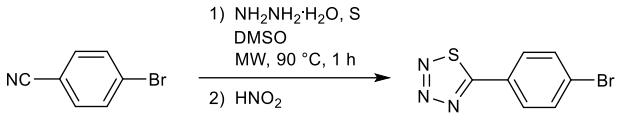

Entry	S	Yield (%)[(b)]
1	1 equiv.	53
2	1.3 equiv.	72
3	1.5 equiv.	74
4	2 equiv.	71

(a) All reactions were carried out on a 0.5 mmol scale in 2 ml DMSO. MW = microwave. (b) Yields (isolated) based on the nitrile precursor.

Table 3: Survey of the influence of reaction temperature and time on the new 1,2,3,4-thiatriazoles synthesis [(a)].

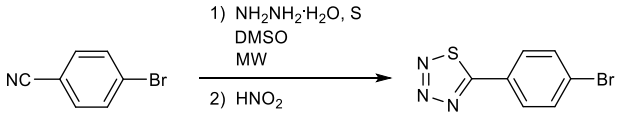

Entry	Temp., time	Yield (%)[(b)]
1	90 °C, 1 h	74
2	80 °C, 1 h	59
3	80 °C, 3 h	72

4	70 °C, 6 h	74
5	60 °C, 24 h	69

(a) All reactions were carried out on a 0.5 mmol scale in 2 ml DMSO. MW = microwave. Temp. = temperature (b) Yields (isolated) based on the nitrile precursor.

Formation of 1,2,3,4-thiatriazoles in this reaction is assumed to propagate through diazotization of the respective thiohydrazide intermediates formed in the first step by nitrous acid used in the second step, however, the detailed mechanism of formation of these thiohydrazide intermediates is still under investigation.

To extend the scope of this synthetic approach, we engaged various nitrile substrates in our one-pot synthetic approach. Thus, a series of 5-aryl-1,2,3,4-thiatriazoles was successfully prepared in good to high yields (51%-80%, **Table 4**), among which many were previously complicated to prepare.[5–14] The reactions are simple and efficient, and the nitrile substrate can contain different functional groups such as halogens or hydroxyl group. Although the reaction is versatile with aromatic nitriles, preparation of 5-alkyl-1,2,3,4-thiatriazoles using benzyl cyanide or *tert*-butyl cyanide was not successful, probably due to the instability of the thioacylating intermediates which have been described previously.[14]

Table 4: Synthesis of 5-aryl-1,2,3,4-thiatriazoles **TT1-TT9** [(a)].

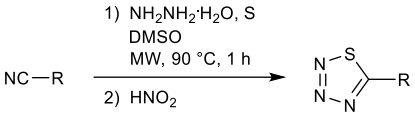

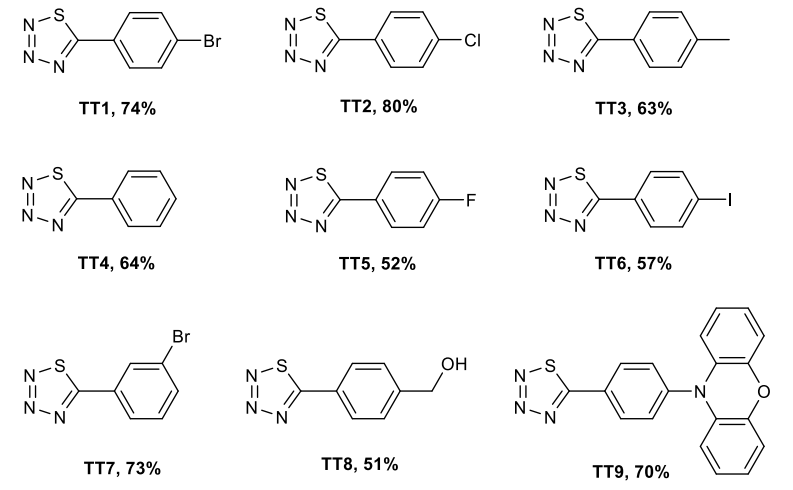

(a) Reactions were carried out on a 0.5 mmol scale in 2 ml DMSO. Yields (isolated) based on the starting nitrile.

With our convenient synthetic approach in hand, we hypothesized that it could be used to prepare donor-acceptor thiatriazole derivatives using appropriate nitrile precursors, and more importantly, 1,2,3,4-thiatriazole could act as a novel electron acceptor for efficient TADF emitters. To our delight, donor-acceptor thiatriazole derivative **TT9** comprising phenoxazine as a donor motif was easily prepared in a high yield (70%) using our approach. **TT9** easily forms yellow crystals, which are stable and could be stored at room temperature for several months without noticeable degradation. The single crystal structure (**Figure 1**) shows a large twisting angle (67°) between the donor (phenoxazine) and acceptor (*i.e.* 1,2,3,4-thiatriazole and phenyl moieties) planes, which is desired to achieve small HOMO-LUMO overlap resulting in a small ΔE_{ST}, a necessary condition for efficient TADF characteristics.

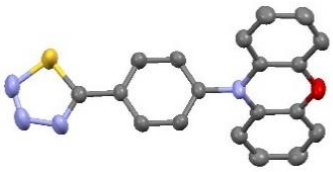

Figure 1: Crystal structure of **TT9**. Hydrogen atoms are omitted for clarity.

6.3 Electrochemistry

The cyclic voltammetry of **TT9** was measured in DCM at room temperature (**Figure 2**). The redox potentials are gathered in **Table 5**. The HOMO and LUMO energy were thus estimated to be 5.35 eV and 3.41 eV from the oxidation and reduction potentials.

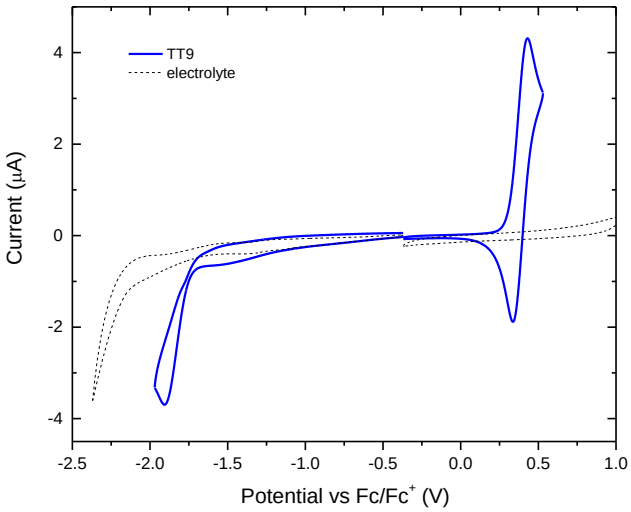

Figure 2: Cyclic voltammetry of **TT9** in DCM at room temperature.

Table 5: Electrochemical properties of **TT9**.

	E_{ox} vs Fc/Fc^+ (V)[a]	E_{red} vs Fc/Fc^+ (V)[a]	HOMO (eV)[b]	LUMO (eV)[c]
TT9	0.25	-1.69	5.35	3.41

(a) Measured in DCM at room temperature by cyclic voltammetry. (b) Estimated from the oxidation potential in DCM, HOMO = E_{ox} + 5.1. (c) Estimated from the reduction potential in DCM, LUMO = E_{red} + 5.1.

The reason why the radical-anions (RAs) of thiatriazoles are not stable (while for example tetrazines RAs are mostly stable) is not clear, but may be linked to its strong basicity, a consequence of its low formation potential.

6.4 Photophysical properties

TT9 exhibits prominent thermally activated delayed fluorescence (TADF) characteristics both in solution and film. The main photophysical properties of **TT9** are depicted in **Table 6**. Like other donor-acceptor molecules, **TT9** shows a clear solvatochromic effect in the excited state (**Figure 3**). It is highly emissive in non-polar media such as methylcyclohexane (MCH), toluene and Zeonex, however very weakly emissive or non-emissive in more polar solvents as typically observed for strong CT systems.[32] Photoluminescence (PL) intensity of **TT9** in MCH increases 6.3-fold in degassed solution relative to the air-equilibrated ones (**Figure 4**), indicating oxygen largely influences the PL of this material.

Table 6: Photophysical properties of **TT9**.

	λ_{PL} (nm)[a]	$\Phi_{PL}^{air}/\Phi_{PL}^{deg}$ (%)	τ_{PF} (ns)[d]	τ_{DF} (µs)[e]	DF/PF[f]
Zeonex film	539	65/99[b]	20.4 ± 0.7	5.5 ± 0.28, 28.0 ± 1.7	2.37
MCH Solution	505,532	12/76[c]	18.6 ± 0.6^{deg}/ 9.0 ± 0.05^{air}	22.2 ± 1.2	2.65

(a) Emission maxima. (b) PLQY in air and N_2 atmosphere. (c) PLQY in air-equilibrated and degassed MCH solution. (d) Prompt fluorescence lifetime determined from PL decay. For MCH solution, the lifetime value for both degassed and air-equilibrated solution are given. (e) Delayed fluorescence lifetime determined from PL decay. (f) Ratio of delayed fluorescence component to prompt fluorescence one.

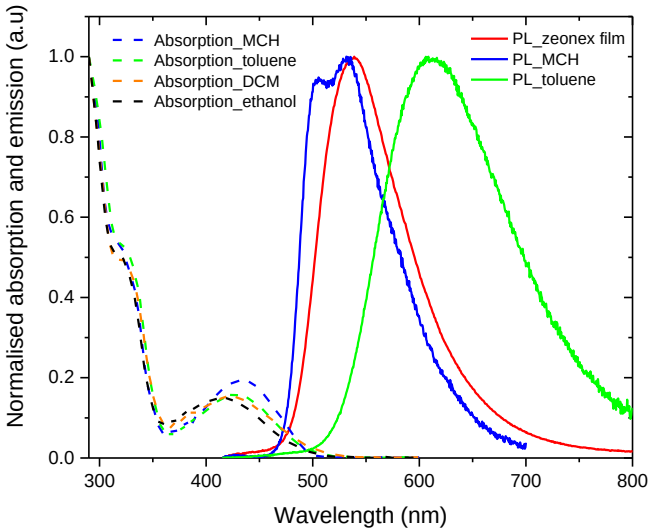

Figure 3: Normalized fluorescence spectra of **TT9** in MCH, toluene and Zeonex 1% (w/w) and normalized absorption spectra in MCH, toluene, DCM and ethanol. Note: DCM and ethanol solutions are virtually non-emissive and their fluorescence spectra are not shown.

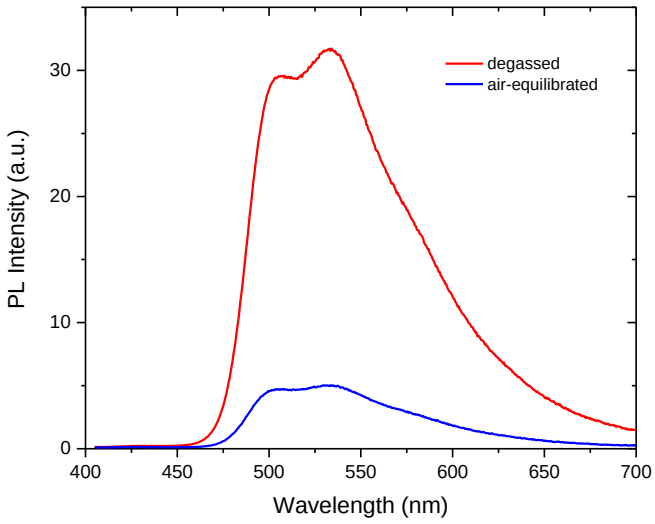

Figure 4: PL spectra of **TT9** in degassed and air-equilibrated MCH at room temperature.

The ratio of delayed to prompt fluorescence components (DF/PF) was determined to be 2.65 from the PL decay of **TT9** in MCH (**Table 6**), indicating that the oxygen not only quenches the triplet state but also the singlet one. This can also be seen by the comparison of PL decays of **TT9** in degassed and air-equilibrated MCH solution. The PL intensity of

prompt fluorescence in air-equilibrated MCH is much lower than in degassed MCH. (**Figure 5**).

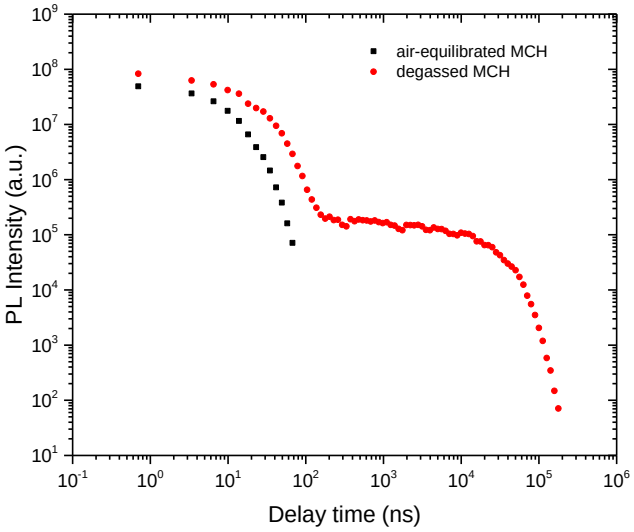

Figure 5: PL decay of **TT9** in degassed and air-equilibrated MCH at room temperature.

PLQY of **TT9** in MCH and Zeonex in air were determined to be 12% and 65%, respectively. Remarkably, the PLQY in degassed MCH increased to 76%, and the PLQY in Zeonex in a nitrogen atmosphere increased to 99%. This is both highly desirable and remarkable, since many CT molecules suffer from a small radiative decay rate and low PLQY due to the spatial separation of HOMO and LUMO because of the molecular design.[15–18]

TT9 exhibits prominent TADF characteristic not only in MCH but also in Zeonex with a DF/PF ratio in the latter equal to 2.37 (**Table 6**). Temperature dependence of the delayed fluorescence of **TT9** recorded in Zeonex (**Figure 6**) is typical for TADF molecules showing clearly the thermal activation of the process.[19] Interestingly, at 80 K the intensity of TADF is still substantial and thus phosphorescence is hardly distinguishable from delayed fluorescence (**Figure 7**). This gives a clear indication that ΔE_{ST} is approaching zero. Prompt fluorescence is completely unaffected by temperature change which indicates that it has almost no effect on non-radiative decay rates of the singlet excited state. This explains the high PLQY of the molecule.

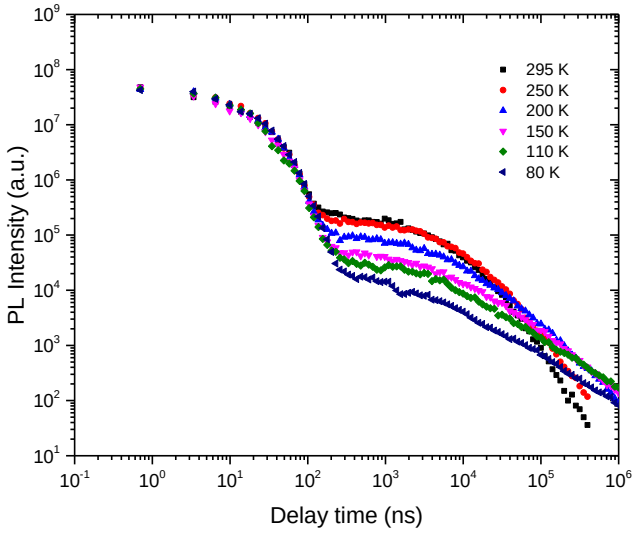

Figure 6: PL decays of **TT9** in Zeonex 1% (w/w) at various temperatures.

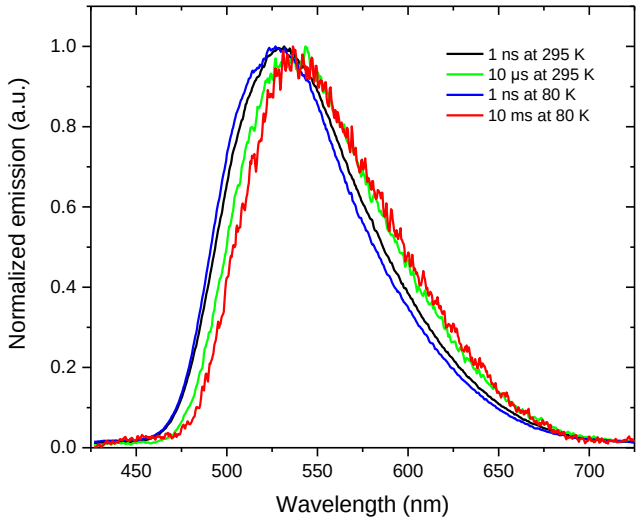

Figure 7: Time-resolved spectra of **TT9** in Zeonex 1% (w/w).

Power dependence of the delayed fluorescence of **TT9** is linear in both MCH and Zeonex which proves that the delayed fluorescence comes from a TADF mechanism and not a triplet-triplet annihilation (TTA) one (**Figure 8, 9**).

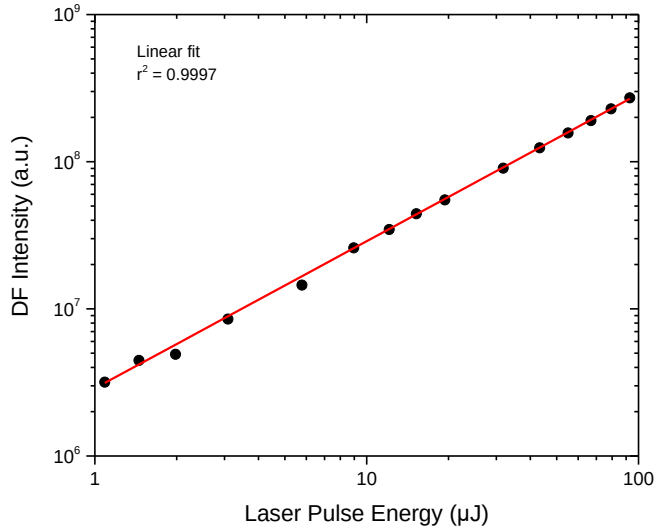

Figure 8: Power dependence of delayed fluorescence of **TT9** in degassed MCH at room temperature.

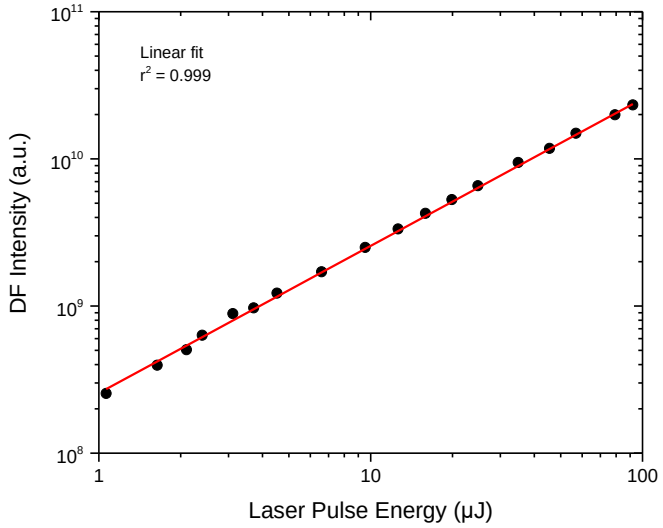

Figure 9: Power dependence of delayed fluorescence of **TT9** in Zeonex in vacuum at room temperature.

6.5 Conclusion

In this chapter, we have confirmed and proved that the solvent plays an important role in the modified Pinner synthesis. In the course of the study of this solvent effect, we have serendipitously discovered a novel and convenient one-pot synthesis of 1,2,3,4-thiatriazoles directly from nitrile substrates in high yields (51%-80%), with no need for

isolating the thioacylating agents. We believe that this work significantly improves access to differently aromatic functionalized 1,2,3,4-thiatriazoles. Using this new one-pot approach a donor-acceptor thiatriazole derivative has been synthesized which proved to be an efficient TADF emitter. This is the first example of 1,2,3,4-thiatriazole used as an electron acceptor in TADF emitters. Our new approach opens up the possibility to use 1,2,3,4-thiatriazole derivatives as a new family of molecules for applications as molecular materials in organic electronic.

6.6 Experimental details

General Methods:

Synthesis. All chemicals were received from commercial sources and used without further purification. Microwave reaction was performed on a microwave synthesis reactor (Anton Paar Monowave 300). Thin layer chromatography (TLC) was performed on silica gel. Flash column chromatography purification was performed on a CombiFlash-Rf system with a variable wavelength UV detector. All mixtures of solvents are given in v/v ratio. NMR spectra were recorded on a JEOL ECS (400 MHz) spectrometer. ^{13}C NMR spectra were proton decoupled. HRMS spectra were measured either on an UPLC/ESI-HRMS device (an Acquity Waters UPLC system coupled to a Waters LCT Premier XE mass spectrometer equipped with an electrospray ion source), or a Q-TOF mass spectrometer (Q-TOF 6540, Agilent) equipped with an APPI ion source.

*All the 1,2,3,4-thiatriazole samples were analyzed in both ESI and APPI HRMS, but only **TT9** gave good result in ESI, and a loss of N_2 was observed for all the 1,2,3,4-thiatriazole samples in APPI which is in accordance with the literature description on the stability of 1,2,3,4-thiatriazoles.[11–13, 33] Nevertheless, **TT9** was confirmed by both ESI HRMS and single crystal XRD measurements. The NMR data of **TT2-TT4** are in accordance with the literature values.[14] The signals observed between 177 and 180 ppm in ^{13}C NMR for all the 1,2,3,4-thiatriazole samples **TT1-TT9** are characteristic of the C=N of 1,2,3,4-thiatriazoles.

The single crystal of compound **TT9** was obtained from slow evaporation of the mixture of solvents (Petroleum ether:CH_2Cl_2 = 1:1). The yellow colour single crystal was mounted on the glass capillary using glue. The crystallographic analysis was performed employing XtaLAB mini diffractometer (Rigaku) with graphite monochromated Mo Kα (λ = 0.71075 Å) X-ray source. The measurements were performed at the temperature of 293 K. Calculations/visualizations were performed using the OLEX2[34] crystallographic software package except for refinement, which was performed using SHELXL.[35] Anisotropic thermal parameters were assigned to all nonhydrogen atoms. The hydrogens were included in the structure factor calculation at idealized positions by using a riding model and refined isotropically.

Photophysics. Zeonex ® 480 blends were prepared from toluene solutions by the drop-cast method and dried in vacuum. All solutions were investigated at 10^{-5} mol dm^{-3} concentration and were degassed using five freeze/pump cycles. Absorption and emission spectra were collected using a UV-3600 double beam spectrophotometer (Shimadzu), and a Fluoromax fluorescence spectrometer (Jobin Yvon) or QePro fluorescence spectrometer (Ocean Optics). Photoluminescence quantum yields of Zeonex films were recorded using an integrating sphere (Labsphere) coupled with a 365 nm LED light source (Ocean Optics)

and a QePro fluorescence spectrometer (Ocean Optics). Photoluminescence quantum yield in MCH solution was measured using Rhodamine 6g (Φ_{PL} = 0.95) as the standard.

Phosphorescence, prompt fluorescence (PF), and delayed fluorescence (DF) spectra and decays were recorded by nanosecond gated luminescence and lifetime measurements (from 400 ps to 1 s) using either third harmonic of a high-energy, pulsed Nd:YAG laser emitting at 355 nm (EKSPLA) or a N2 laser emitting at 337 nm. Emission was focused onto a spectrograph and detected on a sensitive gated iCCD camera (Stanford Computer Optics) of sub-nanosecond resolution. PF/DF time-resolved measurements were performed by exponentially increasing gate and delay times.

Electrochemistry. The electrochemical cell consisted into a platinum electrode with a 1 mm diameter of working area as a working electrode, an Ag electrode as the reference electrode and a platinum coil as an auxiliary electrode. Cyclic voltammetry measurements were conducted at room temperature at a potential rate of 50 mV/s and were calibrated against ferrocene/ferrocenium redox couple. All voltammograms were recorded on a CH Instruments Electrochemical Analyzer model 660 potentiostat. Electrochemical measurements were conducted in 1.0 mM concentrations for all cyclic voltammetry measurements. Electrochemical studies were undertaken in 0.1 M solutions of Bu_4NPF_6, in degassed DCM at room temperature.

General procedure for synthesis of TT1-TT8 (Pinner Synthesis using DMSO as solvent)

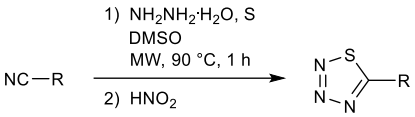

Nitrile substrate (0.5 mmol), sulfur (0.75 mmol, 24 mg) and DMSO (2 ml) were mixed together in a 30 ml microwave reaction tube. Hydrazine monohydrate (5 mmol, 0.25 ml) was added with stirring afterwards. The vessel was sealed and the reaction mixture was heated to 90 °C for 1 hour. (Caution should be exercised due to the elevated pressure in the sealed reaction vessel when heating, particularly attempting scale up). Then 5 ml of CH_2Cl_2 and sodium nitrite (5 mmol, 0.35 g) in 10 ml of H_2O were added to the mixture. Excess acetic acid (20 mmol, 1.14 ml) was then added slowly at 0 °C. The reaction mixture was allowed to stir for another 1 hour at room temperature, and then extracted with dichloromethane. The organic phase was dried over anhydrous magnesium sulfate ($MgSO_4$), filtered and concentrated under reduced pressure. The resulting residue was purified using flash column chromatography.

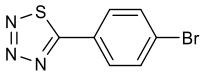

TT1

TT1: A white crystalline solid was obtained after flash column chromatography (Petroleum ether:CH_2Cl_2 = 4:1) (90 mg, yield: 74%). ^{1}H NMR (400 MHz, $CDCl_3$, δ): 7.92 (d, *J* = 8.60 Hz, 2H), 7.71 (d, *J* = 8.60 Hz, 2H) ppm; ^{13}C NMR (100 MHz, $CDCl_3$, δ): 178.24, 133.24, 131.11, 128.21, 125.42 ppm; HRMS-APPI $[M\text{-}N_2]^+$ m/z calcd. for $[C_7H_4BrNS]^+$ 212.9248, found 212.9246.

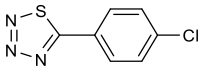

TT2

TT2: A white solid was obtained after flash column chromatography (Petroleum ether:CH_2Cl_2 = 4:1) (79 mg, yield: 80%). ^{1}H NMR (400 MHz, $CDCl_3$, δ): 8.00 (d, *J* = 8.60 Hz, 2H), 7.54 (d, *J* = 8.60 Hz, 2H) ppm; ^{13}C NMR (100 MHz, $CDCl_3$, δ): 178.12, 139.72, 131.01, 130.25, 124.96 ppm; HRMS-APPI $[M\text{-}N_2]^+$ m/z calcd. for $[C_7H_4ClNS]^+$ 168.9753, found 168.9748.

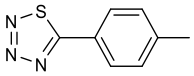

TT3

TT3: A white solid was obtained after flash column chromatography (Petroleum ether:CH_2Cl_2 = 3:1) (56 mg, yield: 63%). ^{1}H NMR (400 MHz, $CDCl_3$, δ): 7.94 (d, *J* = 8.20 Hz, 2H), 7.54 (d, *J* = 8.20 Hz, 2H), 2.45 (s, 3H) ppm; ^{13}C NMR (100 MHz, $CDCl_3$, δ): 179.34, 144.30, 130.57, 129.82, 123.81, 21.87 ppm; HRMS-APPI $[M\text{-}N_2]^+$ m/z calcd. for $[C_8H_7NS]^+$ 149.0299, found 149.0292.

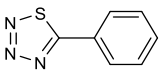

TT4

TT4: A white solid was obtained after flash column chromatography (Petroleum ether:CH_2Cl_2 = 4:1) (52 mg, yield: 64%). ^{1}H NMR (400 MHz, $CDCl_3$, δ): 8.07–8.01 (m, 2H), 7.66–7.51 (m, 3H) ppm; ^{13}C NMR (100 MHz, $CDCl_3$, δ): 179.32, 133.31, 129.86, 129.82, 126.45 ppm; HRMS-APPI $[M\text{-}N_2]^+$ m/z calcd. for $[C_7H_5NS]^+$ 135.0143, found 135.0135.

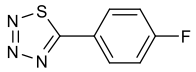

TT5

TT5: A white solid was obtained after flash column chromatography (Petroleum ether:CH_2Cl_2 = 3:1) (47 mg, yield: 52%). ^{1}H NMR (400 MHz, $CDCl_3$, δ): 8.10–8.01 (m, 2H), 7.29–7.20 (m, 2H) ppm; ^{13}C NMR (100 MHz, $CDCl_3$, δ): 178.05 (s), 165.66 (d, $^1J_{CF}$ = 256.03 Hz), 132.15 (d, $^3J_{CF}$ = 8.98 Hz), 122.88 (d, $^4J_{CF}$ = 3.10 Hz), 117.29 (d, $^2J_{CF}$ = 22.33 Hz) ppm; HRMS-APPI $[M\text{-}N_2]^+$ m/z calcd. for $[C_7H_4FNS]^+$ 153.0048, found 153.0045.

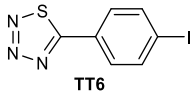

TT6

TT6: A white solid was obtained after flash column chromatography (Petroleum ether:CH_2Cl_2 = 4:1) (82 mg, yield: 57%). ^{1}H NMR (400 MHz, $CDCl_3$, δ): 7.92 (d, *J* = 8.60 Hz, 2H), 7.77 (d, *J* = 8.60 Hz, 2H) ppm; ^{13}C NMR (100 MHz, $CDCl_3$, δ): 178.48, 139.17, 130.98, 125.90, 100.58 ppm; HRMS-APPI $[M\text{-}N_2]^+$ m/z calcd. for $[C_7H_4INS]^+$ 260.9109, found 260.9108.

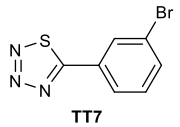

TT7

TT7: A white solid was obtained after flash column chromatography (Petroleum ether:CH_2Cl_2 = 3:1) (88 mg, yield: 73%). ^{1}H NMR (400 MHz, $CDCl_3$, δ): 8.22 (t, *J* = 1.70 Hz, 1H), 7.97 (d, *J* = 7.80 Hz, 1H), 7.74 (d, *J* = 7.80 Hz, 1H), 7.44 (t, *J* = 7.80 Hz, 1H) ppm; ^{13}C NMR (100 MHz, $CDCl_3$, δ): 177.79, 136.16, 132.36, 131.35, 128.47, 128.20, 123.80 ppm; HRMS-APPI $[M\text{-}N_2]^+$ m/z calcd. for $[C_7H_4BrNS]^+$ 212.9248, found 212.9247.

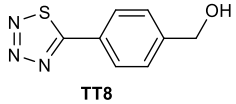

TT8

TT8: A white solid was obtained after flash column chromatography (Petroleum ether:CH_2Cl_2 = 5:2) (49 mg, yield: 51%). ^{1}H NMR (400 MHz, $CDCl_3$, δ): 8.04 (d, *J* = 8.20 Hz, 2H), 7.56 (d, *J* = 8.20 Hz, 2H), 4.83 (s, 2H), 1.97 (s, br, 1H) ppm; ^{13}C NMR (100 MHz, $CDCl_3$, δ): 179.08, 146.62, 130.04, 127.85, 125.55, 64.56 ppm; HRMS-APPI $[M\text{-}N_2]^+$ m/z calcd. for $[C_8H_7NOS]^+$ 165.0248, found 165.0246.

Synthesis of TT9

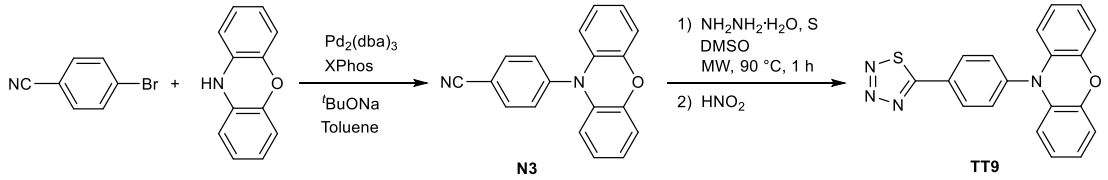

The synthesis of **N3** was described previously in **Chapter 3**.

N3 (0.5 mmol, 142 mg), sulfur (0.75 mmol, 24 mg) and DMSO (2 ml) were mixed together in a 30 ml microwave reaction tube. Hydrazine monohydrate (5 mmol, 0.25 ml) was added with stirring afterwards. The vessel was sealed and the reaction mixture was heated to 90 °C for 1 hour. (Caution should be exercised due to the elevated pressure in the sealed reaction vessel when heating, particularly attempting scale up). Then 5 ml of CH_2Cl_2 and sodium nitrite (5 mmol, 0.35 g) in 10 ml of H_2O were added to the mixture. Excess acetic acid (20 mmol, 1.14 ml) was then added slowly at 0 °C. The reaction mixture was allowed to stir for another 1 hour at room temperature, and then extracted with dichloromethane. The organic phase was dried over anhydrous magnesium sulfate ($MgSO_4$), filtered and concentrated under reduced pressure. The resulting residue was purified using flash column chromatography.

TT9: A yellow crystalline solid was obtained after flash column chromatography (Petroleum ether:CH_2Cl_2 = 3:2) (120 mg, yield: 70%). ^{1}H NMR (400 MHz, $CDCl_3$, δ): 8.29 (d, *J* = 8.20 Hz, 2H), 7.59 (d, *J* = 8.20 Hz, 2H), 6.78–6.59 (m, 6H), 6.01 (d, *J* = 7.80 Hz, 2H) ppm; ^{13}C NMR (100 MHz, $CDCl_3$, δ): 178.17, 144.20, 144.02, 133.57, 132.55, 132.43, 126.34, 123.49, 122.30, 116.04, 113.50 ppm; HRMS-APPI $[M+H-N_2]^+$ m/z calcd. for $[C_{19}H_{13}N_2OS]^+$ 317.0749, found 317.0738; HRMS-ESI $[M]^+$ m/z calcd. for $[C_{19}H_{12}N_4OS]^+$ 344.0732, found 344.0745.

Pinner Synthesis using ethanol as solvent

4-Bromobenzonitrile (0.5 mmol, 91 mg), sulfur (0.75 mmol, 24 mg) and ethanol (2 ml) were mixed together in a 30 ml microwave reaction tube. Hydrazine monohydrate (5 mmol, 0.25 ml) was added with stirring afterwards. The vessel was sealed and the reaction mixture was heated to 90 °C for 1 hour. (Caution should be exercised due to the elevated pressure in the sealed reaction vessel when heating, particularly attempting scale up). Then 5 ml of CH_2Cl_2 and sodium nitrite (5 mmol, 0.35 g) in 10 ml of H_2O were added to the mixture. Excess acetic acid (20 mmol, 1.14 ml) was then added slowly at 0 °C. The reaction mixture was allowed to stir for another 1 hour at room temperature, and then extracted with dichloromethane. The organic phase was dried over anhydrous magnesium sulfate ($MgSO_4$), filtered and concentrated under reduced pressure. The resulting residue was

purified using flash column chromatography (CH_2Cl_2) to give **T1** as a pink solid (42 mg, yield: 43%).

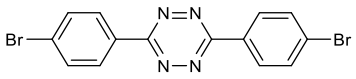

T1

T1[26]**:** ^{1}H NMR (400 MHz, DMSO-d_6, δ): 7.98 (d, *J* = 8.60 Hz, 4H), 7.81 (d, *J* = 8.60 Hz, 4H) ppm; ^{13}C NMR (100 MHz, DMSO-d_6, δ): 167.13, 132.60, 129.59, 128.60, 125.08 ppm.

Pinner Synthesis using acetonitrile as solvent

4-Bromobenzonitrile (0.5 mmol, 91 mg), sulfur (0.75 mmol, 24 mg) and acetonitrile (2 ml) were mixed together in a 30 ml microwave reaction tube. Hydrazine monohydrate (5 mmol, 0.25 ml) was added with stirring afterwards. The vessel was sealed and the reaction mixture was heated to 90 °C for 1 hour. (Caution should be exercised due to the elevated pressure in the sealed reaction vessel when heating, particularly attempting scale up). Then 5 ml of CH_2Cl_2 and sodium nitrite (5 mmol, 0.35 g) in 10 ml of H_2O were added to the mixture. Excess acetic acid (20 mmol, 1.14 ml) was then added slowly at 0 °C. The reaction mixture was allowed to stir for another 1 hour at room temperature, and then extracted with dichloromethane. The organic phase was dried over anhydrous magnesium sulfate ($MgSO_4$), filtered and concentrated under reduced pressure. The resulting residue was purified using flash column chromatography.

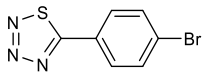

TT1

TT1: Petroleum ether:CH_2Cl_2 = 4:1 (11 mg, yield: 9%), obtained as a white crystalline solid.

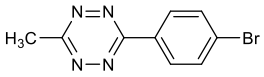

T2

T2[36]**:** Petroleum ether:CH_2Cl_2 = 3:1 (20 mg, yield: 16%), obtained as a red solid. ^{1}H NMR (400 MHz, $CDCl_3$, δ): 8.46 (d, *J* = 8.60 Hz, 2H), 7.73 (d, *J* = 8.60 Hz, 2H), 3.10 (s, 3H) ppm; ^{13}C NMR (100 MHz, $CDCl_3$, δ): 167.60, 163.72, 132.72, 130.83, 129.46, 127.87, 21.36 ppm.

Pinner Synthesis using DMF as solvent

4-Bromobenzonitrile (0.5 mmol, 91 mg), sulfur (0.75 mmol, 24 mg) and DMF (2 ml) were mixed together in a 30 ml microwave reaction tube. Hydrazine monohydrate (5 mmol, 0.25 ml) was added with stirring afterwards. The vessel was sealed and the reaction mixture was heated to 90 °C for 1 hour. (Caution should be exercised due to the elevated pressure in the sealed reaction vessel when heating, particularly attempting scale up). Then 5 ml of CH_2Cl_2 and sodium nitrite (5 mmol, 0.35 g) in 10 ml of H_2O were added to the mixture. Excess acetic acid (20 mmol, 1.14 ml) was then added slowly at 0 °C. The reaction mixture was allowed to stir for another 1 hour at room temperature, and then extracted with dichloromethane. The organic phase was dried over anhydrous magnesium sulfate ($MgSO_4$), filtered and concentrated under reduced pressure. The resulting residue was purified using flash column chromatography.

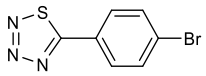

TT1

TT1: Petroleum ether:CH_2Cl_2 = 4:1 (50 mg, yield: 41%), obtained as a white crystalline solid.

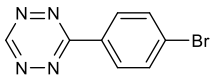

T3

T3[27]**:** Petroleum ether:CH_2Cl_2 = 3:1 (10 mg, yield: 8%), obtained as a red solid. ^{1}H NMR (400 MHz, $CDCl_3$, δ): 10.25 (s, 1H), 8.51 (d, *J* = 8.70 Hz, 2H), 7.76 (d, *J* = 8.70 Hz, 2H) ppm; ^{13}C NMR (100 MHz, $CDCl_3$, δ): 166.12, 158.04, 132.89, 130.62, 129.82, 128.64 ppm.

6.7 Reference

[1] M. Freud, H. P. Schwarz, *Ber. Dtsch. Chem. Ges.* **1896**, 29*,* 2491–2499.

[2] M. Freud, A. Schander, *Ber. Dtsch. Chem. Ges.* **1896**, 29*,* 2500–2505.

[3] E. Lieber, C. N. Pillai, R. D. Hites, *Can. J. Chem.* **1957**, *35*, 832–842.

[4] E. Lieber, J. Ramochandran, *Can. J. Chem.* **1959**, *37*, 101–109.

[5] K. A. Jensen, C. Pedersen, *Adv. Heterocycl. Chem.* **1964**, *3*, 263–284.

[6] A. Holm, *Adv. Heterocycl. Chem.* **1976**, *20*, 145–174.

[7] W. Kirmse, *Chem. Ber.* **1960**, *93*, 2353–2356.

[8] K. A. Jensen, C. Pedersen, *Acta. Chem. Scand.* **1961**, *15*, 1104–1108.

[9] P. A. S. Smith, D. H. Kenny, *J. Org. Chem.* **1961**, *26*, 5221–5224.

[10] E. Lieber, C. N. R. Rao, R. C. Orlowski, *Can. J. Chem.* **1963**, *41*, 926–931.

[11] A. Holm, N. Harrit, N. H. Toubro, *J. Am. Chem. Soc.* **1975**, *97*, 6197–6201.

[12] A. Holm, N. Harrit, I. Trabjerg, *J. Chem. Soc., Perkin Trans. 1*, **1978**, 746–750.

[13] A. Holm, N. H. Toubro, *J. Chem. Soc., Perkin Trans. 1*, **1978**, 1445–1449.

[14] S. Ikeda, T. Murai, H. Ishihara, S. Kato, *Synthesis* **1990**, *5* 415–416.

[15] Y. Im, M. Kim, Y. J. Cho, J.-A Seo, K. S. Yook, J. Y. Lee, *Chem. Mater*. **2017**, *29*, 1946–1963.

[16] M. Y. Wong, E. Zysman-Colman, *Adv. Mater.* **2017**, *29*, 1605444.

[17] Z. Yang, Z. Mao, Z. Xie, Y. Zhang, S. Liu, J. Zhao, J. Xu, Z. Chi, M. P. Aldred, *Chem. Soc. Rev.* **2017**, *46*, 915–1016.

[18] T. Huang, W. Jiang, L. Duan, *J. Mater. Chem. C* **2018**, *6*, 5577–5596.

[19] F. B. Dias, T. J Penfold, A. P Monkman, *Methods Appl. Fluoresc.* **2017**, *5*, 012001

[20] G. Clavier, P. Audebert, *Chem. Rev.* **2010**, *110*, 3299–3314.

[21] F. Miomandre, R. Meallet-Renault, J. J. Vachon, R. B. Pansu, P. Audebert, *Chem. Commun.* **2008**, *16*, 1913–1915.

[22] C. Quinton, V. Alain-Rizzo, C. Dumas-Verdes, G. Clavier, F. Miomandre, P. Audebert, *Eur. J. Org. Chem.* **2012**, *7*, 1394–1403.

[23] J. Malinge, C. Allain, A. Brosseau, P. Audebert, *Angew. Chem. Int. Ed.* **2012**, *51*, 8534–8537.

[24] P. Audebert, F. Miomandre, *Chem. Sci.* **2013**, 4, 575–584.

[25] C. Quinton, S.-H. Chi, C. Dumas-Verdes, P. Audebert, G. Clavier, J. W. Perry, V. Alain-Rizzo, *J. Mater. Chem. C* **2015**, *3*, 8351-8357.

[26] C. Allain, J. Piard, A. Brosseau, M. Han, J. Paquier, T. Marchandier, M. Lequeux, C. Boissière, P. Audebert, *ACS Appl. Mater. Interfaces* **2016**, *8*, 19843–19846.

[27] Y. Qu, F.-X. Sauvage, G. Clavier, F. Miomandre, P. Audebert, *Angew. Chem. Int. Ed.* **2018**, DOI 10.1002/anie.201804878.

[28] A. Pinner, *Ber. Dtsch. Chem. Ges.* **1893**, *26*, 2126–2135.

[29] K. A. Hofmann, O. Ehrhart, *Ber. Dtsch. Chem. Ges.* **1912**, *45*, 2731–2740.

[30] T. Curtius, A. Hess, *J. Prakt. Chem.* **1930**, *125*, 40–53.

[31] J. C. T. Carlson, L. G. Meimetis, S. A. Hilderbrand, R. Weissleder, *Angew. Chem. Int. Ed.* **2013**, *52*, 6917–6920.

[32] F. B. Dias, J. Santos, D. R. Graves, P. Data, R. S. Nobuyasu, M. A. Fox, A. S. Batsanov, T. Palmeira, M. N. Berberan-Santos, M. R. Bryce, A. P. Monkman, *Adv. Sci.* **2016**, *3*, 1600080.

[33] Y. Liu, A. S. Evans, J. P. Toscano, *Phys. Chem, Chem, Phys*. **2012**, *14*, 10438–10444.

[34] O. V. Dolomanov, L. J. Bourhis, R. J. Gildea, J. A. K. Howard, H. Puschmann, *J. Appl. Cryst.* **2009**, *42*, 339–341.

[35] G. M. Sheldrick, *Acta Cryst.* **2008**, *A64*, 112–122.

[36] E. Kozma, G. Estrada Girona, G. Paci, E. A. Lemke, P. Kele, *Chem. Commun.* **2017**, *53*, 6696-6699.

General conclusion and perspectives

This thesis focused on the design, synthesis and characterization of various electron-acceptor derivatives. As a well-known electron-deficient heterocycle and the promising application potentials described in Chapter 1, 1,2,4,5-tetrazine undoubtedly became our first choice for investigation. In addition, the study of this thesis also reached benzonitrile derivatives which are the typical precursors for preparing the 1,2,4,5-tetrazines, and pyridazine derivatives which are the products derived from Inverse Electron Demand Diels–Alder (iEDDA) reaction of 1,2,4,5-tetrazine molecules. Moreover, 1,2,3,4-thiatriazole derivatives, as unpredicted products from modified Pinner synthesis, are also elaborately investigated.

One of the research highlights of this thesis is the development of synthetic methodologies in each chapters. To sum up, Chapter 2 demonstrated a facile and efficient synthetic approach to 3-monosubstituted unsymmetrical 1,2,4,5-tetrazines, which are highly useful for bioorthogonal click chemistry. Chapter 3 described an elaborative synthetic strategy for novel donor-acceptor benzonitrile derivatives which were proved to exhibit interesting photophysical properities, such as TADF, AIE and mechanochromism. Chapter 4 presented a detailed study of Buchwald–Hartwig cross-coupling reaction as an important synthetic methodology in the synthesis and functionalization of tetrazine molecules. Chapter 5 described the study of inverse Electron Demand Diels–Alder (iEDDA) reaction as a synthetic tool to prepare novel pyridazine derivatves. And finally Chapter 6 demonstrated a novel convenient one-pot synthesis of 1,2,3,4-thiatriazoles directly from commercially available nitrile compounds. The important role of solvent in the Pinner synthesis was also presented.

Donor-acceptor structured molecules are valuable in this thesis, because they possess remarkable photophysical and electrochemical properties due to the charge-transfer (CT) states introduced in the donor-acceptor system, which are of particular interest in organic electronics. For example, as described in Chapter 1, donor-acceptor TADF molecules have recently attracted significant interest in electroluminescence (EL) and other applications. Indeed, many of the electron-acceptor derivatives prepared in this thesis possess interesting photophysical and electrochemical properties which have been presented in each chapters. For example, the novel donor-acceptor benzonitrile derivatives exhibit promising TADF, AIE and mechanochromism. As exemplified in Chapter 3, **N10** exhibits prominent TADF and AIE characteristics. It is also important to point out that 1,2,3,4-thiatriazole was for the first time used as an electron acceptor TADF emitters, and donor-acceptor 1,2,3,4-thiatriazole **TT9** exhibits excellent TADF characteristics in both solution and film, as demonstrated in Chapter 6. Additionally, donor-acceptor pyridazine derivatives also show interesting photophysical properties, such as room temperature

phosphorescence (RTP) for **DA3** and **DA6**, which was described in Chapter 5. Finally, it is also important to mention that some of the donor-acceptor tetrazine derivatives exhibit excellent fluorescence turn-on ability after iEDDA reaction as described also in Chapter 5.

It is anticipated that the synthetic methodologies presented in this thesis should be widely utilized to prepare useful materials in the future. For example, the metal-free synthetic approach to 3-monosubstituted 1,2,4,5-tetrazines is expected to be widely employed by researchers to prepare tetrazines useful in several applications, particularly bioorthogonal click chemistry. In addition, it would be interesting to explore the use of DCM as a novel reagent in the synthesis of other heterocycles. Another perspective from the synthetic methodology is to use the novel convenient one-pot synthesis of 1,2,3,4-thiatriazoles to prepare new functionalized 1,2,3,4-thiatriazole derivatives which could be helpful in various applications, especially organic electronics. Moreover, Inverse Electron Demand Diels–Alder (iEDDA) reaction as a convenient and powerful synthetic tool is anticipated to be widely employed to prepare tailored pyridazine materials with various functional groups (e.g., supramolecular or polymeric materials) from the prepared tetrazine derivatives. Additionally, the prepared donor-acceptor benzonitrile and thiatriazole derivatives which exhibit promising TADF characteristics are certainly expected to be investigated for OLED application. Finally, a fruitful perspective would be to combine TADF fluorophore and tetrazine moiety for the application of time-resolved fluorescence imaging (TRFI).

Titre : Design, synthèse et caractérisation de dérivés aromatiques et hétérocycliques électrodéficitaires

Mots clés : tétrazine, benzonitrile, thiatriazole, fluorescence retardée, réaction de couplage, réaction Diels–Alder

Résumé : Cette thèse porte sur la conception, la synthèse et la caractérisation de nouveaux dérivés accepteurs d'électrons. Elle se concentre sur l'étude des dérivés de la 1,2,4,5-tétrazine, mais contient également l'étude de dérivés du benzonitrile, précurseurs typiques de la préparation des 1,2,4,5-tétrazines et de dérivés de la pyridazine, les produits dérivés de la réaction de Diels – Alder à Demande Inverse (IEDDA) des dérivés de la tétrazine. De plus, les dérivés de 1,2,3,4-thiatriazole, en tant que produits imprévus de la synthèse de Pinner modifiée, sont également étudiés de manière approfondie. En raison des états de transfert de charge (CT) introduits dans le système donneur-accepteur, les dérivés préparés accepteur d'électrons présentent en général des propriétés photophysiques et électrochimiques intéressantes, et ont donc un intérêt particulier pour l'électronique organique.

Le point culminant de cette thèse est le développement de méthodologies synthétiques dans chaque chapitre. En résumé, le chapitre 2 met en évidence une nouvelle approche synthétique sans métal pour les 1,2,4,5-tétrazines 3-monosubstituées, qui sont très utiles pour la chimie du click bioorthogonal. Le chapitre 3 décrit une stratégie de synthèse élaborée pour de nouveaux dérivés de benzonitrile donneur-accepteur qui présentent de la TADF, de l' AIE et du mécanochromisme. Le chapitre 4 présente une étude détaillée de la réaction de couplage croisé Buchwald – Hartwig en tant que méthodologie de synthèse importante dans la synthèse de molécules de tétrazine. Le chapitre 5 décrit l'étude de la réaction à l'IEDDA comme un outil synthétique utile pour préparer des dérivés de pyridazine. Le chapitre 6 présente une nouvelle synthèse pratique de 1,2,3,4-thiatriazoles à partir de composés nitriles.

Title : Design, synthesis and characterization of electron-acceptor aromatic and heterocyclic derivatives

Keywords : tetrazine, benzonitrile, thiatriazole, delayed fluorescence, coupling reaction, Diels–Alder reaction

Abstract : This PhD thesis deals with the design, synthesis and characterization of novel electron-acceptor derivatives. It is focused on the study of 1,2,4,5-tetrazine derivatives, but also involves the study of benzonitrile derivatives which are the typical precursors for the preparation of 1,2,4,5-tetrazines, and pyridazine derivatives which are the products derived from Inverse Electron Demand Diels–Alder (IEDDA) reaction of tetrazine derivatives. Moreover, 1,2,3,4-thiatriazole derivatives, as unpredicted products from modified Pinner synthesis, are also elaborately investigated. Due to the charge-transfer (CT) states introduced in the donor-acceptor system, the prepared electron-acceptor derivatives exhibit interesting photophysical and electrochemical properties, and therefore are of particular interest in organic electronics.

The highlight of this thesis is the development of synthetic methodologies in each chapter. To sum up, Chapter 2 demonstrates a novel metal-free synthetic approach to 3-monosubstituted 1,2,4,5-tetrazines, which are highly useful for bioorthogonal click chemistry. Chapter 3 describes an elaborative synthetic strategy for novel donor-acceptor benzonitrile derivatives which exhibit TADF, AIE and mechanochromism. Chapter 4 presents a detailed study of Buchwald–Hartwig cross-coupling reaction as an important synthetic methodology in the synthesis of tetrazine molecules. Chapter 5 described the study of IEDDA reaction as a useful synthetic tool to prepare pyridazine derivatves. Chapter 6 presented a novel convenient one-pot synthesis of 1,2,3,4-thiatriazoles directly from nitrile compounds.

Université Paris-Saclay
Espace Technologique / Immeuble Discovery
Route de l'Orme aux Merisiers RD 128 / 91190 Saint-Aubin, France